HAL
open science

Infections par SARS-COV-2 et par VIH-1 : activations immunitaires aigüe et chronique

Lucy Kundura

To cite this version:

Lucy Kundura. Infections par SARS-COV-2 et par VIH-1 : activations immunitaires aigüe et chronique. Médecine humaine et pathologie. Université Montpellier, 2021. Français. NNT : 2021MONTT034 . tel-03431161

HAL Id: tel-03431161

https://theses.hal.science/tel-03431161

Submitted on 16 Nov 2021

HAL is a multi-disciplinary open access archive for the deposit and dissemination of scientific research documents, whether they are published or not. The documents may come from teaching and research institutions in France or abroad, or from public or private research centers.

L'archive ouverte pluridisciplinaire **HAL**, est destinée au dépôt et à la diffusion de documents scientifiques de niveau recherche, publiés ou non, émanant des établissements d'enseignement et de recherche français ou étrangers, des laboratoires publics ou privés.

THÈSE POUR OBTENIR LE GRADE DE DOCTEUR DE L'UNIVERSITÉ DE MONTPELLIER

En Biologie (Immunologie, Virologie)

École doctorale Sciences Chimiques et Biologiques pour la santé (CBS2) – ED 168

Institut de Génétique Humaine, CNRS Montpellier, France (UMR 9002)

Infections par SARS-COV-2 et par VIH-1 : activations immunitaires aigüe et chronique

Présentée par Lucy KUNDURA
Le 03 novembre 2021

Sous la direction de Pierre CORBEAU et Jacques REYNES

Devant le jury composé de

Philippe VAN DE PERRE, Professeur, Université de Montpellier	Président
Joanna VITTE, Docteur, Aix-Marseille Université	Rapporteur
Jean-Pierre ROUTY, Professeur, Université McGill	Rapporteur
Astrid VABRET, Professeur, Université de Caen	Examinatrice
Christian DEVAUX, Docteur, Aix-Marseille Université	Examinateur
Pierre CORBEAU, Professeur, Université de Montpellier	Directeur
Jacques REYNES, Professeur, Université de Montpellier	Co-Directeur

UNIVERSITÉ DE MONTPELLIER

TABLE DES MATIERES

A- RESUME 3
RESUME EN FRANÇAIS 4
ENGLISH ABSTRACT 5
B- REMERCIEMENTS 6
C- TABLE DES ABREVIATIONS 9
D- INTRODUCTION 13
I. LA REPONSE IMMUNITAIRE 14
A- LES MONOCYTES 14
B- LES LYMPHOCYTES 16
C- LES GRANULOCYTES 17
II. LES DERIVES REACTIFS DE L'OXYGENE 18
III. LA PANDEMIE DE COVID-19 20
IV. LE SARS-COV-2 23
A- LES CORONAVIRUS 23
B- L'ENTREE DU VIRUS DANS LA CELLULE 26
C- LA REPLICATION DU VIRUS 27
D- L'ASSEMBLAGE DES NOUVEAUX VIRIONS ET LA SORTIE VERS LE MILIEU EXTRACELLULAIRE 29
VII. LE LYMPHOHISTIOCYTOSE HEMOPHAGOCYTAIRE 29
VIII. L'ANGIOTENSINE II ET RECEPTEUR CELLULAIRE : ACE2 30
A- LE SYSTEME RENINE-ANGIOTENSINE-ALDOSTERONE 30
B- IMPLICATION DANS L'INFECTIONS SARS-COV-2 31
IX. REPONSE IMMUNITAIRE A UNE INFECTION AU SARS-COV-2 33
X. L'ACTIVATION IMMUNITAIRE ET LE VIH 38
A- LE VIRUS DE L'IMMUNODEFICIENCE HUMAINE 38
B- L'ACTIVATION IMMUNITAIRE, CAUSES ET CONSEQUENCES 39
E- RESULTATS 42
I. ARTICLE «MICROBIAL TRANSLOCATION IS LINKED TO A SPECIFIC IMMUNE ACTIVATION PROFILE IN HIV-1-INFECTED ADULTs WITH SUPPRESSED VIREMIA» 43
II. ARTICLE « RESIDUAL VIREMIA IS LINKED TO A SPECIFIC IMMUNE ACTIVATION PROFILE IN HIV-1-INFECTED ADULTS UNDER EFFICIENT ANTIRETROVIRAL THERAPY» 53
III. ARTICLE « IDENTIFICATION OF DISTINCT IMMUNE ACTIVATION PROFILES IN ADULT HUMANS » 66
IV. ARTCLE « INSULIN RESISTANCE IS LINKED TO A SPECIFIC PROFILE OF IMMUNE ACTIVATION IN HUMAN SUBJECTS. » 82
V. ARTICLE « ANGIOTENSIN II INDUCES REACTIVE OXYGEN SPECIES, DNA DAMAGE, AND T CELL APOPTOSIS IN SEVERE COVID-19 » 94
F- PERSPECTIVES 120
I. PERSPECTIVES CONCERTANT LES PARTIES I A IV DES RESULTATS 121
II. PERSPECTIVES CONCERNANT LA PARTIE V DES RESULTATS 121
G- REFERENCES BIBLIOGRAPHIQUE 123

A- RESUME

Mots-Clés : Activation Immunitaire, SARS-COV-2, VIH, Inflammation, Monocytes, ROS, Lymphopénie, Syndrome Métabolique, Marqueurs d'Activation, Translocation Microbienne, Virémie Résiduelle

Key words : Immune activation, SARS-COV-2, HIV, Inflammation, Monocytes, ROS, Lymphopenia, Metabolic Syndrome, Activation Markers, Microbial Translocation, Residual Viremia

RESUME EN FRANÇAIS

Lors d'une infection, le but principal de la réponse immunitaire est d'éliminer le pathogène. Cependant cette réponse peut avoir des effets secondaires indésirables chroniques, comme chez les personnes vivant avec le VIH avirémiques sous traitement ou aigües, comme dans les formes graves de COVID-19.

Les personnes vivant avec le VIH-1, malgré un traitement antirétroviral efficace, présentent plus de comorbidités que la population générale. Beaucoup de ces comorbidités sont liées à une activation immunitaire persistante. Nous avons montré que différents profils d'activation immunitaire pouvaient être identifiés chez ces patients, dont un était associé à la présence d'une translocation microbienne et un autre à une virémie résiduelle. Nous avons également observé que des profils différents d'activation immunitaire existaient dans une cohorte de personnes issues de la population générale et que les personnes ayant un de ces profils présentaient des signes de résistance à l'insuline et de syndrome métabolique.

Dans un contexte d'infection par le SARS-COV-2, une lymphopénie est observée chez certains patients. Cette lymphopénie est un facteur prédictif de complications entraînant l'admission en soins intensifs, voire la mort. Cette lymphopénie semble survenir avant l'orage cytokinique et pourrait en être une des causes. Nous avons découvert une raison à cette lymphopénie : les monocytes de certains patients admis à l'hôpital produisent des dérivés réactifs de l'oxygène responsables de lésions d'ADN puis d'apoptose dans les lymphocytes circulants. Ces dérivés réactifs de l'oxygène sont produits à cause de la stimulation via le récepteur AT_1R des monocytes par l'angiotensine II, dont la concentration sanguine est augmentée probablement du fait de l'internalisation d'ACE2, enzyme capable de cliver l'angiotensine II, induite par le SARS-COV-2 au cours de son entrée cellulaire.

Nos travaux permettent de mieux comprendre les mécanismes pathogènes dus à l'activation immunitaire induite par deux virus différents et ouvrent par là des perspectives thérapeutiques.

ENGLISH ABSTRACT

During an infection, the main purpose of the immune response is to eliminate the pathogen. However, this response can have chronic side effects, such as in people living with aviremic HIV on treatment or acute, as in severe forms of COVID-19.

People living with HIV-1, despite effective antiretroviral therapy, have more comorbidities compared with the general population. Many of these comorbidities are linked to persistent immune activation. We showed that different immune activation patterns could be identified in these patients, one of which was associated with the presence of microbial translocation and another with residual viremia. We also observed that different immune activation patterns occurred in a cohort of people from the general population and that people with one of these patterns showed signs of insulin resistance and metabolic syndrome.

In a context of SARS-COV-2 infection, lymphopenia is observed in some patients. This lymphopenia is a predictor of complications up to admission into intensive care units or death. This lymphopenia seems to occur before the cytokinetic storm and could be one of the causes. We discovered a potential explanation for this lymphopenia: the monocytes of some patients admitted to the hospital produce reactive oxygen derivatives responsible for DNA damage and then apoptosis in circulating lymphocytes. These reactive oxygen derivatives are produced because of stimulation via the AT1R receptor of monocytes by angiotensin II, whose blood concentration is increased probably due to internalization of ACE2, an enzyme capable of cleaving angiotensin II, induced by SARS-COV-2 during cellular entry.

Our work allows us to better understand the pathogenic mechanisms due to the immune activation induced by two different viruses and thus opens up therapeutic perspectives.

B- REMERCIEMENTS

Je remercie mon directeur de thèse, Pierre Corbeau pour la confiance et la liberté qu'il m'a accordées pour mener à bien les projets de l'équipe et ceux à venir. Merci également pour tous les échanges scientifiques et ton accompagnement précieux dans cette thèse.

Je remercie mon co-directeur de thèse Jacques Reynes. Merci pour le temps que vous m'avez accordé et d'avoir suivi cette thèse tout le long.

Je remercie grandement Alain Makinson, Ariane Sultan et Pascal Seyer de m'avoir suivi lors des comités de thèse, merci pour leurs précieux conseils et leur présence.

Je remercie Astrid Vabret, Christian Devaux et Phillipe Van de Perre d'avoir accepté d'être examinateur de mon travail.

Je remercie également Jean-Pierre Routy et Joanna Vitte d'avoir accepté d'être mes rapporteurs et d'évaluer mon travail.

Je remercie les membres de l'équipe, Sandrine, Clément et Renaud ainsi que Mehwish, Claire, Nicolas et tous les anciens membres de cette équipe pour leur apport scientifique et humain.

Par extension je remercie toutes les personnes de l'Institut de Génétique Humaine avec qui j'ai eu la chance d'échanger ces dernières années.

Je remercie aussi les membres du laboratoire d'Immunologie de Saint Eloi de m'avoir accueillie et accompagnée, particulièrement Pierre, Martine et Claire.

Je remercie les membres du Département des Maladies Infectieuses et Tropicales de Montpellier, en particulier Christine, Céline et Cécile pour leur travail remarquable. Merci également à tous les médecins et les volontaires des cohortes de Nîmes et de Montpellier.

Je remercie également la plate-forme MRI et les services communs de l'Institut de Génétique Humaine d'avoir rendu ma thèse plus simple à bien des égards.

Je remercie la FHU-InCh, Sidaction et MSD Avenir pour le soutien financier des projets de l'équipe.

Je remercie profondément ma famille de m'avoir soutenue tout au long de mes études et plus encore. Je ne remercierai jamais assez mes amis d'Epinay, de la Faculté, du CRI et de Montpellier pour leur présence.

Merci Guillaume d'être entré dans ma vie.

Remerciements non censurés pour les copains

Pierre, merci d'avoir accepté mon excentricité et mes mots mal choisis. Merci d'avoir été compréhensif et humain dans les moments compliqués pour moi.

Clément, si je devais t'offrir en fruits l'équivalent de ce que je te dois, même toi tu n'arriverais pas à tout manger.

Sandrine, je n'ai pas les mots, ton soutien a de loin dépassé le cadre professionnel, tu m'as vu pleurer de tristesse, d'énervement, d'épuisement et de rire. Je te suis reconnaissante de tout ce que j'ai pu accomplir ces dernières années, parce que tu m'as poussé pour le faire.

Pascal, merci beaucoup (beaucoup) pour ton soutien et tes conseils. En plus, j'ai une complémentaire santé grâce à toi, tu ne sais pas combien de temps les gens ont bataillé pour que j'en ai une et il a juste fallu que tu sautes une barrière pour me convaincre ! Vraiment merci.

Mehwish, ce fut bref mais inoubliable. Merci de m'avoir mis le pied à l'étrier de la manière la plus efficace qu'il soit.

Clarita, en quelques mois tu m'as appris tout ce dont j'avais besoin pour survivre les quatre années qui ont suivi et j'ai gagné une amie, merci.

Nicolas, dans le genre inoubliable tu as aussi marqué mon esprit. Merci pour les portes que tu m'as ouvertes, merci pour toute nos conversations.

Benoit, bro, je ne t'appelle jamais bro mais ça correspond bien pourtant, t'es toujours là quand je suis en galère, tu m'accordes tout et tu supportes mes blagues salaces. Merci beaucoup.

Callum, merci pour la recette de gâteau au chocolat, je veux que le monde soit au courant que t'as changé ma perspective sur les desserts. Prochaine étape tu me fais aimer les oignons. Merci Charlotte, t'es géniale !

Elea, merci de m'avoir appris à t'apprendre et merci pour tes idées foisonnantes, t'es mon étudiante préférée tu sais !

Mathilde, chère (ex)colloque, chère amie, t'es ma plus belle rencontre dans cet institut. On est ensemble jusqu'au bout dans ce bail.

Docteur Audrey, ne soit pas jalouse, t'es aussi ma plus belle rencontre dans cet institut. Mais t'es la famille, c'est acté maintenant. Monsieur le mari du Docteur, merci également.

Claire et Alex vous avez également été une merveilleuse rencontre, mais si je dis que tout le monde est ma plus belle rencontre je perds en crédibilité. Merci pour les découvertes œnologiques et spiritueuses (c'est beau dit comme ça).

Pierre et Martine, merci pour votre accueil et votre bonne humeur ! Merci aussi pour les aubergines, mais ce fut un échec agricole de mon côté, désolé…

Je re-remercie la plate-forme MRI et les services communs de l'IGH d'avoir rendu ma thèse bien plus simple, on ne le dit pas assez je trouve. Merci pour les litres de TBS, l'aide administrative et merci Marie-thé pour ta gentillesse.

Merci à toutes les personnes que j'ai rencontrées à l'IGH et qui ont rendu cette aventure plus merveilleuse et humaine chaque jour. Marion, Céline, Quentin, Gael, Eliot, Samira, Antoine, Victor, toute l'équipe Benkirane (merci pour les anticorps) toute l'équipe Pasero (merci pour les anticorps), MT-ACT. Et plus encore merci à vous tous pour les échanges scientifiques ou non, les bières, les blagues, les bars, les photos de chat, merci à la direction d'avoir accepté que j'envoie des mails outrageusement non professionnels à l'ensemble de l'institut pour faire des TGF.

Mes chers parents, merci pour ma curiosité et ce goût de la science, trainer sur des sites pleins de trilobites avant de savoir marcher a eu un léger impact sur moi je crois. Merci de m'avoir fait grandir dans un environnement sain, plein d'amour et riche en découvertes. Merci de m'avoir encouragé et soutenu dans toute mes décisions. Léa, merci pour tous les fringues que je te t'ai taxée, merci d'être là quoi qu'il arrive et de me maintenir dans le monde réel. Remy, reste tranquille, je te remercie mais prends pas la grosse tête. Lyam, petit être de lumière, tu m'as donné envie de créer une famille, merci pour tes sourires.

Papou Pierre, je sais que t'es fier, même si c'est dans le service public. Helena, merci pour tes lettres et tes appels, ta voix me manque. Ghislaine, Stavros, vous quatre, merci pour la bienveillance et l'équilibre que vous m'avez apporté tant que vous le pouviez.

Aux potes d'Epinay, Griveau, Desnos, Rea et tous les membres de la conversation où tout le monde parle de caca, merci pour les soirées onlines, avec et sans jeux, les vacances et le reste des souvenirs qu'on continue à produire.

Coraline, t'es là depuis le début et tu seras là jusqu'à la fin je le sais, merci plus que tout d'être présente.

Mr Prayssac, pareil, ça fait si longtemps et tu es toujours là, c'est plus que des remerciements que je te dois.

Alex & Marion, on a fait ce Master ensemble et clairement sans vous je n'y serais pas arrivée.

Emeline merci beaucoup pour ta présence et tes rires. Chris et Ioana aussi merci d'avoir été là pour le dernier rush, vous m'avez donné l'énergie de continuer.

Par extension les membres d'FDV de la Science Ac' et du CRI, ces environnements peuplés de gens de curieux m'ont forgé humainement, chaque moment a été précieux.

Sithis, tu ne sais pas lire mais t'es dans mon cœur. Polka, pareil, mais si tu arrivais à arrêter de pisser sur mes chaussures j'arriverais à t'aimer encore plus.

Guillaume, t'es rentré dans ma vie et on s'est mis à partager plein de choses, mais ce n'est que le début. On construira encore beaucoup ensemble, c'est une promesse. Je suis impatiente de voir la suite avec toi.

C- TABLE DES ABREVIATIONS

Table des abréviations

7T-GPCR	Récepteurs couplés au protéines G à 7 domaines transmembranaires
ACE	Enzyme de conversion de l'angiotensine
ACE2	Enzyme de conversion n°2 de l'angiotensine
APC	Cellule présentatrice d'antigène
ARDS	Syndrome de détresse respiratoire aigüe
AT_1R	Récepteur pour l'angiotensine II de type 1
AT_2R	Récepteur pour l'angiotensine II de type 2
cART	Multithérapie antirétrovirale
CCL	Ligand à motif CC de chimiokine
COVID-19	Maladie à coronavirus 2019
CoVs	Coronavirinae
CRP	Protéine C-réactive
CTL	Cathepsine L
E	Protéine d'enveloppe
EPCR	Récepteur de la protéine C endothéliale
ER	Réticulum endoplasmique
ERGIC	Compartiment intermédiaire entre le réticulum endoplasmique et l'appareil de Golgi
GM-CSF	Facteur de stimulation des colonies de granulocytes et de macrophages
HOMA	Modèle d'évaluation de l'homéostasie
ICU	Intensive care unit
I-FABP	Protéine intestinale de liaison aux acides gras
IFN	Interféron
Ig	Immunoglobuline
IL	Interleukine
LB	Lymphocytes B

LBP	Protéine de liaison au lipopolysaccharide
HLH	Lymphohistiocytose hémophagocytaire
LPS	Lipopolysaccharide
LT	Lymphocytes T
M	Protéine de la membrane
MCP1	Protéine chimio-attractive des monocytes de type 1
M-CSF	Facteur de stimulation des colonies de macrophages
MERS-COV	Coronavirus du Syndrome Respiratoire du Moyen-Orient
MHC	Complexe majeur d'histocompatibilité
N	Nucléoprotéines
NAC	N-Acétylcystéine
NSP	Protéine non structurale
ORF	Cadres de lecture ouvert
PBMCs	Cellules mononucléées du sang périphérique
PP	Polypeptides
PRR	Récepteurs de reconnaissance de motifs moléculaires
PVVIH	Personnes vivant avec le VIH
RBD	Domaine d'attachement au récepteur
RNS	Dérivés réactifs de l'azote
RONS	Dérivés réactifs de l'oxygène et de l'azote
ROS	Dérivés réactifs de l'oxygène
S	Protéine de surface
SARS-COV-1	Coronavirus de type 1 du Syndrome Respiratoire Aigüe Sévère
SARS-CoV-2	Coronavirus de type 2 du Syndrome Respiratoire Aigüe Sévère
SIDA	Syndrome d'Immunodéficience Acquise
SRAA	Système rénine-angiotensine-aldostérone

TCP2	Two-pore channel 2
TCR	Récepteur des cellules T
TGF-β	Facteur de croissance transformant beta
T_H	Lymphocyte T Helper
TLR	Récepteurs Toll-like
TMPRSS2	Sérine-protéase transmembranaire de type II
TNF-α	Facteur de nécrose tumoral de type alpha
tPA	Activateur tissulaire du plasminogène
Treg	Lymphocyte T régulateur
TRS-s	Séquence régulatrice de transcrit
VIH	Virus de l'immunodéficience Humaine

D- INTRODUCTION

I. LA REPONSE IMMUNITAIRE

En réponse à un pathogène le système immunitaire s'active afin de contrôler l'infection. Idéalement cette activation aigüe est temporaire, avec un bénéfice, l'élimination du pathogène, prévalant sur les effets secondaires. Cependant les effets secondaires peuvent parfois être excessifs et entrainer une pathologie aigüe (exemple de la maladie à coronavirus 2019 (COVID-19)) ou chronique (exemple de l'infection par le virus de l'immunodéficience humaine (VIH) qui, même traitée, peut favoriser des comorbidités liées à l'activation immunitaire chronique).

Dans les cas du COVID-19, le patient peut développer des symptômes graves, le taux de mortalité étant estimé à 0.5% dans la population générale mais variant énormément en fonction de l'âge et des comorbidités de la personne infectée puisque par exemple les sujets de plus de 80 ans ont un taux de mortalité estimé à 8,3%. (O'driscoll et al. 2021)

Dans le cas des personnes vivant avec le VIH-1 (PVVIH), celles-ci présentent une activation immunitaire chronique et développent des comorbidités plus fréquemment et plus précocement que la population générale à âge équivalent. (Maciel et al. 2018; Guaraldi et al. 2011)

Les conséquences potentielles de cette activation immunitaire aigüe ou chronique sont multiples et impliquent de nombreuses cellules et facteurs de l'immunité. Le travail de ma thèse a consisté à contribuer à l'amélioration des connaissances dans ce domaine. Les deux modèles d'infection que j'ai étudiés sont l'infection aigue au Coronavirus de type 2 du Syndrome Respiratoire Aigüe Sévère (SARS-COV-2) chez des patients ayant développé des formes graves de COVID-19 nécessitant une hospitalisation et l'infection chronique par VIH-1 chez des personnes sous traitement antirétroviral efficace.

A- LES MONOCYTES

Les Monocytes sont un des types cellulaires mononucléés du sang périphérique circulant (PBMCs). 7 à 10% des leucocytes sont des monocytes. Dans la moelle osseuse, par un processus impliquant différentes cytokines, les cellules souches hématopoïétiques vont se différencier en cellules précurseurs myéloïdes puis en monoblastes qui vont se développer et se différencier en monocytes.

Les monocytes sont caractérisés par la présence du récepteur CD14 à leur surface. Leur taille et leur structure diffèrent des autres types de cellules du sang : ce sont les plus grandes cellules parmi des PBMCs, faisant 15-18µm de diamètre. Leur noyau est relativement gros et a une forme caractéristique de fer à cheval. Le cytoplasme comprend de plusieurs granules. Il existe trois sous-populations de monocytes chez l'Homme, caractérisées selon leurs récepteurs de surface : les monocytes dit « classiques » représentant 90% des monocytes circulants, sont $CD14^{high}CD16^{-}$, ensuite les « intermédiaires » $CD14^{high}CD16^{+}$ et enfin les « non classiques » $CD14^{low}$ $CD16^{+}$. Les monocytes, particulièrement mobiles, circulent dans le sang. Ils sont très flexibles au niveau de leur différenciation puisqu'ils peuvent également être des précurseurs de cellules dendritiques et de macrophages. Ils ont une durée de vie en circulation dans le sang assez courte, allant jusqu'à 72 heures. (Parham 2005)

Ils jouent un rôle majeur dans l'inflammation et dans la réponse immunitaire innée : leur fonction principale est une réponse directe après rencontre d'un pathogène pour recruter d'autres cellules et l'éliminer, mais cette réponse est polyvalente. Les monocytes sont capables de reconnaitre différents pathogènes et cellules endommagées grâce aux récepteurs de reconnaissance des motifs moléculaire (PRR) présents à leur surface, comme les récepteurs Toll-like (TLR-1 à TLR-10) (Dolganiuc et al. 2006). Lorsqu'ils sont en circulation dans le sang, les monocytes ont des capacités de présentation d'antigènes (APC) aux autres cellules de l'immunité (Jakubzick, Randolph, et Henson 2017), mais ont surtout une capacité de phagocytose. Les cellules monocytaires absorbent et enferment le pathogène dans un phagosome. Dans ce phagosome seront déchargées des molécules chimiques dont des dérivés réactifs de l'oxygène et de l'azote dans le but de déstructurer et de dissoudre l'agent infectieux (Dale, Boxer, et Liles 2008).

Les monocytes sont recrutés dans les tissus endommagés par chimio-attraction via des chimiokines comme la protéine chimio-attractive des monocytes de type 1 (MCP1). Les monocytes, qui passent la barrière endothéliale pour arriver dans les tissus, sont alors différenciés en fonction des cytokines présentes dans la zone. Orekhol et ses collègues ont résumé l'impact des différentes cytokines sur la différenciation des monocytes en macrophage dans la figure 1 suivante (Greter et al. 2012; Orekhov et al. 2019).

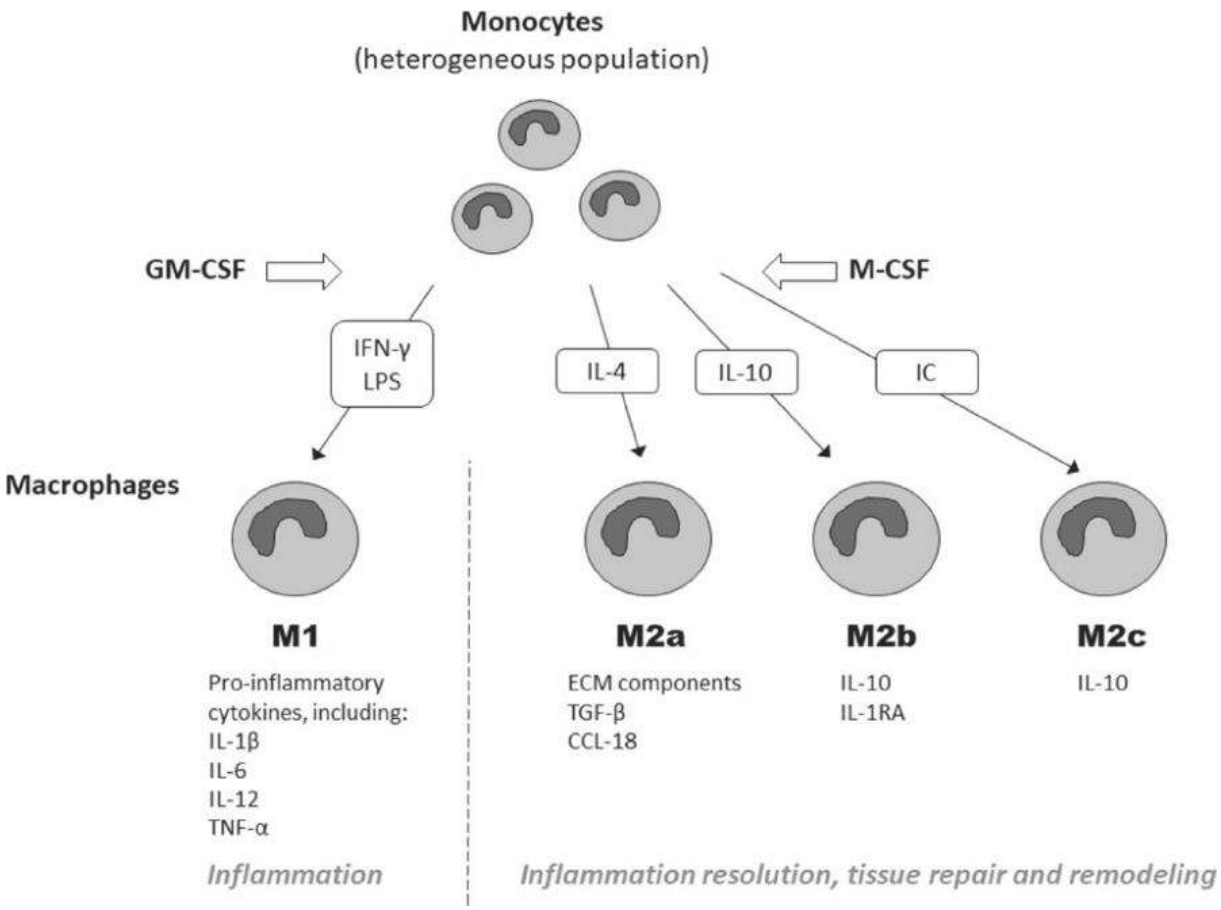

Figure 1 : Principaux régulateurs transcriptionnels de l'activation des macrophages et mécanismes de leur stimulation/inhibition (Orekhov et al. 2019).

B- LES LYMPHOCYTES

Les lymphocytes sont un des types cellulaires des PBMCs. Ils représentent la majorité de ce type cellulaire (70%). Les lymphocytes peuvent être divisés en deux grandes sous-familles : les lymphocytes T (LT), caractérisés par la présence du récepteur CD3 à leur surface, qui ont pour origine la moelle osseuse mais vont se différencier dans le thymus d'où ils sortent à l'état dit « naïf » et les lymphocytes B (LB), avec les marqueurs de surface CD19 et CD20.

Les LB ont pour origine de différenciation la moelle osseuse. Les LB font partie de la réponse spécifique humorale : ils sont capables de reconnaitre spécifiquement un pathogène qu'il leur soit présenté ou non. Ils peuvent se différencier en plasmocytes pour produire des anticorps contre celui-ci ou peuvent conserver une mémoire de la rencontre avec ce pathogène en devenant des LB mémoires. Ils peuvent aussi avoir une action d'APC.

Les LT sont caractérisés par la présence à leur surface du récepteur des cellules T (TCR) qui leur permet de reconnaître un déterminant antigénique associé à un complexe majeur

d'histocompatibilité (MCH). Les LT peuvent être séparés en plusieurs sous-groupes différenciés selon leurs marqueurs de surface et ayant des fonctions distinctes. Pour les LT4 et les LT8 on peut distinguer des sous-populations naïves, mémoires centrales et mémoires effectrices. Les LT4 reconnaissent un déterminant antigénique associé à un MCH de classe II (MCH-II) à la surface des APC tandis que les LT8 reconnaissent un déterminant antigénique associé à un MCH de classe I (MCH-I) à la surface des APC. Les LT8 activés peuvent devenir cytotoxiques et éliminer les cellules infectées par induction d'apoptose. Les LT8 cytotoxiques sont chargés en perforine (qui déstabilise la membrane des cellules), granzyme (des sérine-protéases), granulysine et serglycine (des protéoglycanes). Elles sont aussi capables de produire de l'interféron-γ (IFN-γ) et de l'IL-2.

Parmi les LT4 effectrices on peut différencier plusieurs populations de cellules dites « helper » ou « auxiliaire » qui vont aider d'autres cellules du système immunitaire en les activant. Les LT Helper 1 (T_H1) sont capables de produire de l'IL-2, du TNF-α et de l'IFN-γ. Elles peuvent en particulier activer les macrophages, leur permettant de détruire le pathogène qu'ils ont internalisé. Les LT Helper 2 (T_H2) peuvent produire de l'IL-4, de l'IL-5, de l'IL-6, de l'IL-10 et de l'IL-13. Elles peuvent activer les basophiles, les mastocytes et les LB, par exemple en cas d'infection par des parasites multicellulaires. Les LT Helper 17 (T_H17) peuvent activer les neutrophiles en particulier lors de réponses à des pathogènes fongiques ou des bactéries a développement extra cellulaire. Les T_H17 peuvent produire de l'IL-22 et de l'IL-17. Enfin, les T régulateurs (Treg) peuvent produire du facteur de croissance transformant beta (TGF-B), de l'IL-10 et de l'IL-35 et réguler négativement les autres T helper. (Parham 2005)

C- LES GRANULOCYTES

Les granulocytes, caractérisés par la présence des granules dans leur cytoplasme, sont une famille des cellules de l'immunité innée issue des même cellules souches que les monocytes. Il existe plusieurs types de granulocytes : les neutrophiles, les éosinophiles et les basophiles. Les neutrophiles sont les cellules majoritaires circulante dans le sang (40% des globules blanc). Ils font partie des premières réponses immunitaires puisque ce sont généralement les premières cellules mobilisées sur un site d'infection. Les neutrophiles ont une demi-vie de 6h en circulation et de 48h après diapédèse.

L'activation du complément sur le site d'infection et en particulier le relargage de C5a permet le recrutement de neutrophiles. Les neutrophiles ont une capacité de phagocytose non

spécifique de tout pathogène ou cellule infectée : l'agent est alors détruit dans des phagosomes par l'action de dérivés oxygénés, de protéases à sérine, de défensines et d'autre peptides antimicrobiens (Reusch et al. 2021). Ils relarguent également des cytokines. En présence d'une cellule infectée les neutrophiles sont activés par des cytokines pro-inflammatoires, des protéines dénaturées issues des pathogènes et des dérivés des lipides membranaires présents dans l'environnement. Un des marqueurs de sévérité du COVID-19 est un changement de ratio entre le nombre lymphocytes qui décroît et le nombre de neutrophiles qui augmente (Vitte et al. 2020).

II. LES DERIVES REACTIFS DE L'OXYGENE

« Dérivés réactifs de l'oxygène » (ROS) est le nom général donné aux différentes molécules hautement réactives et radicaux libres dérivés de l'oxygène. Les ROS ont d'abord été étudiés dans des contextes pathologiques comme pro-mutagène, endommageant l'ADN, les tissus et accélérant le vieillissement biologique (Roy et al. 2017) . Aujourd'hui, on sait que les ROS régulent également l'homéostasie cellulaire et sont un élément clé dans la médiation des signaux de transduction. Ils peuvent donc avoir une action directe ou être à l'origine d'un signal d'activation d'autres voies dont celles de NFκB, MAPK, PI3K-AKT, Keap1-Nrf2-ARE mais aussi du système d'ubiquitination/protéasome. (Zhang et al. 2016 ; D'Autréaux et Toledano 2007).

Produits par toutes les cellules en quantité physiologique, ils sont les sous-produits de nombreuses réactions enzymatiques et peuvent donc provenir de nombreux compartiments de la cellule comme le réticulum endoplasmique, les péroxysomes, le cytoplasme et les mitochondries. Dans des conditions physiologiques, les ROS sont bien tolérés dans les cellules humaines. C'est un excès de ROS qui peut poser des problèmes et aboutir à un stress oxydatif. Le stress oxydatif est défini comme la disproportion entre les quantités de dérivés oxygénés et d'antioxydants présents dans un élément biologique donné, une cellule ou un environnement biologique. (Ray, Huang, et Tsuji 2012).

Il existe plusieurs types de ROS tout comme il existe également des dérivés réactifs de l'azote (RNS), le tout formant la famille des RONS.

Les cellules phagocytaires comprennent les neutrophiles, les monocytes et les macrophages. Tous les phagocytes sont capables de produire des RONS dans leurs phagolysosomes par quatre complexes différents mais interdépendants. Le complexe NADPH-

oxydase produit des superoxyde $O_2^{\bullet -}$. Les superoxydes réagissent avec eux-mêmes et produisent du peroxyde d'hydrogène H_2O_2, on parle de dismutation. Le complexe oxyde nitrique synthase produit du monocyte d'azote NO et enfin le complexe myélopéroxydase produit des anions hypochlorites l'OCl^- (Babior, 2000.). Tous les produits de ces réactions ont des temps de demi-vie cellulaire de l'ordre de quelques secondes (Rubio et Cerón 2021).

Le complexe NADPH-oxydase est un mécanisme d'oxydoréduction via l'oxydation de NADPH. La formule de la réaction est la suivante : $NADPH + 2O_2 \rightarrow NADP^+ + H^+ + 2O_2^{\bullet -}$. Ce mécanisme d'oxydoréduction ne s'enclenche que lorsque le phagocyte est activé. (Babior, 2000.)

Il a été montré que les ROS pouvaient induire des dommages à l'ADN. Cela va entrainer de multiples réponses aux dommages à l'ADN, allant de la réparation à l'apoptose cellulaire en passant par l'activation immunitaire et la production de plus de ROS. (Kang et al. 2012; Srinivas et al. 2019). Ils sont aussi impliqués dans des mécanismes pro-cancéreux : les ROS activent les voies des MAPK, PI3K-AKT et NFκB, toutes trois pouvant être dérégulées dans différent cancers. En plus, H_2O_2 à faible dose stimule la prolifération cellulaire dans de nombreux types de cellules cancéreuses.(Liou et Storz 2010). Les ROS peuvent également induire des dommages aux tissus, cela a encore été récemment démontré dans le COVID-19 par des ROS provenant des neutrophiles.(Laforge et al. 2020) Enfin, les ROS induisent l'activation de l'inflammasome, entrainant la production de cytokines pro-inflammatoires. (Harijith, Ebenezer, et Natarajan 2014). Ce mécanisme est donc évoqué parmi les raisons de l'activation de l'inflammasome dans l'infection au SARS-COV-2 (Vora, Lieberman, et Wu 2021)

III. LA PANDEMIE DE COVID-19

Le COVID-19 est due à une infection au SARS-COV-2, un coronavirus humain. C'est un virus à ARN positif, enveloppé. Le SARS-COV-2 est plus contagieux chez l'Homme que le SARS-COV-1 de 2003, ce qui explique en partie sa rapide dispersion dans le monde (Nguyen et al. 2020). Je développerai le cycle de réplication du virus et ses conséquences dans l'organisme hôte plus loin et vais commencer par décrire la pathologie liée au COVID-19.

Les premiers cas confirmés de patients infectés par le SARS-COV-2 datent du 12/12/2019 à Wuhan, en Chine. (P. Zhou et al. 2020) Le virus a officiellement été découvert et nommé le 9 janvier 2020 lorsque la chine a communiqué publiquement la séquence du virus. Celui-ci était initialement appelé « 2019-nCoV » Wuhan Coronavirus Novel Coronavirus avant d'être renommé SARS-COV-2. Le 11 mars 2020 l'Organisation Mondiale de la Santé a déclaré que le COVID-19 peut être qualifiée de pandémie. Les origines du virus ne sont pas complètement élucidées et les discussions autour sont riches (Casadevall, Weiss, et Imperiale 2021) mais la transmission depuis une espèce sauvage, impliquant les chauves-souris, est ce qui semble le plus logique à privilégier. (H. Zhou et al. 2021)

Le COVID-19 ne se développe pas systématiquement lors d'une infection à SARS-COV-2. Les premiers chiffres issus des données épidémiologiques en Chine donnent ceci : 80% des personnes positives au SARS-COV-2 n'auront soit pas de symptômes soit des symptômes modérés, 20% nécessiteront des soins hospitaliers allant jusqu'à l'assistance respiratoire et un quart d'entre eux développeront les formes les plus graves de COVID-19 (Wu et McGoogan 2020). Ces chiffres varient beaucoup en fonction des pays et de leur capacité hospitalière. (Carbone et al. 2021; Batah et Fabro 2021; Polak et al. 2020; dos Santos 2020).

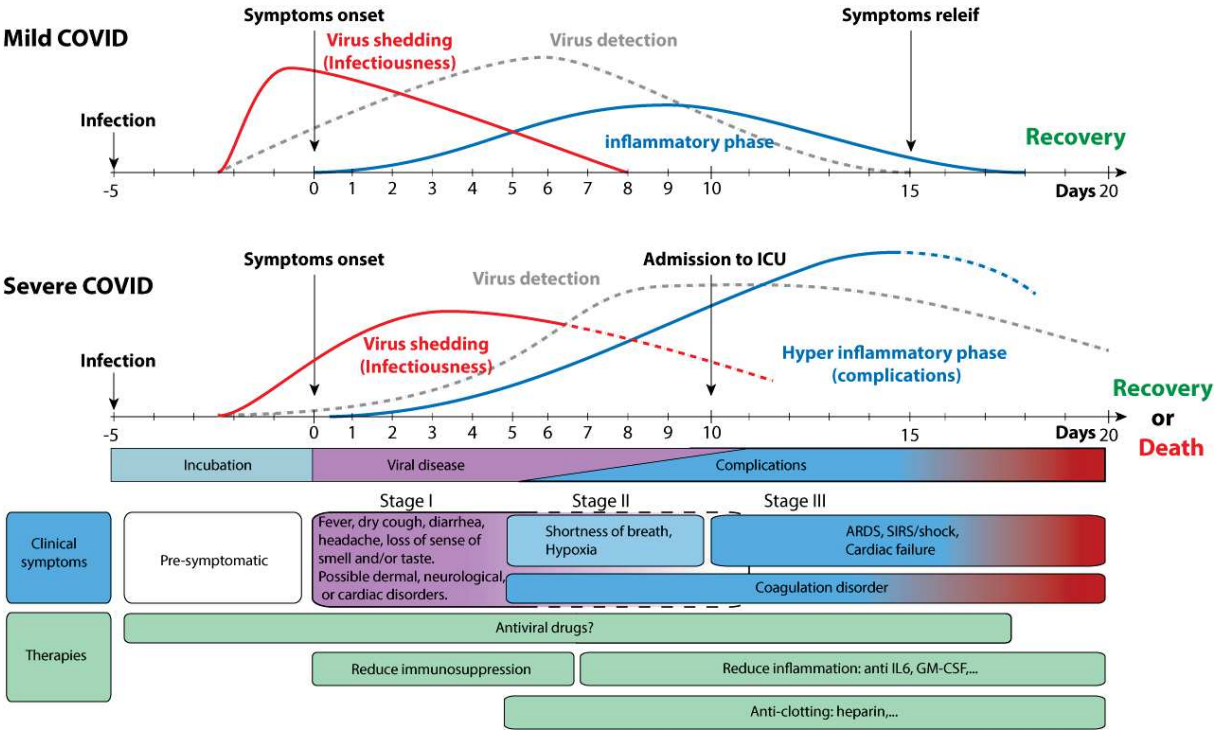

Figure 2: Evolution de la pathologie COVID-19 selon le niveau de gravité et traitements – ViralZone ; https://viralzone.expasy.org/9116

Tous les patients infectés sont totalement asymptomatiques durant toute la période d'incubation virale, période pendant laquelle le virus commence à se répliquer mais ne semble pas ou peu détecté par l'organisme. 40% des personnes infectées ne présenteront aucun symptôme même après cette période d'incubation, pourtant même ces personnes peuvent avoir des lésions au niveau des poumons détectables par tomodensitométrie (Chen et al. 2021) . Les premiers symptômes clinques du COVID-19 apparaissent jusqu'à 11 à 12 jours post-infection (Figure 2). Le nombre de symptômes et leur sévérité dépendent de plusieurs facteurs, dont les caractéristiques du patient : son âge, son sexe et également d'éventuelles comorbidités associées à la gravité de la maladie.

Les premiers symptômes et les plus fréquents de COVID-19 sont une fièvre modérée à sévère (plus de 38°c) une toux, une dyspnée, parfois une respiration accélérée et superficielle et surtout une perte de l'odorat (anosmie). L'anosmie est un symptôme fréquent chez les patients développant un COVID-19 (46% en France) (Ferdenzi et al. 2021). Le mécanisme a été décrit par de Melo et coll. chez le hamster : le SARS-COV-2 est capable d'infecter les cellules de l'épithélium olfactif, formant une inflammation locale et entrainant une perte temporaire des

ciliations de l'épithélium olfactif chez les Hamster. De plus, ils ont observé que de l'ARN viral était détectable dans les muqueuses de l'épithélium olfactif de patients anosmique plus de 100 jours après leurs premiers symptômes de COVID-19 ainsi que des marqueurs d'inflammation locale (de Melo et al. 2021). Chez l'homme, le SARS-COV-2 est également capable d'infecter les cellules olfactives et d'entrer dans le système nerveux central (Meinhardt 2021; Keyhanian et al. 2021).

L'âge, l'obésité, le diabète de type II, les maladies cardiovasculaires et l'hypertension, l'insuffisance rénale ou respiratoire, la cirrhose à un stade B ou C, le cancer, un antécédent de transplantation d'organes sont des comorbidités qui sont associées aux cas les plus graves de COVID-19 (Ejaz et al. 2020). Dans ces cas, le patient déclenche un orage cytokinique, c'est à dire un état d'activation aigüe incontrôlée du système immunitaire caractérisé par une surproduction brutale de cytokines inflammatoires, pouvant impliquer des dommages multiples dans divers organes du patient, entrainant leur dysfonction, en particulier des poumons, des reins et du cœur. (Tay et al. 2020) 70% des décès de patients ayant développé un COVID-19 sont dus à une détresse respiratoire. Le syndrome de détresse respiratoire aigüe (ARDS) est secondaire à des lésions des cellules pulmonaires avec accumulation de liquide dans les alvéoles, une réduction de l'oxygènémie. Jusqu'à 28% des cas de décès présentent une septicémie. 40% des patients décédés ont également une thrombose des veines profonde. (Tay et al. 2020; Edler et al. 2020; Bösmüller et al. 2020)

Même après résolution de l'infection, des cas de « COVID long » ont été constatés. Il s'agit de personnes ayant encore des symptômes de fatigue, de douleurs et des troubles respiratoires plusieurs semaines voire plusieurs mois après le diagnostic de COVID-19. (Domingo et al. 2021)

IV. LE SARS-COV-2

A- LES CORONAVIRUS

Un virus est un parasite intracellulaire obligatoire. Le SARS-COV-2 respecte cette règle.

Parmi les coronavirinae (CoVs) il y a quatre genres connus aujourd'hui : alpha, beta, gamma et delta. (ViralZone (Hulo et al. 2011)) Les genres alpha et beta semblent avoir émergé de virus de chauve-souris tandis que les gamma et delta de virus aviaires (Totura et Bavari 2019). Concernant les CoVs humains connus, ils ne proviennent que du genre alpha ou beta coronavirus. Plus de 500 CoVs ont été identifiés chez les chauves-souris à ce jour en Chine uniquement, la diversité des CoVs étant estimée à plus de 5000 CoVs différents chez cette même espèce (Lin et al. 2017 ; Latinne, 2020. ; H. Zhou et al. 2021).

Sept coronavirus humains ont été dénombrés à ce jour, tous de l'ordre des nidoviridae, famille des coronaviridae et de la sous-famille des coronavirinae. Quatre impliquent des rhumes et des syndromes grippaux hivernaux sans gravité : HKU1, NL63, OC43 et 299E, le virus restant généralement dans les parties supérieures des voies respiratoires, soit la bouche, le nez, le larynx et le pharynx. Les trois autres virus impliquent des syndromes respiratoires sévères : Le Coronavirus de type 1 du Syndrome Respiratoire Aigüe Sévère (SARS-COV-1), le SARS-COV-2 et le Coronavirus du Syndrome Respiratoire du Moyen-Orient (MERS-COV). Ces virus sont capables de se répliquer dans les voies respiratoires inférieures, de la trachée aux poumons. Ces virus se transmettent par des gouttelettes de salive suspendue dans l'air ainsi que par contact avec des surfaces contaminées (V'kovski et al. 2021)

Le SARS-COV-1 est apparu en 2003 en Chine, dans la province de Wuhan. L'épidémie a duré un an et a été complètement contrôlée, dans le sens où plus aucun cas issu du milieu naturel n'a été détecté depuis. 8096 personnes ont été contaminées dans 29 pays et 774 personnes en sont mortes, le taux de mortalité étant estimé à 3%. Le réservoir intermédiaire du virus entre la chauve-souris et l'homme est connu, c'est la civette. (*https://www.who.int/health-topics/severe-acute-respiratory-syndrome#tab=tab_1*)

Le MERS-COV est apparu en 2012 au Moyen-Orient, en Arabie Saoudite et il y a encore des cas sporadiques de personnes contaminées de nos jours. En 2021, 2574 cas ont été

recensés dont 886 morts. Le taux de mortalité du virus est estimé à 34.4%. Le réservoir intermédiaire du MERS-COV est le dromadaire (*https://www.who.int/health-topics/middle-east-respiratory-syndrome-coronavirus-mers#tab=tab_1 ; http://www.emro.who.int/health-topics/mers-cov/mers-outbreaks.html*).

Le SARS-COV-2 fait partie de la famille des Coronaviridae, sous famille des orthocoronavirinae, du genre betacoronaviridae et sous genre sarbecoronavirus (https://talk.ictvonline.org/taxonomy/). C'est un virus enveloppé. La structure du SARS-COV-2 est sphérique. Le virion fait entre 60 et 120 nm de diamètre et est recouvert de protéines de surface (S) : des « spikes », soit des épines de 9 à 12nm directement impliquées dans la capacité du virus à entrer dans la cellule (Ke, 2020).

Le virion est également structuré par un complexe de protéines ribonucléiques composé de glycoprotéines virales membranaires (M), de petites protéines d'enveloppe (E), supportées par la membrane du réticulum endoplasmique capturé lors du cycle viral précédent dans la cellule hôte. Attachée à l'intérieur de cette enveloppe il y a la nucléocapside composée de Nucléoprotéines (N) entourant l'ARN (+) viral et le protégeant (Klein et al. 2020).

Son cycle cellulaire est, jusqu'à preuve du contraire, considéré comme équivalent à celui du SARS-COV-1 et des autres coronavirus qui ont été largement étudiés et les articles publiés jusqu'alors le confirment. Je soulignerai les différences. Le cycle viral du SARS-COV-2 passe par plusieurs phases (Figure 3).

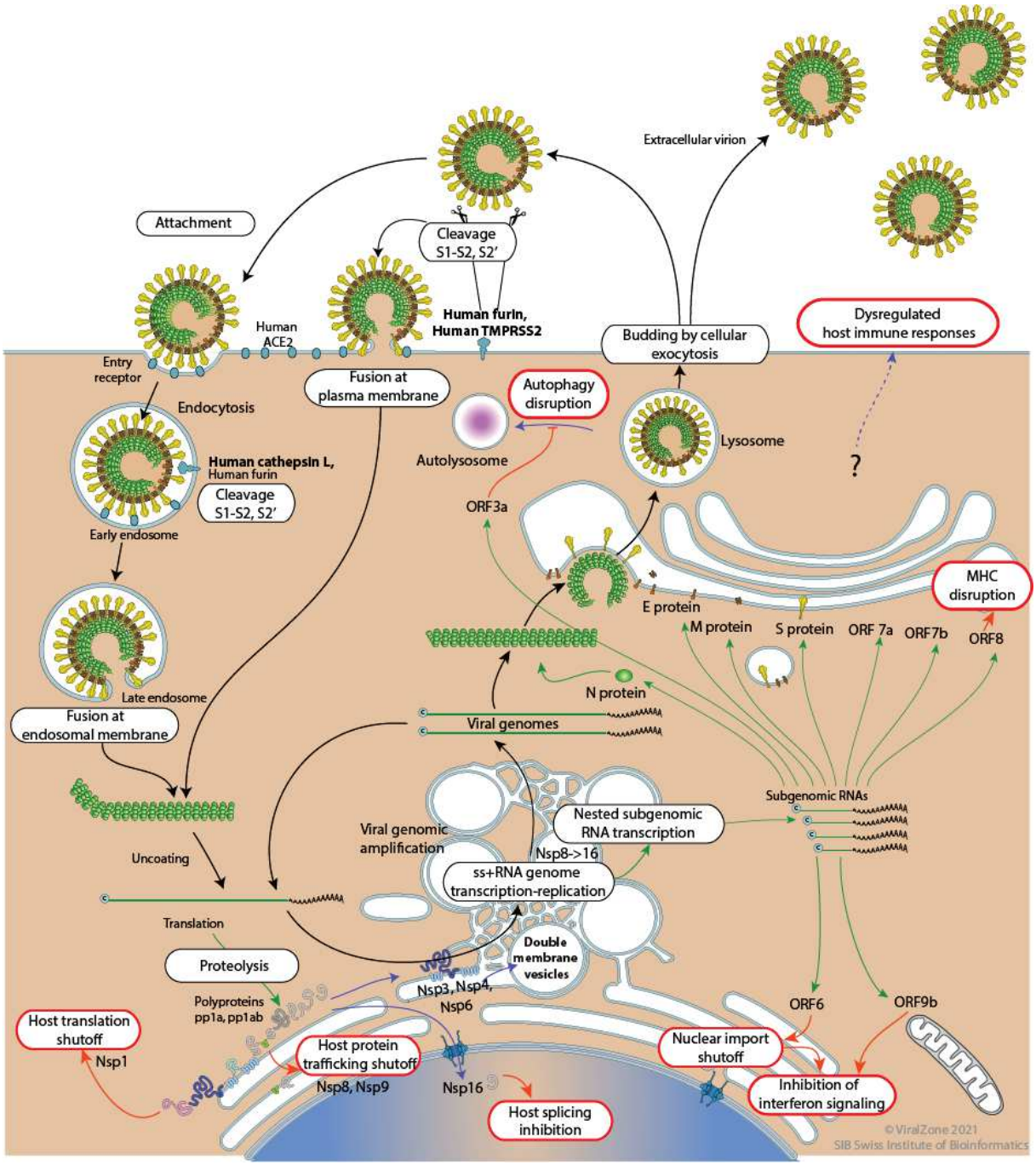

Figure 3 : Cycle viral des coronavirus – ViralZone ; https://viralzone.expasy.org/9096. L'entrée du virus peut se faire par endocytose ou par fusion des membranes. La réplication du génome se produit dans des vésicules à double membrane et l'assemblage des nouveaux virions au niveau du compartiment intermédiaire entre le réticulum endoplasmique et l'appareil de Golgi. L'export des nouveaux virions se fait via des lysosomes par exocytose.

B- L'ENTREE DU VIRUS DANS LA CELLULE

La protéine spike est directement impliquée dans ce processus, elle interagit avec le récepteur ACE2 présent à la surface de la cellule pour y entrer, ce qui induit l'internalisation d'ACE2. Un corécepteur est nécessaire : on connait la sérine-protéase transmembranaire de type II (TMPRSS2) et la cathepsine L (CTL, une cystéine protéase), chez les coronavirus. TMPRSS2 ET CTL ont une action de clivage de la protéine S entre les domaines S1 et S2 enclenchant la fusion de celle-ci avec la membrane cellulaire et donc l'entrée du virus mais c'est vraiment TMPRSS2 qui a été démontré pour le SARS-COV-2 actuellement (Hoffmann et al. 2020 ; Hoffmann, Kleine-Weber, et Pöhlmann 2020 ; Bayati, 2020. ; Shang et al. 2020).

Les deux SARS-COVs partagent 85% de séquence en moyenne et 75% d'acides aminées en commun au niveau du domaine S^B. Ce domaine joue un rôle important dans le mécanisme d'entrée et la particulièrement haute virulence du SARS-COV-2. Le site de clivage pour former S1 et S2 est un des points qui distingue SARS-COV-1, SARS-CoV-2 et MERS des autres coronavirus humain. Le SARS-COV-2 et le MERS ont un site de clivage par la furine, (Peacock, Goldhill, et AL. 2021) ce site n'étant pas nécessaire pour l'entrée du SARS-COV-1 dont le clivage est dépendant de la CTL (Follis, York, et Nunberg 2006). Cependant il a été montré que le niveau de CTL était élevé après une infection par SARS-COV-2 et qu'une inhibition de celle-ci réduisait fortement l'infection du SARS-COV-2 dans des souris humanisées (Zhao 2021).

La protéine S s'attache dans un premier temps au corécepteur. S est trimérique et a un site de clivage la séparant en deux segments : S1-Cter et S2-Nter. C'est le segment S1 qui contient un domaine d'attachement au récepteur (RBD) ACE2. Ce domaine est muté chez beaucoup des variant apparus jusqu'alors, ce qui pourrait expliquer les différences de virulence selon le variant. (Peacock, Sheppard, et al. 2021 ; Escalera et al. 2021 ; Scudalleri et al. 2021)

Le segment S1 va s'accrocher à la partie extracellulaire du récepteur ACE2 en N-terminal. Le changement conformationnel du segment S2 va faciliter la fusion entre l'enveloppe virale et la membrane cellulaire. Ce complexe sera alors intégré à l'intérieur de la cellule par deux voies possibles. Elle peut se faire par endocytose, le virus étant englobé par un endosome qui lui permet d'entrer. L'autre chemin, utilisé principalement par le SARS-COV-2, consiste en une fusion entre l'enveloppe virale et la membrane plasmique après le clivage par TMPRSS2.

(Peacock, Goldhill, et al. 2021). Dans les deux cas, ACE2 est internalisé et n'est donc plus disponible à la surface cellulaire.

La fusion entre l'enveloppe virale et la membrane plasmique entraine une décapsidation directe du virus et un relargage du génome viral dans le cytoplasme. La voie endosomale nécessite une étape intermédiaire. L'endocytose est un mécanisme dépendant du pH : une fois le virus englobé dans l'endosome précoce, c'est essentiellement l'action de la pompe H+-ATPase de type V qui entraine une réduction progressive du pH dans l'endosome passant de 6 à 5 puis à 4.6 pour l'endosome tardif, qui se transforme alors en lysosome.

Dans le lysosome se produit la fusion des membranes et ce mécanisme implique plusieurs protéases. La CTL est présente dans les lysosomes cellulaires. Elle permet de dégrader la matrice cellulaire, ce qui participerait également à la décapsidation du SARS-COV-2. (Gomes et al. 2020). La fusion des membranes peut aussi être induite via « two-pore channel 2 » (TCP2), un canal ionique transmembranaire présent sur le lysosome et qui permet de fusionner le lysosome avec l'enveloppe du virus (Peacock, Goldhill, et al. 2021). Par des échanges ioniques Na+/Ca+, TCP2 va entrainer l'ouverture du lysosome, libérant la nucléocapside dans le cytoplasme. Reste la décapsidation : c'est également TCP2 qui semble être impliqué dans la décapsidation, soit la disparition de la nucléocapside (N) libérant l'ARN viral, sans que le détail des probables phosphorylations impliquées dans ce mécanisme ne soit connu (Z. Zhao, Qin, et Huang 2021).

C- LA REPLICATION DU VIRUS

Une fois la décapsidation effectuée, il ne reste que l'ARN génomique du virus. Le piratage de la machinerie cellulaire permet au virus de produire ses propres protéines, son génome, et de reproduire de nouveaux virions. Le génome du virus est un ARN simple brin positif. Il est particulièrement long pour un virus à ARN : il fait entre 26 000 et 32000 paires de bases. Il est coiffé en 5′ et polyadénylé en 3'. L'ARN génomique viral servira pour plusieurs choses : d'ARN messager pour la production des protéines virales et de modèle pour les étapes de transcription et de réplication. Ce seul ARN génomique va permettre la production de 27 protéines différentes. Pour ce faire, deux stratégies sont utilisées.

Dans un premier temps, l'ARN génomique comme ARN messager va être lu directement par des ribosomes cellulaires qui le traduiront en de grandes polypeptides (PP). Ces polypeptides seront par la suite découpées en plusieurs protéines dites non structurales (NSP) c'est-à-dire qu'elles serviront au bon déroulement du cycle du virus mais ne feront pas partie des virions (Kim et al. 2020).

La traduction des NSP se fait via 2 cadres de lecture ouvert (ORF) : ORF1a et ORF1b. L'ORF1a en lecture directe permet la production du polypeptide 1a (pp1a) qui sera ensuite clivé en 11 NSP (NSP-1 à NSP-11). Très vite, NSP-1 permet l'arrêt des mécanismes de traduction des protéines de la cellule hôte en s'attachant à la sous-unité 40S du ribosome (Schubert et al. 2020). De plus NSP-1 entraine la dégradation des ARN messagers cellulaires, reconnaissant et détruisant leur partie 5'UTR non virale (Finkel, Gluck, et al. 2021). NSP-1 bouche également les canaux entre le noyau et le cytoplasme empêchant l'export des ARNm cellulaires (K. Zhang et al. 2021). Un décalage du cadre de lecture arrive régulièrement dans une séquence dite glissante de génome viral (UUUAAC) accélérant la vitesse de lecture et empêchant l'action du codon stop. Cela entraine la traduction de l'ORF1b en polypeptide 1ab qui sera ensuite clivé en 15 NSP (NSP-1 à NSP-15). Le clivage protéolytique, particulièrement de NSP-1 et NSP-2, est assuré par les protéases virales NSP-3 (ayant un domaine de protéase papaïne-like) et surtout NSP-5 (ayant un domaine de protéase 3C-like) capables de cliver sur 11 sites les pp1a et pp1ab (Haque et al. 2020; Kim et al. 2020).

Des ARN sous-génomiques négatifs sont copiés de manière discontinue avec un évènement de saut vers la partie 3'UTR leur donnant à tous également la même séquence « leader » en 5'. Cet évènement de saut est dû à une partie du génome viral appelé séquence régulatrice de transcrit (TRS-s) qui contient 6-7 nucléotides conservés et qui, par des interactions ARN-ARN peut sauter directement vers la partie équivalente TRS-l située en 5', continuant la transcription jusqu'au 5'UTR. Les ARN sous-génomiques négatifs produits sont copiés en ARN sous-génomiques positifs. Chacun des ARN sous-génomiques contient un ORF pour traduire les protéines de structure utilisées pour l'assemblage des nouveaux virions soit les protéines S (Spike, ORF3), E (enveloppe, ORF4), M (membrane, ORF5) et N (nucléocapside, ORF9). Sont aussi traduites les protéines accessoires 3a, 6, 7a, 7b, 8 et 10, (aux ORF du même nom) non nécessaires pour la réplication virale mais capitales dans la pathogénicité

virale. Enfin, pour la réplication, la NSP-12 a une activité polymérase dépendante de l'ARN (RdRP). Le complexe NSP-12-NSP-7-NSP-8 permet la copie du génome viral entier en ARN simple brin négatif, puis à nouveau en plusieurs ARN simple brin positif qui seront les ARN génomiques empaquetés dans les nouveaux virions. (Haque et al. 2020; Raj 2021; Finkel, Gluck, et al. 2021; Finkel, Mizrahi, et al. 2021)

D- L'ASSEMBLAGE DES NOUVEAUX VIRIONS ET LA SORTIE VERS LE MILIEU EXTRACELLULAIRE

L'assemblage de nouveaux virions se fait en plusieurs étapes, au niveau du compartiment intermédiaire entre le Réticulum Endoplasmique (ER) et l'appareil de golgi (ERGIC). La protéine N va permettre d'enrouler à nouveau le génome viral et de l'encapsider d'un côté tandis que les protéines S, M et E composant l'enveloppe virale s'organisent et s'attachent aux parois de l'ERGIC. La protéine M est la clé des interactions protéines permettant à toute la structure des nouveaux virions de tenir, mais ne suffit pas à elle seule à la formation des nouveaux virions, la protéine E étant nécessaire également. Le domaine C-terminal de la protéine M va s'attacher au domaine C-terminal de la protéine N. La membrane du ER composée des protéines virales S, M et E va entourer la nucléocapside jusqu'à construire entièrement les virions dans des lysosomes.

Les virions produits seront ensuite amenés vers la membrane cellulaire via ces lysosomes de transport où un événement de bourgeonnement par exocytose se fera pour chaque virion, leur permettant d'atteindre le milieu extracellulaire (Haque et al. 2020; Klein et al. 2020).

VII. LE LYMPHOHISTIOCYTOSE HEMOPHAGOCYTAIRE

La lymphohistiocytose hémophagocytaire (HLH) est un syndrome amenant à une réponse inflammatoire excessive. Elle se divise en deux formes, primaire et secondaire. L'origine de la forme primaire est génétique : 40% des personnes atteinte de ce syndrome ont une mutation soit sur le gène qui code pour la perforine, soit sur un gène impliqué dans la dégranulation des perforines. La forme secondaire peut être dû à certaines infections virales et amener à un orage cytokinique, soit une production excessive de cytokines pro-inflammatoires. (Eloseily et Cron 2018). La comparaison avec l'orage cytokinique visible dans les cas grave de

COVID-19 a été faite (Mehta et al. 2020). Bien qu'il présente de forts points communs, la HLH n'est pas toujours ce qui se produit lors des cas graves de COVID-19 : des marqueurs peuvent ne pas correspondre comme les taux de CRP et de ferritine présents dans les HLH. Les connaissances actuelles sur la HLH primaire et secondaire peuvent être utile pour comprendre le COVID-19 et la survenue de l'orage cytokinique, ne serait-ce que pour mieux les différencier. (Otsuka et Seino 2020)

VIII. L'ANGIOTENSINE II ET RECEPTEUR CELLULAIRE : ACE2

A- LE SYSTEME RENINE-ANGIOTENSINE-ALDOSTERONE

L'angiotensine II est un peptide dérivé de l'angiotensine. Le système rénine-angiotensine-aldostérone (SRAA) est une cascade d'événements physiologiques permettant entre autres la régulation du flux sanguin par constriction et dilatation des vaisseaux sanguins. Il implique plusieurs organes dont le foie, les reins et aussi le système cardiovasculaire.

L'angiotensinogène (DRVYIHPFHLVHN) est un glycopeptide synthétisé essentiellement par le foie. Il est libéré dans le plasma et circule alors jusqu'aux reins où la rénine, une enzyme produite par l'appareil juxtaglomérulaire, va partiellement le protéolyser entre la leucine et la valine pour obtenir l'angiotensine I, un décapeptide (DRVYIHPFHL) inactif.

L'angiotensine I sera transporté via l'endothélium et hydrolysé par l'enzyme de conversion de l'angiotensine (ACE), une carboxypeptidase membranaire présente à la surface de certains types cellulaires, dont les petites et les grandes cellules épithéliales alvéolaires (ou pneumocytes de type 1 et de type 2 respectivement) tapissant les poumons.

L'ACE va cliver les deux acides aminés en C-terminal de l'angiotensine I, pour obtenir cette fois l'angiotensine II (DRVYIHPF), octapeptide 1-8 qui lui est actif. Il se lie à deux récepteurs : le récepteur pour l'angiotensine II de type 1 (AT_1R) et le récepteur pour l'angiotensine II de type 2 (AT_2R). Les deux récepteurs font partie de la famille des récepteurs couplés au protéines G à 7 domaines transmembranaires (7T-GPCR). AT_1R enclenche un mécanisme de vasoconstriction tandis que AT_2R enclenche un mécanisme de vasodilatation, mais comme ce dernier est très peu exprimé dans le système vasculaire, l'angiotensine II a donc essentiellement un effet vasoconstricteur. (Forrester et al. 2018).

Il existe également une carboxypeptidase homologue à ACE, ACE2, mais qui ne va cliver qu'un seul acide aminé en C-terminal. L'ACE2 est également présent sur les pneumocytes de type 1 et surtout de type 2 (Ziegler et al. 2020). Son action principale consiste à réguler négativement le système rénine-angiotensine puisqu'il permet de convertir l'angiotensine II en angiotensine 1-7, un vasodilatateur puissant qui agit sur les récepteurs mitochondrial assembly 1 (MAS-1). Du fait de la pluralité de substrat et de l'action combinée d'ACE et ACE2 ainsi que d'autres exoprotéases du sang, il y aura formation d'une variété de peptides ayant des activités antagonistes selon le récepteur qu'ils vont activer : l'angiotensine III (RVYIHPF 2-8) qui agit sur les mêmes récepteurs que l'angiotensine II, l'angiotensine 1-9 (DRVYIHPFH) qui agit sur AT_2R ou peut être converti en 2-8 ou 1-7, l'angiotensine 1-7 qui peut être convertie en angiotensine 1-5 (Forrester et al. 2018).

B- IMPLICATION DANS L'INFECTIONS SARS-COV-2

L'angiotensine II est impliquée dans la signalisation de plusieurs cellules de l'immunité. La présence d'angiotensine I et II ainsi que d'AT_1R dans les monocytes a été démontrée (Hahn et al. 1994). La production de dérivés oxygénés via l'activation de NADH/NADPH oxydase induite par l'angiotensine II a été décrite avec le modèle de cellules musculaires lisses des vaisseaux (Griendling et al., 1994.) et de nombreux liens ont été faits entre la production de dérivés oxygénés médiée par l'angiotensine II et l'hypertension dans différent modèles dont des macrophages mais aussi beaucoup de modèles de rongeurs. (Rajagopalan et al. 1996; Wang et al. 2001 ; Justin Rucker et Crowley 2017) .

La revue très complète de Forrester et ses collègues de 2018 nous donne un tableau résumant ce qui a été démontré quant à l'action de l'angiotensine II sur les cellules immunitaires (Tableau 1).

Table 9. *Roles of immune cell subtypes in ANG II pathophysiology*

Cell Type	Pathophysiology	Model	Mediators	Reference Nos.
Macrophages	Hypertension ↓	IL-1R1−/−	Renal NKCC2	1249
	VSMC proliferation ↓	Clodronate	C1q/β-catenin	1010
	AAA ↓	apoE−/− Notch+/− BMT	Notch1	353
	AAA ↑	LDLr−/− Nox2−/− BMT	ROS/IL-1β	490
	Intracranial aneurysm ↓	Clodronate	MCP1	453
	Cardiac inflammation ↑	Atg5+/−	Autophagy/ROS	1265
	Renal fibrosis (UUO) ↑	AT_{1A}Rf/f RysM-Cre	M1 cytokines/IL-1R	1250
	Cognitive dysfunction ↓	Clodronate or AT_{1A}R−/− BMT	Nox2/ROS	271
T cells	Hypertension ↓	AT_{1A}R−/− T cell transfer	Nox/ROS/TNF-α	348
	Hypertension ↓	CTLA4-Ig, B7(CD80/86)−/−	Inflammation	1093
	Hypertension ↓	IL-17−/−	ROS/cytokines	630
	Hypertension ↓	$AT_{1A}R^{ff}$ CD4-Cre	Th1 cytokines	1251
	Vascular dysfunction ↓	Tbx21−/−	IFN-γ/ROS/NK cell	511
T cells ($CD8^+$)	Hypertension ↓	CD8−/−, $CD8^+$ T cell transfer	Kidney T cell R	1066
γδ T cells	Hypertension ↓	TCRδ−/−	EC dysfunction	109
Tregs	Hypertension ↓	Treg adoptive transfer	ROS/Inflammation	54
	Hypertension/fibrosis ↓	Treg adoptive transfer	CD39/neutrophils	263
B cells	Hypertension ↓	BAFF-R−/−	IgG/macrophage	134
	Atherosclerosis	apoE−/− BAFF-R−/−	IL-10 Bregs	830
NK cells	Vascular dysfunction ↓	NK1.1 depletion antibody	Inflammation	511
Neutrophils	Aortic dissection ↓	Anti-Gr-1 antibody	MMP9	525
MDSCs	Hypertension ↑	MDSC depletion	H_2O_2	940

Tableau 1 : Rôle des différentes sous-populations cellulaires dans la physiopathologie due à l'angiotensine II. (Forrester et al. 2018) page 1697.

Peu de choses sont connues sur l'action de l'angiotensine II dans les monocytes. L'angiotensine II induit une production d'IL-1β et de TNF-α significativement plus élevée dans les monocytes de donneurs ayant des problèmes d'hypertension par rapport aux monocytes de donneurs sains (Dörffel et al. 1999). Dans un contexte pathologique d'anévrisme de l'aorte abdominale chez la souris, une infusion d'angiotensine II induit une augmentation de TREM-1 (pour Triggering Receptor Expressed on Myeloid cells-1) dans les monocytes (Vandestienne et al. 2021). TREM-1 activé induit une production de cytokines pro-inflammatoires. (Varanat et al. 2017). L'angiotensine II induirait une production de ROS et de MC1-P dans les cellules mésangiales humaines (Chen et al. 2009). Enfin, bien que cela soit régulièrement évoqué et logique au vu des résultats précédemment décrits, le fait que l'angiotensine II induise une production de ROS dans les monocytes n'a pas été démontré.

Le SARS-COV-2 a pour récepteur d'entrée dans la cellule ACE2. Son action sur le SRAA a donc été étudiée. Furuhashi et ses collègues ont résumé les différents impacts que pourrait causer le SARS-COV-2 sur le système SRAA (Figure 4). Malgré l'homologie entre ACE et ACE2 seul ACE2 interagit avec certains coronavirus (Lubbe et al. 2020). Les raisons seraient à trouver dans l'espace d'interaction en C-terminal : il est plus grand au niveau d'ACE2 que pour ACE,

permettant une interaction avec la protéine Spike. La protéine Spike du SARS-COV-2 possède un site de clivage à la furine que n'a pas celle du SARS-COV-1. Ceci pourrait expliquer en partie le fait que l'affinité du SARS-COV-2 pour le récepteur ACE2 est meilleure que celle du SARS-COV-1 (Walls et al. 2020 ; Ke, 2020.). Lors de l'entrée du SARS-COV-2, ACE2 est co-internalisé avec le virus. Ceci pourrait aboutir à une moindre conversion de l'Angiotensine II en Angiotensine 1-7 et par là à un taux d'angiotensine II élevé dans l'environnement des cellules infectées.

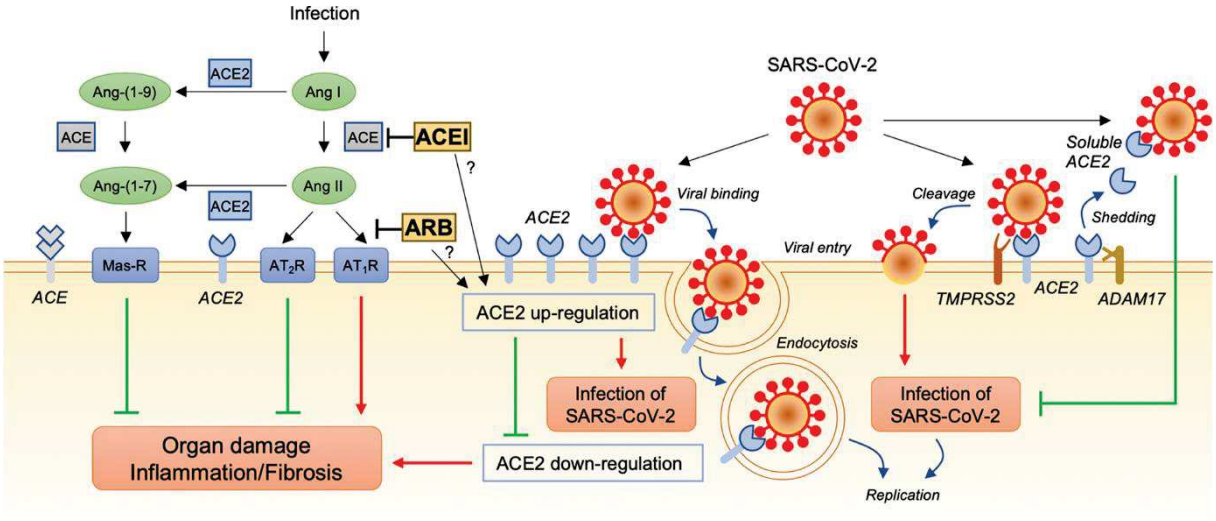

Figure 4 : Possibles associations entre le SRAA et les dommages pulmonaires observés lors d'une infection par SARS-COV-2 (Furuhashi et al. 2020).

IX. REPONSE IMMUNITAIRE A UNE INFECTION AU SARS-COV-2

On observe plusieurs étapes dans la réponse du système immunitaire visant à contrôler puis résoudre l'infection par SARS-COV 2. La réplication du virus est cytopathique (Buchrieser et al. 2020; Li et al. 2020). Le SARS-COV-2 déclencherait via sa protéine virale ORF3a des mécanismes d'apoptose et possiblement de pyroptose dans les cellules où il réplique par l'activation de la caspase 8, de la caspase 3 mais pas par l'activation de la caspase 1 (Ren et al. 2020, 3; Li et al. 2020, 8). La pyroptose est une mort cellulaire particulièrement pro-inflammatoire, comme son nom le laisse entendre (*pyro* = feu ; *ptosis* = chute). C'est un mécanisme induit par l'activation de caspases qui va déclencher la production de plusieurs cytokines dont l'IL-1β et l'IL-18 (Bergsbaken, Fink, et Cookson 2009). Les caspases 1, 3 et 8 sont capables de déclencher la pyroptose (Yu et al. 2021).

La cellule infectée va donc produire des cytokines pro-inflammatoires comme l'IL-1β attirant les cellules de l'immunité innée comme les monocytes se différenciant alors en macrophages mais aussi les cellules NK et les neutrophiles. (Maucourant et al. 2020; Jinghe Zhang et al. 2021; Reusch et al. 2021)

Dans un second temps, ce sont les cellules LT4 et LT8 qui sont recrutées dans les tissus infectés et qui à leur tour enclencheront des mécanismes d'élimination du pathogène et des cellules infectées plus spécifique, et surtout de mémoire du SARS-COV-2 (Schultze et Aschenbrenner 2021, 19).

Dans la majeure partie des cas, ces mécanismes seront parfaitement efficaces. Ils peuvent être à l'origine de la fièvre et d'autres symptômes faibles à modérés du patient accompagnant la résolution de l'infection et ne nécessitant pas d'hospitalisation. Mais dans les cas les plus graves, un orage cytokinique se déclenche et le pronostic vital de la personne peut se trouver engagé. L'orage cytokinique déclenché est défini par la production fulminante et disproportionnée de cytokines par les cellules immunitaires, particulièrement par les macrophages mais aussi les monocytes et les neutrophiles infiltrés à cause des lésions. Les raisons pour lesquelles certains patients développent un orage cytokinique sont encore sujet à discussion.

Localement, la cellule en apoptose qui relargue des cytokines pro-inflammatoires, va, en plus d'attirer les cellules de l'immunité, déclencher un signal de danger aux cellules adjacentes qui à leur tour vont envoyer un signal de danger, créant une boucle positive de production en continu de cytokines pro-inflammatoires (Coperchini et al. 2020).

Beaucoup de cytokines pro-inflammatoires sont impliquées dans ce processus : des interférons (IFN), des Interleukines (IL), les facteurs de croissance transformant beta (TGF-β), des facteurs stimulant les colonies (CSF) des granulocytes et des macrophages, des chimiokines (C, CXC, CC ou CX3C selon leur structure) et particulièrement le facteur de nécrose tumorale alpha (TNF-α). Celles qui semblent être les plus impliquées dans la pathologie de COVID-19 sont le TNF-α, l'IL-1β, l'IL-6 et l'IL-18 (Fajgenbaum et June 2020; Mangalmurti et Hunter 2020). Les patients présentent un niveau élevé de TNF-α, d'IL-1β, d'IL-6 et d'IL-18 dans le tractus

respiratoire (Jinghe Zhang et al. 2021). Dans le plasma on observe un plus haut taux d'IL-6, d'IL-18, d'IL-10 et d'IL-4 (Rodrigues et al. 2021).

De plus, dans les cellules infectées, un mécanisme d'inflammation particulier est activé : l'inflammasome. C'est un complexe protéique formé par le récepteur NOD-like NLRP3, le domaine de recrutement de caspase CARD et la procaspase 1. Ce complexe permet de cliver la procaspase 1, ce qui l'active en caspase 1 et induit l'activation des cytokines pro-inflammatoires IL-1β et l'IL-18 en clivant leurs précurseurs. De plus la caspase 1 est capable de déclencher la pyroptose. Dans le contexte du SARS-COV-2, l'activation de l'inflammasome dans les cellules infectées est probablement induite par l'ORF3a, comme avec le SARS-COV-1 (Chen et al. 2019). La protéine N semble également être impliquée dans l'activation de l'inflammasome via NLRP3 (Pan et al. 2021, 2).

L'activation de l'inflammasome a été détectée dans des PBMCs et potentiellement aussi dans des cellules endothéliales de patients COVID-19 (Rodrigues et al. 2021; Paul et al. 2021). Les monocytes et les macrophages peuvent être infectés par le SARS-COV2 mais de façon non productive (Boumaza et al. 2021). Pour entrer dans les monocytes le mécanisme du virus est particulier. Les monocytes présentent très peu d'ACE2 à leur surface, mais le virus pourrait utiliser une autre voie d'entrée : les virions liés à des anticorps anti-spike seraient internalisés par les monocytes via le récepteur FcγR, (Vora, Lieberman, et Wu 2021), un article de bio-arxiv donne des premiers éléments pour le démontrer en induisant une infection des monocytes pré-incubés avec du plasma de patients (Junqueira, 2021.). Cependant cela déclenche l'apoptose des cellules infectées et participe également à l'inflammation locale (Zheng et al. 2021). l'ORF3a est capable d'activer le mécanisme de pyroptose des macrophages ce qui induit la production de cytokines pro-inflammatoires pouvant participer au déclenchement de l'orage cytokinique (Jinghe Zhang et al. 2021; Ferreira et al. 2021). De plus, les monocytes infectés vont également voir leur inflammasome s'activer par la présence des protéines virales de la nucléocapside, produire des dérivés oxygénés, activer la caspase 1 et relarguer des cytokines dont de l'IL-1β (Vora, Lieberman, et Wu 2021).

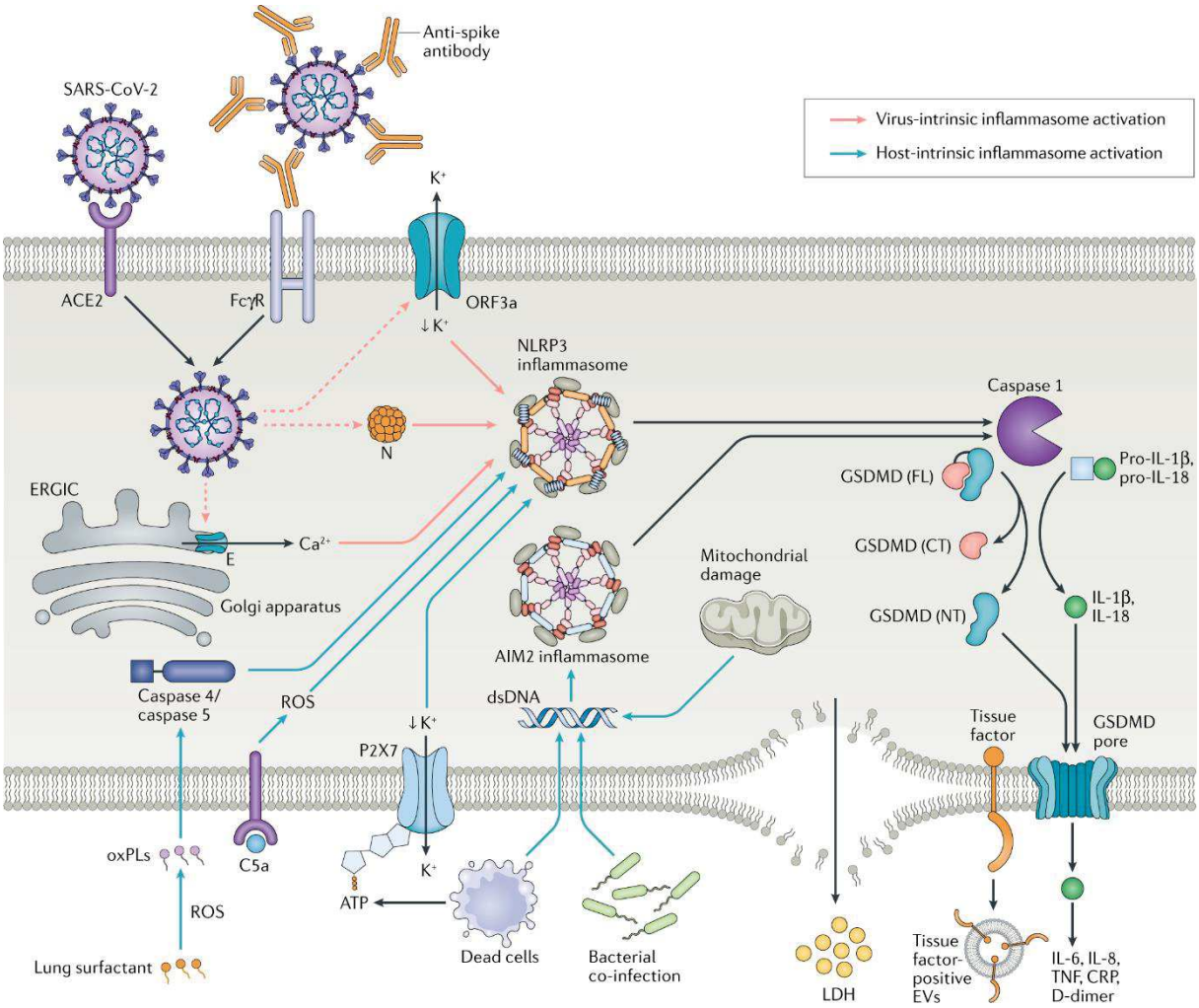

Figure 5 : Voies d'activation de l'inflammasome NLRP3 : Il peut être activé par le SARS-COV-2 et par les ROS (Vora, Lieberman, et Wu 2021)

L'action directe des monocytes différenciés en macrophages et de la réaction inflammatoire locale va entrainer une pneumopathie (Xu et al. 2020, 1). Ces lésions pulmonaires, si elles s'accumulent, vont-elles-même entraîner des conséquences directes puisque le patient peut alors développer un ARDS qui est fatal dans 40% des cas hospitalisés (Maca et al. 2017).

De manière générale les patients avec les formes les plus graves de COVID-19 ont une action des LT déficiente par rapport aux patients asymptomatiques. Une lymphopénie, c'est-à-dire un nombre de lymphocytes inférieur à 1000/mm^3 de sang, est également observée chez ces patients. Les origines de cette lymphopénie sont encore en discussion puisqu'elle semble précéder l'orage cytokinique et font l'objet central de ma thèse. (Cappanera et al. 2021) Nous proposons qu'une des causes pourrait être les ROS issus des monocytes.

Chez les patients COVID-19, on observe une lymphopénie, en particulier parmi les LT8 (Westmeier et al. 2020) ce qui paradoxalement devrait réduire la quantité de cytokines pro-inflammatoire chez le patient. Cependant une hyperactivation des LT8 restants, sans épuisement de leur action de sécrétion de cytokines pro-inflammatoires, a été rapportée (Rha et al. 2021). Également, au niveau des LT4, un déficit quantitatif est observé, mais de façon moins prononcée que pour les T8 (Z. Chen et John Wherry 2020). Selon les patients, une activation T_H2 ou T_H1 a été observée et cette activation serait prédictive du devenir pathologique du patient. (Ganneru et al. 2021; Roncati et al. 2020, 2) D'autre études sont encore en cours pour mieux comprendre ces différences d'activation (ClinicalTrials.gov Identifier : NCT04403061).

On observe aussi dans les formes graves de la maladie des anomalies de coagulation, avec des microthrombi disséminés dans les vaisseaux favorisant les complications précédemment évoquées du COVID-19 (Jose et Manuel 2020). Le taux de D-dimères chez les patients COVID-19 est élevé et un facteur prédictif de la survie du patient. (Chocron et al. 2021)

X. L'ACTIVATION IMMUNITAIRE ET LE VIH

A- LE VIRUS DE L'IMMUNODEFICIENCE HUMAINE

Le VIH est un rétrovirus à ARN, découvert en 1983 par Françoise Barré-Sinoussi et ses collègues à l'Institut Pasteur de Paris (Barre-Sinoussi et al. 1983) . Il existe 2 types de VIH (1 et 2) chacun ayant une diversité génétique élevée (Désiré et al. 2018; Gao et al. 1994). Le VIH-1 est divisible en sous-familles : M, N ; O et P. Le VIH-1 M est largement majoritaire, c'est le seul qui est vraiment pandémique (B. S. Taylor et al. 2008). L'infection par VIH est une zoonose, provenant du chimpanzé et du gorille pour VIH-1 et du singe sooty mangabey pour VIH-2. Tous viennent de la région centrale du continent Africain. L'épidémie de VIH-1 a commencé à se développer à Kinshasa dans les années 1920 avec le développement industriel (Sharp et Hahn 2011).

La médiane de survenue du Syndrome d'Immunodéficience Acquise (SIDA) chez une personne séropositive au VIH non traitée était estimée à 8 à 10 ans après infection. Une fois que la personne a développé un SIDA, sans traitement antirétroviral, son espérance de vie était réduite à un à deux ans. (https://www.who.int/news-room/q-a-detail/hiv-aids)

Sans traitement, l'infection par le VIH passe par quatre phases. Le VIH en phase aigüe, pendant quelques semaines, active potentiellement toutes les types de cellules immunitaires dont les lymphocytes T4, détruisant ces dernières. Vient ensuite une phase asymptomatique où un équilibre s'installe entre la dynamique de la réplication virale et la réponse immunitaire antivirale, équilibre se traduisant par une virémie plus ou moins élevée mais moindre qu'en phase aigüe. La troisième phase est la phase symptomatique où le système immunitaire devient moins efficace pour combattre les pathologies dues à des agents microbiens et/ou des cancers. Finalement, le SIDA est déclaré lorsque le système immunitaire de la personne infectée est au plus bas, c'est la dernière phase d'infection au VIH avant la mort du patient par un pathogène opportuniste, un cancer ou toute autre pathologie en l'absence de traitement (Deeks et al. 2015; Miller et al. 2010; Gonçalves, Uldrick, et Yarchoan 2017).

Les efforts de recherche ont abouti à des traitements antirétroviraux efficaces transformant une pathologie mortelle en une pathologie chronique permettant de vivre jusqu'à 100 ans (patient de Lisbonne), ceci en l'espace d'une décennie entre la découverte officielle du virus et les premiers essais de thérapies combinées (Hammer et al. 1996).

B- L'ACTIVATION IMMUNITAIRE, CAUSES ET CONSEQUENCES

Aujourd'hui avec la multithérapie antirétrovirale (cART), une combinaison de molécules agissant à plusieurs points clé du cycle de réplication virale, l'espérance de vie des personnes vivant avec le VIH (PVVIH) a augmenté considérablement pour être presque aussi élevée que celle de la population générale. Cet écart est particulièrement faible pour les personnes les plus récemment infectées et qui ont commencé précocement leur traitement, avec un taux de LT4 élevé (Marcus et al. 2020; Smiley et al. 2021)

Ces personnes ont tout de même des comorbidités non attribuables à des infections, survenant plus tôt que dans la population générale (Guaraldi et al. 2011; Marcus et al. 2020). Les comorbidités les plus étudiées sont les maladies cardiovasculaires, l'hypertension, l'insuffisance rénale et le diabète de type 2.

Malheureusement, en France, 29% des personnes dépistées positives le sont à un stade avancé de l'infection (Cazein 2019).

Sous un traitement approprié les PVVIH peuvent rester en phase asymptomatique toute leur vie avec une charge virale globalement sous le seuil de détection de 50 copies/mL et restaurer au moins en partie leur taux de lymphocytes.

Mais les PVVIH traitées ont une activation immunitaire résiduelle et persistante. Cette activation immunitaire peut avoir plusieurs causes et entrainer plusieurs conséquences. Cette thématique est centrale pour l'équipe de recherche dans laquelle j'ai fait ma thèse.

Plusieurs études ont comparé l'incidence des causes de morbi-mortalité entre les PVVIH et la population générale. Ces études ont ensuite permis de faire des méta-analyses qui rendent compte de ce que l'on sait aujourd'hui des causes de mortalité des PVVIH sous traitement efficace. Les maladies du foie, les maladies cardiovasculaires et les cancers non liés au VIH restent les causes de mort les plus fréquentes et ont un taux d'incidence plus élevé que dans la population générale (Aldaz et al. 2011; Croxford et al. 2017).

Les causes de cette activité immunitaire sont plurielles. D'abord il y a la production occasionnelle de virions par les cellules réservoirs. La virémie résiduelle peut dépendre de la cART du patient (Nolan 2003; Darcis et al. 2020). Mais il y a aussi la question de l'infection *de novo* d'une cellule, même abortive, par ces virions : l'accumulation de rétrotranscrits même

lors d'un cycle d'infection incomplet, induit l'apoptose ou la pyroptose via la voie des caspases et une réaction inflammatoire dans les cellules voisine (Doitsh et al. 2010). Une deuxième cause d'activation immunitaire sont les co-infections, par exemple par le cytomégalovirus et les virus de l'hépatite B et C. On peut aussi citer comme cause d'activation immunitaire la lymphopénie des LT4, responsable d'une production d'IL7, ayant une activité pro inflammatoire (Sereti et al. 2009). Une autre cause d'activation immunitaire peut-être un déficit quantitatif en cellules Treg. Les cellules Treg ayant un effet inhibiteur sur les autres sous-populations de LT4 (T_H1, T_H2, T_H17), leur inactivité peut favoriser l'activation immunitaire (Kanwar, Favre, et McCune 2010). La translocation microbienne est également très décrite comme cause d'AI. La translocation microbienne est le passage d'un agent microbien commensal ou d'une partie de celui-ci d'une muqueuse dans la circulation générale en l'absence d'infection manifeste (Sandler et Douek 2012). La translocation microbienne peut induire une activation du système immunitaire pouvant se traduire par des taux circulants de CD14 soluble, de protéine intestinale de liaison aux acides gras (I-FABP) et de LPS-binding protein (LBP) élevés. La présence de LPS circulant est un autre marqueur de translocation microbienne (Brenchley et al. 2006).

L'immunosénescence présente chez certaines PVVIH peut être à la fois une cause et une conséquence de l'activation immunitaire. La sénescence des cellules immunitaires peut les amener à produire des facteurs pro-inflammatoires (Freund et al. 2010), et ces facteurs peuvent engendrer une sénescence prématurée des cellules immunitaires (Sokoya et al. 2017).

Pour chaque acteur de l'immunité, des marqueurs d'activation ont été identifiés chez les PVVIH comme résumé dans la Figure 6.

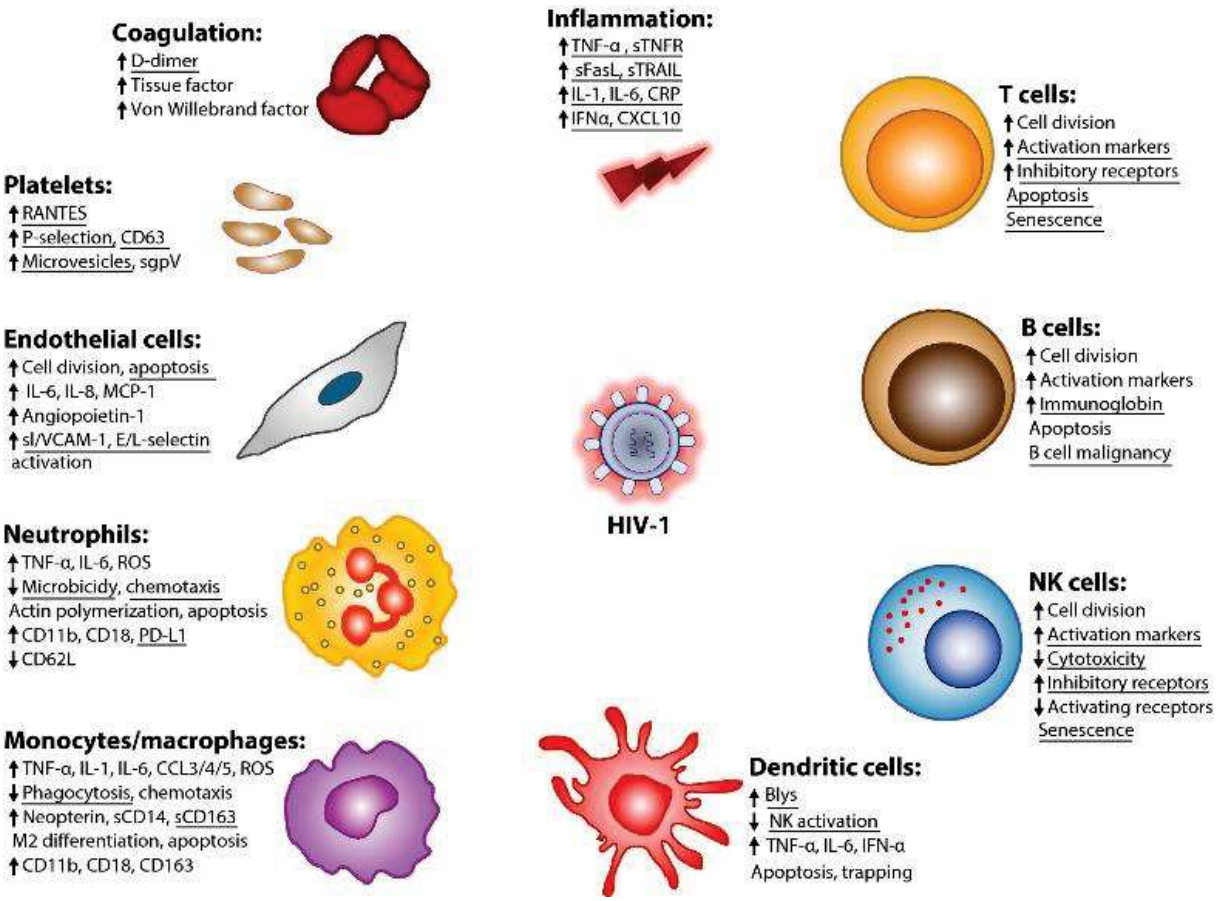

Figure 6 : Marqueurs et cellules impliqués dans l'activation immunitaire chez les PVVIH. (M Younas et al. 2016) les marqueurs soulignés peuvent être persistants après mise sous cART.

L'activation immunitaire résiduelle semble influer sur le développement de comorbidités dites non liées au SIDA rencontrées chez les PVVIH comme le syndrome métabolique, l'athérotrombose, les troubles neurocognitifs, la stéatose hépatique, l'ostéoporose, l'atteinte rénale, une fragilité générale, voire certains cancers (M Younas et al. 2016).

En 2015 l'équipe de Pierre Corbeau a publié un article développant l'idée que les PVVIH ont plusieurs profils d'activation immunitaire distincts. Chaque profil est caractérisé par une association spécifique de marqueurs d'activation immunitaire (Psomas et al. 2016). Ce premier travail a ouvert la voie au sein de l'équipe à plusieurs études auxquelles j'ai contribué. Les premiers résultats publiés sont présentés dans cette thèse.

E- RESULTATS

I. ARTICLE «MICROBIAL TRANSLOCATION IS LINKED TO A SPECIFIC IMMUNE ACTIVATION PROFILE IN HIV-1-INFECTED ADULTS WITH SUPPRESSED VIREMIA»

Dans ce travail et dans la continuité du projet ACTIVIH (Psomas et al. 2016) nous avions plusieurs objectifs : démontrer la robustesse du profilage des PVVIH avirémiques sous cART, c'est-à-dire établir que celui-ci n'est pas spécifique de la cohorte établie précédemment, et tester si une cause potentielle d'activation immunitaire, la translocation microbienne, pouvait être associée à un profil particulier (Brenchley et al. 2006).

Pour tester la robustesse du profilage, 20 patients d'une cohorte de PVVIH avirémiques plus jeunes et infectés depuis moins longtemps ont été ajoutés aux 120 premiers patients. Ces 20 patients nouveaux ont été analysés comme les 120 patients précédents d'ACTIVIH en observant plus de 60 marqueurs d'activation immunitaire dans leur sang périphérique. L'ensemble des patients a pu être profilé à nouveau et les groupes renommés en conséquence de A à E.

Nous avons observé que les volontaires d'un profil (le profil D) avait deux marqueurs de translocation microbienne plus élevés que les volontaires ayant un autre profil. Le premier marqueur de translocation microbienne était la LBP. LBP est une protéine de phase aiguë de la réponse immunitaire à une attaque bactérienne, induite par la présence de LPS bactérien, capable de se lier à ce LPS pour faciliter sa reconnaissance par les PRR. En temps normal, le LBP est présent dans des concentrations allant de 5 à 15µg/mL dans le plasma humain (Zweigner et al. 2001). Dans notre cohorte la moyenne était à 29.2µg/mL pour les PVVIH (Figure 2G). Ceci a également été démontré dans plusieurs travaux chez les PVVIH (Baroncelli et al. 2020; Funderburg et al. 2016; Brenchley et al. 2006). De plus les LBP induit elle-même une production de cytokines pro-inflammatoires (Brenchley et al. 2006). Un deuxième marqueur de translocation microbienne que nous avons utilisé était la I-FABP. I-FABP est une protéine produite essentiellement par les entérocytes (Agellon, Toth, et Thomson 2002), un des quatre types cellulaires du tube digestif. La présence de cette protéine dans le plasma est anormale, causée par la mort de ces cellules fragilisant la barrière intestinale et entrainant de la translocation microbienne (Lau 2016; Skowyra et al. 2015). Nous avons également observé que la quantité de LT8 épuisés (présentant le marqueur PD-1 à leur surface) était liée non seulement à la quantité d'ADN ribosomal 16s bactérien présente dans le plasma des patients mais également à la quantité de LBP plasmatique (Figure 2L et 2N).

frontiers in Immunology

ORIGINAL RESEARCH
published: 13 September 2019
doi: 10.3389/fimmu.2019.02185

Microbial Translocation Is Linked to a Specific Immune Activation Profile in HIV-1-Infected Adults With Suppressed Viremia

Mehwish Younas[1†], Christina Psomas[1,2†], Christelle Reynes[3], Renaud Cezar[4], Lucy Kundura[1], Pierre Portales[5], Corinne Merle[2], Nadine Atoui[2], Céline Fernandez[2], Vincent Le Moing[2,6,7], Claudine Barbuat[8], Olivier Moranne[9], Albert Sotto[7,8], Robert Sabatier[3], Pascale Fabbro[10], Thierry Vincent[5,7], Catherine Dunyach-Remy[11], Audrey Winter[1], Jacques Reynes[2,6,7], Jean-Philippe Lavigne[11] and Pierre Corbeau[1,4,7]*

[1] Institute of Human Genetics, CNRS-Montpellier University, UMR9002, Montpellier, France, [2] Infectious Diseases Department, University Hospital, Montpellier, France, [3] Institute for Functional Genomics, Montpellier University, UMR5203, Montpellier, France, [4] Immunology Department, University Hospital, Nîmes, France, [5] Immunology Department, University Hospital, Montpellier, France, [6] IRD UMI 233, INSERM U1175, Montpellier University, Montpellier, France, [7] Montpellier University, Montpellier, France, [8] Infectious Diseases Department, University Hospital, Nîmes, France, [9] Nephrology Department, University Hospital, Nîmes, France, [10] Medical Informatics Department, University Hospital, Nîmes, France, [11] U1047, INSERM, Microbiology University Hospital Nîmes, Montpellier University, Nîmes, France

OPEN ACCESS

Edited by:
Mario Mago Clerici,
University of Milan, Italy

Reviewed by:
Nicholas Funderburg,
The Ohio State University,
United States
Suresh Pallikkuth,
University of Miami, United States
Giulia Carla Marchetti,
University of Milan, Italy

***Correspondence:**
Pierre Corbeau
pcorbeau@igh.cnrs.fr

†These authors have contributed equally to this work

Specialty section:
This article was submitted to Viral Immunology, a section of the journal Frontiers in Immunology

Received: 31 May 2019
Accepted: 29 August 2019
Published: 13 September 2019

Citation:
Younas M, Psomas C, Reynes C, Cezar R, Kundura L, Portales P, Merle C, Atoui N, Fernandez C, Le Moing V, Barbuat C, Moranne O, Sotto A, Sabatier R, Fabbro P, Vincent T, Dunyach-Remy C, Winter A, Reynes J, Lavigne J-P and Corbeau P (2019) Microbial Translocation Is Linked to a Specific Immune Activation Profile in HIV-1-Infected Adults With Suppressed Viremia. Front. Immunol. 10:2185. doi: 10.3389/fimmu.2019.02185

Persistent immune activation in virologically suppressed HIV-1 patients, which may be the consequence of various factors including microbial translocation, is a major cause of comorbidities. We have previously shown that different profiles of immune activation may be distinguished in virological responders. Here, we tested the hypothesis that a particular profile might be the consequence of microbial translocation. To this aim, we measured 64 soluble and cell surface markers of inflammation and CD4+ and CD8+ T-cell, B cell, monocyte, NK cell, and endothelial activation in 140 adults under efficient antiretroviral therapy, and classified patients and markers using a double hierarchical clustering analysis. We also measured the plasma levels of the microbial translocation markers bacterial DNA, lipopolysaccharide binding protein (LBP), intestinal-fatty acid binding protein, and soluble CD14. We identified five different immune activation profiles. Patients with an immune activation profile characterized by a high percentage of CD38+CD8+ T-cells and a high level of the endothelial activation marker soluble Thrombomodulin, presented with higher LBP mean (± SEM) concentrations (33.3 ± 1.7 vs. 28.7 ± 0.9 μg/mL, $p = 0.025$) than patients with other profiles. Our data are consistent with the hypothesis that the immune activation profiles we described are the result of different etiological factors. We propose a model, where particular causes of immune activation, as microbial translocation, drive particular immune activation profiles responsible for particular comorbidities.

Keywords: bacterial translocation, cell activation, inflammation, coagulation, endothelium

INTRODUCTION

Immune activation plays a major role during HIV-1 infection. In the short term, it is the main driver of CD4 T-cell loss (1). In the long term, it fuels non-AIDS-linked morbidities such as atherothrombosis, osteoporosis, metabolic syndrome, neurocognitive disorders, liver steatosis, kidney failure, frailty, and certain types of cancer, even under antiretroviral therapy (ART) (2). These diseases are responsible for over 80% of deaths among virologic responders (3). It is therefore of major interest to better understand the causes and the phenotypes of this immune activation, as well as the pathophysiological mechanisms resulting in its consequences.

Via cell-surface and soluble markers, we recently analyzed the state of activation of the immune system in 120 efficiently treated HIV-1 patients. Using two independent hierarchical clustering analyses, we identified five patient groups characterized by very different immune activation profiles (4). This observation highlights the fact that virological responders do not all present with the same types of immune activation. It is notable that one of these five immune activation profiles was strongly linked to insulin resistance (Odds Ratio 17.06 [95% CI 2.14–135.60], $p = 0.007$). These findings provoke the interesting possibility that certain immune activation profiles might lead to specific comorbidities. It is also logical to hypothesize that these immune activation profiles might be the consequences of specific causes. Various causes of immune activation have been unveiled, including residual viral production, coinfections, CD4 T-cell lymphopenia, immune senescence, metabolism disorders, CD4 T-cell subset deregulation, and microbial translocation (5). In a given virologic responder, some of these causes may prevail. For instance, microbial translocation is present in some individuals but not in others (6). Likewise, some patients have restored their CD4 count, whereas others have not. In addition, the level of persistent HIV production is also variable among virologic responders.

Microbial translocation is the passage of microbes and/or microbial products from the gut lumen into the organism in absence of bacteremia. It has been recognized as a potential source of immune activation in HIV infection (7). It is caused by the conjunction of physical destruction (8) and loose junctions (9) of the epithelium and immunological (CD4 T-cell, and particularly Th17 lymphopenia (10), neutrophil accumulation) (11) lesions of the gut mucosa. It may be noted that some degree of mucosa alteration and microbial translocation may persist under efficient ART (6). Various biomarkers are used to evaluate microbial translocation. Lipopolysaccharide (LPS) and bacterial DNA peripheral blood concentrations are direct markers. LPS-binding protein (LBP) (12) and soluble CD14 (sCD14), the production of which is induced by the presence of LPS, are indirect markers. Intestinal fatty acid binding protein (I-FABP), released by damaged gut epithelial cells, is a marker of epithelium destruction (13). More recently, dysbiosis, an imbalance in bacterial taxa, has been described in the microbiota of HIV patients, linked to microbial translocation and immune activation (14–16). Yet, this dysbiosis might be more linked to sexual preference than to HIV infection (17), and its role as a cause and/or a consequence of immune dysregulation remains yet to be clarified.

In the present study, to test the hypothesis that some causes of immune activation might specifically fuel certain profiles of immune activation, we looked for a link between microbial translocation and the immune activation profiles that we identified in virologic responders.

MATERIALS AND METHODS

Study Design

In the previous ACTIVIH trial, we had analyzed 120 HIV-1 patients over 45 years of age with pre-therapeutic CD4 cell counts below 350 cells per μL. In order to diversify our study population, we recruited 20 additional adults infected by HIV-1 without age or CD4 nadir limitations. All individuals were aviremic (<50 copies per mL) for at least 6 months while under stable antiretroviral regimen. Pregnant or breastfeeding women, persons under immunomodulatory treatment or presenting with diseases likely to modify their immune system were not included. Fourty-seven HIV-negative control subjects matched for age were also recruited. This study was approved by the Ethics Committee of Montpellier University Hospital. All patients had provided written informed consent. The trial was registered on ClinicalTrials.gov under the reference NCT02334943.

Quantification of Cell Surface and Soluble Markers

Cell surface markers were analyzed by flow cytometry as previously described (4). Soluble markers of immune, endothelial, and coagulation activation were analyzed as in the ACTIVIH study (4). The 64 markers are listed in Supplementary Table 1 (4). 16s ribosomal DNA (rDNA) was quantified by PCR (18). LBP (Enzo Life Sciences) and I-FABP (Hycult Biotech) were measured in plasma using commercial ELISA kits.

TABLE 1 | Bioclinical characteristics of the study populations.

Characteristic	Variable	Patients	Controls
Number of individuals		140	47
Age (years)	Mean (± SD)	56 (± 9)	56 (± 13)
% CD4+ T cell	Mean (± SD)	49.3 (± 11.4)	NA
CD4 Count (cell/mm3)	Mean (± SD)	733 (± 375)	NA
CD4/CD8 Ratio	Mean (± SD)	1.24 (± 0.88)	NA
Pre-therapeutic nadir CD4 count (cells/μL)	Mean (± SD)	199 (± 119)	NA
Pre-therapeutic viremia (RNA copies/ml)	Mean (± SD)	1437216 (± 9602969)	NA
Years of HIV infection	Mean (± SD)	16 (± 8)	NA
Months of viral suppression	Mean (± SD)	95 (± 49)	NA
Male sex (%)	*N* (%)	113 (81)	23 (50)

Statistical Analysis

We used the squared Euclidean distance of scaled data to measure dissimilarities between patients and the square of (1-(pearson correlation coefficient)^2) to measure dissimilarities between markers. The classifications used the Ward method (on the squared distance) as a metric. The heatmap was generated using R software. We tested different criteria to choose the number of clusters, and finally chose five clusters as it was consistent with the dendrogram structure and gave homogenous and distinct profiles. We used the Mann-Whitney test to compare patients and controls, and Profile D with other profiles. The links between biomarkers were determined by Spearman rank correlations.

RESULTS

Study Subjects

Compared with the first 120 patients we recruited for the ACTIVIH study, the 20 new patients were younger (50.4 ± 12.9 vs. 56.5 ± 8.1 years of mean ± SD age, $p = 0.054$), and presented with shorter durations of HIV infection (8.9 ± 7.1 vs. 17.2 ± 7.4 years, $p = 0.004$), shorter durations of aviremia (56 ± 40 vs. 102 ± 47 months, $p < 0.001$), and a mean pre-therapeutic CD4 cell count tending to be higher (239 ± 169 vs. 192 ± 108 cells per μL, $p = 0.112$). The bioclinical characteristics of all 140 patients and of HIV-negative controls are given in **Table 1**.

Immune Activation Profiling

As previously performed, for the 20 additional patients living with HIV-1, we determined the proportions of CD4+ and CD8+ T-cells, naïve, central memory, and effector memory T-cells, based on CD45RA and CD27 expression, activated (HLA-DR+ and/or CD38+), exhausted (PD-1+), and senescent (CD57+, eventually CD27– and CD28–) T-cells. The percentages of activated (HLA-DR+), dysfunctional (CD56–), and senescent (CD57+) NK cells were also measured. Immunoglobulin (Ig)G, IgA, IgM, and soluble CD163 (sCD163) peripheral blood levels were used as markers of B-cell and monocyte activation, respectively. It should be noted that sCD14 was not used as an activation marker, but as a microbial translocation marker. Inflammation was evaluated via soluble Tumor Necrosis Factor receptor type I (sTNFRI-1) and C-reactive protein (CRP) concentrations, and endothelium activation was evaluated via soluble Endothelial Protein C Receptor (sEPCR), soluble

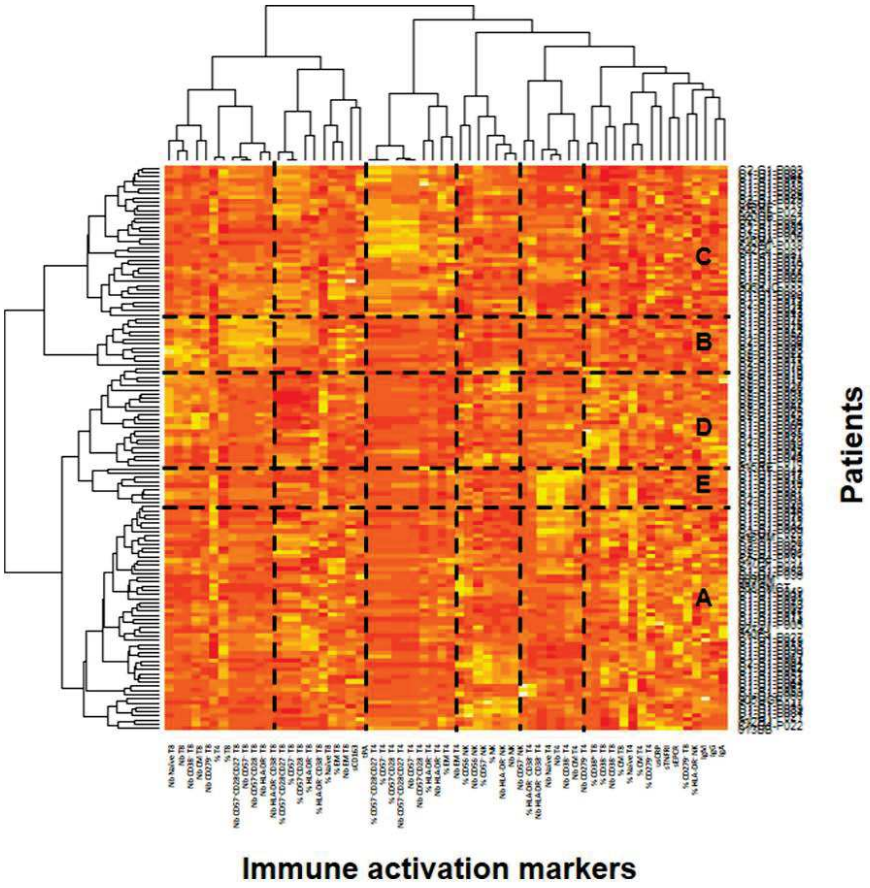

FIGURE 1 | Identification of the patient's immune activation profiles. Heatmap showing the hierarchical clustering of the activation markers (vertical) and of the patients (horizontal). The five profiles of immune activation issued from the patients clustering **(A–E)** are indicated.

Thrombomodulin (sThrombomodulin), and tissue Plasminogen Activator (tPA) concentrations in peripheral blood.

In the ACTIVIH study, two independent hierarchical clustering analyses of the activation markers and of the 120 patients had identified five groups of individuals presenting with very different profiles of immune activation. We carried out the same analysis on all 140 patients (**Figure 1**). Interestingly, although the 20 additional patients presented with divergent bioclinical characteristics, this new analysis again identified five different immune activation profiles. The bioclinical characteristics of the patients are given according to their immune activation profile in **Table 2**. Each profile may be characterized by a specific marker. As compared with the other patients, patients with Profile A present with a high percentage of central memory CD8+ T-cells (31 ± 13 vs. 22 ± 9%, $p < 0.001$, **Figure 2A**), and patients with Profile B present with the lowest CD4:CD8 ratio (0.64 ± 0.30 vs. 1.29 ± 0.90, $p < 0.001$, **Figure 2B**). Profile C patients have the higher percentage of HLA-DR+ CD4+ T-cells (32 ± 15 vs. 19 ± 10%, $p < 0.001$, **Figure 2C**), whereas Profile D patients have the higher percentage of CD8+ T-cells expressing CD38 (53 ± 3 vs. 43 ± 1%, $p = 0.001$, **Figure 2D**). Finally, Profile E is remarkable for its elevated proportion of CD38-positive CD4+ T-cells (73 ± 11 vs. 56 ± 12%, $p < 0.001$, **Figure 2E**).

Microbial Translocation Markers

Next, for these 140 patients we measured peripheral blood mean (±SEM) levels of rDNA, LBP, sCD14, and I-FABP. Plasma concentrations of rDNA (16.6 ± 2.0 vs. 9.9 ± 0.9 copies/μL, $p < 0.001$, **Figure 2F**), LBP (29.2 ± 0.8 vs. 16.0 ± 1.0 μg/mL, $p < 0.001$, **Figure 2G**), and sCD14 (3.41 ± 0.09 vs. 1.65 ± 0.02 μg/mL, $p < 0.001$, **Figure 2H**) were significantly higher, whereas I-FABP concentrations (470 ± 39 vs. 333 ± 46 pg/mL, $p = 0.557$, **Figure 2I**) were non-significantly higher in HIV patients than in HIV-negative controls matched for age. In our search for correlations between microbial translocation markers, we observed a link between rDNA and LBP ($r = 0.279$, $p < 0.001$, **Figure 2J**), and an almost significant link between sCD14 and I-FABP ($r = 0.153$, $p = 0.071$, **Figure 2K**).

Relationships Between Microbial Translocation and Immune Activation Markers

As microbial translocation has been linked to immune activation, we looked for correlations between the microbial translocation and the immune activation markers we had quantified. This analysis revealed that the direct marker of microbial translocation rDNA was linked to CD8+ T-cell exhaustion ($r = 0.253$, $p = 0.003$, **Figure 2L**) and to the endothelium activation marker sThrombomodulin ($r = 0.239$, $p = 0.004$, **Figure 2M**). The indirect marker of microbial translocation LBP was not only linked to CD8+ T-cell exhaustion ($r = 0.226$, $p = 0.008$, **Figure 2N**), but also to sThrombomodulin ($r = 0.278$, $p = 0.002$, **Figure 2O**), the inflammation marker CRP ($r = 0.204$, $p = 0.017$, **Figure 2P**) as well. The other indirect marker of microbial translocation, sCD14, correlated with the expression of the immune activation marker HLA-DR on CD4+ T-cells ($r = 0.187$, $p = 0.028$, **Figure 2Q**).

Microbial Translocation Is Linked to a Specific Immune Activation Profile

Next, we analyzed whether the levels of microbial translocation were similar among the five immune activation profiles identified. Compared with the other patients, we observed that patients with Profile D presented a non-significant higher mean (±SEM) rDNA levels (29 ± 10 vs. 14 ± 1 copies/μL, $p = 0.589$). Their sCD14 (3.7 ± 0.2 vs. 3.3 ± 0.1 μg/mL, $p = 0.102$) and I-FABP (564 ± 85 vs. 410 ± 36 pg/mL, $p = 0.067$, **Figure 3A**) concentrations also tended to be higher. Moreover, their LBP levels were significantly higher (33.3 ± 1.7 vs. 28.7 ± 0.9 μg/mL, $p = 0.025$, **Figure 3B**), with an odds ratio (OR) per unit increase in LBP of 1.05 (95% CI, 1.01–1.11, $p = 0.034$).

Patients with Profile D were younger than the other patients (52 ± 7 vs. 57 ± 9 years, $p = 0.003$). A multivariate analysis, adjusted with age as a covariate, still revealed their risk of higher LBP (OR per unit increase in LBP of 1.06, 95% CI, 1.01–1.11, $p = 0.030$). Their CD4 nadir (148 ± 108 vs. 163 ± 104 cells/μL, $p = 0.501$) and duration of aviremia (85 ± 45 vs. 100 ± 49 months, $p = 0.188$) were not different. Although their CD8+

TABLE 2 | Bioclinical characteristics of the participants according to their immune activation profile.

Characteristic	Variable	Profile A	Profile B	Profile C	Profile D	Profile E
Number of individuals		56	13	37	25	9
Age (years)	Mean (± SD)	57 (± 9)	57 (± 5)	59 (± 11)	52 (± 7)	54 (± 4)
% CD4+ T cell	Mean (± SD)	48.8 (± 11.7)	36.5 (± 10.7)	47.3 (± 10.8)	53.2 (± 9.6)	63.4 (± 11.6)
CD4 Count (cell/mm^3)	Mean (± SD)	606 (± 279)	800 (± 344)	678 (± 280)	731 (± 301)	1567 (± 451)
CD4/CD8 Ratio	Mean (± SD)	1.17 (± 0.57)	0.64 (± 0.30)	1.08 (± 0.53)	1.38 (± 0.61)	2.64 (± 2.37)
Pre-therapeutic nadir CD4 count (cells/μL)	Mean (± SD)	148 (± 112)	147 (± 83)	180 (± 98)	148 (± 108)	201 (± 93)
Pre-therapeutic viremia (RNA copies/ml)	Mean (± SD)	2,774,841 (±15,256,275)	148,346 (± 151,297)	492,278 (± 1,835,761)	1,130,295 (± 2,941,405)	447,255 (± 503,358)
Years of HIV infection	Mean (± SD)	15 (± 7)	20 (± 6)	17 (± 8)	14 (± 9)	16 (± 7)
Months of viral suppression	Mean (± SD)	96 (± 44)	81 (± 43)	114 (± 58)	85 (± 45)	99 (± 44)
Male sex	*N* (%)	48 (85)	12 (92)	31 (83)	18 (71)	5 (55)

T-cells expressed higher levels of the activation marker CD38 (**Figure 2D**) they expressed lower levels of the senescence marker CD57 (23 ± 3 vs. 34 ± 1%, $p < 0.001$, **Figure 3C**) than the rest of the patients. Profile D was also remarkable because of a high level of mean (±SEM) sThrombomodulin (117 ± 13 vs. 89 ± 5 ng/mL, $p = 0.030$, **Figure 3D**).

DISCUSSION

We had previously described five different immune activation profiles in 120 patients with a mean age of 58 years, a mean pre-therapeutic CD4 count of 192 cells per μL, and a mean duration of infection of 17 years. It was important to assess whether

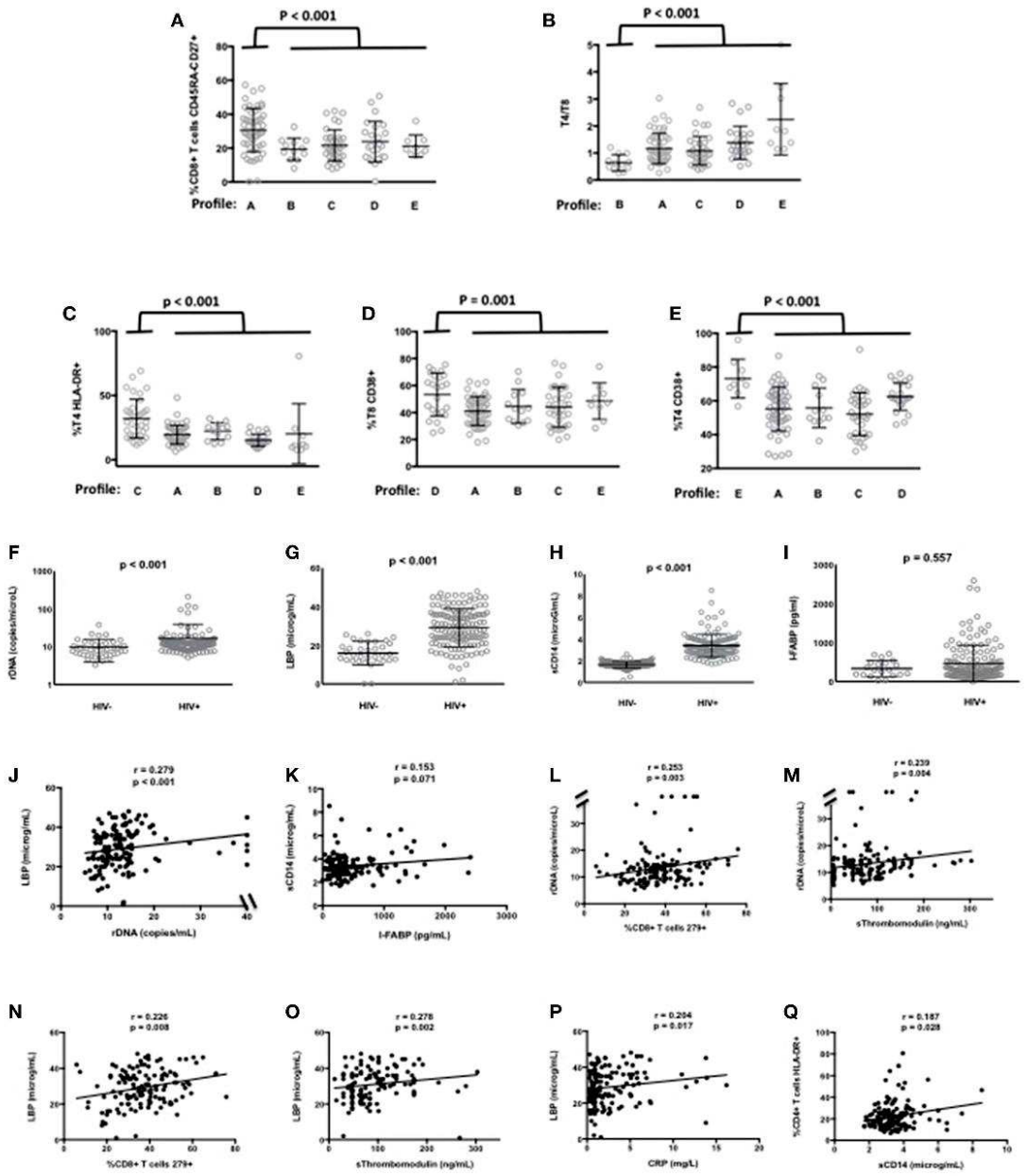

FIGURE 2 | Characterization of the immune activation profiles **(A–E)**. Differences in the level of various activation markers between each cluster of patients and the other clusters are shown. Microbial translocation in patients and healthy donors **(F–K)**. Plasma levels of rDNA **(F)**, LBP **(G)**, sCD14 **(H)**, and I-FABP **(I)** are presented as mean values and standard deviation; *p*-values are shown. Correlations between rDNA and LBP **(J)**, and between sCD14 and I-FABP **(K)** in patients are shown. Correlations between microbial translocation and immune activation markers in patients **(L–Q)**.

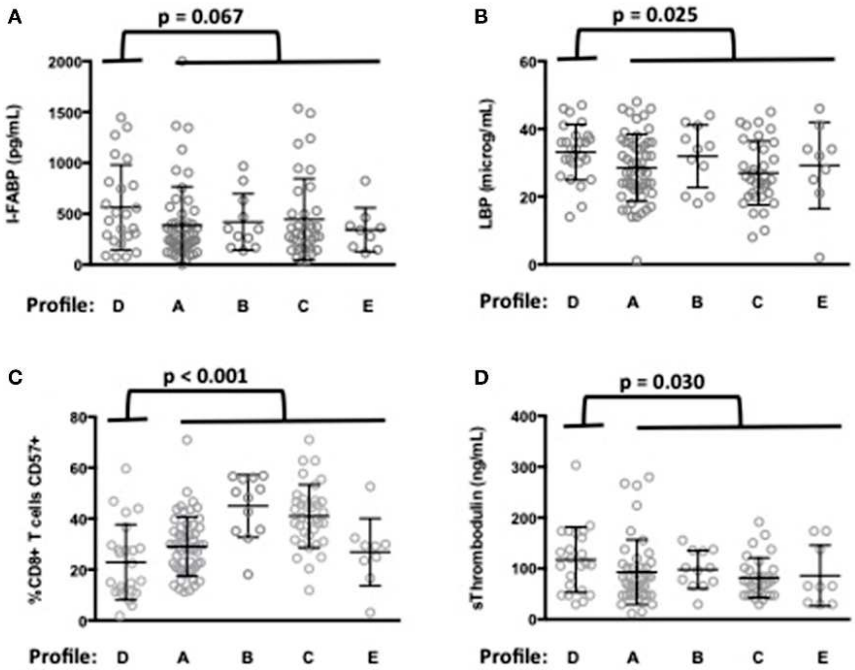

FIGURE 3 | Microbial translocation markers are elevated in patients with immune activation profile D. I-FABP **(A)** and LBP **(B)** mean values and standard deviations in patients according to their immune activation profile. *p*-value of the difference for each microbial translocation marker between Profile D and the other immune activation profiles is indicated. Characterization of the immune activation profile D **(C,D)**. Differences in the percentage of CD8+ T-cells expressing CD57 **(C)** and in the level of sThrombomodulin **(D)** between profile D and the other profiles are shown.

the same kind of profiles could be found after having added a divergent group of patients. Here we show that adding to this cohort 20 younger individuals with a shorter period of infection and aviremia and a higher CD4 count before ART, did not disrupt the hierarchical clustering. This observation argues for the fact that our classification is robust rather than specific for a particular set of patients. Yet, this remains to be confirmed with a greater number of patients with a higher diversity.

In the present study, we found elevated microbial translocation markers in some of the virological responders we analyzed. Globally, the peripheral blood concentrations of bacterial DNA and indirect translocation markers (LBP and sCD14) were higher in infected than in non-infected individuals. It is important to note that we observed a correlation between rDNA and LBP. In contrast, we did not establish any relationship between either rDNA, LBP, sCD14, or I-FABP, and sCD163, an alternative marker for monocyte activation. This is in line with a fact we had already unraveled in the ACTIVIH study, that sCD14 and sCD163 are clustered far apart from each other in the hierarchical clustering of the activation markers (**Figure 1**). This further emphasizes the fact that sCD14 and sCD163 correspond to different forms of monocyte activation.

We also unveiled links between microbial translocation markers and some of the immune activation markers we measured. We noticed a link between the level of circulating bacterial DNA as well as LBP and CD8+ T-cell exhaustion and sThrombomodulin. Thrombomodulin is released from activated endothelial cells, in the course of sepsis for example (19). Therefore, sThrombomodulin is considered as an endothelial activation marker (20). Vascular endothelial cells have been reported to express the LPS receptor TLR4, particularly under proatherogenic stimuli (21). Consequently, under LPS exposure, these cells release the inflammatory cytokines IL-6 and IL-8, produce TNFα and IL-1β mRNA and express the adhesion molecules ICAM-1, VCAM, and E-selectin (21, 22). In line with the hypothesis that microbial translocation might directly activate endothelial cells, sCD14 has been shown to correlate with the markers of endovascular dysfunction, symmetric, and asymmetric dimethylarginine (23).

The main result of our work is the report of a correlation between the markers of microbial translocation LBP and I-FABP, and one profile of immune activation. Although our data do not allow to state that this link is causative, it is noteworthy that patients with Profile D present high levels of sThrombomodulin, since microbial translocation is known to induce endothelial activation (22). This argues for a causative relationship between microbial translocation and Profile D immune activation. The link between LBP and Profile D that we established strengthens the hypothesis that the immune activation profiles we observed might be fueled by specific causes. Yet we cannot exclude the possibility that, inversely, Profile D immune activation favors microbial translocation. For instance,

we discovered a link between LBP and CRP, as previously observed (24). On the one hand, microbial translocation may cause inflammation, but on the other hand, inflammation may increase gut epithelium permeability and thereby microbial translocation. So there may be a bidirectional link between Profile D and microbial translocation.

As we have previously shown that a specific immune activation profile is strongly linked to a pathogenic process, insulin resistance, the present data have important consequences. Microbial translocation has been reported to be a driver of morbi-mortality, including insulin resistance (25), hypertension (26), cardiovascular disease (27), neurocognitive disorders (28), depression (29), liver disease progression (30), and non-Hodgkin lymphoma (31). Linking microbial translocation to Profile D and, in the future, eventually linking Profile D to specific morbidities, will help to specify which comorbidity microbial translocation may fuel. Early diagnosis of microbial translocation may then orientate the prevention and screening toward particular morbidities. Moreover, our observation opens the possibility to identify the pathophysiological pathways between microbial translocation and phenotypes of immune activation specific to Profile D and these phenotypes to comorbidities driven by Profile D. It will also be of interest to monitor the effect of probiotics and prebiotics tested in HIV infection (32) on Profile D. Furthermore, the influence of the dysbiosis described in HIV patients on Profile D will also have to be tested.

From a more general point of view, our observations may benefit other situations where microbial translocation occurs, including inflammatory bowel disease, pancreatitis, non-alcoholic steato-hepatitis, hepatitis B and C virus infection, graft vs. host disease, alcoholism, and aging. It would be of interest to study whether the same immune activation phenotype may be observed in these situations.

DATA AVAILABILITY

The datasets generated for this study are available on request to the corresponding author.

ETHICS STATEMENT

The studies involving human participants were reviewed and approved by Ethics Committee of the University Hospital of Montpellier. The patients/participants provided their written informed consent to participate in this study.

AUTHOR CONTRIBUTIONS

MY and LK contributed to the design of the flow cytometry study, acquired, analyzed, interpreted cell surface, and soluble marker data. CP contributed to the design of the study, the enrolment of patients, acquired, analyzed, and interpreted the data. RC, PP, and TV contributed to the design of the flow cytometry study, acquired, analyzed, and interpreted cell surface markers. CR, RS, AW, and PF contributed to the design of the statistical study, acquired, analyzed, and interpreted the statistical data. CM, NA, CF, VL, CB, and AS acquired, analyzed, and interpreted clinical data. CD-R, OM, and J-PL contributed to the design, analysis, and interpretation of the microbial translocation data. JR contributed to the design of the study, analyzed and interpreted the data. PC contributed to the design of the study, analyzed, interpreted data, and wrote the first draft of the manuscript. All authors revised and approved the final version.

FUNDING

The study was funded by MSD, MSDAvenir, and the University Hospitals of Montpellier and Nîmes. These sponsors had no role in the study design, the collection, analysis, or interpretation of data, the writing of the report, nor in the decision to submit the paper for publication.

ACKNOWLEDGMENTS

We are grateful to the persons who volunteered for this study, and to Teresa Sawyers for the critical reading of the manuscript.

REFERENCES

1. Nasi M, Pinti M, Mussini C, Cossarizza A. Persistent inflammation in HIV infection: established concepts, new perspectives. *Immunol Lett.* (2014) 161:184–8. doi: 10.1016/j.imlet.2014.01.008
2. Hunt PW. HIV and inflammation: mechanisms and consequences. *Curr HIV/AIDS Rep.* (2012) 9:139–47. doi: 10.1007/s11904-012-0118-8
3. Antiretroviral Therapy Cohort C. Causes of death in HIV-1-infected patients treated with antiretroviral therapy, 1996-2006: collaborative analysis of 13 HIV cohort studies. *Clin Infect Dis.* (2010) 50:1387–96. doi: 10.1086/652283
4. Psomas C, Younas M, Reynes C, Cezar R, Portales P, Tuaillon E, et al. One of the immune activation profiles observed in HIV-1-infected adults with suppressed viremia is linked to metabolic syndrome: the ACTIVIH study. *EBioMed.* (2016) 8:265–76. doi: 10.1016/j.ebiom.2016.05.008
5. Younas M, Psomas C, Reynes J, Corbeau P. Immune activation in the course of HIV-1 infection: causes, phenotypes and persistence under therapy. *HIV Med.* (2016) 17:89–105. doi: 10.1111/hiv.12310
6. Jiang W, Lederman MM, Hunt P, Sieg SF, Haley K, Rodriguez B, et al. Plasma levels of bacterial DNA correlate with immune activation and the magnitude of immune restoration in persons with antiretroviral-treated HIV infection. *J Infect Dis.* (2009) 199:1177–85. doi: 10.1086/597476
7. Brenchley JM, Price DA, Schaker TW, Asher TE, Silvestri G, Rao S, et al. Microbial translocation is a cause of systemic immune activation in chronic HIV infection. *Nat Med.* (2006) 12:1365–71. doi: 10.1038/nm1511
8. Nazli A, Chan O, Dobson-Belaire WN, Ouellet M, Tremblay MJ, Gray-Owen SD, et al. Exposure to HIV-1 directly impairs mucosal epithelial barrier integrity allowing microbial translocation. *PLoS Pathog.* (2010) 6:e1000852. doi: 10.1371/journal.ppat.1000852
9. Li Q, Schacker T, Carlis J, Beilman G, Nguyen P, Haase AT. Functional genomic analysis of the response of HIV-1-infected lymphatic tissue to antiretroviral therapy. *J Infect Dis.* (2004) 189:572–82. doi: 10.1086/381396
10. Schuetz A, Deleage C, Sereti I, Rerknimitr R, Phanuphak N, Phuang-Ngern Y, et al. Initiation of ART during early acute HIV infection preserves mucosal Th17 function and reverses HIV-related immune activation. *PLoS Pathog.* (2014) 10:e1004543. doi: 10.1371/journal.ppat.1004543

11. Somsouk M, Estes JD, Deleage C, Dunham RM, Albright R, Inadomi JM, et al. Gut epithelial barrier and systemic inflammation during chronic HIV infection. *AIDS*. (2015) 29:43–51. doi: 10.1097/QAD.0000000000000511
12. Stehle JR Jr, Leng X, Kitzman DW, Nicklas BJ, Kritchevsky SB, High KP. Lipopolysaccharide-binding protein, a surrogate marker of microbial translocation, is associated with physical function in healthy older adults. *J Gerontol A Biol Sci Med Sci*. (2012) 67:1212–8. doi: 10.1093/gerona/gls178
13. Hunt PW, Sinclair E, Rodriguez B, Shive C, Clagett B, Funderburg N, et al. Gut epithelial barrier dysfunction and innate immune activation predict mortality in treated HIV infection. *J Infect Dis*. (2014) 210:1228–38. doi: 10.1093/infdis/jiu238
14. Dillon SM, Lee EJ, Kotter CV, Austin GL, Dong Z, Hecht DK, et al. An altered intestinal mucosal microbiome in HIV-1 infection is associated with mucosal and systemic immune activation and endotoxemia. *Mucosal Immunol*. (2014) 7:983–94. doi: 10.1038/mi.2013.116
15. Lozupone CA, Li M, Campbell TB, Flores SC, Linderman D, Gebert MJ, et al. Alterations in the gut microbiota associated with HIV-1 infection. *Cell Host Microbe*. (2013) 14:329–39. doi: 10.1016/j.chom.2013.08.006
16. Vujkovic-Cvijin I, Dunham RM, Iwai S, Maher MC, Albright RG, Broadhurst MJ, et al. Dysbiosis of the gut microbiota is associated with HIV disease progression and tryptophan catabolism. *Sci Transl Med*. (2013) 5:193ra191. doi: 10.1126/scitranslmed.3006438
17. Noguera-Julian M, Rocafort M, Guillen Y, Rivera J, Casadella M, Nowak P, et al. Gut microbiota linked to sexual preference and HIV infection. *EBio Med*. (2016) 5:135–46. doi: 10.1016/j.ebiom.2016.01.032
18. Psomas C, Lavigne JP, Barbuat C, Trabelsi S, Ghosn J, Lascoux-Combe C, et al. Maraviroc-induced decrease in circulating bacterial products is not linked to an increase in immune activation in HIV-infected individuals. *Blood*. (2013) 122:2282–3. doi: 10.1182/blood-2013-06-507012
19. Faust SN, Levin M, Harrison OB, Goldin RD, Lockhart MS, Kondaveeti S, et al. Dysfunction of endothelial protein C activation in severe meningococcal sepsis. *N Engl J Med*. (2001) 345:408–16. doi: 10.1056/NEJM200108093450603
20. Page AV, Liles WC. Biomarkers of endothelial activation/dysfunction in infectious diseases. *Virulence*. (2013) 4:507–16. doi: 10.4161/viru.24530
21. Zeuke S, Ulmer AJ, Kusumoto S, Katus HA, Heine H. TLR4-mediated inflammatory activation of human coronary artery endothelial cells by LPS. *Cardiovasc Res*. (2002) 56:126–34. doi: 10.1016/S0008-6363(02)00512-6
22. Meroni PL, Raschi E, Testoni C, Tincani A, Balestrieri G, Molteni R, et al. Statins prevent endothelial cell activation induced by antiphospholipid (anti-beta2-glycoprotein I) antibodies: effect on the proadhesive and proinflammatory phenotype. *Arthritis Rheum*. (2001) 44:2870–8. doi: 10.1002/1529-0131(200112)44:12<2870::AID-ART475>3.0.CO;2-Y
23. Pedersen KK, Manner IW, Seljeflot I, Kvale D, Os I, Gerstoft J, et al. Monocyte activation, but not microbial translocation, is independently associated with markers of endovascular dysfunction in HIV-infected patients receiving cART. *J Acquir Immune Defic Syndr*. (2014) 67:370–4. doi: 10.1097/QAI.0000000000000339
24. Canipe A, Chidumayo T, Blevins M, Bestawros M, Bala J, Kelly P, et al. A 12 week longitudinal study of microbial translocation and systemic inflammation in undernourished HIV-infected Zambians initiating antiretroviral therapy. *BMC Infect Dis*. (2014) 14:521. doi: 10.1186/1471-2334-14-521
25. Pedersen KK, Pedersen M, Troseid M, Gaardbo JC, Lund TT, Thomsen C, et al. Microbial translocation in HIV infection is associated with dyslipidemia, insulin resistance, and risk of myocardial infarction. *J Acquir Immune Defic Syndr*. (2013) 64:425–33. doi: 10.1097/QAI.0b013e31829f919d
26. Manner IW, Baekken M, Kvale D, Oektedalen O, Pedersen M, Nielsen SD, et al. Markers of microbial translocation predict hypertension in HIV-infected individuals. *HIV Med*. (2013) 14:354–61. doi: 10.1111/hiv.12015
27. Steele AK, Lee EJ, Vestal B, Hecht D, Dong Z, Rapaport E, et al. Contribution of intestinal barrier damage, microbial translocation and HIV-1 infection status to an inflammaging signature. *PLoS ONE*. (2014) 9:e97171. doi: 10.1371/journal.pone.0097171
28. Monnig MA, Kahler CW, Cioe PA, Monti PM, Mayer KH, Pantalone DW, et al. Markers of microbial translocation and immune activation predict cognitive processing speed in heavy-drinking men living with HIV. *Microorganisms*. (2017) 5:E64. doi: 10.3390/microorganisms5040064
29. Zhou Z, Guille C, Ogunrinde E, Liu R, Luo Z, Powell A, et al. Increased systemic microbial translocation is associated with depression during early pregnancy. *J Psychiatr Res*. (2018) 97:54–7. doi: 10.1016/j.jpsychires.2017.11.009
30. French AL, Evans CT, Agniel DM, Cohen MH, Peters M, Landay AL, et al. Microbial translocation and liver disease progression in women coinfected with HIV and hepatitis C virus. *J Infect Dis*. (2013) 208:679–89. doi: 10.1093/infdis/jit225
31. Epeldegui M, Magpantay L, Guo Y, Halec G, Cumberland WG, Yen PK, et al. A prospective study of serum microbial translocation biomarkers and risk of AIDS-related non-Hodgkin lymphoma. *AIDS*. (2018) 32:945–54. doi: 10.1097/QAD.0000000000001771
32. Bandera A, De Benedetto I, Bozzi G, Gori A. Altered gut microbiome composition in HIV infection: causes, effects and potential intervention. *Curr Opin HIV AIDS*. (2018) 13:73–80. doi: 10.1097/COH.0000000000000429

Conflict of Interest Statement: The authors declare that the research was conducted in the absence of any commercial or financial relationships that could be construed as a potential conflict of interest.

Copyright © 2019 Younas, Psomas, Reynes, Cezar, Kundura, Portales, Merle, Atoui, Fernandez, Le Moing, Barbuat, Moranne, Sotto, Sabatier, Fabbro, Vincent, Dunyach-Remy, Winter, Reynes, Lavigne and Corbeau. This is an open-access article distributed under the terms of the Creative Commons Attribution License (CC BY). The use, distribution or reproduction in other forums is permitted, provided the original author(s) and the copyright owner(s) are credited and that the original publication in this journal is cited, in accordance with accepted academic practice. No use, distribution or reproduction is permitted which does not comply with these terms.

L'ajout de 20 PVVIH plus jeunes, infectés et sous traitement depuis moins longtemps en moyenne que les patients ACTIVIH a permis de tester la robustesse du modèle de profilage décrit dans ACTIVIH. Cet ajout n'a pas perturbé la classification dans son ensemble, confirmant la solidité de cette classification ascendante hiérarchique. Depuis ce travail nous avons encore confirmé cette robustesse sur un total de près de 300 patients.

L'étude a permis d'établir un lien entre un profil et la translocation microbienne, cause connue d'activation immunitaire chez les PVVIH avirémique sous cART. Nous supposons plutôt que la translocation microbienne cause ce profil particulier d'activation immunitaire, mais on ne peut exclure qu'en plus ou à la place de ce lien causal, le schéma inverse soit possible. Effectivement, l'inflammation entrainée par l'activation immunitaire peut accroître la perméabilité de la barrière intestinale et ainsi la translocation microbienne.

II. ARTICLE « RESIDUAL VIREMIA IS LINKED TO A SPECIFIC IMMUNE ACTIVATION PROFILE IN HIV-1-INFECTED ADULTS UNDER EFFICIENT ANTIRETROVIRAL THERAPY»

Dans cet article nous avons démontré qu'une autre cause d'activation immunitaire chez les PVVIH, la virémie résiduelle, était liée à un autre profil d'activation immunitaire. A partir de la même cohorte de patients et la même classification que celle développée dans le travail sur la translocation microbienne (Younas et al. 2019), nous avons établi un lien entre le profil E et le niveau de virémie résiduelle ainsi que le nombre de virémies détectables transitoirement ou 'blips' sur deux ans de ces patients.

Généralement le statut viral des PVVIH peut être divisé en deux grandes catégories : virémique et avirémique selon que la charge virale plasmatique du patient est supérieure ou inférieure au seuil de détection qui, aux CHU de Nîmes et de Montpellier est placé à 20 copies d'ARN VIH/mL. Dans ce travail nous avons étudié plus en détail le statut viral des avirémiques. La virémie des PVVIH dits avirémiques a donc été précisée. Un patient peut être en dessous du seuil de détection mais présenter entre 1 et 20 copies d'ARN viral/mL de plasma : on considère alors que sa virémie est détectable bien que résiduelle. Ou alors un patient peut ne présenter aucune molécule d'ARN VIH-1 détectable dans son sang : il a une virémie indétectable. Les blips quant à eux sont définis comme une augmentation transitoire de la virémie du patient au-dessus du seuil de détection (ici 20 copies/mL). Cette augmentation n'est pas considérée comme un signe d'échec virologique tant que la virémie redescend sous le seuil de détection à la détermination suivante.

Durant les deux années précédant l'inclusion dans la cohorte, les patients du profil E présentaient en moyenne une plus grande fréquence de virémie détectable (66.7%) que les patients d'un autre profil (23.8%). Ces patients du profil E ont également eu plus de blips que les autres (39.5% contre 21.1%) durant cette période.

Nous avons observé que les patients de ce profil E présentent un haut niveau de LT4 et particulièrement de LT4 activés (présentant le marqueur CD38 à leur surface). La présence de LT4 CD38+ a encore récemment été associée à la taille du réservoir chez les PVVIH avirémique sous cART (Song et al. 2020).

Nous avons également observé une corrélation entre le taux de D-Dimère présent dans le plasma des patients au moment de l'étude et le pourcentage de blips observé dans les deux ans précédents l'étude. Les D-dimères sont produits lors de la dégradation de la fibrine. Dans ce profil le taux d'activateur tissulaire du plasminogène (tPA) présent dans leur plasma était corrélé au pourcentage de virémies détectées les deux années précédant l'étude (figure 4F). Le tPA est un marqueur d'activation endothélial jouant un rôle clé dans la fibrinolyse : il empêche la formation de thromboses. Les patients du profil E ont également plus de récepteur de la protéine C endothéliale (EPCR) soluble dans leur plasma, qui est également un marqueur d'activation endothélial (Figure 4E)

frontiers in Immunology

ORIGINAL RESEARCH
published: 30 March 2021
doi: 10.3389/fimmu.2021.663843

Residual Viremia Is Linked to a Specific Immune Activation Profile in HIV-1-Infected Adults Under Efficient Antiretroviral Therapy

OPEN ACCESS

Edited by:
Remi Cheynier,
INSERM U1016 Institut Cochin,
France

Reviewed by:
Jean-Pierre Routy,
McGill University, Canada
Petronela Ancuta,
Université de Montréal, Canada

***Correspondence:**
Pierre Corbeau
pcorbeau@igh.cnrs.fr

†These authors have contributed equally to this work and share first authorship

Specialty section:
This article was submitted to Viral Immunology, a section of the journal Frontiers in Immunology

Received: 03 February 2021
Accepted: 15 March 2021
Published: 30 March 2021

Citation:
Younas M, Psomas C, Reynes C, Cezar R, Kundura L, Portalès P, Merle C, Atoui N, Fernandez C, Le Moing V, Barbuat C, Sotto A, Sabatier R, Winter A, Fabbro P, Vincent T, Reynes J and Corbeau P (2021) Residual Viremia Is Linked to a Specific Immune Activation Profile in HIV-1-Infected Adults Under Efficient Antiretroviral Therapy. Front. Immunol. 12:663843. doi: 10.3389/fimmu.2021.663843

*Mehwish Younas[1†], Christina Psomas[1,2†], Christelle Reynes[3], Renaud Cezar[4], Lucy Kundura[1], Pierre Portalès[5], Corinne Merle[2], Nadine Atoui[2], Céline Fernandez[2], Vincent Le Moing[2,6,7], Claudine Barbuat[8], Albert Sotto[7,8], Robert Sabatier[3], Audrey Winter[1], Pascale Fabbro[9], Thierry Vincent[5,7], Jacques Reynes[2,6,7] and Pierre Corbeau[1,4,7]**

[1] Institute for Human Genetics, CNRS, Montpellier, France, [2] Infectious Diseases Department, Montpellier University Hospital, Montpellier, France, [3] Institute for Functional Genomics, Montpellier University, Montpellier, France, [4] Immunology Department, University Hospital, Nîmes, France, [5] Immunology Department, University Hospital, Montpellier, France, [6] IRD UMI 233, INSERM U1175, Montpellier University, Montpellier, France, [7] Faculty of Medicine, Montpellier University, Montpellier, France, [8] Infectious Diseases Department, University Hospital, Nîmes, France, [9] Medical Informatics Department, University Hospital, Nîmes, France

Chronic immune activation persists in persons living with HIV-1 even though they are aviremic under antiretroviral therapy, and fuels comorbidities. In previous studies, we have revealed that virologic responders present distinct profiles of immune activation, and that one of these profiles is related to microbial translocation. In the present work, we tested in 140 HIV-1-infected adults under efficient treatment for a mean duration of eight years whether low-level viremia might be another cause of immune activation. We observed that the frequency of viremia between 1 and 20 HIV-1 RNA copies/mL (39.5 ± 24.7% versus 21.1 ± 22.5%, p = 0.033) and transient viremia above 20 HIV-1 RNA copies/mL (15.1 ± 16.9% versus 3.3 ± 7.2%, p = 0.005) over the 2 last years was higher in patients with one profile of immune activation, Profile E, than in the other patients. Profile E, which is different from the profile related to microbial translocation with frequent CD38+ CD8+ T cells, is characterized by a high level of CD4+ T cell (cell surface expression of CD38), monocyte (plasma concentration of soluble CD14), and endothelium (plasma concentration of soluble Endothelial Protein C Receptor) activation, whereas the other profiles presented low CD4:CD8 ratio, elevated proportions of central memory CD8+ T cells or HLA-DR+ CD4+ T cells, respectively. Our data reinforce the hypothesis that various etiological factors shape the form of the immune activation in virologic responders, resulting in specific profiles. Given the type of immune activation of Profile E, a potential causal link between low-level viremia and atherosclerosis should be investigated.

Keywords: low-level viremia, blip, inflammation, virologic responder, endothelium activation, coagulation

INTRODUCTION

Immune activation (IA)-related comorbidities are becoming a major concern in aviremic HIV-infected persons under antiretroviral therapy (ART) (1). For instance, atherosclerosis has been linked to inflammation and coagulation, interleukin-6 (IL-6) and D-dimer correlating positively with a greater risk of fatal cardiovascular disease (2), as well as to CD8+ T cell activation (HLA-DR and CD38 coexpression) (3) and monocyte (soluble CD163 level and cell surface coexpression of CD14 and CD16) activation (3, 4). It is therefore important to better identify the causes of this IA. HIV itself may be one of these drivers. Although HIV RNA levels are below the detection level of routine tests in these patients, most of them still produce low levels of virus, and HIV (glyco)proteins may be detected in their lymph nodes (5). Many HIV components may directly activate the innate immune system. For example, gp120 (6) Nef and Vpr (7) have been reported to directly activate monocytes and macrophages, and gp41 T cells (8). It has also been reported that HIV RNA induces interferon-α production by plasmacytoid dendritic cells *via* TLR-7 and TLR-9. Moreover, HIV antigens detected by specific B lymphocytes and T cells trigger an adaptive immune response. Finally, even a truncated CD4+ T cell infection may induce caspase-1 activation and IL-1β production in CD4+ T cells (9). In addition, HIV might also favor other causes of IA (10). Thus, Nef protein is also known to interact with the adenosine-triphosphate-binding cassette A1 transporter. This interaction interferes with cholesterol metabolism, and may promote pro-inflammatory metabolic disorders (11). Likewise, HIV-mediated IA might promote immune senescence, which is an additional cause of IA.

Yet authors looking for correlations between residual viremia and IA markers obtained contradictory results. Some authors found a link between residual viremia and inflammation (12), CD4+ T cell activation (13), and monocyte activation (12). By contrast, other authors did not observe such correlations (14–17).

Recent data however argue for a role of persistent viral production in IA. First, in virologic responders, higher levels of the inflammatory markers C-reactive protein (CRP), Tumor Necrosis Factor α (TNFα), IL-6, interferon γ (IFNγ) and/or the monocyte activation marker soluble CD14 (sCD14) have been reported in non-fully adherent patients than in fully adherent patients (18, 19). Second, in elite controllers, who are aviremic in the absence of treatment, intermittent bouts of viremia, so-called blips, are associated with a low CD4/CD8 ratio which is a global marker of IA (20). Moreover, the initiation of ART in these patients reduces CD4+ T cell and CD8+ T cell activation in the blood as well as in the gastrointestinal associated lymphoid tissues (21). Third, switching from a 3-drug regimen to some 2-drug ART regimens may result in an increase in CD8+ T cell counts (22, 23).

Knowing whether low-level viremia is a cause of IA is particularly important at a time when 2-drug regimens rather than 3-drug ART regimens (24), day-on, day-off schedules (25), and intermittent four-days-a-week treatments (26) are being proposed.

In a previous study, we analyzed 64 soluble and cell surface markers of inflammation and CD4+ and CD8+ T cell, B cell, monocyte, NK cell, and endothelial activation in 140 adults under effective ART. A double hierarchical clustering of patients and markers unveiled that these virologic responders had 5 different IA profiles (27). The first profile was characterized by a high percentage of central memory CD8+ T cells, the second by a low CD4:CD8 ratio, the third by frequent HLA-DR+ CD4+ T cells, and the two last profiles by an elevated proportion of CD38-expressing CD8+ and CD4+ T cells, respectively. In this present study, we looked for a link between one of those profiles and residual viremia.

MATERIALS AND METHODS

Study Design

This cross-sectional observational study has already been previously described (27). We recruited 140 HIV-1-infected adults with CD4 count above 200 cells/μL. Viremia of all participants, under stable ART, was below 50 copies per mL for at least 6 months before inclusion. We also recruited 150 persons with a mean ± SD age of 62 ± 4 years in the general population. Pregnant or breastfeeding women, persons under treatment or presenting a disease likely to modify the immune system were not included. Blood samples for immune profiling were collected once between April 2014 and June 2016. This study was approved by the Ethics Committee of Montpellier University Hospital. All patients provided written informed consent. The trial was registered on ClinicalTrials.gov (NCT02334943).

Immune Activation Markers

Using flow cytometry as previously described (28), we determined cell surface markers for the differentiation, activation, senescence, and/or exhaustion of CD4+ T lymphocytes, CD8+ T lymphocytes, and NK cells. We used ELISA to quantify soluble TNF receptor I (sTNFRI), sCD14 and soluble CD163 (sCD163), tissue Plasminogen Activator (tPA), soluble Thrombomodulin (sTM), and soluble Endothelial Protein C Receptor (sEPCR) and, by turbidimetry, CRP, immunoglobulins (Ig) and D-dimers also as previously reported (28).

Residual Viremia

HIV-1 RNA plasma level was quantified using the Amplicor HIV-1 Monitor test (Roche Diagnostic Systems). The test has a positive threshold of 20 copies/mL, and discriminates samples containing no detectable copies in 1mL from samples containing 1 to 20 copies/mL. We also recorded the percentage of blips, defined as isolated episodes of viremia > 20 copies/mL, within the 2 years preceding the analysis of the immune profile. The frequency of detectable viremia and blips over the 2 last years was determined on 4 to 8 measurements.

Statistical Analysis

Fisher's exact test or $\chi 2$ test was used to compare qualitative covariates. For quantitative covariates, on one hand, when comparing two groups (e.g. undetectable vs detectable viremia), we compared the distributions of covariates using the Student T-test or the Wilcoxon-Mann-Whitney test as appropriate. On the other hand, when comparing profiles together for example (i.e. more than two groups), the comparison was made using Anova or the Kruskal-Wallis H test as appropriate. Correlations were evaluated by Pearson, Spearman or Kendall test as appropriate. Normality was assessed using the Shapiro-Wilk test.

All analyses were performed using R software, version 3.6.1 (R Development Core Team, A Language and Environment for Statistical Computing, Vienna, Austria, 2016. https://www.R-project.org/).

Funding Source

Nîmes and Montpellier University Hospitals, MSD and MSDAVENIR.

RESULTS

Study Subjects

HIV-1-infected adults (n = 140), under efficient ART for a mean (SD) duration of 7.9 (4.1) years, were recruited at the University Hospitals of Nîmes and Montpellier, France. Eighty-one percent of patients were male, with a mean age of 56 (9) years. Their pretherapeutic CD4 count and viremia were 199 (119) cells/μL and 1,4372,216 (9,602,969) HIV RHA copies/mL, respectively. Their current mean CD4 count was 733 ± 375 cells/μL, and their CD4/CD8 ratio 1.24 (0.88). ART regimens and co-infections are given in **Table 1**.

Residual Viremia

In this study population, the frequency of residual viremia (1-20 copies/mL) at the time of study was 26%. There was no difference, neither in age (56.1 ± 8.5 versus 55.9 ± 10.1 years, p = 0.771), duration of infection (14.5 ± 8.0 versus 16.8 ± 7.7 years, p = 0.168) nor aviremia (7.0 ± 3.5 versus 8.3 ± 4.2 years, p = 0.155), nor in pretherapeutic CD4 count (164 ± 110 versus 159 ± 103 cells/mL, p = 0.980) nor pretherapeutic viremia (4,782,630 ± 20,381,332 versus 530,006 ± 1,733,809 copies/mL, p = 0.831) between patients with detectable and undetectable viremia, respectively. Likewise, no link could be established between residual viremia and the use of nucleoside reverse transcriptase inhibitors (p = 0.999), non-nucleoside reverse transcriptase inhibitors (p = 0.999), protease inhibitors (p = 0.969), or integrase inhibitors (p = 0.900).

The percentage of samples with detectable viremia (1-20 HIV-1 RNA copies/mL) or blips (isolated viremia > 20 HIV-1 RNA copies/mL) during the two years preceding the study was available for 135 out of 140 participants. These percentages of samples with detectable viremia (47.1 ± 21.0% versus 19.0 ± 21.0%, $p < 10^{-4}$, **Figure 1A**) and blips (9.8 ± 11.5% versus 2.1 ± 5.9%, $p < 10^{-4}$, **Figure 1B**) were higher in patients with detectable viremia than in patients with undetectable viremia at the time of the study.

TABLE 1 | Bioclinical characteristics of the study population.

Characteristics		HIV+ Treated
Number of individuals		140
Nucleoside reverse transcriptase inhibitor	N (%)	128 (91)
Non-nucleoside reverse transcriptase inhibitor	N (%)	50 (36)
Protease inhibitor	N (%)	67 (48)
Integrase inhibitor	N (%)	44 (31)
HBs Ag+	N (%)	3 (2)
Anti-HBs Ab+	N (%)	61 (44)
Anti-HBc Ab+	N (%)	54 (39)
HCV coinfection	N (%)	6 (4)
CMV coinfection	N (%)	124 (89)
EBV coinfection	N (%)	138 (99)
HAV coinfection	N (%)	97 (69)

HBs Ag, Hepatitis B surface antigen; HBc, Hepatitis B core; HCV, Hepatitis C Virus; CMV, Cytomegalovirus; EBV, Epstein-Barr Virus; HAV, Hepatitis A Virus.

Relationships Between Residual Viremia and Biomarkers

We determined the numbers and percentages of the following subpopulations: (i) activated (HLA-DR+ and/or CD38+), exhausted (PD-1+), senescent (CD57+, eventually CD27- and CD28-), naïve (CD45RA+CD27+), central and effector (CD45RA-CD27+ and CD45RA-CD27-, respectively) memory CD4+ and CD8+ T cells, (ii) activated (HLA-DR+), dysfunctional (CD56-), and senescent (CD57+) NK cells. Monocyte activation was evaluated by measuring sCD14 and sCD163, and B cell activation by measuring IgM, IgG, and IgA levels. Inflammation was monitored by quantifying sTNFRI and CRP. tPA, sTM, and sEPCR were used as markers of endothelium activation, and D-dimers were used as an indicator of fibrinolysis.

We compared residual viremia and blip frequency, i.e. for each participant, the frequency where the participant displayed low-level viremia or blips during the two last years with each one of these markers. The only link we revealed was with D-dimers. Patients with 1-20 HIV-1 RNA copies at the time of the study presented higher D-dimer levels than patients with undetectable viremia (n = 119, 708 ± 841 versus 411 ± 535 ng/mL, p = 0.015, **Figure 1C**). Moreover, there was a correlation between blip frequency over the two last years and D-dimer levels (n = 119, Kendall coefficient = 0.190, p = 0.009, **Figure 1D**). Looking for correlations between D-dimers and patient characteristics as well as other markers, we observed links between the coagulation marker, participant age (r = 0.295, p = 0.001, **Figure 2A**), pretherapeutic CD4 count (r = -0.182, p = 0.046, **Figure 2B**), the inflammation markers CRP (r = 0.364, $p < 10^{-4}$, **Figure 2C**) and sTNFRI (r = 0.293, p = 0.001, **Figure 2D**), the monocyte activation marker sCD163 (r = 0.253, p = 0.005, **Figure 2E**), and the endothelial activation marker sEPCR (r = 0.265, p = 0.003, **Figure 2F**).

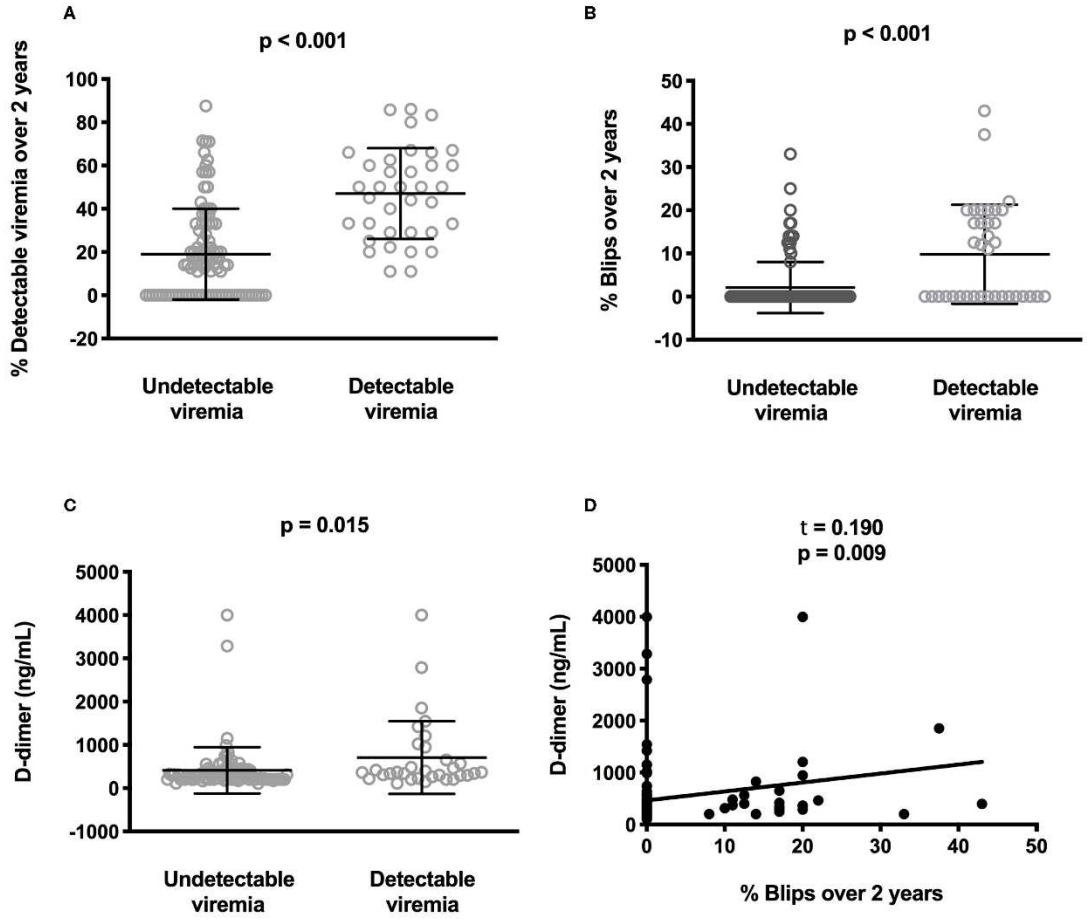

FIGURE 1 | Correlations between low-level viremia, blips, and D-dimer plasma levels. Difference for each participant in the frequency where the participant displayed low-level viremia **(A)** or blips **(B)** over the two last years between participants with or without current detectable viremia. Difference in circulating D-dimer concentrations between participants with or without current detectable viremia. Statistical analyses were performed using a Mann-Whitney test **(C)**. Correlation between the frequency of blips over the two last years and D-dimer plasma levels. Statistical analysis was performed using Kendall correlation **(D)**.

Residual Viremia Over Time Is Related to a Specific Immune Activation Profile

We previously reported that two independent hierarchical clustering analyses of the activation markers for the 140 patients had identified 5 groups of individuals presenting different IA profiles (Profiles A to E). Duration of infection and aviremia, nadir CD4, pretherapeutic viral load and CD4:CD8 ratio, as well as age were not different between Profile E and the other Profiles (27). There was differences neither in nucleoside reverse transcriptase inhibitor (p = 0.565), non-nucleoside reverse transcriptase inhibitor (p = 0.999), protease inhibitor (p = 0.165), nor in integrase inhibitor (0.999) usage between Profile E and the other profiles. The only difference was a tendency to a higher proportion of females in Profile E (p = 0. 061) (27). Yet, the frequency of detectable viremia (p = 0.999) or blips (p = 0.278) during the two years were not different between males and females (data not shown).

Interestingly, one of these profiles, Profile D, was linked to microbial translocation (27). We reasoned that another IA profile could be linked to another cause of IA, residual viral production. To test this hypothesis, we compared the frequency of residual viremia and the occurrence of blips over time between the IA profiles. Detectable viremia at the time of the study was more frequent in patients with Profile E than in the other patients (66.7% versus 23.8%, p = 0.011, **Figure 3A**). The frequency of detectable viremia over the 2 last years was also higher in Profile E patients than in patients with other profiles (39.5 ± 24.7% versus 21.1 ± 22.5%, p = 0.033, **Figure 3B**). Likewise, previous blip frequency was higher in Profile E patients than in the patients with other profiles (15.1 ± 16.9% versus 3.3 ± 7.2%, p = 0.005, **Figure 3C**).

Characterization of the Immune Activation Profile Related to Residual Viremia

No difference in duration of infection (p = 0.191) and of viral suppression (p = 0.285), in pretherapeutic viremia (p = 0.881) or

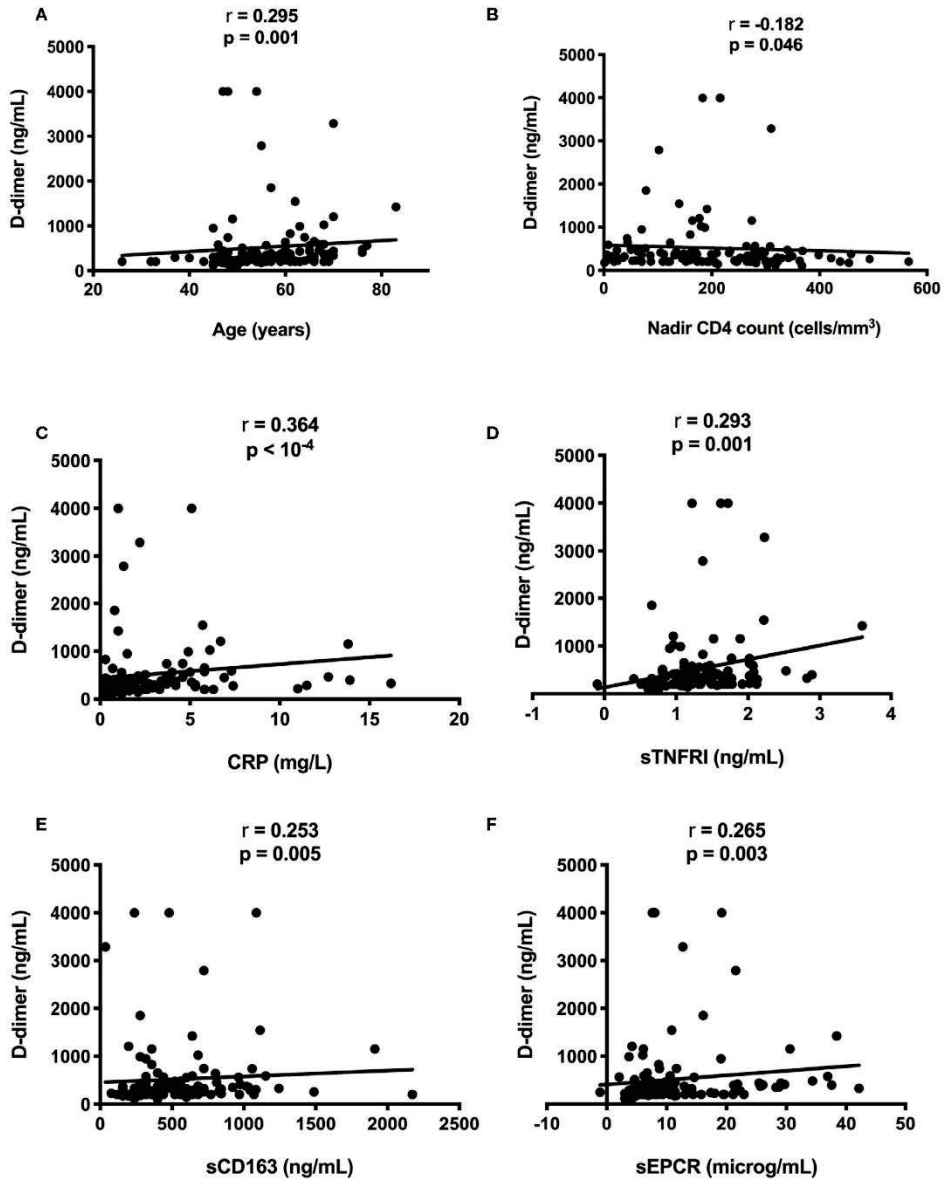

FIGURE 2 | Correlations between D-dimer level, participant age **(A)** and pretherapeutic CD4 count **(B)**, CRP **(C)**, sTNFRI **(D)**, sCD163 **(E)**, and sEPCR **(F)**.

CD4 count (0.285), and in age (p = 0.138) was observed between Profile E patients and patients with other profiles (data not shown). Compared with the other patients, Profile E patients had higher CD4 counts (1567 ± 451 versus 669 ± 288 cells/mL, $p < 10^{-4}$, **Figure 4A**) and CD4:CD8 ratios (2.79 ± 2.48 versus 1.14 ± 0.57, p < 0.001, **Figure 4B**). They also presented higher levels of sCD14 (3.76 ± 0.50 versus 3.37 ± 1.08 mg/mL, p = 0.030, **Figure 4C**) and higher percentages of CD38-positive CD4+ T-cells (73.1 ± 11.4% versus 55.9 ± 12.4%, $p < 10^{-4}$, **Figure 4D**) compared with the other patients. Profile E was also characterized by a high level of the endothelium activation marker sEPCR (18 ± 12% versus 10 ± 8%, p = 0.035, **Figure 4E**). Moreover, in Profile E patients there was a strong link between frequency of detectable viremia over the 2 last years and another endothelium activation marker, tPA (r = 0.687, p = 0.006, **Figure 4F**).

DISCUSSION

It is logical to assume that residual viremia should fuel immune activation in virological responders. Yet, although some authors have indeed found a link between low-level

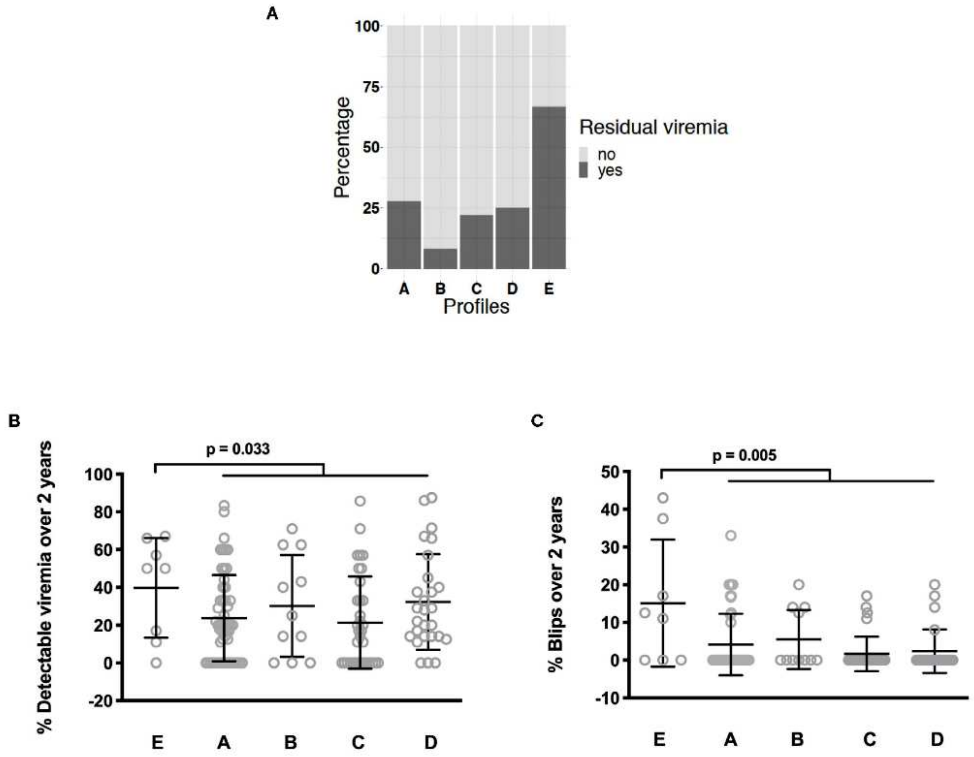

FIGURE 3 | Differences in the frequency of current low-level viremia between the various IA profiles. Statistical analyses were performed using a Kruskal-Wallis H test **(A)**. Differences in the frequency of low-level viremia **(B)** and blips **(C)** over the two last years between the various IA profiles. Statistical analyses were performed using a Mann-Whitney test.

viremia and IA (12, 13), others have not (14–17). This discrepancy might be due to differences in the size and/or bioclinical characteristics of the populations under study, as well as the actual definition of residual viremia. Here, we show that the frequency of detectable HIV-1 RNA and blips over a period of 2 years is associated with a specific profile of IA, Profile E. There may be two explanations for why we observed such a correlation whereas other authors had failed to identify it. First, a 24-month follow-up of viral load is more sensitive than a single measurement. Second, our two-step approach, consisting of clustering IA profiles in the patient population and thereafter looking for correlations between each of these profiles and residual viremia, may have unveiled links which would have been hidden in searches for such links in the global population. For instance, in our study, whereas high sCD14 levels and percentages of CD4+ T cells expressing CD38 characterize Profile E, these markers are not associated with residual viremia when taking into account the 140 participants.

The high circulating concentrations of sCD14 that we observed in Profile E patients is in line with the link between this IA marker and residual viremia reported by other authors (12). This link might be explained by the fact that the presence of viral components within the gut-associated lymphoid tissues might be responsible for local inflammation and thereby an increase in gut permeability facilitating microbial translocation (29). This could thus be a first argument in favor of a causal link between residual viremia and Profile E.

Previously, CD4+ T cell activation has also been found to be associated with residual viremia (13). Here again, it may be the presence of viral components that trigger this form of IA. Indeed, gp41 has been reported to interact with the T cell receptor and to facilitate thereby T lymphocyte activation (8). Moreover, Doitsh et al. observed that the presence of HIV DNA in CD4+ T cell provokes inflammasome activation, even though the viral life cycle is truncated (9). Consequently, CD4+ T cell activation in Profile E patients may be induced by the presence of the virus.

Compared with the other IA profiles, Profile E is also characterized by a high level of sEPCR. sEPCR results from the cleavage of the external portion of the protein C receptor on the surface of endothelial cells activated by thrombin, TNFα, IL-1 or endotoxins (30). An increase in sEPCR has already been reported in HIV infection (31, 32). A decrease in sEPCR under 48-week ART has even been correlated with HIV RNA changes (32). This is in line with the hypothesis that the presence of HIV may provoke EPCR cleavage, and further argues for a model in which Profile E is the consequence of residual viral production.

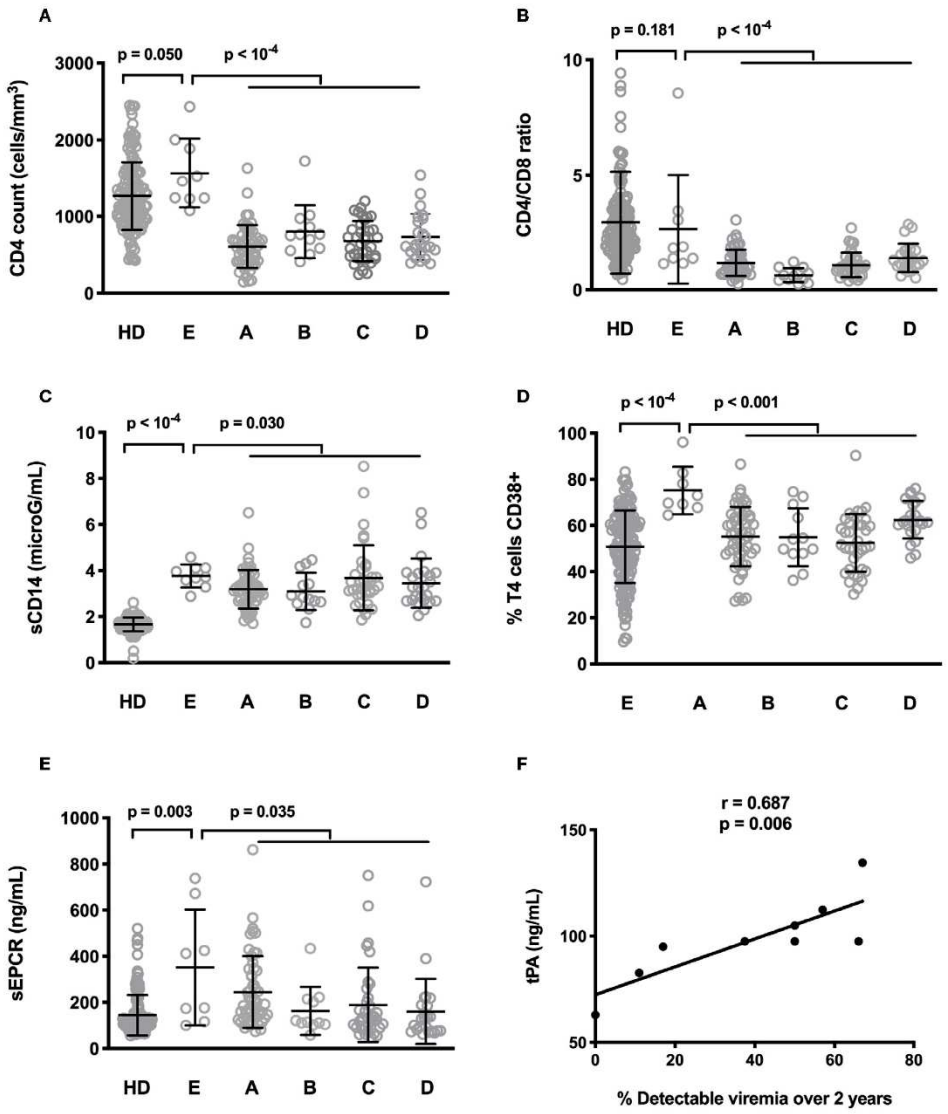

FIGURE 4 | Differences in CD4 count **(A)**, CD4:CD8 ratio **(B)**, sCD14 **(C)**, frequency of CD4+ T cells expressing CD38 **(D)**, and sEPCR **(E)** between healthy donors (HD) and people living with HIV-1 with the five IA profiles. Statistical analyses were performed using a Mann-Whitney test. Correlation between low-level viremia over the two last years and tPA in Profile E participants. Statistical analysis was performed using Spearman correlation **(F)**.

One consequence of our results is that we now know that residual viremia should be sought in patients with increased proportions of CD38+CD4+ T cell, sCD14 and/or sEPCR. Moreover, in these patients, potential causes of this residual viremia, e.g., non-optimal adherence to treatment or partial resistance to the current antiretroviral regimen, should also be investigated.

Globally, the present data support the idea that, depending on the etiological factor at work, microbial translocation for Profile D patients (27) and residual viremia for Profile E patients (present study), virologic responders develop a particular IA profile. As we have also established that a specific IA profile may be related to a specific comorbidity, insulin resistance (28), we propose a model in which a cause of IA may fuel an IA profile that may favor an IA-related morbidity. To further test this hypothesis, tissue evaluation of the IA, particularly in secondary lymphoid organs, and functional assays would be necessary. According to this model, the fact that we have shown that residual viremia is associated with a marker of monocyte activation (sCD14), two markers of endothelial activation (sEPCR and tPA), and a marker of coagulation (D-dimer), three forms of activation known to favor atherothrombosis (33–35), should encourage us to search for a link between residual viremia and atherosclerosis.

DATA AVAILABILITY STATEMENT

The raw data supporting the conclusions of this article will be made available by the authors, without undue reservation.

ETHICS STATEMENT

The studies involving human participants were reviewed and approved by Ethics Committee of Montpellier University Hospital, France. The patients/participants provided their written informed consent to participate in this study.

AUTHOR CONTRIBUTIONS

MY and LK contributed to the design of the flow cytometry study, and acquired, analyzed, and interpreted cell surface and soluble marker data. CP contributed to the design of the study, the enrolment of patients, and acquired, analyzed and interpreted the data. RC, PP, and TV contributed to the design of the flow cytometry study and acquired, analyzed and interpreted cell surface markers. CR, RS, AW, and PF contributed to the design of the statistical study and acquired, analyzed, and interpreted the statistical data. CM, NA, CF, VL, CB, and AS acquired, analyzed, and interpreted clinical data. JR contributed to the design of the study and analyzed and interpreted the data. PC contributed to the design of the study, analyzed, and interpreted data, and wrote the first draft of the manuscript. All authors contributed to the article and approved the submitted version.

FUNDING

The study was funded by MSD, MSDAvenir, and the university hospitals of Montpellier and Nîmes. These sponsors had no role in the study design, the collection, analysis, or interpretation of data, the writing of the report, nor in the decision to submit the paper for publication.

ACKNOWLEDGMENTS

We are grateful to the persons who volunteered for this study and to Teresa Sawyers for the critical reading of the manuscript.

REFERENCES

1. Miller CJ, Baker JV, Bormann AM, Erlandson KM, Hullsiek KH, Justice AC, et al. Adjudicated morbidity and mortality outcomes by age among individuals with HIV infection on suppressive antiretroviral therapy. *PLoS One* (2014) 9:e95061. doi: 10.1371/journal.pone.0095061
2. Nordell AD, McKenna M, Borges AH, Duprez D, Neuhaus J, Neaton JD, et al. Severity of cardiovascular disease outcomes among patients with HIV is related to markers of inflammation and coagulation. *J Am Heart Assoc* (2014) 3:e000844. doi: 10.1161/JAHA.114.000844
3. Longenecker CT, Funderburg NT, Jiang Y, Debanne S, Storer N, Labbato DE, et al. Markers of inflammation and CD8 T-cell activation, but not monocyte activation, are associated with subclinical carotid artery disease in HIV-infected individuals. *HIV Med* (2013) 14:385–90. doi: 10.1111/hiv.12013
4. Fitch KV, Srinivasa S, Abbara S, Burdo TH, Williams KC, Eneh P, et al. Noncalcified coronary atherosclerotic plaque and immune activation in HIV-infected women. *J Infect Dis* (2013) 208:1737–46. doi: 10.1093/infdis/jit508
5. Popovic M, Tenner-Racz K, Pelser C, Stellbrink H-J, van Lunzen J, Lewis G, et al. Persistence of HIV-1 structural proteins and glycoproteins in lymph nodes of patients under highly active antiretroviral therapy. *Proc Natl Acad Sci U S A* (2004) 102:14807–12. doi: 10.1073/pnas.0506857102
6. Planès R, Serrero M, Leghmari K, BenMohamed L, Bahraoui B. HIV-1 Envelope Glycoproteins Induce the Production of TNF-α and IL-10 in Human Monocytes by Activating Calcium Pathway. *Sci Rep Sci Rep* (2018) 8(1):17215. doi: 10.1038/s41598-018-35478-1
7. Lawn SD, Butera ST, Folks TM. Contribution of immune activation to the pathogenesis and transmission of human immunodeficiency virus type 1 infection. *Clin Microbiol* (2001) 14:753–77. doi: 10.1128/CMR.14.4.753-777.2001
8. Yakovian O, Schwarzer R, Sajman J, Neve-Oz Y, Razvag Y, Herrmann A, et al. Gp41 dynamically interacts with the TCR in the immune synapse and promotes early T cell activation. *Sci Rep* (2018) 8:9747. doi: 10.1038/s41598-018-28114-5
9. Doitsh G, Cavrois M, Lassen KG, Zepeda O, Yang Z, Santiago ML, et al. Abortive HIV infection mediates CD4 T cell depletion and inflammation in human lymphoid tissue. *Cell* (2010) 143:789–801. doi: 10.1016/j.cell.2010.11.001
10. Younas M, Psomas C, Reynes J, Corbeau P. Immune activation in the course of HIV-1 infection: Causes, phenotypes and persistence under therapy. *HIV Med* (2016) 17:89–105. doi: 10.1111/hiv.12310
11. Mujawar Z, Rose H, Morrow MP, Pushkarsky T, Dubrovsky L, Mukhamedova N, et al. Human immunodeficiency virus impairs reverse cholesterol transport from macrophages. *PLoS Biol* (2006) 4:e365. doi: 10.1371/journal.pbio.0040365
12. Falasca F, Di Carlo D, De Vito C, Bon I, d'Ettorre G, Fantauzzi A, et al. Evaluation of HIV-DNA and inflammatory markers in HIV-infected individuals with different viral load patterns. *BMC Infect Dis* (2017) 17:581. doi: 10.1186/s12879-017-2676-2
13. Hatano H, Jain V, Hunt PW, Lee TH, Sinclair E, Do TD, et al. Cell-based measures of viral persistence are associated with immune activation and programmed cell death protein 1 (PD-1)-expressing CD4+ T cells. *J Infect Dis* (2013) 213:370–8. doi: 10.1093/infdis/jis630
14. Guihot A, Dentone C, Assoumou L, Parizot C, Calin R, Seang S, et al. Residual immune activation in combined antiretroviral therapy-treated patients with maximally suppressed viremia. *AIDS* (2016) 30:327–30. doi: 10.1097/QAD.0000000000000815
15. Gandhi RT, McMahon DK, Bosch RJ, Lalama CM, Cyktor JC, Macatangay BJ, et al. Levels of HIV-1 persistence on antiretroviral therapy are not associated with markers of inflammation or activation. *PLoS Pathog* (2011) 13:e1006285. doi: 10.1371/journal.ppat.1006285
16. Chun T-W, Murray D, Justement JS, Hallahan CW, Moir S, Kovacs C, et al. Relationship between residual plasma viremia and the size of HIV proviral DNA reservoirs in infected individuals receiving effective antiretroviral therapy. *J Infect Dis* (2011) 204:135–8. doi: 10.1093/infdis/jir208
17. Allavena C, Rodallec A, Sécher S, Reliquet V, Baffoin S, André-Garnier E, et al. Evaluation of residual viremia and quantitation of soluble CD14 in a large cohort of HIV-infected adults on a long-term non-nucleoside reverse transcriptase inhibitor-based regimen. *J Med Virol* (2013) 85:1878–82. doi: 10.1002/jmv.23679
18. Castillo-Mancilla JR, Brown TT, Erlandson KM, Palella FJJ, Gardner EM, Macatangay BJC, et al. Suboptimal Adherence to Combination Antiretroviral Therapy Is Associated With Higher Levels of Inflammation Despite HIV Suppression. *Clin Infect Dis* (2016) 63:1661–7. doi: 10.1093/cid/ciw650
19. Castillo-Mancilla JR, Morrow M, Boum Y, Byakwaga H, Haberer JE, Martin JN, et al. Brief Report: Higher ART Adherence Is Associated With Lower

Systemic Inflammation in Treatment-Naive Ugandans Who Achieve Virologic Suppression. *J Acquir Immune Defic Syndr* (2018) 77:507–13. doi: 10.1097/QAI.0000000000001629

20. Chereau F, Madec Y, Sabin C, Obel N, Ruiz-Mateos E, Chrysos G, et al. Impact of CD4 and CD8 dynamics and viral rebounds on loss of virological control in HIV controllers. *PLoS One* (2017) 12:e0173893. doi: 10.1371/journal.pone.0173893
21. Hatano H, Yukl SA, Ferre AL, Graf EH, Somsouk M, Sinclair E, et al. Prospective antiretroviral treatment of asymptomatic, HIV-1 infected controllers. *PLoS Pathog* (2013) 9:e1003691. doi: 10.1371/journal.ppat.1003691
22. Mussini C, Lorenzini P, Cozzi-Lepri A, Marchetti G, Rusconi S, Gori A, et al. Switching to dual/monotherapy determines an increase in CD8+ in HIV-infected individuals: an observational cohort study. *BMC Med* (2018) 16:79. doi: 10.1186/s12916-018-1046-2
23. Quiros-Roldan E, Magro P, Raffetti E, Izzo I, Borghetti A, Lombardi F, et al. Biochemical and inflammatory modifications after switching to dual antiretroviral therapy in HIV-infected patients in Italy: a multicenter retrospective cohort study from 2007 to 2015. *BMC Infect Dis* (2018) 18285. doi: 10.1186/s12879-018-3198-2
24. Moreno S, Perno CF, Mallon PW, Behrens G, Corbeau P, Routy JP, et al. Two-drug vs. three-drug combinations for HIV-1: Do we have enough data to make the switch? *HIV Med* (2019) 20(Suppl 4):2–12. doi: 10.1111/hiv.12716
25. Costantini A, Tontini C, Rocchi M, Martini M, Butini L. Day-On, Day-Off emtricitabine, tenofovir disoproxil fumarate and efavirenz single tablet regimen (DODO) as maintenance therapy in HIV-infected patients. *Infez Med* (2018) 26:126–32.
26. de Truchis P, Assoumou L, Landman R, Mathez D, Le Dû D, Bellet J, et al. Four-days-a-week antiretroviral maintenance therapy in virologically controlled HIV-1-infected adults: the ANRS 162-4D trial. *J Antimicrob Chemother* (2018) 73:738–47. doi: 10.1093/jac/dkx434
27. Younas M, Psomas C, Reynes C, Cezar R, Kundura L, Portales P, et al. Microbial Translocation Is Linked to a Specific Immune Activation Profile in HIV-1-Infected Adults With Suppressed Viremia. *Front Immunol* (2019) 10:2185. doi: 10.3389/fimmu.2019.02185
28. Psomas C, Younas M, Reynes C, Cezar R, Portales P, Tuaillon E, et al. One of the immune activation profiles observed in HIV-1-infected adults with suppressed viremia is linked to metabolic syndrome: The ACTIVIH study. *EBioMedicine* (2016) 8:265–76. doi: 10.1016/j.ebiom.2016.05.008
29. Reus S, Portilla J, Sánchez-Payá J, Giner L, Francés R, Such J, et al. Low-level HIV viremia is associated with microbial translocation and inflammation. *J Acquir Immune Defic Syndr* (2013) 62:129–34. doi: 10.1097/QAI.0b013e3182745ab0
30. Van de Wouwer M, Collen D, Conway EM. Thrombomodulin-protein C-EPCR system: integrated to regulate coagulation and inflammation. *Arterioscler Thromb Vasc Biol* (2004) 24:1374–83. doi: 10.1161/01.ATV.0000134298.25489.92
31. Nozza S, Pogliaghi M, Chiappetta S, Spagnuolo V, Fontana G, Razzari C, et al. Levels of soluble endothelial protein C receptor are associated with CD4+ changes in Maraviroc-treated HIV-infected patients. *PLoS One* (2012) 7:e37032. doi: 10.1371/journal.pone.0037032
32. Chiappetta S, Ripa M, Galli L, Razzari C, Longo V, Galli A, et al. Soluble endothelial protein C receptor (sEPCR) as an inflammatory biomarker in naive HIV-infected patients during ART. *J Antimicrob Chemother* (2016) 71:1627–31. doi: 10.1093/jac/dkw010
33. Reynolds HR, Buyon J, Kim M, Rivera TL, Izmirly P, Tunick P, et al. Association of plasma soluble E-selectin and adiponectin with carotid plaque in patients with systemic lupus erythematosus. *Atherosclerosis* (2010) 210:569–74. doi: 10.1016/j.atherosclerosis.2009.12.007
34. Masiá M, Padilla S, García JA, García-Abellán J, Fernández M, Bernardino I, et al. Evolving understanding of cardiovascular, cerebrovascular and peripheral arterial disease in people living with HIV and role of novel biomarkers. A study of the Spanish CoRIS cohort, 2004-2015. *PLoS One* (2019) 14:e0215507. doi: 10.1371/journal.pone.0215507
35. Engelberger RP, Limacher A, Kucher N, Baumann F, Silbernagel G, Benghozi R, et al. Biological variation of established and novel biomarkers for atherosclerosis: Results from a prospective, parallel-group cohort study. *Clin Chim Acta* (2015) 447:16–22. doi: 10.1016/j.cca.2015.05.003

Conflict of Interest: The authors declare that the research was conducted in the absence of any commercial or financial relationships that could be construed as a potential conflict of interest.

Copyright © 2021 Younas, Psomas, Reynes, Cezar, Kundura, Portalès, Merle, Atoui, Fernandez, Le Moing, Barbuat, Sotto, Sabatier, Winter, Fabbro, Vincent, Reynes and Corbeau. This is an open-access article distributed under the terms of the Creative Commons Attribution License (CC BY). The use, distribution or reproduction in other forums is permitted, provided the original author(s) and the copyright owner(s) are credited and that the original publication in this journal is cited, in accordance with accepted academic practice. No use, distribution or reproduction is permitted which does not comply with these terms.

Alors que la translocation microbienne est une cause reconnue d'activation immunitaire chez le PVVIH avirémique (Sandler et Douek 2012), la virémie résiduelle est encore discutée comme étiologie. Cette question est importante puisque l'on cherche aujourd'hui à alléger la trithérapie des PVVIH (Moreno et al. 2019). Jusque-là, pour la grande majorité des patients, même après des dizaines d'années de traitement l'arrêt total de thérapie entraine une augmentation de la charge virale (S. Taylor et al. 2007).

Ce qui a été démontré c'est qu'il existait des liens fort entre l'athérosclérose et certains marqueurs d'activation endothéliale (tPA, sEPCR) et de coagulation (D-dimère) (Steins et al. 1999; Ireland et al. 2005; Engelberger et al. 2015). Nous avons trouvé un lien entre un profil d'activation immunitaire et la virémie résiduelle et nous avons également remarqué des liens entre ce profil et un haut niveau des marqueurs d'activation (tPA, sEPCR et CRP). L'étape suivante consisterait à mieux comprendre les liens entre la virémie résiduelle et l'athérosclérose, qui est une conséquence de l'activation immunitaire chez les PVVIH sous traitement efficace (Younas et al. 2016).

Le modèle que nous testons est celui de différentes causes d'activation immunitaire entraînant de façon plus ou moins spécifique l'établissement de différents profils d'activation immunitaire, lesquels profils d'activation immunitaire entraîneraient de façon plus ou moins spécifique certaines comorbidités. A terme, notre idéal serait de proposer des profils simples à établir grâce à quelques marqueurs distincts et spécifiques. Nous travaillons donc au perfectionnement de ce profilage en ajoutant un nombre conséquent de patients : presque 300 à ce jour ont été profilés par Mehwish Younas, Renaud Cezar ou moi-même ces dernières années avec un suivi sur plusieurs années de ceux-ci. L'ajout de ces patients a permis de refaire un classification hiérarchique ascendante des patients en fonction de leurs marqueurs d'activation immunitaire plus robuste encore. Elle nous a permis d'identifier que certains profils présentaient plus de troubles neurocognitifs que les autres. Nous cherchons également actuellement des liens entre certains de ces profils d'activation immunitaire et la fragilité chez des PPVIH de plus de 70 ans.

L'intérêt potentiel de ce travail est multiple :

- Mieux comprendre comment certaines causes d'activation immunitaire façonnent certains profils d'activation immunitaire et comment certains profils d'activation immunitaire favoriseraient certaines comorbidités
- Faire un diagnostic étiologique d'activation immunitaire chez chaque patient, ce qui pourrait orienter un traitement étiologique
- Identifier des signatures simples permettant en routine d'identifier le profil d'activation immunitaire d'un patient ce qui pourrait guider le dépistage et la prévention de comorbidités
- Identifier des facteurs immunologiques jouant un rôle clef dans le développement de morbidités facilitées par l'activation immunitaire qui pourraient être des cibles thérapeutiques.

III. ARTICLE « IDENTIFICATION OF DISTINCT IMMUNE ACTIVATION PROFILES IN ADULT HUMANS »

Après avoir réussi à distinguer différents profils d'activation immunitaire chez les PVVIH sous cART efficace et avoir commencé à caractériser certains profils, l'idée que des profils distincts soient également présents dans la population générale a été très vite envisagée. Certaines causes d'activation immunitaire chez les PVVIH comme la sénescence cellulaire, la translocation microbienne ou la présence latente de pathogènes sont également observées dans la population générale. Par exemple, l'infection par des herpes virus humains est très fréquente allant à plus de 90% de séroprévalence chez l'adulte pour l'herpèsvirus humain 6 (Zaravinos, Bizakis, et Spandidos 2009). La translocation microbienne est également source de débat quant à son implication dans les cas de diabètes de type 2 (Jensen et Marette 2020).

Une étude a donc été mise en place au centre de sécurité social de Nîmes où 150 personnes volontaires âgées de 55 à 70 ans ont donné leur accord pour participer à cette cohorte. Un point à souligner est le contexte socio-économique précaire des personnes ayant accepté d'entrer dans cette étude qui est un biais de sélection quant à leur santé générale. De la même manière que pour l'étude ACTIVIH, 48 marqueurs d'activation immunitaire ont été analysés à la surface cellulaire des PBMC et dans le plasma des personnes incluses. Tous ces marqueurs ont été utilisés pour effectuer une classification ascendante hiérarchique des personnes incluses dans la cohorte, comme dans l'étude ACTIVIH. La classification a donné cinq profils d'activation.

www.nature.com/scientificreports

scientific reports

OPEN

Identification of distinct immune activation profiles in adult humans

Renaud Cezar[1,10], Audrey Winter[2,10], Delphine Desigaud[2], Manuela Pastore[3], Lucy Kundura[2], Anne-Marie Dupuy[4], Chantal Cognot[5], Thierry Vincent[5], Christelle Reynes[3], Catherine Dunyach-Remy[6], Jean-Philippe Lavigne[6], Robert Sabatier[3], Patricia Le Merre[7], Elisabeth Maggia[7] & Pierre Corbeau[1,2,8,9]✉

Latent infectious agents, microbial translocation, some metabolites and immune cell subpopulations, as well as senescence modulate the level and quality of activation of our immune system. Here, we tested whether various in vivo immune activation profiles may be distinguished in a general population. We measured 43 markers of immune activation by 8-color flow cytometry and ELISA in 150 adults, and performed a double hierarchical clustering of biomarkers and volunteers. We identified five different immune activation profiles. Profile 1 had a high proportion of naïve T cells. By contrast, Profiles 2 and 3 had an elevated percentage of terminally differentiated and of senescent CD4+T cells and CD8+T cells, respectively. The fourth profile was characterized by NK cell activation, and the last profile, Profile 5, by a high proportion of monocytes. In search for etiologic factors that could determine these profiles, we observed a high frequency of naïve Treg cells in Profile 1, contrasting with a tendency to a low percentage of Treg cells in Profiles 2 and 3. Moreover, Profile 5 tended to have a high level of 16s ribosomal DNA, a direct marker of microbial translocation. These data are compatible with a model in which specific causes, as the frequency of Treg or the level of microbial translocation, shape specific profiles of immune activation. It will be of interest to analyze whether some of these profiles drive preferentially some morbidities known to be fueled by immune activation, as insulin resistance, atherothrombosis or liver steatosis.

Persistent immune activation (IA) fuels major chronic morbidities, including insulin resistance, metabolic syndrome, diabetes, atherothrombosis, neurocognitive disorders or liver steatosis. A model for IA is HIV-1 infection under efficient combined antiretroviral therapy. In people living with HIV-1, the immune system remains potentially activated, even if viral replication is controled by the treatment[1]. To better characterize IA in this model, we previously measured a series of cell-surface and soluble markers, in 120 efficiently treated HIV patients. A hierarchical clustering analysis identified 5 different IA profiles in these people[2]. To test whether the IA profiles were robust rather than specific to the 120 patients we had analyzed, we recruited 20 more HIV patients with divergent bioclinical characteristics, and performed the hierarchical clustering analysis again[3]. Once more, we observed 5 different IA profiles in these 140 HIV patients. We also analyzed the possibility that these IA profiles were the consequence of different causes. In favour of this model, we found a link between microbial translocation and one of the IA profiles[3].

The general population, particularly in old age, shares many of the causes of IA with people living with HIV-1. First, we all harbour infectious agents that trigger our immune system[4]. Second, there is a low level of microbial translocation in each individual that increases over time[5]. Third, metabolic disorders that may stimulate the immune system also increase with age[4]. Fourth, as with any senescent cell, immune cells in aging individuals release factors responsible for IA[4]. And last, the efficiency of Treg cells, a CD4+T cell subpopulation whose function is to downregulate IA, decreases over time[6]. Therefore, we reasoned that a more general population

[1]Immunology Department, Nîmes University Hospital, Place du Pr Debré, 30029 Nîmes, France. [2]Institute of Human Genetics, CNRS-Montpellier University UMR9002, 141 rue de la Cardonille, 34396 Montpellier Cedex 5, France. [3]Institute of Functional Genomics UMR5203 and BCM, CNRS-INSERM-Montpellier University, 141 rue de la Cardonille, 34396 Montpellier, France. [4]Biochemestry Department, Montpellier University Hospital, 371 Avenue du Doyen Gaston Giraud, 34295 Montpellier, France. [5]Immunology Department, Montpellier University Hospital, 80 Avenue Auguste Fliche, 34295 Montpellier, France. [6]U1047, INSERM, Microbiology, Nîmes University Hospital, Montpellier University, Place du Pr Debré, 30029 Nîmes, France. [7]Caisse Primaire d'Assurance Maladie, 14 rue du Cirque Romain, Nîmes, France. [8]Montpellier University, 5 Boulevard Henri IV, 34967 Montpellier, France. [9]Fédération Hospitalo-Universitaire Infections Chroniques, Montpellier-Nîmes, France. [10]These authors contributed equally: Renaud Cezar and Audrey Winter. ✉email: pcorbeau@igh.cnrs.fr

might also present with different IA profiles driven by these various etiologic factors. To test this hypothesis, we looked in the present study for the presence of distinct IA profiles in a general population, and for potential etiologic factors linked to these profiles.

Materials and methods

Study design. We recruited 150 adults over 55 years and below 70 years of age, affiliated to the French Social Security system who volunteered for a free health checkup at a Social Security Center in Nîmes, France. Pregnant women, people under immunomodulatory treatment or with diseases likely to modify their immune system were not included. This study was approved by the French Ethics Committee Sud Est IV. All methods were carried out in accordance with the French guidelines and regulations. All individuals had provided written informed consent. The trial was registered on ClinicalTrials.gov under the reference NCT04028882.

Flow cytometry. Monoclonal antibodies conjugated with fluorescein isothiocyanate (FITC), phycoerythrin (PE), energy-coupled dye (ECD), PE-Cyanine5.5 (PC5.5), PE-Cyanine7 (PC7), allophycocyanine (APC), APCAlexa700, or APCAlexa750 were purchased from Beckman Coulter (Villepinte, France). The antibodies were used in the following combinations; CD57-FITC/CD279-PE/CD45RA-ECD/CD28-PC5.5/CD27-PC7/CD8-APC/CD4-APCAlexa700/CD3-APCAlexa750, CD20-FITC/CD38-PE/HLADR-PC7/CD8-APC/CD4-APCAlexa700/CD3-APCAlexa750, CD57-FITC/CD14-PE/CD56-PC5.5/HLADR-PC7/CD16-APC/CD3-APCAlexa750, CD4-FITC/CD45RA-ECD/CD25-PC7/FoxP3-APC/CD127-APC750. Whole blood collected in EDTA tubes was stained within one hour for 10 mn at room temperature in the dark with the cocktail of antibodies and fixed using Immunoprep Reagent kit (Beckman Coulter) according to the manufacturer's protocol.

For Treg quantification, cells were first fixed with Reagent 1 of the IntraPrep Permeabilization kit (Beckman Coulter) in the dark, and then stained with the CD4-FITC/CD45RA-ECD/CD25-PC7/CD127-APC750 cocktail of antibodies. Secondly, cells were permeabilized and an anti-FoxP3-APC antibody was added. Finally, red blood cells were lysed using Reagent 2. After one hour, cells were washed with Reagent 3.

Cells were run on a Navios flow cytometer and results were analyzed by using Kaluza® software (Beckman Coulter). A minimum of 20,000 lymphocytes were gated to analyze the subpopulations. We controled the inter-run variability with the same batch of Rainbow 8-peak beads (Beckman Coulter). During the study, no voltage adjustment was necessary to keep the beads into their respective defined targets.

Soluble immunologic markers in peripheral blood. ELISA was used to quantify soluble TNF receptor I (sTNFRI), soluble CD14 and soluble CD163 (sCD163) (Quantikine, R&D systems, Rennes, France), as well as tissue Plasminogen Activator (tPA) and soluble Endothelial Protein C Receptor (sEPCR) (Asserachrom, Stago, Asnières-sur-Seine, France) in plasma collected in EDTA Vacutainer tubes (Becton Dickinson, Le Pont-de-Claix, France) and frozen. C-Reactive Protein (CRP) and immunoglobulins (Ig) were measured by turbidimetry in plasma collected by the same way. 16s ribosomal bacterial DNA was measured in plasma by quantitative PCR as previously described[7].

Statistical analysis. All data were standardized before statistical analysis. Next, a visual assessment of the possibility to cluster the data was made using principal component analysis, and also by seeking a cluster structure in the distance matrix. Next, the Hopkins statistic was calculated, with a value of 1 indicating the highest possibility to cluster the data[8]. Second, we determined the optimal number of clusters using several indexes (e.g., Silhouette[9], Gap statistic[10]). The majority rule was used to determine the optimal number of clusters. Third, we performed two hierarchical clustering analyses. One clustering analysis was carried for volunteers, using the Euclidian distance to measure the distance between individuals and the other one for markers, using 1-abs (correlation) as a distance. For both of them, Ward's minimum variance method was used as a linkage method. We then generated a heatmap using the classification of volunteers and markers. We evaluated the appropriateness of the classification through an internal validation test. We used two indexes, based on compactness and separation, (i) the silhouette width which varies between − 1 and 1 representing a wrong and perfect classification[9], respectively, and (ii) the Dunn index which varies from 0 to infinity and should be maximized[11,12]. In addition, to analyze the significance of the hierarchical classification, we performed a permutation test on volunteer groups. To this aim, we computed the ratio between between-group and within-group variability in the true groups using the *lda* function of the MASS package (MASS_7.3-51.6) of the R software (R version 4.0.2 (2020-06-22)). This function computes the singular values, which give the ratio of the between- and within-group standard deviations on the linear discriminant variables. Their squares are the canonical F-statistics. The sum of all singular values provides the global ratio among between-group and within-group variability. In parallel we generated random groups by permutation of group labels. We repeated the permutation 1000 times and visualized their distribution compared to the ratio obtained from true groups.

In order to characterize each immune profile, a V-test was calculated[13]. The bigger the absolute value of the V-test is, the more characteristic the variable is. All analyses were performed using version 3.6.1 R software (R Development Core Team, A Language and Environment for Statistical Computing, Vienna, Austria, 2016. https://www.R-project.org/).

We used the Mann–Whitney test to compare markers and IA profiles. The links between biomarkers were determined by Spearman rank correlations.

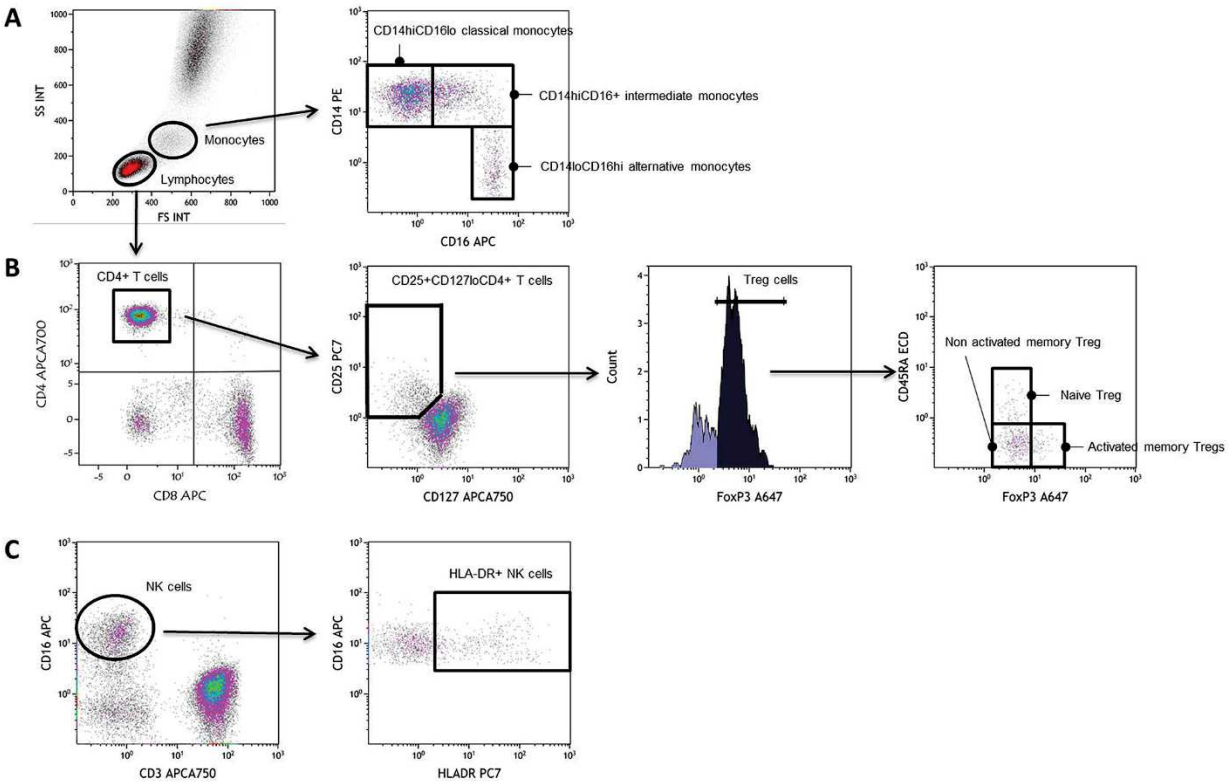

Figure 1. Examples of flow cytometry staining of monocytes **(A)**, CD4+ T cells including Treg cells **(B)**, CD8+ T cells **(B)**, and NK cells **(C)**.

Results

Different immune activation profiles may be distinguished in adults. We recruited 74 (49%) women and 76 (51%) men with a mean ± SD age of 62 ± 4 years. We determined the proportions of CD4+ and CD8+ T cells, of naïve (CD27+ CD45RA+), central memory (CD27+ CD45RA-), effector memory (CD27- CD45RA-), and terminally differentiated T cells (CD27-CD45RA+), activated (HLA-DR+ and/or CD38+), exhausted (PD-1+), and senescent (CD57+, eventually CD27- and CD28-) T cells. The percentages of activated (HLA-DR+), dysfunctional (CD56-), and senescent (CD57+) NK cells were also measured. For monocytes, we quantified the classical (CD14hiCD16lo), intermediate (CD14hiCD16+), and alternative CD14loCD16hi) subpopulations. Examples of our gating strategy are shown in Fig. 1. IgG, IgA, IgM, and sCD163 peripheral blood levels were used as markers of B-cell and monocyte activation, respectively. Inflammation was evaluated via sTNFRI and CRP concentrations, and endothelium activation via sEPCR and tPA concentrations in peripheral blood.

For both markers and individuals, a clustering tendency was observed (Hopkins statistics: 0.68 and 0.73, respectively). We performed two independent hierarchical clustering analyses, one for the activation markers and another one for the volunteers. The number of clusters chosen for markers and donors were 2 and 5, respectively, as they corresponded to the results obtained with the majority of the indexes we tested. Thus, the analysis of volunteers identified 5 groups of individuals presenting with different IA profiles (Fig. 2). Concerning the internal validation step, the Dunn index and the silhouette width were 0.26 and 0.06 for individuals, and 0.39 and 0.12 for markers, respectively. To show that the groups identified by hierarchical classification reflect a true structure of the data, we generated random groups of the same size as the true ones. The within-group and between-group variability allow to investigate the quality of clusters, as "good" clusters are compact (individuals in the same group have similar properties, reflected in a low within-group variability) and far from each other (individuals in different groups present distinct profiles, reflected in high between-group variability). Hence, random groups, or data with no defined clusters, would show a lower ratio between between-group and within-group variability. The distribution of the ratio of the between- and within-group standard deviations on the linear discriminant variables is represented in the Fig. 3. The histogram shows that the between/within ratio is much better for the real groups as the "best" random group exhibits a much lower ratio. Indeed, the median values for the random groups is 15.22 (minimum, 12.04 and maximum, 18.92), whereas it is 42.85 for the true groups, identified by the hierarchical classification ($p < 0.001$). Next, we computed a Principal Component Analysis of the volunteers (Fig. 4).

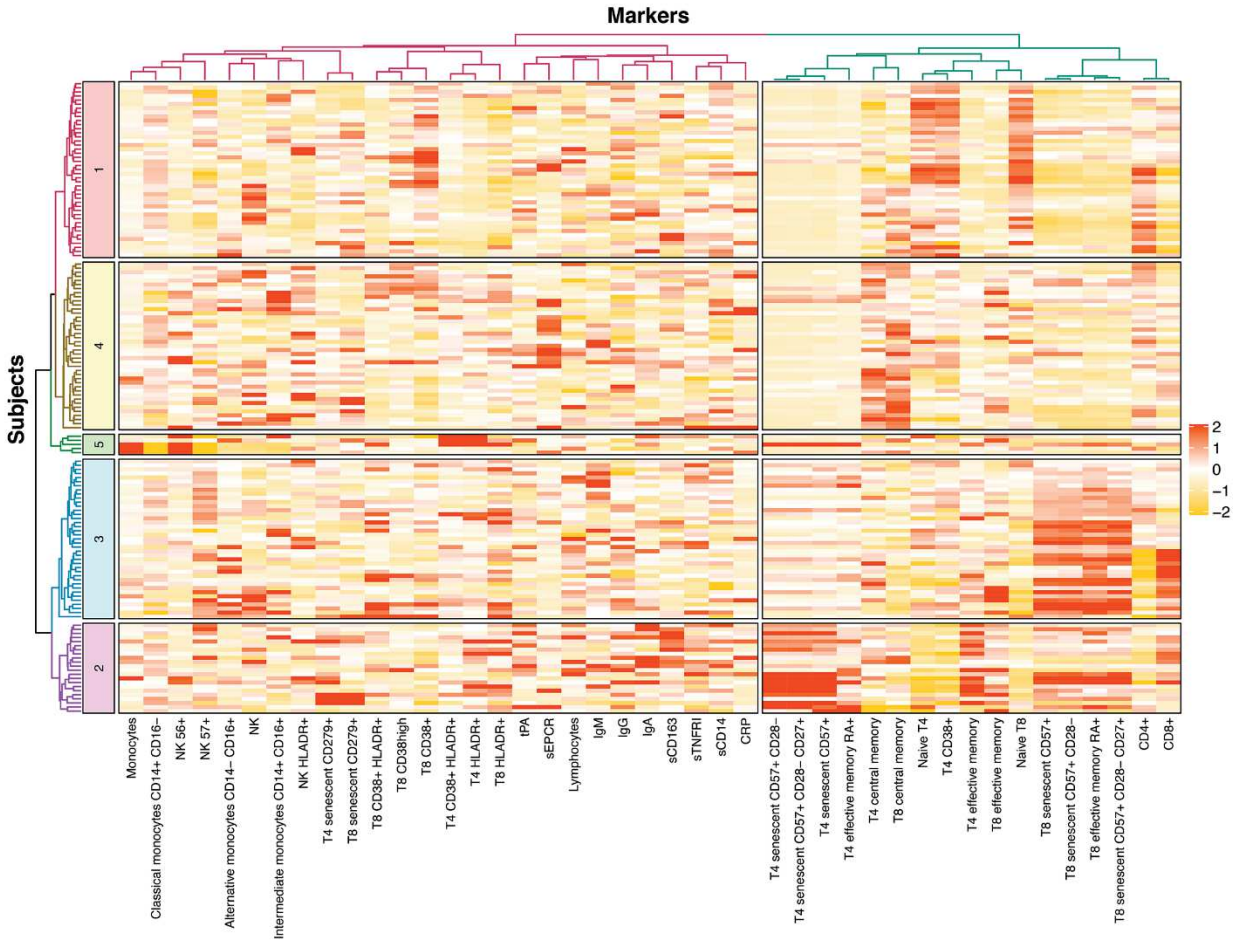

Figure 2. Individuals have different immune activation profiles. Heatmap showing the hierarchical clustering of activation markers (vertical) and volunteers according to their immune activation profile (horizontal). Each immune activation profile is indicated.

Characterization of the immune activation profiles observed. The age, sex, and ethnicity of the individuals are given according to their IA profile in Table 1. There are gender differences in the immune activation profiles ($p < 0.001$). For each profile, we compared each marker mean with the overall mean, using the V-test (Table 2). Each profile may be characterized by specific markers, comparatively to other profiles. Thus, individuals with Profile 1 had a high mean (± SD) percentage of naïve CD4+ T cells (55 ± 12 versus 37 ± 14, $p < 10^{-4}$, Fig. 5A) and naïve CD8+ T cells (53 ± 12 versus 31 ± 12, $p < 10^{-4}$, Fig. 5B) contrasting with a low frequency of terminally differentiated (1 ± 1 versus 3 ± 6, $p < 10^{-4}$, Fig. 5C) and CD57+ senescent (2 ± 2 versus 7 ± 9, $p < 10^{-4}$, Fig. 5D) CD4+ T cells, as well as of terminally differentiated (12 ± 8 versus 27 ± 18, $p < 10^{-4}$, Fig. 5E) and senescent (17 ± 10 versus 34 ± 16, $p < 10^{-4}$, Fig. 5F) CD8+ T cells. Profiles 2 and 3 were at the opposite end of the spectrum. Profile 2 was characterized by an elevated percentage of terminally differentiated (9 ± 11 versus 2 ± 3, $p < 10^{-4}$, Fig. 5C) and CD57+ senescent (19 ± 12 versus 4 ± 4, $p < 10^{-4}$, Fig. 5D) CD4+ T cells. In Profile 3, it is the CD8+ T cells that were more terminally differentiated (41 ± 12 versus 16 ± 14, $p < 10^{-4}$, Fig. 5E), and senescent (45 ± 12 versus 24 ± 14, $p < 10^{-4}$, Fig. 5F). Profile 4 presented a high proportion of activated NK cells (23 ± 13 versus 14 ± 11, $p < 10^{-4}$, Fig. 5G). Finally, a high proportion of monocytes (41 ± 33 versus 9 ± 4, $p = 0.018$, Fig. 5H) was noteworthy in Profile 5.

Links between immune activation profiles and etiologic factors. In Humans, various factors may be responsible for chronic immune activation. Thus, for instance, a deficiency in the mechanisms responsible for downregulating IA may be responsible for an overactivity of the immune system. Microbial translocation, the entry into our organism of microbial products originating from our microbiota, is another potential cause of IA. In a given individual, only some of these etiologic factors may be at work, e.g., immune dysregulation, but not microbial translocation. Therefore, we tested the hypothesis that the IA profiles that we unraveled might be

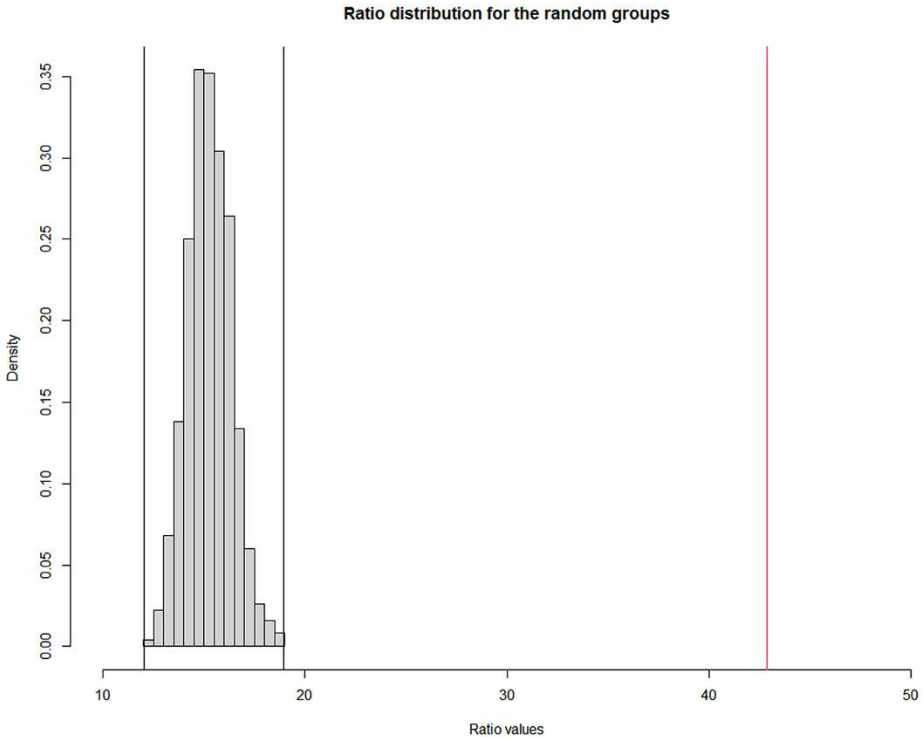

Figure 3. Analyse of the quality of the hierarchical clustering of the volunteers by permutation test. Distribution of the ratio between-group standard deviations: within-group standard deviations for the random groups (grey bars) and the true groups (red line).

fueled by specific causes. To this aim, we searched for correlations between potential etiologic factors and each profile. Treg is a CD4+ T cell subpopulation playing a major role in IA downregulation [14]. Therefore, we measured the proportions and numbers of total Treg (CD4+ CD25+ FOXP3+ CD127lo), naïve Treg (CD4+ CD25+ FOXP3+ CD45RA+CD127lo), and memory Treg, activated (CD4+CD25hiFOXP3hiCD45RA-CD127lo) or not (CD4+CD25+FOXP3+CD45RA-CD127lo) in each individual. As compared with the other profiles, Profile 1, characterized by a low level of differentiated and senescent T cells, had a high percentage of naïve Treg (6.6 ± 4.4 versus 5.3 ± 5.0, p = 0.017, Fig. 6A), a reservoir of cells able to inhibit IA. Moreover, this percentage was linked to the proportions of naïve CD4+ T cells (r = 0.190, p = 0.022, Fig. 6B) and of naïve CD8+ T cells (r = 0.248, p = 0.003, Fig. 6C) in the whole population. By contrast, Profiles 2 and 3, characterized by a high level of differentiated and senescent T cells, tended to have a low percentage of Treg (5.4 ± 1.8 versus 5.9 ± 1.9, p = 0.080, Fig. 6D), in comparison with Profiles 1, 4, and 5. In addition, this percentage was negatively correlated with the proportions of terminally differentiated (r = -0.242, p = 0.003, Fig. 6E) and senescent (r = -0.197, p = 0.017, Fig. 6F) CD4+ T cells in the whole population.

Another potential cause of IA is the intensity of microbial translocation which increases with age[5]. A direct marker of microbial translocation is the presence of bacterial DNA in the circulation quantified by PCR targeting conserved sequences of the 16s ribosomal gene (rDNA). Strikingly, we observed a high, although not significant, level of rDNA in Profile 5 people (45 ± 59 versus 14 ± 13 copies/mL, p = 0.242, Fig. 6G), comparatively to the other volunteers.

Discussion

In this study, we have shown that various IA profiles may be distinguished using an unsupervised learning method in a population of adults volunteering for a health checkup. We revealed 5 distinct IA profiles that may be characterized according to their levels of CD4+ T cell, CD8+ T cell, NK cell and monocyte frequency, activation, and/or differentiation. One profile, Profile 1, has the lowest level of differentiated and senescent T cells, of activated NK cells, and the lowest percentage of monocytes. It may therefore be considered as the less activated profile. Of note, it is the group with the highest percentage of women. Profiles 2 and 3 are remarkable by their reduced percentages of naïve T cells and their elevated percentages of differentiated and senescent T cells. These profiles may therefore be considered as the T cell activated profiles. In Profile 4 it is the NK cells that are activated, and in Profile 5 it is the frequency of circulating monocytes that is noteworthy.

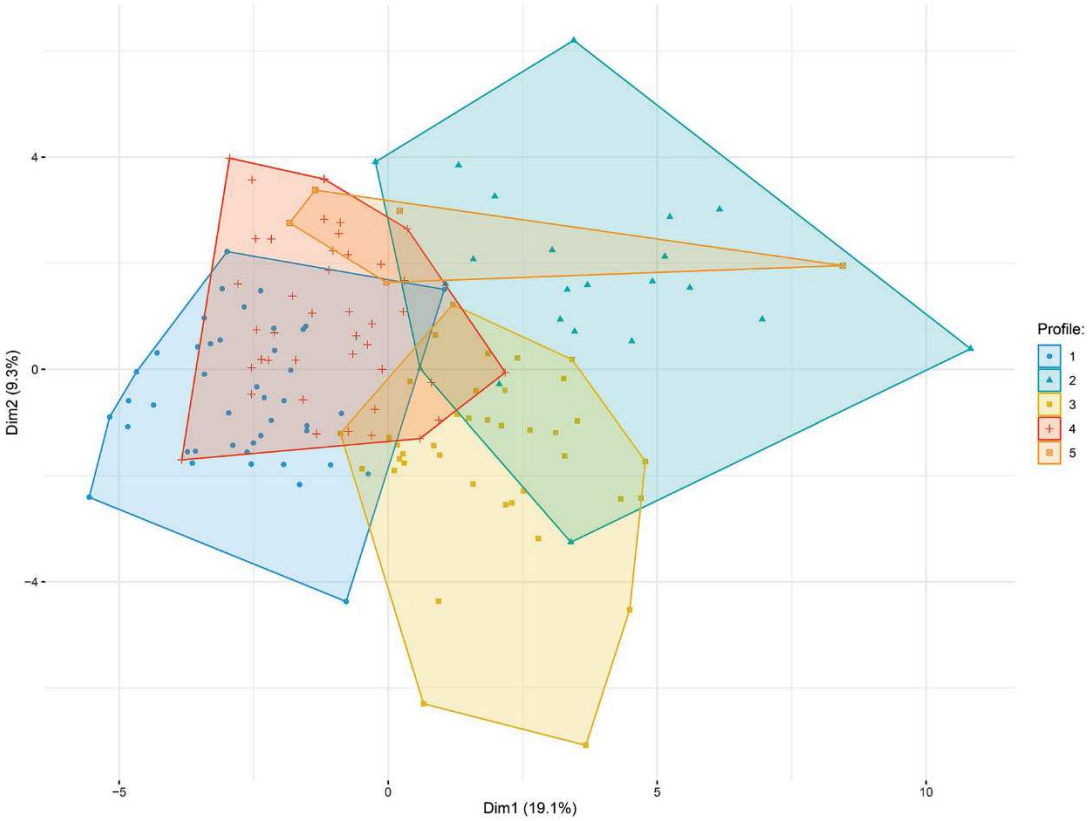

Figure 4. Subjects' map resulting from principal component analysis.

Characteristic	Variable	All profiles	Profile 1 (N = 43)	Profile 2 (N = 22)	Profile 3 (N = 39)	Profile 4 (N = 41)	Profile 5 (N = 5)
Age	Mean (SD)	61.7 (4.3)	61.4 (4.6)	61.8 (4.8)	62.8 (4.3)	61.2 (3.8)	61.0 (2.1)
Sex Female Male	% %	48 52	67 33	23 77	59 41	39 61	20 80
Ethnicity African Caucasian	% %	8 92	10 90	14 86	10 90	2 98	0 100

Table 1. Volunteers characteristics.

A second finding of this study is that some of these IA profiles are linked to potential causes of IA. Thus, Profile 5 individuals, characterized by a high frequency of peripheral blood monocytes, have a high circulating bacterial DNA load. Yet, the difference in rDNA level between Profile 5 and the other profiles was not significant, probably due to the small number of participants with this Profile (n = 5). Yet, this link between microbial translocation and the frequency of circulationg monocytes is in line with the observation that bacterial products may boost monopoiesis via TLR signaling[15]. Profiles 2 and 3 which are particular because of their high degree of CD4+ T cell and CD8+ T cell differentiation and senescence, tend to have low percentages of Treg. As Treg are known to interrupt the process of T cell activation[16], these low Treg levels might participate in the increased T cell differentiation and senescence specific to these profiles. This hypothesis is supported by our observation of an inverse correlation between the percentage of Treg cells on one hand, and of differentiated and senescent CD4+ T cells on the other hand. Conversely, the high percentage of naïve Treg cells in Profile 1 may at least partly explain the low level of T cell differentiation and senescence in that profile.

Profile	Variable	Mean (SD) in profile	Overall mean (SD)	V-test
Profile 1	Percentage of T8 naive	53.52 (12.38)	37.19 (16.2)	7.8
	Percentage of T4 naive	54.82 (11.7)	41.86 (15.87)	6.32
	Percentage of T8 senescent CD57+	16.72 (10.01)	29.26 (16.42)	− 5.91
	Percentage of T4 CD38	62.22 (13.3)	50.82 (15.71)	5.61
	Percentage of T8 HLA-DR+	27.12 (13.01)	39.5 (17.48)	− 5.48
	Percentage of T8 senescent CD57+CD28−	13.71 (8.91)	24.65 (16.03)	− 5.28
	Percentage of T8 senescent CD57+CD28−CD27−	9.76 (6.98)	19.93 (15.68)	− 5.02
	Percentage of T8 terminally differentiated	12.06 (8.21)	22.98 (17.32)	− 4.88
	Percentage of T4 effector memory	6.06 (2.97)	11.47 (9.16)	− 4.58
	Percentage of T4 HLA-DR+	9.61 (4.63)	15.9 (11.06)	− 4.4
	Percentage of T8 CD38+	37.54 (13.11)	29.94 (13.49)	4.36
	Percentage of T8 effector memory	5.42 (2.87)	9.34 (7.17)	− 4.23
	Percentage of T4	72.88 (9.32)	66.77 (11.54)	4.1
	Percentage of T4 senescent CD57+	1.96 (2.25)	5.88 (7.87)	− 3.86
	Percentage of T8	23.4 (8.33)	28.45 (10.16)	− 3.85
	Percentage of T4 senescent CD57+CD28−	1.14 (1.77)	3.83 (5.81)	− 3.58
	Percentage of T4 senescent CD57+CD28−CD27−	0.99 (1.69)	3.61 (5.8)	− 3.5
	Percentage of T4 central memory	38.3 (9.66)	43.62 (11.86)	− 3.47
	Percentage of NK CD57+	42.16 (14.66)	49.21 (16.36)	− 3.33
	Percentage of NK HLA-DR+	11.58 (10.63)	16.55 (12.11)	− 3.18
	Percentage of NK CD56−	9.55 (6.17)	16.4 (17.15)	− 3.09
	Percentage of T8 CD38+HLA-DR+	8.37 (4.69)	11.63 (8.79)	− 2.87
	Percentage of T4 CD38+HLA-DR+	3.92 (1.54)	5.36 (3.98)	− 2.81
	Percentage of T4 terminally differentiated	0.82 (1.43)	2.75 (5.37)	− 2.77
	Percentage of classical monocytes CD14hiCD16lo	83.32 (6.84)	79.9 (14.37)	1.84
	Percentage of monocytes	7.6 (2.84)	9.67 (9.06)	− 1.77
	IgM	1.09 (0.53)	1.26 (0.73)	− 1.75
	sEPCR	126.89 (69.32)	146.45 (89.39)	− 1.69
	Percentage of T4 exhausted CD279+	8.72 (4.94)	10.57 (8.83)	− 1.62
	sCD163	625.84 (287.63)	683.64 (283.54)	− 1.58
	Percentage of alternative monocytes CD14loCD16hi	4.64 (3.1)	5.53 (4.84)	− 1.43
	CRP	2.16 (2.49)	2.83 (3.68)	− 1.41
	sTNFRI	1.48 (0.26)	1.55 (0.39)	− 1.39
	sCD14	1708.43 (204.85)	1657.59 (298.19)	1.32
	IgA	2.32 (1)	2.5 (1.15)	− 1.27
	Percentage of intermediate monocytes CD14hiCD16+	9.09 (4.63)	9.99 (6.73)	− 1.04
	tPA	9.75 (4.93)	10.51 (6.09)	− 0.96
	Percentage of T8 central memory	28.99 (10.49)	30.51 (12.69)	− 0.92
	Lymphocytes	1838.49 (556.16)	1904.7 (593.2)	− 0.86
	Percentage of T8 CD38hi	2.8 (2.05)	2.66 (2.79)	0.41
	Percentage of T8 exhausted CD279+	16.24 (10.09)	15.93 (12.13)	0.2
	IgG	9.91 (2.07)	9.93 (2.07)	− 0.07
	Percentage of NK	8.21 (5.89)	8.22 (5.34)	− 0.02

Continued

Profile	Variable	Mean (SD) in profile	Overall mean (SD)	V-test
Profile 2	Percentage of T4 senescent CD57+	18.76 (12.2)	5.88 (7.87)	8.28
	Percentage of T4 senescent CD57+CD28−	13.03 (8.45)	3.83 (5.81)	8.01
	Percentage of T4 senescent CD57+CD28−CD27−	12.6 (8.73)	3.61 (5.8)	7.85
	Percentage of T4 effector memory	23.87 (13.55)	11.47 (9.16)	6.85
	Percentage of T4 terminally differentiated	8.87 (10.58)	2.75 (5.37)	5.78
	Percentage of T4 naive	24.9 (14.44)	41.86 (15.87)	− 5.41
	Percentage of T4 CD38+	34.39 (12.73)	50.82 (15.71)	− 5.29
	Percentage of T4 exhausted CD279+	19.29 (17.63)	10.57 (8.83)	5
	sCD163	940.28 (397.75)	683.64 (283.54)	4.58
	IgA	3.39 (1.95)	2.5 (1.15)	3.9
	Percentage of T8 naive	24.93 (8.32)	37.19 (16.2)	− 3.83
	Percentage of T8 effector memory	14.74 (9.67)	9.34 (7.17)	3.81
	Percentage of T8 CD38+	21.43 (9.64)	29.94 (13.49)	− 3.19
	Percentage of T4 HLA-DR+	22.51 (11.26)	15.9 (11.06)	3.03
	Percentage of T8 terminally differentiated	32.35 (18.21)	22.98 (17.32)	2.74
	Percentage of T4	60.9 (10.24)	66.77 (11.54)	− 2.57
	tPA	13.58 (6.24)	10.51 (6.09)	2.55
	Percentage of T8 HLA-DR+	47.89 (18.53)	39.5 (17.48)	2.43
	Percentage of T8	33.22 (10.96)	28.45 (10.16)	2.37
	Percentage of T8 senescent CD57+	36.86 (16.98)	29.26 (16.42)	2.34
	Lymphocytes	2179.32 (763.19)	1904.7 (593.2)	2.34
	IgG	10.74 (2.16)	9.93 (2.07)	1.98
	Percentage of T8 exhausted CD279+	20.62 (18.36)	15.93 (12.13)	1.96
	Percentage of T8 senescent CD57+CD28−CD27−	25.94 (17.09)	19.93 (15.68)	1.94
	Percentage of alternative monocytes CD14loCD16hi	3.93 (2.58)	5.53 (4.84)	− 1.67
	Percentage of NK CD57+	54.4 (15.15)	49.21 (16.36)	1.6
	Percentage of T8 senescent CD57+CD28−	29.67 (17.09)	24.65 (16.03)	1.58
	sTNFRI	1.67 (0.42)	1.55 (0.39)	1.57
	Percentage of classical monocytes CD14hiCD16lo	84.32 (7.23)	79.9 (14.37)	1.55
	Percentage of T4 central memory	40.32 (15.23)	43.62 (11.86)	− 1.41
	sCD14	1725.62 (274.65)	1657.59 (298.19)	1.15
	Percentage of T8 CD38hi	2.06 (1.83)	2.66 (2.79)	− 1.09
	Percentage of T8 central memory	28.14 (12.79)	30.51 (12.69)	− 0.95
	Percentage of intermediate monocytes CD14hiCD16+	9.08 (6.7)	9.99 (6.73)	− 0.69
	Percentage of T4 CD38+HLA-DR+	4.99 (2.1)	5.36 (3.98)	− 0.47
	Percentage of NK CD56−	14.85 (12)	16.4 (17.15)	− 0.46
	IgM	1.32 (0.77)	1.26 (0.73)	0.43
	Percentage of T8 CD38+HLA-DR+	10.94 (6.19)	11.63 (8.79)	− 0.4
	Percentage of NK HLA-DR+	17.48 (12.22)	16.55 (12.11)	0.39
	Percentage of monocytes	10.23 (6.9)	9.67 (9.06)	0.31
	CRP	3.01 (3.65)	2.83 (3.68)	0.26
	Percentage of NK	8 (4.58)	8.22 (5.34)	− 0.21
	sEPCR	148.49 (81.15)	146.45 (89.39)	0.12

Continued

Profile	Variable	Mean (SD) in profile	Overall mean (SD)	V-test
Profile 3	Percentage of T8 terminally differentiated	41.34 (12.49)	22.98 (17.32)	7.67
	Percentage of T8 senescent CD57+CD28−CD27−	36.46 (12.84)	19.93 (15.68)	7.63
	Percentage of T8 senescent CD57+CD28−	41.04 (11.73)	24.65 (16.03)	7.4
	Percentage of T8 senescent CD57+	44.89 (11.88)	29.26 (16.42)	6.89
	Percentage of T8 central memory	20.8 (6.07)	30.51 (12.69)	− 5.53
	Percentage of T4	60.04 (13.06)	66.77 (11.54)	− 4.22
	Percentage of T8	34.36 (10.92)	28.45 (10.16)	4.21
	Percentage of T8 CD38+HLA-DR+	16.75 (12.82)	11.63 (8.79)	4.21
	Percentage of T8 naive	28 (13.42)	37.19 (16.2)	− 4.11
	Percentage of NK CD57+	56.9 (14.01)	49.21 (16.36)	3.4
	Percentage of T8 HLA-DR+	46.84 (18.3)	39.5 (17.48)	3.04
	Percentage of alternative monocytes CD14loCD16hi	7.41 (6.98)	5.53 (4.84)	2.81
	IgM	1.51 (0.75)	1.26 (0.73)	2.5
	Percentage of T8 exhausted CD279+	12.34 (9.18)	15.93 (12.13)	− 2.14
	sEPCR	122.18 (42.08)	146.45 (89.39)	− 1.96
	sCD14	1594.01 (373.68)	1657.59 (298.19)	− 1.54
	sCD163	624.32 (191.54)	683.64 (283.54)	− 1.51
	Percentage of NK CD56−	12.89 (7.33)	16.4 (17.15)	− 1.48
	Percentage of T4 effector memory	13.13 (8.14)	11.47 (9.16)	1.31
	CRP	2.17 (2.75)	2.83 (3.68)	− 1.28
	Lymphocytes	2007.18 (531.31)	1904.7 (593.2)	1.25
	tPA	9.63 (4.39)	10.51 (6.09)	− 1.04
	Percentage of monocytes	8.42 (3.78)	9.67 (9.06)	− 1
	Percentage of NK HLA-DR+	14.92 (9.6)	16.55 (12.11)	− 0.97
	IgA	2.36 (0.75)	2.5 (1.15)	− 0.93
	Percentage of T4 exhausted CD279+	9.69 (5.54)	10.57 (8.83)	− 0.72
	Percentage of T4 CD38+HLA-DR+	5.75 (2.47)	5.36 (3.98)	0.7
	Percentage of T8 CD38hi	2.92 (4.36)	2.66 (2.79)	0.67
	IgG	10.09 (1.97)	9.93 (2.07)	0.56
	Percentage of T4 naive	40.68 (13.93)	41.86 (15.87)	− 0.54
	Percentage of T8 effector memory	9.86 (7.72)	9.34 (7.17)	0.53
	Percentage of T4 terminally differentiated	3.11 (3.19)	2.75 (5.37)	0.49
	sTNFRI	1.57 (0.33)	1.55 (0.39)	0.47
	Percentage of T8 CD38+	30.71 (12.99)	29.94 (13.49)	0.41
	Percentage of T4 central memory	43.08 (10.12)	43.62 (11.86)	− 0.33
	Percentage of T4 senescent CD57+CD28−	4.07 (2.91)	3.83 (5.81)	0.3
	Percentage of T4 senescent CD57+CD28−CD27−	3.81 (2.9)	3.61 (5.8)	0.25
	Percentage of classical monocytes CD14hiCD16lo	79.45 (11.29)	79.9 (14.37)	− 0.23
	Percentage of T4 CD38+	51.29 (13.08)	50.82 (15.71)	0.22
	Percentage of T4 senescent CD57+	6.1 (3.32)	5.88 (7.87)	0.2
	Percentage of intermediate monocytes CD14hiCD16+	10.15 (6.31)	9.99 (6.73)	0.17
	Percentage of T4 HLA-DR+	15.76 (6.71)	15.9 (11.06)	− 0.09
	Percentage of NK	8.17 (5.42)	8.22 (5.34)	− 0.07

Continued

Profile	Variable	Mean (SD) in profile	Overall mean (SD)	V-test
Profile 4	Percentage of T8 central memory	42.14 (10.29)	30.51 (12.69)	6.86
	Percentage of T4 central memory	51.7 (9.52)	43.62 (11.86)	5.1
	Percentage of T8 terminally differentiated	12.58 (8.44)	22.98 (17.32)	− 4.5
	Percentage of NK HLA-DR+	22.92 (13.49)	16.55 (12.11)	3.94
	Percentage of T8 senescent CD57+CD28−CD27−	12.05 (8.37)	19.93 (15.68)	− 3.76
	sEPCR	187.69 (127.81)	146.45 (89.39)	3.45
	Percentage of T4 senescent CD57+CD28−	1.32 (2.19)	3.83 (5.81)	− 3.24
	Percentage of T4 senescent CD57+CD28−CD27−	1.16 (2.17)	3.61 (5.8)	− 3.16
	Percentage of T8 senescent CD57+CD28−	18.37 (11.17)	24.65 (16.03)	− 2.93
	Percentage of T4 senescent CD57+	2.83 (2.54)	5.88 (7.87)	− 2.9
	Lymphocytes	1704.27 (539)	1904.7 (593.2)	− 2.53
	Percentage of T4 terminally differentiated	1.01 (1.82)	2.75 (5.37)	− 2.42
	Percentage of T8 senescent CD57+	24.16 (11.32)	29.26 (16.42)	− 2.32
	Percentage of NK CD56−	21.7 (20.08)	16.4 (17.15)	2.32
	CRP	3.92 (5.13)	2.83 (3.68)	2.23
	Percentage of T4 effector memory	8.93 (3.47)	11.47 (9.16)	− 2.08
	Percentage of T8	25.83 (6.88)	28.45 (10.16)	− 1.93
	Percentage of T4	69.68 (8.17)	66.77 (11.54)	1.89
	Percentage of intermediate monocytes CD14hiCD16+	11.61 (8.2)	9.99 (6.73)	1.8
	Percentage of T8 CD38+	26.9 (12.4)	29.94 (13.49)	− 1.69
	Percentage of T4 naive	38.36 (10.86)	41.86 (15.87)	− 1.65
	IgG	9.54 (2.08)	9.93 (2.07)	− 1.41
	Percentage of T4 exhausted CD279+	8.92 (4.47)	10.57 (8.83)	− 1.4
	IgA	2.31 (0.78)	2.5 (1.15)	− 1.27
	Percentage of T4 CD38+	48.55 (12.48)	50.82 (15.71)	− 1.08
	Percentage of T8 CD38+HLA-DR+	10.41 (6.3)	11.63 (8.79)	− 1.04
	Percentage of NK	8.9 (5.15)	8.22 (5.34)	0.95
	Percentage of T8 naive	35.64 (11.54)	37.19 (16.2)	− 0.72
	IgM	1.19 (0.86)	1.26 (0.73)	− 0.67
	Percentage of monocytes	8.9 (4.19)	9.67 (9.06)	− 0.64
	Percentage of NK CD57+	50.54 (12.77)	49.21 (16.36)	0.61
	sCD14	1634.07 (315.53)	1657.59 (298.19)	− 0.59
	Percentage of T4 CD38+HLA-DR+	5.07 (1.91)	5.36 (3.98)	− 0.56
	Percentage of T8 HLA-DR+	40.59 (12.26)	39.5 (17.48)	0.47
	Percentage of alternative monocytes CD14loCD16hi	5.82 (4.17)	5.53 (4.84)	0.46
	Percentage of T4 HLA-DR+	15.31 (5.43)	15.9 (11.06)	− 0.39
	sCD163	671.56 (216.79)	683.64 (283.54)	− 0.32
	Percentage of T8 effector memory	9.64 (6.14)	9.34 (7.17)	0.31
	tPA	10.71 (7.88)	10.51 (6.09)	0.25
	Percentage of classical monocytes CD14hiCD16lo	80.24 (10.75)	79.9 (14.37)	0.18
	Percentage of T8 exhausted CD279+	16.2 (12.07)	15.93 (12.13)	0.17
	Percentage of T8 CD38hi	2.72 (2.06)	2.66 (2.79)	0.16
	sTNFRI	1.54 (0.52)	1.55 (0.39)	− 0.14
Continued				

Profile	Variable	Mean (SD) in profile	Overall mean (SD)	V-test
Profile 5	Percentage of monocytes	41.04 (33.36)	9.67 (9.06)	7.85
	Percentage of T4 CD38+HLA-DR+	18.86 (13.95)	5.36 (3.98)	7.68
	Percentage of classical monocytes CD14hiCD16lo	31.83 (37.9)	79.9 (14.37)	− 7.58
	Percentage of NK CD56−	65.91 (35.69)	16.4 (17.15)	6.54
	Percentage of T4 HLA-DR+	46.66 (33.09)	15.9 (11.06)	6.3
	Percentage of NK CD57+	16.1 (19.1)	49.21 (16.36)	− 4.59
	Percentage of NK	4.23 (4.07)	8.22 (5.34)	− 1.7
	IgG	8.48 (1.54)	9.93 (2.07)	− 1.58
	Percentage of T4 CD38+	40.04 (14.8)	50.82 (15.71)	− 1.56
	Percentage of T8 CD38+	20.92 (11.12)	29.94 (13.49)	− 1.52
	Percentage of alternative monocytes CD14loCD16hi	3.16 (5.94)	5.53 (4.84)	− 1.11
	Percentage of T8 effector memory	12.76 (6.82)	9.34 (7.17)	1.08
	IgA	2.99 (1.28)	2.5 (1.15)	0.95
	Percentage of T8 CD38hi	1.55 (0.92)	2.66 (2.79)	− 0.9
	IgM	0.97 (0.24)	1.26 (0.73)	− 0.9
	Percentage of intermediate monocytes CD14hiCD16+	7.37 (11.31)	9.99 (6.73)	− 0.88
	Percentage of T8 senescent CD57+	23.5 (12.51)	29.26 (16.42)	− 0.79
	Lymphocytes	2110 (431.86)	1904.7 (593.2)	0.78
	Percentage of T8 central memory	34.27 (13.99)	30.51 (12.69)	0.67
	Percentage of T8 terminally differentiated	17.9 (18.36)	22.98 (17.32)	− 0.67
	tPA	8.76 (6.84)	10.51 (6.09)	− 0.65
	CRP	3.86 (3.34)	2.83 (3.68)	0.64
	Percentage of T8 senescent CD57+CD28−	20.29 (13.26)	24.65 (16.03)	− 0.62
	Percentage of T4 senescent CD57+CD28−CD27−	5.14 (10.52)	3.61 (5.8)	0.6
	Percentage of T4 senescent CD57+CD28−	5.26 (10.51)	3.83 (5.81)	0.56
	sCD163	613.39 (191.72)	683.64 (283.54)	− 0.56
	Percentage of T4 exhausted CD279+	8.51 (5.55)	10.57 (8.83)	− 0.53
	Percentage of T8 senescent CD57+CD28−CD27−	16.71 (14.99)	19.93 (15.68)	− 0.47
	Percentage of CD8	26.38 (8.14)	28.45 (10.16)	− 0.46
	Percentage of T8 exhausted CD279+	18.34 (11.25)	15.93 (12.13)	0.45
	Percentage of T8 HLA-DR+	42.78 (23.01)	39.5 (17.48)	0.43
	sTNFRI	1.48 (0.3)	1.55 (0.39)	− 0.41
	Percentage of T4 terminally differentiated	3.68 (7.41)	2.75 (5.37)	0.4
	sCD14	1610 (228.56)	1657.59 (298.19)	− 0.36
	Percentage of T4	68.56 (9.39)	66.77 (11.54)	0.35
	Percentage of T4 central memory	41.9 (11.33)	43.62 (11.86)	− 0.33
	Percentage of T8 naive	35.08 (14.41)	37.19 (16.2)	− 0.3
	Percentage of T8 CD38+HLA-DR+	12.73 (9.87)	11.63 (8.79)	0.28
	sEPCR	156.75 (70.83)	146.45 (89.39)	0.26
	Percentage of T4 naive	43.03 (17.31)	41.86 (15.87)	0.17
	Percentage of NK HLA-DR+	15.72 (8.84)	16.55 (12.11)	− 0.16
	Percentage of T4 senescent CD57+	6.3 (11.33)	5.88 (7.87)	0.12
	Percentage of T4 effector memory	11.38 (8.06)	11.47 (9.16)	− 0.02

Table 2. Description of the immune activation profiles using the V-test. Markers are presented from the most to the least characteristic by profile.

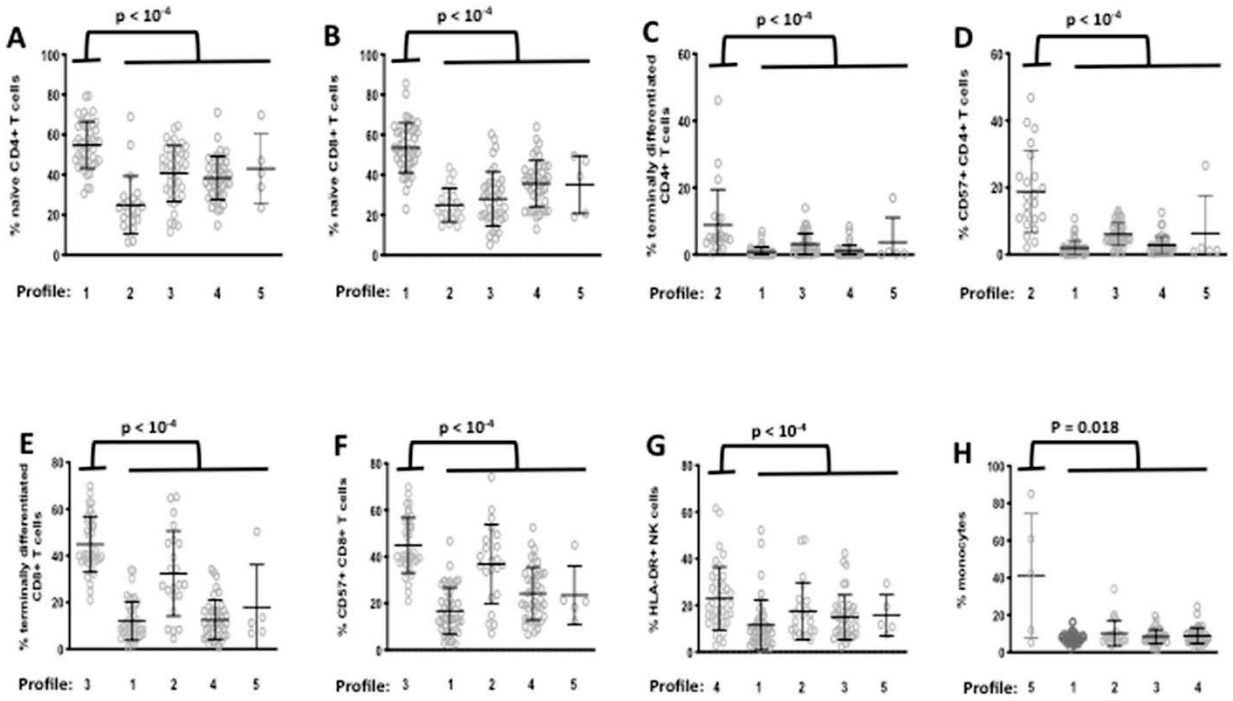

Figure 5. IA profiles are characterized by specific markers. Differences in the level of various activation markers between volunteers with Profile 1 **(A,B)**, 2 **(C,D)**, 3 **(E,F)**, 4 **(G)**, and 5 **(H)**, and the other profiles.

One of the limitations of our study is that it is cross-sectional, highlighting only correlations. Further analysis is needed to definitively establish causative links between etiologic factors and IA profiles. Also, additional etiologic factors, different from the one we tested, could shape the IA profiles, as for instance the genetic background and the clinical history. Moreover, the stability over time of IA profiles has to be verified. Our study is also limited by the technology we used. Thus, we did not test the functionality of the various immune cell subpopulations we analyzed. The immune phenotyping could also be more precise by using single-cell transcriptomics analysis, high dimensional flow cytometry or CyTOF. On the other hand, our ultimate goal is to identify a simple signature of easily measurable markers characteristic of immune activation profiles that could fuel immune activation-induced morbidities. This goal may be achievable in routine with the tools we used.

Globally, we show that different IA profiles may be distinguished in a general population, and that some of these profiles are linked to potential etiologic factors such as Treg frequency and microbial translocation.

We propose a model where in each individual one or a few specific causes of IA shape a specific IA profile. Of interest, the different IA profiles we describe here may fuel different morbidities among those driven by IA, as insulin resistance, atherothrombosis or liver steatosis for instance, In this hypothesis, immune profiling might help to tailor the prevention and the screening of these IA-induced diseases. Moreover, deciphering soluble immune factors favoring each of these morbidities might open the way to new therapeutic strategies. In the near future, the immune activation profile of each individual might be identified via a simple signature of a reduced number of activation markers easily measurable, and this immune activation profile might predict the chronic morbidiites this individual is at risk of developing.

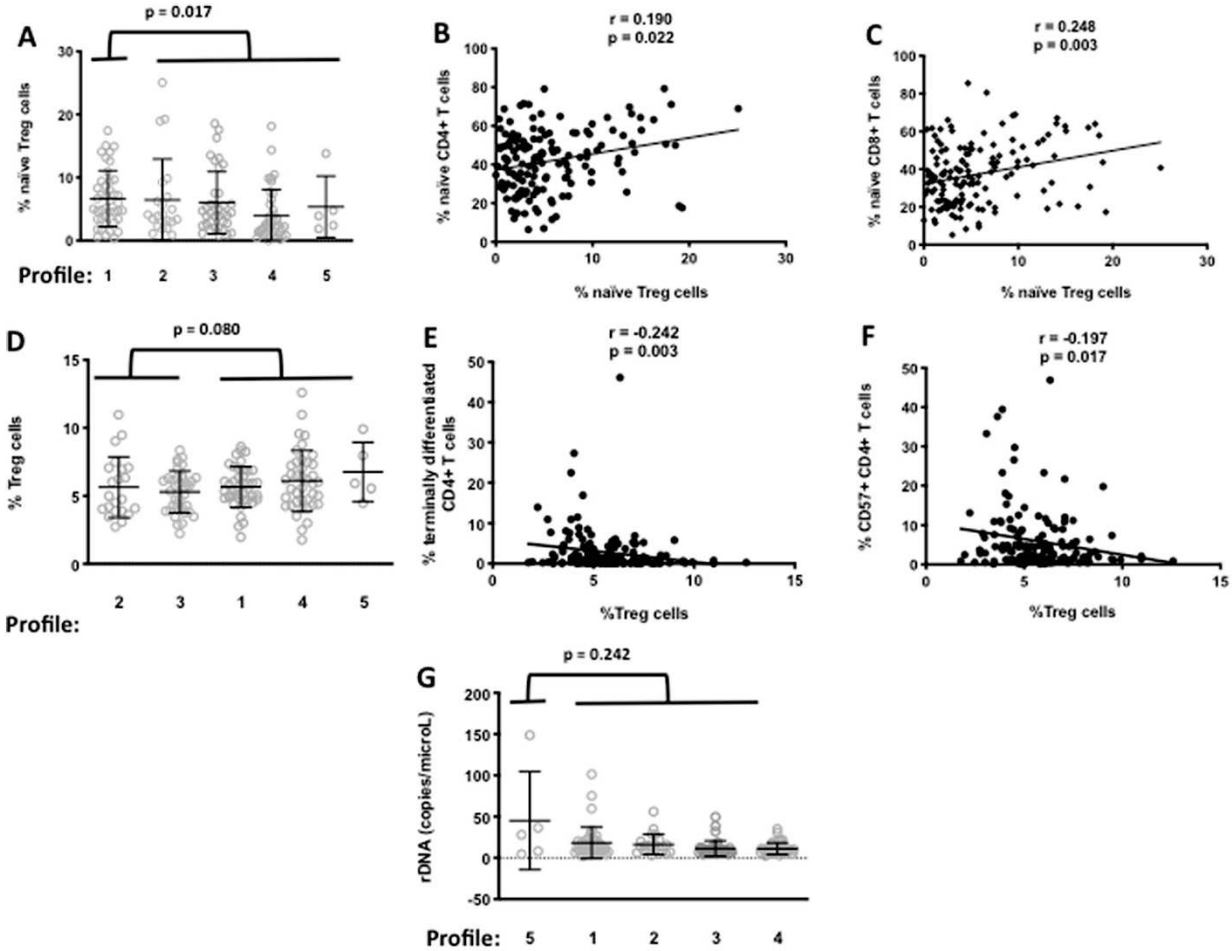

Figure 6. Immune activation Profiles 1, 2, 3, and 5 may be characterized by specific etiologic factors. Naïve Treg frequencies in Profile 1 as compared with the other profiles **(A)**, and correlations with naïve CD4+ T cell **(B)** and naïve CD8+ T cell **(C)** subpopulations. Treg frequencies in Profiles 2 and 3 comparatively to Profiles 1, 4, and 5 **(D)**, and correlations with terminally differentiated **(E)** and senescent **(F)** CD4+ T cells. Circulating bacterial DNA levels in Profile 5 in comparison with the other profiles **(G)**.

Received: 12 August 2020; Accepted: 30 October 2020
Published online: 30 November 2020

References

1. Younas, M., Psomas, C., Reynes, J. & Corbeau, P. Immune activation in the course of HIV-1 infection: Causes, phenotypes and persistence under therapy. *HIV Med.* **17**, 89–105. https://doi.org/10.1111/hiv.12310 (2016).
2. Psomas, C. *et al.* One of the immune activation profiles observed in HIV-1-infected adults with suppressed viremia is linked to metabolic syndrome: The ACTIVIH study. *EBioMedicine* **8**, 265–276. https://doi.org/10.1016/j.ebiom.2016.05.008 (2016).
3. Younas, M. *et al.* Microbial translocation is linked to a specific immune activation profile in HIV-1-infected adults with suppressed viremia. *Front. Immunol.* **10**, 2185. https://doi.org/10.3389/fimmu.2019.02185 (2019).
4. Lopez-Otin, C., Blasco, M. A., Partridge, L., Serrano, M. & Kroemer, G. The hallmarks of aging. *Cell* **153**, 1194–1217. https://doi.org/10.1016/j.cell.2013.05.039 (2013).
5. Stehle, J. R., Jr. *et al.* Lipopolysaccharide-binding protein, a surrogate marker of microbial translocation, is associated with physical function in healthy older adults. *J. Gerontol. Ser. A Biol. Sci. Med. Sci.* **67**, 1212–1218, https://doi.org/10.1093/gerona/gls178 (2012).
6. Schmitt, V., Rink, L. & Uciechowski, P. The Th17/Treg balance is disturbed during aging. *Exp. Gerontol.* **48**, 1379–1386. https://doi.org/10.1016/j.exger.2013.09.003 (2013).
7. Psomas, C. *et al.* Maraviroc-induced decrease in circulating bacterial products is not linked to an increase in immune activation in HIV-infected individuals. *Blood* **122**, 2282–2283. https://doi.org/10.1182/blood-2013-06-507012 (2013).
8. Hopkins, B. & Skellam, J. G. A new method for determining the type of distribution of plant individuals. *Ann. Bot.* **18**, 213–227 (1954).
9. Rousseeuw, P. J. Silhouettes: A graphical aid to the interpretation and validation of cluster analysis. *J. Comput. Appl. Math.* **20**, 53–65 (1987).
10. Tibshirani, R., Walther, G., Hastie, T. Estimating the number of clusters in a data set via the gap statistic. *J. R. Stat. Soc. Ser. B Stat. Methodol.* **63**, 411–423 (2001).
11. Dunn, J. C. Well-separated clusters and optimal fuzzy partitions. *J. Cybern.* **4**, 95–104 (1974).
12. Dunn, J. C. A fuzzy relative of the ISODATA process and its use in detecting compact well-separated clusters. *J. Cybern.* **3**, 32–57 (1973).

13. Lê, S., Josse, J. & Husson, F. FactoMineR: An R package for multivariate analysis. *J. Stat. Softw.* **25**, 1–18 (2008).
14. Sakaguchi, S. Naturally arising Foxp3-expressing CD25+CD4+ regulatory T cells in immunological tolerance to self and non-self. *Nat. Immunol.* **6**, 345–352. https://doi.org/10.1038/ni1178 (2005).
15. Serbina, N. V., Hohl, T. M., Cherny, M. & Pamer, E. G. Selective expansion of the monocytic lineage directed by bacterial infection. *J. Immunol.* **183**, 1900–1910. https://doi.org/10.4049/jimmunol.0900612 (2009).
16. Sojka, D. K., Hughson, A., Sukiennicki, T. L. & Fowell, D. J. Early kinetic window of target T cell susceptibility to CD25+ regulatory T cell activity. *J. Immunol.* **175**, 7274–7280. https://doi.org/10.4049/jimmunol.175.11.7274 (2005).

Acknowledgements
We are grateful to the persons who volunteered for this study, and to Teresa Sawyers for the critical reading of the manuscript.

Author contributions
R.C. and T.V. contributed to the conception and design of the flow cytometry study, acquired, analyzed and interpreted cell surface markers data. D.D., A.M.D., C.G. and L.K. acquired, analyzed and interpreted soluble markers data. P.L.M. and E.M. contributed to the conception and design of the study, the volunteers' enrolment, acquired, analyzed and interpreted clinical data. A.W., C.R., M.P. and R.S. contributed to the conception and design of the statistical study, acquired, analyzed and interpreted statistical data. C.D.R. and J.P.L. contributed to the design, analysis and interpretation of the data. P.C. contributed to the conception and design of the study, analyzed and interpreted data, and wrote the first draft of the manuscript. All authors revised and approved the final version.

Funding
The study was funded by MSD, MSDAvenir, and by the University Hospital of Nîmes. These sponsors had not any role, neither in the study design, in the collection, analysis, and interpretation of data, in the writing of the report, nor in the decision to submit the paper for publication.

Competing interests
The authors declare no competing interests.

Additional information
Correspondence and requests for materials should be addressed to P.C.

Reprints and permissions information is available at www.nature.com/reprints.

Publisher's note Springer Nature remains neutral with regard to jurisdictional claims in published maps and institutional affiliations.

Open Access This article is licensed under a Creative Commons Attribution 4.0 International License, which permits use, sharing, adaptation, distribution and reproduction in any medium or format, as long as you give appropriate credit to the original author(s) and the source, provide a link to the Creative Commons licence, and indicate if changes were made. The images or other third party material in this article are included in the article's Creative Commons licence, unless indicated otherwise in a credit line to the material. If material is not included in the article's Creative Commons licence and your intended use is not permitted by statutory regulation or exceeds the permitted use, you will need to obtain permission directly from the copyright holder. To view a copy of this licence, visit http://creativecommons.org/licenses/by/4.0/.

© The Author(s) 2020

Chaque profil peut donc se distinguer des autres par un ou plusieurs marqueurs caractéristiques. (Tableau 2) Les personnes du profil 1 ont un taux de LT naïfs plus élevé. Les personnes du profil 2 ont en moyenne plus de LT4 sénescents que les autres profils tandis que ceux du profil 3 ont plus de LT8 sénescents. Les personnes du profil 4 sont caractérisées par un grand nombre de LT mémoire centrale et enfin les personnes du profil 5 ont beaucoup de monocytes par rapport aux autres profils.

IV. ARTCLE « INSULIN RESISTANCE IS LINKED TO A SPECIFIC PROFILE OF IMMUNE ACTIVATION IN HUMAN SUBJECTS. »

Dans un second travail à partir de cette même cohorte de 150 personnes nous avons décrit plus finement un profil précédemment établi. Le profil 2 présente des caractéristiques d'insulinorésistance et de syndrome métabolique. En effet, les personnes incluses dans ce profil ont un plus haut taux d'insulinémie, de triglycéridémie et un HOMA plus élevé à 3.9 en moyenne contre 2.4 dans les autres profils (Figure 1). Un HOMA élevé est un signe d'insulinorésistance (Horáková et al. 2019). En plus, les personnes du profil 2 ont un rapport taille/hanche plus important que les autres profils, signe d'une obésité viscérale (Brook et al. 2001) (Figure 1). Cette caractéristique clinique a encore récemment été soulignée comme marqueur significatif de risque d'hypertension artérielle, même chez les personnes avec un IMC dit normal, dans la cohorte Constance en France (Wiernik et al. 2019). De plus, nous avons observé des liens entre les différents marqueurs caractéristiques de ce profil 2 (tPA, CRP, IgA , LT4 sénescent, sCD163 et sTNF-R1) et l'insulinémie ou le HOMA (Figure 5). L'élévation de sTNF-R1 est un argument pour un lien causal entre ce profil 2 et la résistance à l'insuline. Enfin, des liens sont visibles entre des marqueurs de syndrome métabolique (triglycéridémie, hypertension, niveau de HDL bas et obésité viscérale) et les marqueurs caractéristiques du profil 2 (Figure 6).

Les PVVIH sous cART ont une activation immunitaire globalement bien plus élevée que les personnes observées dans METACTIV mais nous avons voulu comparer au sein des cohortes les caractéristiques immunologiques de chaque profil associé à l'insulinorésistance et ils présentent des points communs. Le niveau de LT8 naïf est plus bas dans ces deux profils comparés aux autres profils. Ces personnes ont également plus de LT8 activés et plus de sTNFR1 avec des différences à chaque fois plus prononcées pour le profil issu de la cohorte ACTIVIH.

www.nature.com/scientificreports

scientific reports

OPEN

Insulin resistance is linked to a specific profile of immune activation in human subjects

Renaud Cezar[1], Delphine Desigaud[2], Manuela Pastore[3], Lucy Kundura[2], Anne-Marie Dupuy[4], Chantal Cognot[5], Thierry Vincent[5], Christelle Reynes[3], Robert Sabatier[3], Elisabeth Maggia[6] & Pierre Corbeau[1,2,7,8]✉

We tested the hypothesis that a particular immune activation profile might be correlated with insulin resistance in a general population. By measuring 43 markers of immune, endothelial, and coagulation activation, we have previously shown that five different immune activation profiles may be distinguished in 150 volunteers. One of these profiles, Profile 2, characterized by CD4+T cell senescence, inflammation, monocyte, B cell, and endothelial activation, presented elevated insulinemia, glycemia, triglyceridemia, and γ-glutamyl transferase, a marker of liver injury, in comparison with other profiles. Our data are compatible with a model in which a particular immune activation profile might favor the development of insulin resistance and metabolic syndrome. In this hypothesis, identification of this profile, that is feasible with only 3 markers with an error rate of 5%, might allow to personalize the screening and prevention of metabolic syndrome-driven morbidities as liver steatosis.

Metabolic Syndrome (MetS) is a cluster of bioclinical abnormalities including hypertension, central obesity, impaired glucose metabolism, hypertriglyceridemia, and low high-density lipoprotein (HDL) cholesterolemia[1]. These abnormalities are risk factors for developing cardiovascular disease, nonalcoholic fatty liver, type 2 diabetes, neurocognitive disorders, and death from all causes[2]. The prevalence of MetS is on the increase worldwide and affects more than 20% of the global adult population[3]. A root cause of MetS is insulin resistance (IR)[1]. It is therefore of major interest to identify the causes of IR and the biomarkers able to predict its development.

IR is fueled by immune activation (IA). Thus, for instance, the inflammatory cytokines tumor necrosis factor α (TNFα), interleukin (IL)-1β, and IL-6 inhibit insulin signaling[4]. We have recently shown, using 43 cell surface and soluble markers, that distinct IA profiles may be distinguished by a double hierarchical clustering in 150 people aged 55–69 years who were visiting a health center for routine check-up[5]. Moreover, some of these profiles were linked to potential causes of IA as a low level of regulatory T cells, a CD4+ T cell subpopulation able to downregulate IA, or microbial translocation[5].

People living with HIV-1 on efficient antiretroviral therapy present with persistent chronic IA[6]. We have previously identified in 120 virologic responders 5 different IA profiles[7]. Among these profiles, Profile 2, was linked to IR. One feature of this profile was an elevated plasma levels of soluble TNF receptor I (sTNFRI). As sTNFRI correlates with TNFα production, and as TNFα induces IR, this is in favor of a causative link between Profile 2 and IR.

Here we probed whether, in a same way one of the IA Profiles we described in a general population could also be linked to IR.

[1]Immunology Department, Nîmes University Hospital, Place du Pr Debré, 30029 Nîmes, France. [2]Institute of Human Genetics, CNRS-Montpellier University UMR9002, 141 rue de la Cardonille, 34396 Montpellier Cedex 5, France. [3]Institute of Functional Genomics UMR5203 and Biocampus UAR3426, CNRS, Inserm, Montpellier University, 141 rue de la Cardonille, 34396 Montpellier, France. [4]Biochemestry Department, Montpellier University Hospital, 371 avenue du Doyen Gaston Giraud, 34295 Montpellier, France. [5]Immunology Department, Montpellier University Hospital, 80 avenue Auguste Fliche, 34295 Montpellier, France. [6]Caisse Primaire D'Assurance Maladie, 14 rue du cirque Romain, Nîmes, France. [7]Montpellier University, 5 Boulevard Henri IV, 34967 Montpellier, France. [8]Fédération Hospitalo-Universitaire Infections Chroniques, Montpellier-Nîmes, France. ✉email: pcorbeau@igh.cnrs.fr

Characteristic	Variable	All profiles	Profile 1 (N = 43)	Profile 2 (N = 22)	Profile 3 (N = 39)	Profile 4 (N = 41)	Profile 5 (N = 5)
Age	Mean (SD)	61.7 (4.3)	61.4 (4.6)	61.8 (4.8)	62.8 (4.3)	61.2 (3.8)	61.0 (2.1)
Sex							
Female	%	48	67	23	59	39	20
Male	%	52	33	77	41	61	80
Ethnicity							
African	%	8	10	14	10	2	0
Caucasian	%	92	90	86	90	98	100
Body Mass Index	Mean (SD)	26.6 (4.6)	25.6 (4.9)	27.3 (5.0)	26.8 (4.0)	27.4 (4.9)	25.8 (4.8)
Waist circumference (cm)	Mean (SD)	88.8 (13.3)	85.5 (14.2)	93.4 (14.0)	87.6 (10.5)	90.6 (13.3)	90.8 (16.3)
Female	Mean (SD)	81.5 (10.8)	78.2 (11.2)	80.6 (9.0)	83.6 (10.9)	83.4 (10.8)	95.0
Male	Mean (SD)	95.5 (11.5)	94.5 (11.8)	95.4 (10.7)	96.9 (13.1)	94.9 (12.3)	91.7 (9.8)
Hip circumference (cm)	Mean (SD)	100.5 (8.6)	99.5 (8.6)	99.6 (8.7)	102.2 (8.3)	100.6 (8.6)	97.2 (10.2)
Systolic blood pressure (mmHg)	Mean (SD)	138 (17)	137 (20)	141 (12)	137 (17)	138 (19)	137 (20)
Diastolic blood pressure (mmHg)	Mean (SD)	83 (10)	81 (11)	84 (8)	83 (10)	82 (10)	84 (9)
Glycemia (mM)	Mean (SD)	5.58 (1.17)	5.54 (1.51)	6.16 (1.70)	5.36 (0.69)	5.56 (0.82)	5.40 (0.60)
Cholesterol (mM)	Mean (SD)	2.24 (0.45)	2.22 (0.36)	2.26 (0.55)	2.20 (0.53)	2.25 (0.42)	2.31 (0.42)
HDL (mM)	Mean (SD)	0.59 (0.16)	0.65 (0.20)	0.55 (0.14)	0.60 (0.13)	0.55 (0.13)	0.58 (0.13)
LDL (mM)	Mean (SD)	1.42 (0.38)	1.36 (0.30)	1.40 (0.45)	1.40 (0.43)	1.49 (0.39)	1.49 (0.38)
Triglyceridemia (mM)	Mean (SD)	1.19 (0.68)	1.12 (0.64)	1.54 (1.03)	1.09 (0.54)	1.15 (0.59)	1.26 (0.57)
Insulinemia (µU/mL)	Mean (SD)	10.2 (6.3)	9.7 (5.6)	13.3 (9.2)	9.3 (5.4)	10.1 (5.7)	9.5 (7.3)
Antidiabetic therapy	Number (%)	9 (6%)	4 (9%)	3 (14%)	1 (3%)	1 (2%)	0 (0%)
Antihyperlipidemic therapy	Number (%)	31 (21%)	6 (14%)	8 (36%)	10 (26%)	6 (15%)	0 (0%)
High blood pressure therapy	Number (%)	36 (24%)	8 (19%)	7 (32%)	10 (26%)	8 (19%)	0 (0%)

Table 1. Patients characteristics.

Results

A specific immune activation profile is linked to insulin resistance and metabolic syndrome. We recruited 74 women and 76 men with a mean (± SD) age of 61.7 (± 4.3) years. We have previously shown that 5 different IA profiles may be distinguished in this cohort. Profile 1 is characterized by a high proportion of naïve T cells, Profiles 2 and 3 by elevated percentages of terminally differentiated and senescent CD4+ T cells and CD8+ T cells, respectively, Profile 4 by a high proportion of activated NK cells, and Profile 5 by an increase in the percentage of monocytes[5].

We tested to see whether one of the IA profiles we had observed in the 150 subjects we have previously analyzed was associated with IR and MetS. The levels of the risk factors defining MetS are given in Table 1 for each IA profile. Compared with the other volunteers, Profile 2 individuals presented higher insulinemia (13.3 ± 9.2 vs 9.7 ± 5.6 µU/mL, $p = 0.016$, Fig. 1a), higher homeostatic model assessment (HOMA) (3.9 ± 3.4 vs 2.4 ± 1.6, $p = 0.014$, Fig. 1b), a larger waist/hip circumference (0.93 ± 0.09 vs 0.87 ± 0.10, $p = 0.005$, Fig. 1c), and higher triglyceridemia (1.5 ± 1.0 vs 1.1 ± 0.6 mM, $p = 0.041$, Fig. 1d). Their glycemia (6.2 ± 1.7 vs 5.5 ± 1.0 mM, $p = 0.122$, Fig. 1e) and systolic blood pressure (141 ± 12 vs 137 ± 18 mmHg, $p = 0.172$, Fig. 1f), were non-significantly higher than the other volunteers, and their HDL (0.55 ± 0.14 vs 0.60 ± 0.16 mM, $p = 0.350$, Fig. 1g) non-significantly lower.

In line with these biological data, Profile 2 volunteers were more often treated with antihyperlipidemic drugs than the other volunteers (36.4 vs 17.2%, $p = 0.038$), as shown in Table 1. Antidiabetic (13.6 vs 4.7%, $p = 0.128$) and antihypertensive drugs (31.8 vs 20.3%, $p = 0.229$) were non-significantly more often prescribed to Profile 2 individuals than to individuals with another profile.

Characterization of the immune activation profile linked to insulin resistance. As Profile 2 is associated with IR and MetS markers, we further analyzed the characteristics of this profile. Consistently with their high proportions of circulating terminally differentiated and senescent CD4+ T cells, people with Pro-

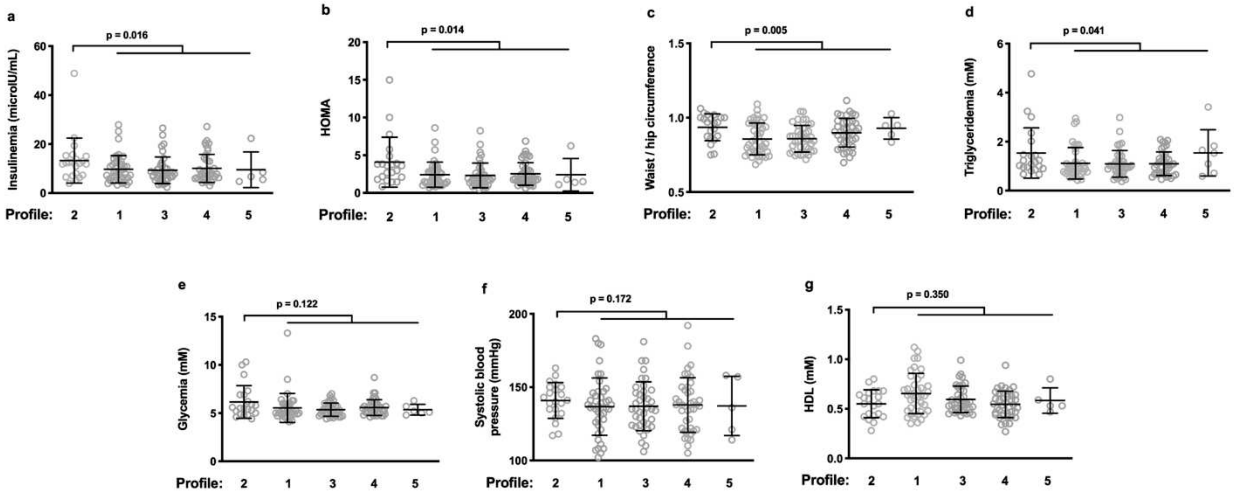

Figure 1. Profile 2 presents with features of insulin resistance and metabolic syndrome. Profile 2 people have higher insulinemia (**a**), HOMA (**b**), waist/hip ratio (**c**), triglyceridemia (**d**), glycemia (**e**), systolic blood pressure (**f**), and HDL (**g**) than the rest of the volunteers.

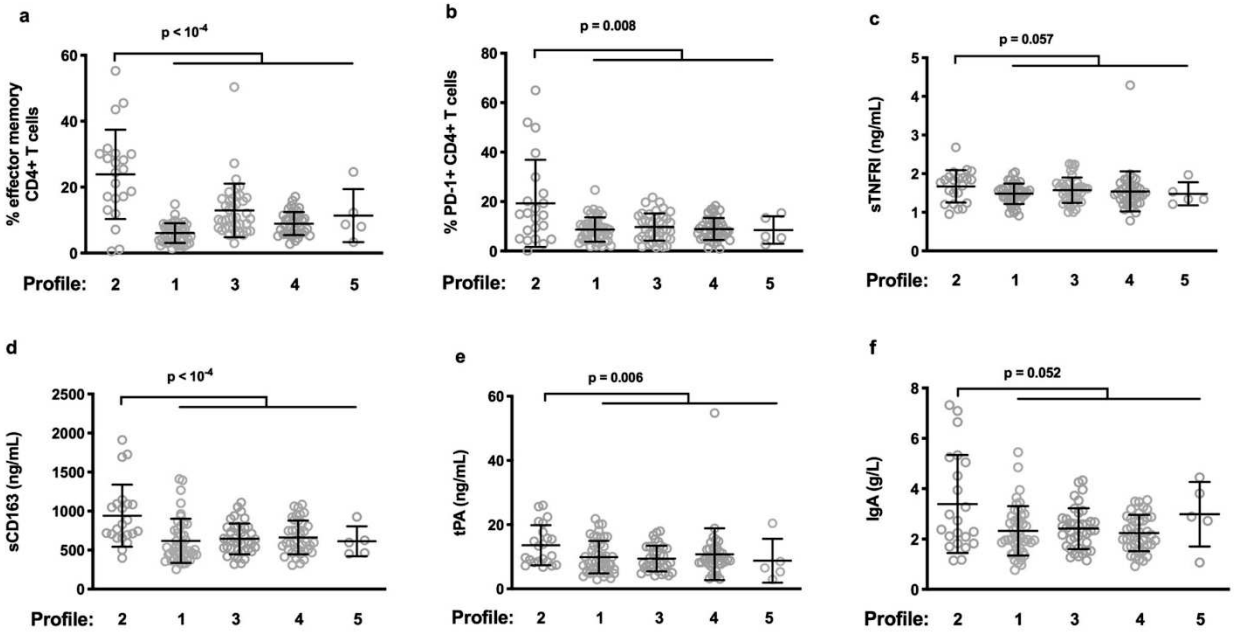

Figure 2. Immune characteristics of Profile 2. Differences between the level of various activation markers in Profile 2 and the other profiles (**a**–**f**).

file 2 presented with high proportions of effector memory (24 ± 13 vs 9 ± 6%, $p < 10^{-4}$, Fig. 2a) and exhausted (19 ± 18 vs 9 ± 5%, $p = 0.008$, Fig. 2b) CD4+ T cells than the other participants. In addition, their plasma levels of sTNFRI (1.7 ± 0.4 vs 1.5 ± 0.4 mg/L, $p = 0.057$, Fig. 2c), soluble CD163 (sCD163), a marker of monocyte activation (940 ± 398 vs 639 ± 234 ng/mL, $p < 10^{-4}$, Fig. 2d), tissue Plasminogen Activator (tPA), a marker of endothelial activation (14 ± 6 vs 10 ± 6 ng/mL, $p = 0.006$, Fig. 2e), and immunoglobulin (Ig)A (3.4 ± 1.9% vs 2.3 ± 0.9 g/L, $p = 0.052$, Fig. 2f), were, or tended to be, also higher than those of the other individuals.

In the hierarchical clustering we have previously performed on all the IA markers, sCD163, tPA, sTNFRI, and IgA were close[5]. Accordingly, in the 150 volunteers, sCD163 ($r = 0.291$, $p < 0.001$, Fig. 3a) and tPA ($r = 0.230$, $p = 0.005$, Fig. 3b) levels correlated with sTNFRI plasma concentrations. sCD163 ($r = 0.295$, $p < 0.001$, Fig. 3c) and tPA ($r = 0.344$, $p < 10^{-4}$, Fig. 3d) also correlated with C-reactive protein (CRP).

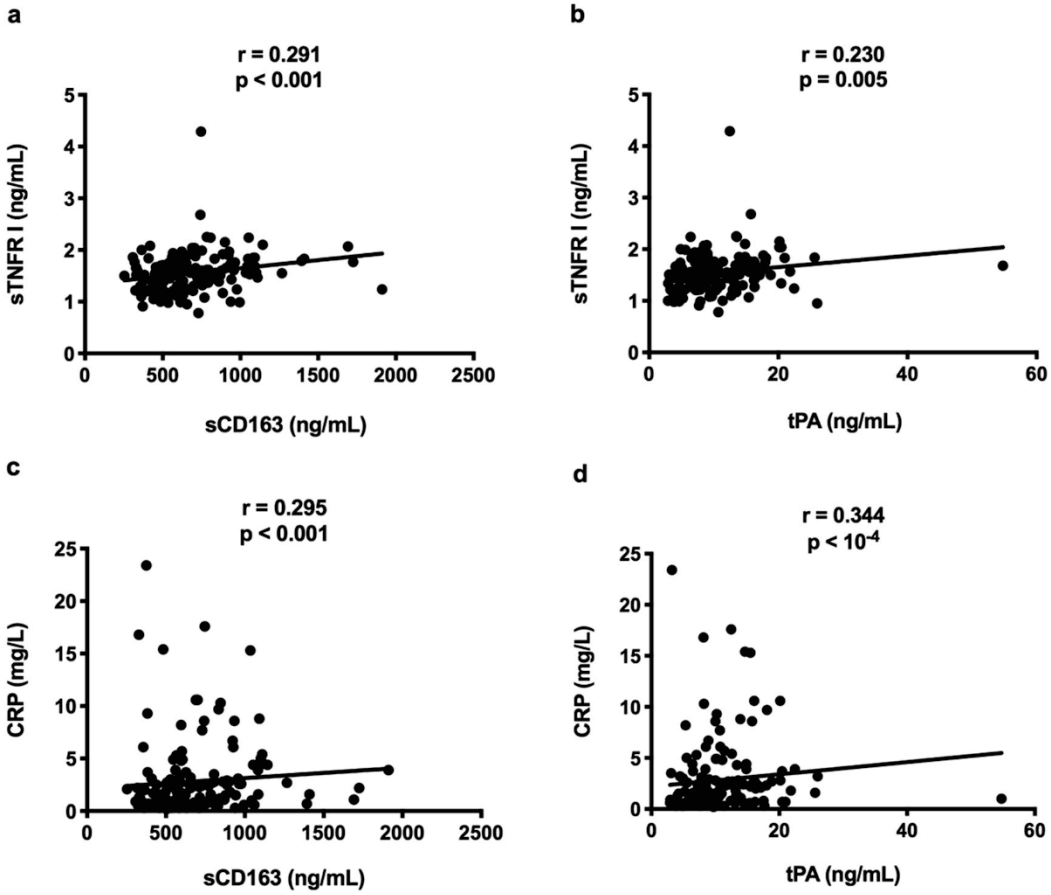

Figure 3. Links between various activation markers in the whole population.

Biomarker selection for Profile 2 signature. Interestingly, using only three markers, the percentage of senescent (CD57+) CD4+ T cells, the circulating levels of IgA and sCD163, we were able to determine whether a volunteer presented or not with Profile 2 with an error rate of 5%, a specificity of 99%, and a sensibility of 77%.

The IA profiles linked to insulin resistance in HIV-positive individuals and in the general populations have similarities. We tested whether the IR-associated IA profile we have just unveiled in the general population presented common traits with the IR-associated IA profile we have previously identified in people living with HIV-1[7]. Indeed, as compared with the other profiles, HIV-positive Profile 2 was also characterized by high levels of sTNFRI (1.46 ± 0.31 vs 1.23 ± 0.50 ng/mL, $p = 0.012$, Fig. 4a) and high percentages of effector memory CD4+ T cells (15.3 ± 8.1 vs 10.4 ± 6.2%, $p = 0.017$, Fig. 4b). Both Profiles 2 presented a low proportion of naïve CD4+ T cells (24.9 ± 14.4 vs 44.8 ± 14.2%, $p < 10^{-4}$, Fig. 4c and 30.7 ± 9.6 vs 40.2 ± 17.1%, $p = 0.039$, Fig. 4d in the general population and in HIV-positive adults, respectively) and a high proportion of activated, HLA-DR-positive, CD4+ T cells (22.5 ± 11.3 vs 14.8 ± 10.7%, $p < 10^{-4}$, Fig. 4e and 25.9 ± 7.9 vs 21.7 ± 13.1%, $p = 0.019$, Fig. 4f, respectively). Likewise, in these Profiles 2 there weas a low percentage of naïve CD8+ T cells (24.9 ± 8.3 vs 39.3 ± 16.3%, $p < 10^{-4}$, Fig. 4g and 22.8 ± 5.8 vs 40.0 ± 14.7%, $p < 10^{-4}$, Fig. 4h, respectively) contrasting with a high percentage of effector memory CD8+ T cells (14.7 ± 9.7 vs 8.4 ± 6.2%, $p < 10^{-3}$, Fig. 4i and 10.6 ± 5.5 vs 7.1 ± 5.0%, $p = 0.017$, Fig. 4j, respectively). Finally, two common characteristics of Profiles 2 were high proportions of HLA-DR-positive, CD8+ T cells (47.9 ± 18.5 vs 38.1 ± 17.0%, $p = 0.015$, Fig. 4k and 71.4 ± 14.6 vs 52.4 ± 17.9%, $p < 10^{-3}$, Fig. 4l, respectively) and of senescent, CD57+, CD8+ T cells (36.9 ± 17.0 vs 27.9 ± 16.0%, $p = 0.020$, Fig. 4m and 48.5 ± 7.1 vs 30.4 ± 14.0%, $p < 10^{-4}$, Fig. 4n, respectively).

Correlations between immune activation and Metabolic Syndrome markers. Next, we sought links between the characteristics of Profile 2 and markers of IR in the whole population. As a relationship between CD4+ T cell senescence and IR has been recently reported[8], we looked for such a link in our cohort. We found that the number of senescent CD4+ T cells tended to correlate with insulinemia ($r = 0.143$, $p = 0.087$, Fig. 5a). In addition, plasma levels of insulinemia correlated with those of sTNFRI ($r = 0.217$, $p = 0.008$, Fig. 5b) and of another inflammation marker, CRP ($r = 0.173$, $p = 0.034$, Fig. 5c). Moreover, insulin concentrations were also strongly linked to the other soluble markers overexpressed in IA Profile 2, sCD163 ($r = 0.283$, $p < 0.001$, Fig. 5d), tPA ($r = 0.542$, $p < 10^{-4}$, Fig. 5e), and IgA ($r = 0.265$, $p < 0.001$, Fig. 5f). The same was true for HOMA

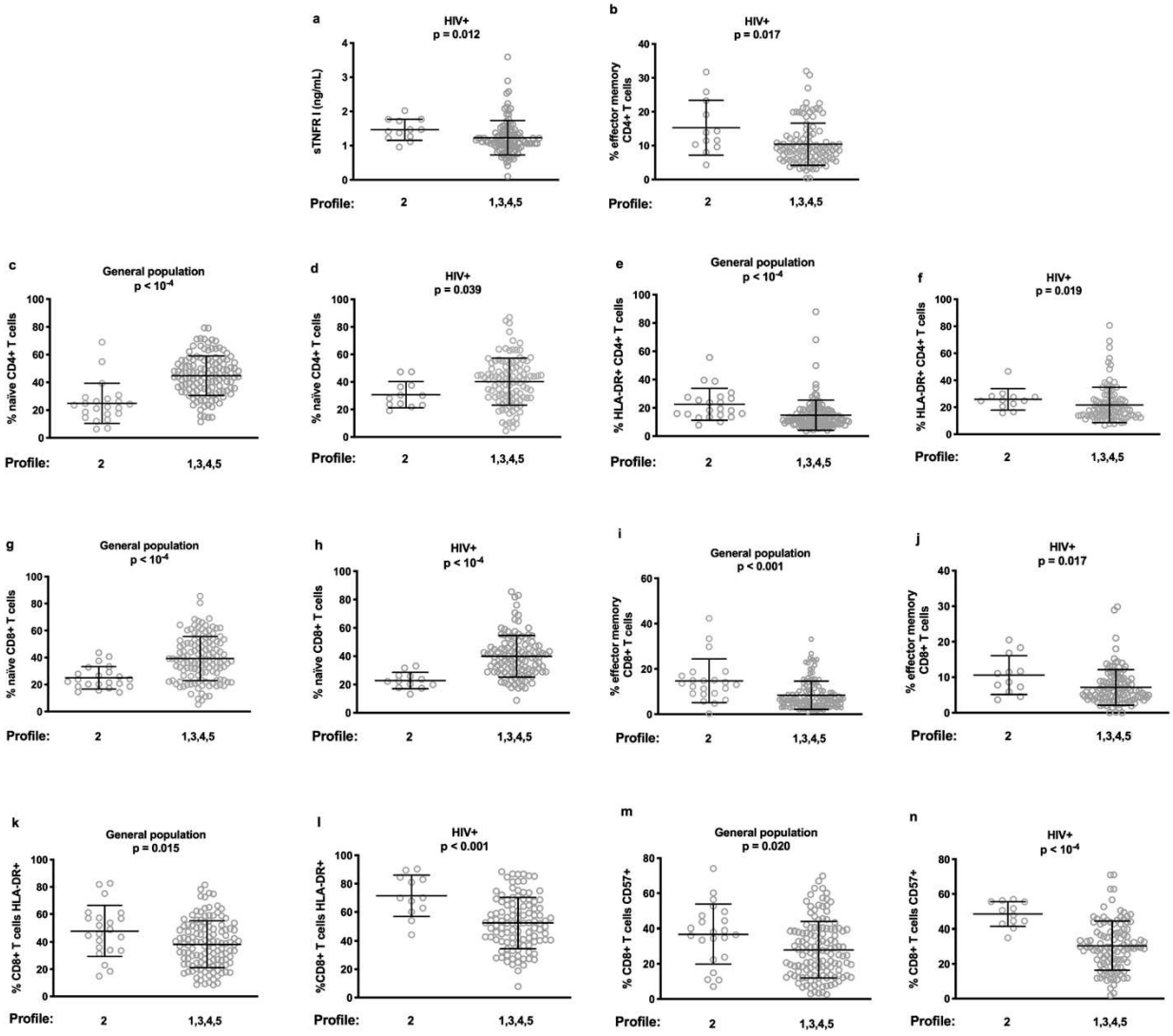

Figure 4. Common immunological characteristics between the general population Profile 2 and the HIV patients Profile 2. The expression of each marker in Profile 2 is compared with its expression in the other profiles.

that correlated with sTNRF1 ($r = 0.239$, $p = 0.004$, Fig. 5g), sCD163 ($r = 0.276$, $p < 0.001$, Fig. 5h), tPA ($r = 0.593$, $p < 10^{-4}$, Fig. 5i), and IgA ($r = 0.264$, $p = 0.001$, Fig. 5j).

We also looked for links between increased markers in Profile 2 and markers of MetS. Senescent CD4+ T cell count was linked to triglyceridemia ($r = 0.202$, $p = 0.015$, Fig. 6a) and waist/hip ratio ($r = 0.182$, $p = 0.029$, Fig. 6b). sTNFRI and tPA correlated with blood pressure, waist/hip ratio, triglyceridemia, and HDL levels (Fig. 6c–j). IgA and sCD163 correlated with blood pressure, waist/hip ratio, and HDL levels (Fig. 6k–p).

IA Profile 2 is linked to high γGT levels. One of the consequences of MetS is liver steatosis[2]. Liver steatosis is the most common cause of elevated gamma-glutamyltransferase (γGT)[9]. To test the hypothesis that persons with IA Profile 2 might develop more frequently this disease, we compared γGT levels in the persons who volunteered for this study according to their IA profile. Individuals with IA Profile 2 presented with higher levels of γGT than the other individuals (76 ± 88 vs 38 ± 34 UI/L, $p = 0.007$, Fig. 7a). Another potential cause of elevated serum γGT levels is alcohol consumption, but there was no difference in alcohol use between participants with Profile 2 and the other participants (6.1 ± 10.9 vs 8.2 ± 22.1 g, $p = 0.846$, Fig. 7b).

Discussion

In this study, we have shown that one IA profile is clearly linked to some markers of IR and MetS, eventhough subjects with this profile received antidiabetic, antihyperlipidemic and antihypertensive therapies more often than the other subjects. This is phenocopying our report of a link between one IA profile and hyperinsulinemia as well as hypertriglyceridemia in HIV patients[7]. Of note, both IR-linked IA profiles, in people living with HIV-1

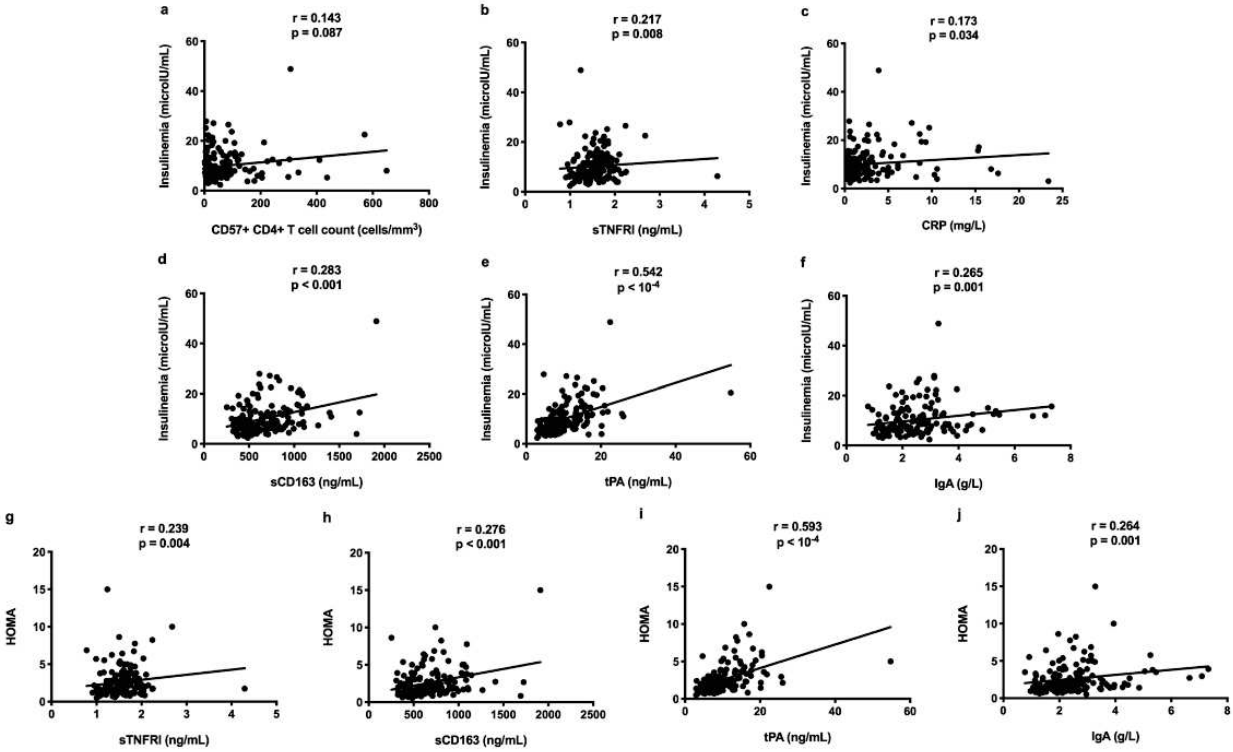

Figure 5. Links between various activation markers, insulinemia and HOMA in the whole population.

and in a general population, present many common immunological characteristics. This is also in line with the correlation between adipose tissue inflammation and IR reported by many studies[10]. In particular, macrophage activation, TNFα overproduction[11], and CD163 shedding[12] have been observed in human obese adipose tissue. Even activated B cells have been shown in this tissue[13].

Strikingly, in this present work we found that the IA profile linked to insulin resistance was characterized by a high level of sTNFRI, a finding common to our observation in people living with HIV[7]. As sTNFRI is a marker of TNFα production, and as TNFα inhibits insulin signaling[4], both findings argue for a causative link between IA Profile 2 and insulin resistance.

We also observed that hyperinsulinemia was linked to the levels of circulating sCD163. In the course of inflammation, CD163 is shed from the surface of monocytes and macrophages by the metalloproteinase TNFα-converting enzyme (TACE), which is also responsible for the release of TNFα from the surface of immune cells[14]. Therefore, sCD163 is considered as a marker of monocyte and macrophage activity and of TNFα production. Indeed, TNFα production and sCD163 levels have previously been shown to be related[15] as we observed here (Fig. 3a). White adipose tissue (WAT) inflammation and IR are inter-related[16]. This WAT inflammation results in CD163 mRNA overexpression in WAT macrophages[17] which correlates with sCD163 blood concentrations[12]. Accordingly, sCD163 levels have been reported to be linked to adiposity[18–22] on one hand and to IR[15,20,21,23–25] on the other hand. sCD163 has even be identified as a predictive marker of type 2 diabetes in the general population independently of age or BMI[23]. Thus, the fact that sCD163 levels in Profile 2 are higher than in the other profiles may be considered as an additional argument for a causative link between Profile 2 and IR.

tPA is released by activated endothelial cells functioning both as a serine protease favoring thrombolysis by converting plasminogen to plasmin and as an inflammatory cytokine[26]. tPA activates NFκB, inducing inflammatory cytokines production, and modulates inflammatory infiltration, particularly macrophage migration, in various organs[26–30]. In line with these proinflammatory properties, tPA levels have been linked to CRP and fibrinogen levels in another study[31], and to sTNFRI as well as to CRP in the present study (Fig. 3b,d). These characteristics might explain why tPA is correlated with IR and predictive for the development of type 2 diabetes[32–34]. Thus, the high level of tPA in Profile 2 may be interpreted as a third argument for a causative link between Profile 2 and IR.

In addition to monocyte/macrophage and T cell activation, B cell overactivity has been observed in the visceral adipose tissue (VAT) of obese mice[35,36] and men[13]. In VAT, B cell activation induces the production of IFNγ and other inflammatory cytokines by T cells, fueling IR[36]. This aligns with the fact that B cell deficient mice on a high fat diet show better insulin sensitivity than wild-type mice[36]. One consequence of this B cell activation might be an increase in serum IgA levels which has been linked to obesity[37,38], MetS[37,38], and diabetes[37], as we observed here in Profile 2.

Globally, these data lead to a model where IA Profile 2 favors IR. Yet, it may be argued that conversely, IR may favor Profile 2. First, IR is responsible for an increase in circulating free fatty acids able to activate hepatic macrophages and thereby to increase the level of sCD163[39]. In addition, IR and hyperglycemia cause oxidative

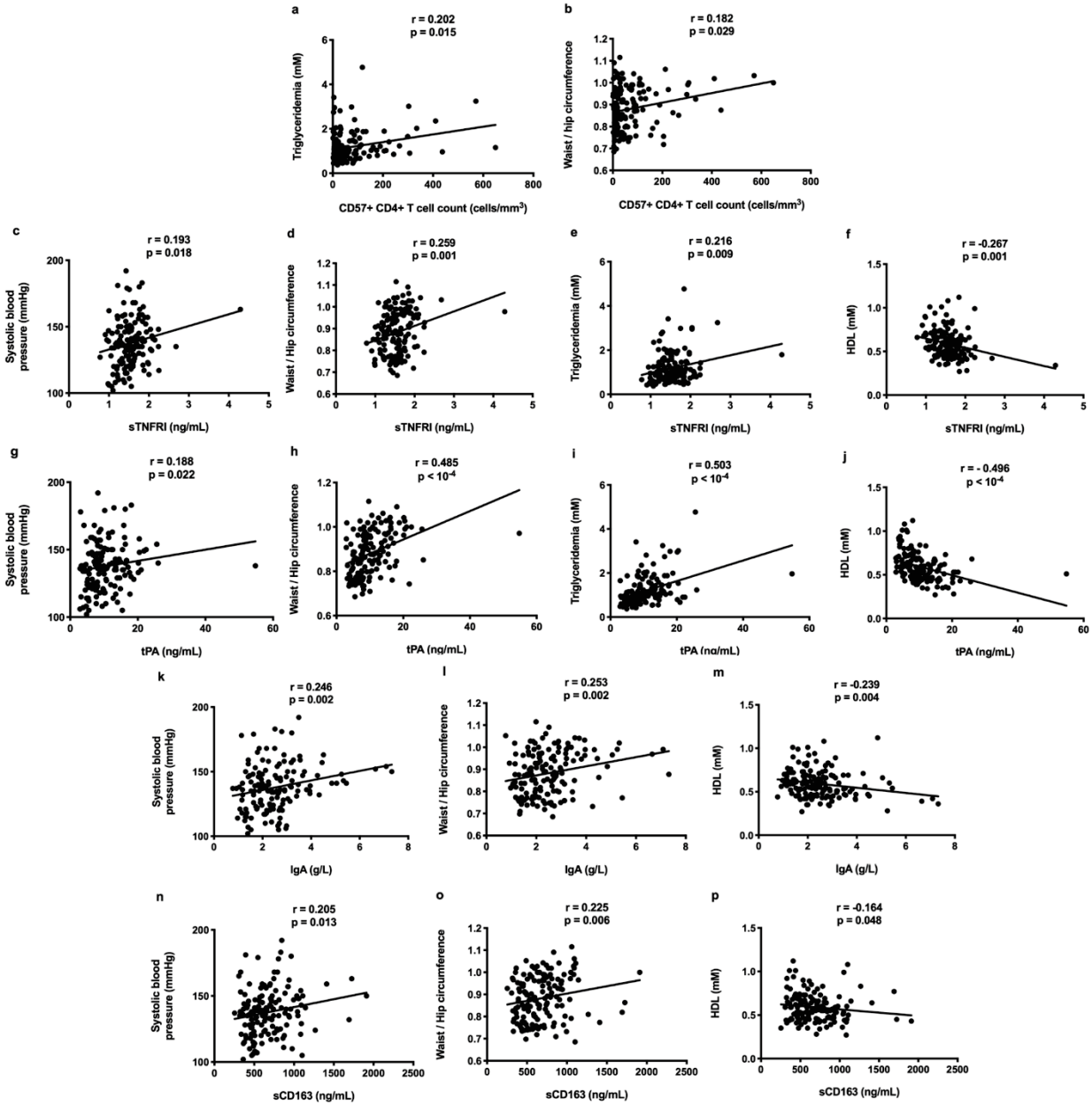

Figure 6. Links between various activation markers and markers of metabolic syndrome in the whole population.

stress, TACE activation, and CD163 shedding[14]. Second, a positive causal effect of IR on tPA has been revealed via a Mendelian randomization analysis[32]. This causal effect could be mediated by a defect in endothelium-derived nitric oxide[40]. Third, hyperproduction of IgA might also be a consequence of metabolic disorders, as suggested by the report that treatment of morbid obesity by adjustable gastric banding leads to reduction in IgA values[41].

Thus, the links between Profile 2 and IR might be bidirectional, resulting in a vicious circle. Whatever the nature of these links, it would be interesting to test whether Profile 2 is predictive for the establishment of MetS and for the morbidities it fuels. The combination of activation markers characterizing Profile 2 might then provide us with a predictive signature. The possibility of reducing the size of this signature to three markers adapts immune profiling to routine. Last, but not least, deciphering the soluble factors which are overproduced by Profile 2 individuals, and which may cause IR might uncover pathways to pharmacologically target and prevent MetS.

One of the limitation of our work is that our study population is not representative of the general population. We recruited adults who volunteered for a free health checkup. Therefore, the majority of these volunteers were in a precarious socio-economical situation, and overweight. Another limitation is that the present study is cross-sectional, highlighting only correlations. Further analysis is needed to establish whether there are causative links between some types of immune activation and IR.

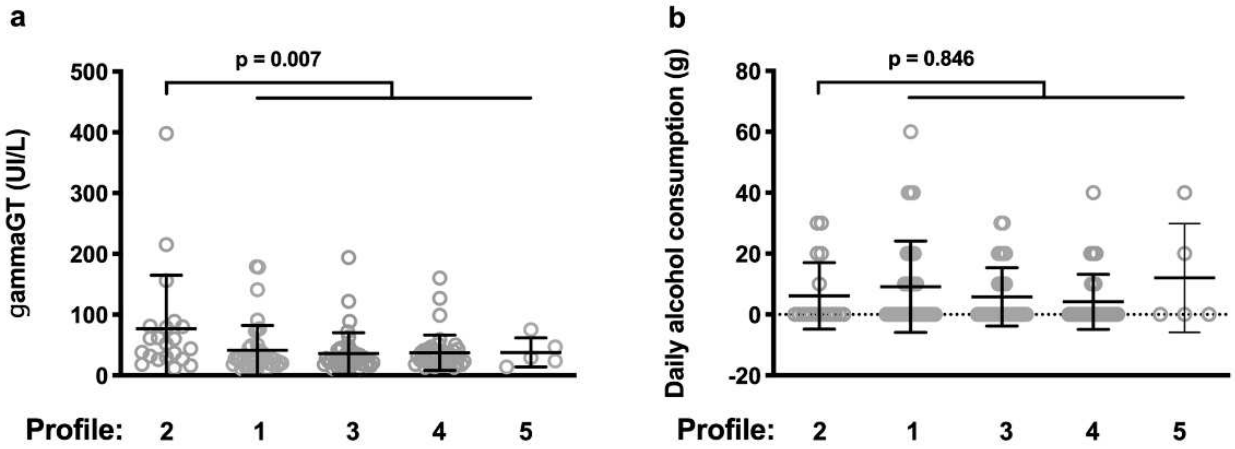

Figure 7. Profile 2 participants present with high yGT levels (**a**) but similar alcohol use (**b**) as compared with the other participants.

Globally, we show that one of the IA profiles observed in a general population is linked to IR, MetS, and possibly to one consequence of MetS, liver steatosis. Our findings open the way to the identification of markers predictive for metabolic syndrome and the morbidities it drives, and of new causative factors.

Methods

Study design. We have previously described the characteristics of the 150 volunteers we enrolled for this study[5]. Pregnant or breastfeeding women, people under immunomodulatory treatment, with cancer, acute infection, autoimmune or autoinflammatory disease were not included. Fifty-nine percent of these volunteers were in a precarious socio-economical situation. Our protocol was performed in accordance with the relevant guidelines and regulations and approved by the French Ethics Committee Sud Est IV. All patients had provided written informed consent. The trial was registered on ClinicalTrials.gov under the reference NCT04028882.

Metabolic and immunologic markers in peripheral blood. Blood was collected after eight hours of fasting on EDTA Vacutainer tubes (Becton Dickinson, Le Pont-de-Claix, France), immediately centrifuged (delay < 4 h) and plasma was frozen at -80 °C on several aliquots until analysis. Insulinemia were measured using electrochemiluminescence immunoassay "ECLIA" on Cobas e602 analyzer from Roche (Roche diagnostic, Meylan, France) using Roche reagent kits and calibrators. Insulinemia was determined from plasma aliquot never thawed. Lower detection limit was 0.2 µU/mL (1.39 pmol/L) and intra-and inter-assay was < 1.5% and < 5%, respectively. Blood triglycerides, HDL, LDL, and total cholesterol levels were quantified on the Cobas8000/c502© analyzer from serum collected into SST II Vacutainer tubes (Becton Dickinson). The determination of the other markers has been previously described[5].

Statistical analysis. We used t-test or Mann–Whitney test to compare markers and IA profiles. The links between markers were determined by Spearman rank correlations. Fisher test or χ^2 test was used to compare qualitative covariates.

The R software version R 3.5.1 (July, 2018) was used to perform the analysis described in this section. To select an optimal number of variables and create a parsimonious predictive model of the Profile 2, we chose genetic algorithms (GAs)[42,43]. GAs are optimization algorithms, inspired by Charles Darwin's idea of natural selection. They provide approximate solutions to complex optimization problems. In a first step, a population of potential solutions is randomly generated. Then, this population evolves through the iterative application of mutation, cross-over and selection. The natural selection preferentially preserves the fittest individuals over the successive generations. An evolutionary algorithm improves the selection over time and allows the best solution to emerge from the best of prior solutions.

In our application[44,45], solutions are subsets (combinations) of the immunological markers (the features) mentioned above. Specifically, the mutation randomly alters a solution by feature addition, removal or substitution. The cross-over randomly combines the features of two solutions. Selection is the only operator increasing the quality of solutions across generations. It relies on a fitness function (to be optimized) quantifying the solution quality.

A Linear Discriminant Analysis (LDA)[46] is applied on each solution using the R package MASS. To avoid over-fitting a cross-validation is used to evaluate the accuracy. The fitness function uses this accuracy penalized by the subset size to favor parsimonious solutions. In this goal, we also chose 10 as the maximal size for subsets. In order to favor solution robustness, the genetic algorithm was run four times and all solutions of the final generations were evaluated through 30 runs of independent linear discriminant analysis with 2-fold cross validation. Solutions were ranked according to their average correct classification rate during the cross-validation process.

Received: 3 March 2021; Accepted: 19 May 2021
Published online: 10 June 2021

References

1. Alberti, K. G. *et al.* Harmonizing the metabolic syndrome: A joint interim statement of the International Diabetes Federation Task Force on Epidemiology and Prevention; National Heart, Lung, and Blood Institute; American Heart Association; World Heart Federation; International Atherosclerosis Society; and International Association for the Study of Obesity. *Circulation* **120**, 1640–1645. https://doi.org/10.1161/CIRCULATIONAHA.109.192644 (2009).
2. Brede, S., Serfling, G., Klement, J., Schmid, S. M. & Lehnert, H. Clinical scenario of the metabolic syndrome. *Visceral Med.* **32**, 336–341. https://doi.org/10.1159/000449028 (2016).
3. Saklayen, M. G. The global epidemic of the metabolic syndrome. *Curr. Hypertens. Rep.* **20**, 12. https://doi.org/10.1007/s11906-018-0812-z (2018).
4. Boucher, J., Kleinridders, A. & Kahn, C. R. Insulin receptor signaling in normal and insulin-resistant states. *Cold Spring Harbor Perspect. Biol.* **6**, 1. https://doi.org/10.1101/cshperspect.a009191 (2014).
5. Cezar, R. *et al.* Identification of distinct immune activation profiles in adult humans. *Sci. Rep.* **10**, 20824 (2020).
6. Younas, M., Psomas, C., Reynes, J. & Corbeau, P. Immune activation in the course of HIV-1 infection: Causes, phenotypes and persistence under therapy. *HIV Med.* **17**, 89–105. https://doi.org/10.1111/hiv.12310 (2016).
7. Psomas, C. *et al.* One of the immune activation profiles observed in HIV-1-infected adults with suppressed viremia is linked to metabolic syndrome: The ACTIVIH study. *EBioMedicine* **8**, 265–276. https://doi.org/10.1016/j.ebiom.2016.05.008 (2016).
8. Yi, H. S. *et al.* T-cell senescence contributes to abnormal glucose homeostasis in humans and mice. *Cell Death Dis.* **10**, 249. https://doi.org/10.1038/s41419-019-1494-4 (2019).
9. Ekstedt, M. *et al.* Long-term follow-up of patients with NAFLD and elevated liver enzymes. *Hepatology* **44**, 865–873 (2006).
10. Zatterale, F. *et al.* Chronic adipose tissue inflammation linking obesity to insulin resistance and type 2 diabetes. *Front. Physiol.* **10**, 1607. https://doi.org/10.3389/fphys.2019.01607 (2019).
11. Hotamisligil, G. S., Arner, P., Caro, J. F., Atkinson, R. L. & Spiegelman, B. M. Increased adipose tissue expression of tumor necrosis factor-alpha in human obesity and insulin resistance. *J. Clin. Investig.* **95**, 2409–2415. https://doi.org/10.1172/JCI117936 (1995).
12. Kracmerova, J. *et al.* Soluble CD163 is associated with CD163 mRNA expression in adipose tissue and with insulin sensitivity in steady-state condition but not in response to calorie restriction. *J. Clin. Endocrinol. Metab.* **99**, E528-535. https://doi.org/10.1210/jc.2013-3348 (2014).
13. McDonnell, M. E. *et al.* B lymphocytes in human subcutaneous adipose crown-like structures. *Obesity* **20**, 1372–1378. https://doi.org/10.1038/oby.2012.54 (2012).
14. Etzerodt, A., Maniecki, M. B., Moller, K., Moller, H. J. & Moestrup, S. K. Tumor necrosis factor alpha-converting enzyme (TACE/ADAM17) mediates ectodomain shedding of the scavenger receptor CD163. *J. Leukoc. Biol.* **88**, 1201–1205. https://doi.org/10.1189/jlb.0410235 (2010).
15. Kawarabayashi, R. *et al.* The association between monocyte surface CD163 and insulin resistance in patients with type 2 diabetes. *J. Diabetes Res.* **2017**, 6549242. https://doi.org/10.1155/2017/6549242 (2017).
16. Hardy, O. T., Czech, M. P. & Corvera, S. What causes the insulin resistance underlying obesity?. *Curr. Opin. Endocrinol. Diabetes Obes.* **19**, 81–87. https://doi.org/10.1097/MED.0b013e3283514e13 (2012).
17. Shakeri-Manesch, S. *et al.* Diminished upregulation of visceral adipose heme oxygenase-1 correlates with waist-to-hip ratio and insulin resistance. *Int. J. Obes.* **33**, 1257–1264. https://doi.org/10.1038/ijo.2009.160 (2009).
18. Sorensen, L. P. *et al.* Visceral obesity is associated with increased soluble CD163 concentration in men with type 2 diabetes mellitus. *Endocr. Connect.* **4**, 27–36. https://doi.org/10.1530/EC-14-0107 (2015).
19. Fjeldborg, K. *et al.* Intrahepatic fat content correlates with soluble CD163 in relation to weight loss induced by Roux-en-Y gastric bypass. *Obesity* **23**, 154–161. https://doi.org/10.1002/oby.20942 (2015).
20. Zanni, M. V., Burdo, T. H., Makimura, H., Williams, K. C. & Grinspoon, S. K. Relationship between monocyte/macrophage activation marker soluble CD163 and insulin resistance in obese and normal-weight subjects. *Clin. Endocrinol.* **77**, 385–390. https://doi.org/10.1111/j.1365-2265.2011.04284.x (2012).
21. Fjeldborg, K. *et al.* The macrophage-specific serum marker, soluble CD163, is increased in obesity and reduced after dietary-induced weight loss. *Obesity* **21**, 2437–2443. https://doi.org/10.1002/oby.20376 (2013).
22. Al-Daghri, N. M. *et al.* Soluble CD163 is associated with body mass index and blood pressure in hypertensive obese Saudi patients. *Eur. J. Clin. Investig.* **42**, 1221–1226. https://doi.org/10.1111/j.1365-2362.2012.02714.x (2012).
23. Moller, H. J., Frikke-Schmidt, R., Moestrup, S. K., Nordestgaard, B. G. & Tybjaerg-Hansen, A. Serum soluble CD163 predicts risk of type 2 diabetes in the general population. *Clin. Chem.* **57**, 291–297. https://doi.org/10.1373/clinchem.2010.154724 (2011).
24. Parkner, T. *et al.* Soluble CD163: a biomarker linking macrophages and insulin resistance. *Diabetologia* **55**, 1856–1862. https://doi.org/10.1007/s00125-012-2533-1 (2012).
25. Reid, M. *et al.* Higher CD163 levels are associated with insulin resistance in hepatitis C virus-infected and HIV-infected adults. *AIDS* **31**, 385–393. https://doi.org/10.1097/QAD.0000000000001345 (2017).
26. Lin, L. & Hu, K. Tissue plasminogen activator and inflammation: from phenotype to signaling mechanisms. *Am. J. Clin. Exp. Immunol.* **3**, 30–36 (2014).
27. Cao, C. *et al.* Endocytic receptor LRP together with tPA and PAI-1 coordinates Mac-1-dependent macrophage migration. *EMBO J.* **25**, 1860–1870. https://doi.org/10.1038/sj.emboj.7601082 (2006).
28. Higazi, A. A. *et al.* Immunomodulatory effects of plasminogen activators on hepatic fibrogenesis. *Clin. Exp. Immunol.* **152**, 163–173. https://doi.org/10.1111/j.1365-2249.2008.03606.x (2008).
29. Roelofs, J. J. *et al.* Tissue-type plasminogen activator modulates inflammatory responses and renal function in ischemia reperfusion injury. *J. Am. Soc. Nephrol.* **17**, 131–140. https://doi.org/10.1681/ASN.2005010089 (2006).
30. Lin, L., Wu, C. & Hu, K. Tissue plasminogen activator activates NF-kappaB through a pathway involving annexin A2/CD11b and integrin-linked kinase. *J. Am. Soc. Nephrol.* **23**, 1329–1338. https://doi.org/10.1681/ASN.2011111123 (2012).
31. Eliasson, M., Jansson, J. H., Nilsson, P. & Asplund, K. Increased levels of tissue plasminogen activator antigen in essential hypertension. A population-based study in Sweden. *J. Hypertens.* **15**, 349–356. https://doi.org/10.1097/00004872-199715040-00005 (1997).
32. Nowak, C. *et al.* Protein biomarkers for insulin resistance and type 2 diabetes risk in two large community cohorts. *Diabetes* **65**, 276–284. https://doi.org/10.2337/db15-0881 (2016).
33. Eliasson, M. C., Jansson, J. H., Lindahl, B. & Stegmayr, B. High levels of tissue plasminogen activator (tPA) antigen precede the development of type 2 diabetes in a longitudinal population study. The Northern Sweden MONICA study. *Cardiovasc. Diabetol.* **2**, 19. https://doi.org/10.1186/1475-2840-2-19 (2003).
34. Festa, A., D'Agostino, R. Jr., Tracy, R. P., Haffner, S. M. & Insulin Resistance Atherosclerosis, S. Elevated levels of acute-phase proteins and plasminogen activator inhibitor-1 predict the development of type 2 diabetes: The insulin resistance atherosclerosis study. *Diabetes* **51**, 1131–1137. https://doi.org/10.2337/diabetes.51.4.1131 (2002).
35. Duffaut, C., Galitzky, J., Lafontan, M. & Bouloumie, A. Unexpected trafficking of immune cells within the adipose tissue during the onset of obesity. *Biochem. Biophys. Res. Commun.* **384**, 482–485. https://doi.org/10.1016/j.bbrc.2009.05.002 (2009).

36. Winer, D. A. *et al.* B cells promote insulin resistance through modulation of T cells and production of pathogenic IgG antibodies. *Nat. Med.* **17**, 610–617. https://doi.org/10.1038/nm.2353 (2011).
37. Gonzalez-Quintela, A. *et al.* Serum levels of immunoglobulins (IgG, IgA, IgM) in a general adult population and their relationship with alcohol consumption, smoking and common metabolic abnormalities. *Clin. Exp. Immunol.* **151**, 42–50. https://doi.org/10.1111/j.1365-2249.2007.03545.x (2008).
38. Bassols, J. *et al.* Increased serum IgG and IgA in overweight children relate to a less favourable metabolic phenotype. *Pediatr. Obes.* **9**, 232–238. https://doi.org/10.1111/j.2047-6310.2013.00160.x (2014).
39. Rosso, C. *et al.* Crosstalk between adipose tissue insulin resistance and liver macrophages in non-alcoholic fatty liver disease. *J. Hepatol.* **71**, 1012–1021. https://doi.org/10.1016/j.jhep.2019.06.031 (2019).
40. Baron, A. D. The coupling of glucose metabolism and perfusion in human skeletal muscle. The potential role of endothelium-derived nitric oxide. *Diabetes* **45**(Suppl 1), S105-109. https://doi.org/10.2337/diab.45.1.s105 (1996).
41. Sakcak, I. *et al.* Comparison of early and late changes in immunoglobulins and acute phase reactants after laparoscopic adjustable gastric banding in patients with morbid obesity. *Obes. Surg.* **20**, 610–615. https://doi.org/10.1007/s11695-009-0061-y (2010).
42. Goldberg, D. E. *Genetic Learning in Optimization, Search and Machine Learning* (Addisson Wesley, 1994).
43. Reeves, C. & Rowe, J. E. *Genetic Algorithms: Principles and Perspectives: A Guide to GA Theory* Vol. 20 (Springer, 2002).
44. Reynes, C., de Souza, S., Sabatier, R., Figuères, G. & Vidal, B. Selection of discriminant wavelength intervals in NIR spectrometry with genetic algorithms. *J. Chemom.* **20**, 136–145 (2006).
45. Gil, M. *et al.* Discrimination of rosé wines using shotgun metabolomics with a genetic algorithm and MS ion intensity ratios. *Sci. Rep.* **10**, 1170 (2020).
46. Hastie, T., Tibshirani, R. & Friedman, J. *The Elements of Statistical Learning: Data Mining, Inference, and Prediction* (Springer, 2009).

Acknowledgements
We are grateful to the persons who volunteered for this study, and to Teresa Sawyers for the critical reading of the manuscript. The study was funded by MSD, MSDAvenir, and by the University Hospital of Nîmes. These sponsors had not any role, neither in the study design, in the collection, analysis, and interpretation of data, in the writing of the report, nore in the decision to submit the paper for publication.

Author contributions
R.C. and T.V. contributed to the conception and design of the flow cytometry study, acquired, analyzed and interpreted cell surface markers data. D.D., A.M.D., C.G. and L.K. acquired, analyzed and interpreted soluble markers data. E.M. contributed to the conception and design of the study, the patients' enrollement, acquired, analyzed and interpreted clinical data. C.R., M.P. and R.S. contributed to the conception and design of the statistical study, acquired, analyzed and interpreted statistical data. P.C. contributed to the conception and design of the study, analyzed and interpreted data, and wrote the first draft of the manuscript. All authors revised and approved the final version.

Competing interests
The authors declare no competing interests.

Additional information
Correspondence and requests for materials should be addressed to P.C.

Reprints and permissions information is available at www.nature.com/reprints.

Publisher's note Springer Nature remains neutral with regard to jurisdictional claims in published maps and institutional affiliations.

Open Access This article is licensed under a Creative Commons Attribution 4.0 International License, which permits use, sharing, adaptation, distribution and reproduction in any medium or format, as long as you give appropriate credit to the original author(s) and the source, provide a link to the Creative Commons licence, and indicate if changes were made. The images or other third party material in this article are included in the article's Creative Commons licence, unless indicated otherwise in a credit line to the material. If material is not included in the article's Creative Commons licence and your intended use is not permitted by statutory regulation or exceeds the permitted use, you will need to obtain permission directly from the copyright holder. To view a copy of this licence, visit http://creativecommons.org/licenses/by/4.0/.

© The Author(s) 2021

Là où les PVVIH avirémique sous cART ont un activation immunitaire résiduelle visible, étudiée depuis un moment et comparée bien souvent avec les normes présentes dans la population générale, nous avons voulu observer ici si même au sein d'une population donnée, sans pathologie particulière, nous pouvions distinguer des profils d'activation et ce fut le cas. Dans un second temps nous avons observé un lien entre un profil et la résistance à l'insuline, mais d'autre perspectives peuvent être envisagées. Certains profils peuvent au contraire être particulièrement exempt de tout symptôme clinique ou physiologique. Leur profil immunologique est tout aussi intéressant à suivre puisqu'il peut permettre d'exclure des causes possibles d'activation.

Ainsi, même au sein d'une population générale sans pathologie particulière, nous pouvons distinguer des profils d'activation immunitaire différents. Cette observation élargit notre modèle de profils d'activation immunitaire sous-tendus par des étiologies spécifiques et sous-tendant des morbidités spécifiques à la population générale.

V. ARTICLE « ANGIOTENSIN II INDUCES REACTIVE OXYGEN SPECIES, DNA DAMAGE, AND T CELL APOPTOSIS IN SEVERE COVID-19 »

Soumis à PNAS le 14/07/2021

Une lymphopénie est observée chez les personnes développant un COVID-19 modéré à sévère, sans que les mécanismes en cause ne soient décrits. Nous avons cherché à comprendre pourquoi cette lymphopénie était présente. Nous avons recruté 58 personnes positive à un test PCR de SARS-COV-2. 29 d'entre elle étaient admises au département des maladies infectieuses du CHU de Nîmes parce qu'elles avaient développé des symptômes de COVID-19 nécessitant une hospitalisation (« non-ICU » pour « non intensive care unit »). 29 personnes étaient admises en soins intensifs et avaient besoin d'une assistance respiratoire (« ICU » pour « intensive care unit »). Nous avons également recruté un groupe de témoins dont l'âge et le sexe correspondaient aux groupes de patients étudiés.

Premièrement nous avons observé que les monocytes du groupe de patients « non-ICU » produisaient spontanément plus de dérivés oxygénés que le groupe de patients ICU et que le groupe témoin. De plus, parmi les ICU, les patients qui n'ont pas survécu au COVID-19 étaient également ceux qui produisaient le plus de ROS. Précisément, j'ai utilisée le CM-H2DCFDA comme sonde de détection dans les monocytes, elle détecte globalement le stress oxydatif dans les cellules en réagissant avec les radicaux peroxyl (ROO (Figure 1).

Nous avons montré que cette production de ROS pouvait induire des dommages à l'ADN dans les cellules adjacentes et que ces dommages induisaient plus d'apoptose dans les LT (Figure 2). En plus, les PBMCs de patients présentaient eux-mêmes des dommages à l'ADN. Finalement, nous avons trouvé une forte corrélation entre le niveau de production de ROS des monocytes et le pourcentage de LT8 en apoptose, mais aussi entre l'importance des lésions d'ADN et le nombre de lymphocytes circulant chez ces patients, appuyant l'hypothèse d'un lien entre cette production de ROS et la lymphopénie (Figure 3E et 3F).

Nous nous sommes ensuite demandé quel était le déclencheur de cette production de ROS. Nous avons émis l'hypothèse que l'angiotensine II pouvait déclencher la production de ROS dans les monocytes. D'une part nous avons mesuré la quantité d'angiotensine II présente dans le plasma des patients (Figure 4D). Ce sont également les patients du groupe non-ICU qui ont le plus d'angiotensine II dans le plasma. D'autre part nous avons observé que l'incubation

des PBMCs de donneurs sains avec de l'angiotensine II induisait la production monocytaire de ROS. De plus, cette production peut être inhibée avec une molécule anti-AT_1R, le Losartan. Ce mécanisme passe donc par AT_1R. Enfin, nous observons une corrélation entre la concentration en angiotensine II présente dans le plasma et d'une part la quantité de ROS mesurée dans les monocytes et d'autre part la capacité de ces monocytes à induire des dommages à l'ADN.

PNAS
www.pnas.org

Main Manuscript for

Angiotensin II induces reactive oxygen species, DNA damage, and T cell apoptosis in severe COVID-19

Lucy KUNDURA[1], Sandrine GIMENEZ[1], Renaud CEZAR[2], Sonia ANDRÉ[3], Mehwish YOUNAS[1], Yea-Lih LIN[1], Pierre PORTALES[4], Claire LOZANO[4], Vincent THIERRY[4], Clément METTLING[1], Philippe PASERO[1], Laurent MULLER[5], Jean-Yves LEFRANT[5], Claire ROGER[5], Pierre-Géraud CLARET[6], Sandra DUVNJAK[7], Paul LOUBET[8], Albert SOTTO[8], Tu-Anh TRAN[9], Jérôme ESTAQUIER[3,10], Pierre CORBEAU[1,2*]

[1]Institute of Human Genetics, CNRS UMR9002 and Montpellier University, Montpellier, France; [2]Immunology Department, Nîmes University Hospital: Nîmes, France; [3]INSERM-U1124, Université de Paris: Paris, France ; [4]Immunology Department, Montpellier University Hospital: Montpellier, France; [5]Surgical Intensive Care Department, Nîmes University Hospital: Nîmes, France; [6]Medical and Surgical Emergency Department, Nîmes University Hospital: Nîmes, France; [7]Gerontology Department, Nîmes University Hospital: Nîmes, France; [8]Infectious diseases Department, Nîmes University Hospital: Nîmes, France; [9]Pediatrics Department, Nîmes University Hospital: Nîmes, France; [10]Laval University Research Center: Quebec City, Quebec, Canada.

*Corresponding author: Pierre Corbeau, Institute of Human Genetics, CNRS UPR1142, 141 rue de la Cardonille, 34396 Montpellier cedex 5, France. Tel : +33 434 359 932, fax: +33 434 359 901, e-mail address: pcorbeau@igh.cnrs.fr, ORCID 0000-0002-8576-6683

Author Contributions: Conceptualization: PC, JE; Methodology: LK, SG, RC, MY, YLL, PP, CL, CM, TAT, JE, PC; Investigation: LK, SG, RC, SA, LM, JYL, CR, PGC, SD, PL, AS, TAT; Funding acquisition: PC, JE; Project administration: PC, JE; Supervision: PC, JE; Writing – original draft: PC; Writing – review & editing: LK, SG, RC, SA, MY, YLL, PP, CL, VT, CM, PP, LM, JYL, CR, PGC, SD, PL, AS, TAT, JE, PC.

Competing Interest Statement: The authors have declared that no conflict of interest exists.

Classification: Biological Sciences / Immunology and Inflammation

Keywords: SARS-CoV-2, lymphopenia, monocytes, pathogenesis, Angiotensin receptor I

This PDF file includes:

Main Text
Figures 1 to 4
Tables 1

Abstract

Lymphopenia is strongly predictive of survival in Coronavirus disease 2019 (COVID-19) patients. Yet, the cause of a lymphocyte count drop in severe forms of SARS-CoV-2 infection is unknown. Here, we show that the monocytes of certain COVID-19 patients spontaneously released reactive oxygen species (ROS) able to induce DNA damage and apoptosis in neighboring cells. Of note, high ROS production was predictive of death in intensive care unit patients. Accordingly, in most patients, we observed the presence of DNA damage in up to 50% of their peripheral mononuclear blood cells, with double-strand DNA breaks, and T-cell apoptosis. Moreover, the intensity of this DNA damage was linked to lymphopenia. SARS-CoV-2 is known to induce the internalization of its receptor, Angiotensin Converting Enzyme 2, a protease able to catabolize Angiotensin II. Accordingly, we observed in certain COVID-19 patients high plasma levels of Angiotensin II. Looking for the stimulus responsible for their monocytic ROS production, we unveiled that Angiotensin II triggers ROS production by monocytes via Angiotensin receptor I. ROS released by Angiotensin II-activated monocytes induced DNA damage and apoptosis in neighboring cells. We conclude that mononuclear cell apoptosis provoked via DNA damage due to the release of monocytic ROS could play a major role in COVID-19 pathogenesis. Unveiling this new pathogenic pathway opens up new therapeutic possibilities for COVID-19.

Significance Statement

Here we show that in severe forms of COVID-19, Angiotensin II induces reactive oxygen species (ROS) monocytic production responsible for DNA damage in peripheral blood cells and programed T lymphocyte death. As the level of ROS production was predictive of death and as lymphopenia has been previously linked to disease severity, this pathogenic pathway could play a major role in critical SARS-CoV-2 infection. The finding of this cascade of pathological events unveils new therapeutic angles for COVID-19.

Introduction

COVID-19 is an infectious disease caused by severe acute respiratory syndrome coronavirus 2 (SARS-CoV-2). The most severe forms of COVID-19 are due to acute lung damage which is strongly linked to hyperactivation of the immune system (1). A hallmark of critical COVID-19 is lymphopenia (2), observed in up to 63% of COVID-19 patients, and predictive of an unfavorable outcome (3). Yet, the cause of peripheral blood T-cell, B-cell, and NK-cell loss remains unclear. Indeed, this loss may be the consequence of a decrease in lymphocyte production, the trapping of these cells in the respiratory tract and/or a high rate of lymphocyte death. As lymphocyte counts are strongly predictive of survival, understanding the causes of lymphopenia is of major importance.

Various ribonucleic acid (RNA) viruses have been reported to induce ROS production and antioxidant system depletion. For instance, the influenza virus increases the level of ROS production in the host cells and decreases the concentration of antioxidants (4). Moreover, the oxidative stress provoked by the virus is responsible for lung damage that may be prevented by antioxidants or by targeting nicotinamide adenine dinucleotide phosphate (NADP) oxidase-2 (4). Likewise, respiratory syncytial virus infection causes ROS expression (5) and decreases the expression of antioxidant genes, contributing to bronchiolitis (6). SARS-CoV-1 modifies the oxidoreductase system of the mitochondria, via an interaction between its non-structural protein 10 and cytochrome oxidase II (7). In line with this mechanism, oxidative stress has been reported in the lungs of SARS-CoV-1-infected mice (8). Likewise, SARS-CoV-2-infected monocytes overproduce mitochondrial ROS, and an increased expression of oxidative stress-associated genes has been observed in monocytes of bronchoalveolar fluid from COVID-19 patients (9). In the peripheral blood of these patients, markers of Nox2 activation(10), impaired antioxidant

activity(11) and oxidative stress(12) have been revealed as possibly being linked to the severity of the disease.

As ROS can cause DNA damage resulting in apoptosis (13), we analyzed the level of monocytic ROS production in COVID-19 patients at different stages, as well as its causes and consequences.

Results

Patient enrollment

We enrolled 29 PCR-positive SARS-CoV-2-infected patients upon admission to Intensive Care Units (ICUs) for an oxygen saturation of less than 90% and/or PaO2 below 60 mmHg in room air, or an oxygen saturation of less than 90% while receiving 5L/min of oxygen. We also recruited 29 PCR-positive SARS-CoV-2-infected patients upon admission to the Infectious Diseases Department (non-ICU) for an oxygen saturation of less than 96% in room air and/or deterioration in their general condition. Age- and sex-matched healthy donor (HDs: age range, 28 to 95 years) were used as negative controls. The bioclinical characteristics of these patients are shown in Table 1.

Monocytes from COVID-19 patients overproduce ROS

To test whether monocytes from COVID-19 patients produced ROS, we labeled the peripheral blood mononuclear cells (PBMCs) of SARS-CoV-2-infected individuals with dichloro-dihydro-fluorescein diacetate (DCFH-DA), which reacts with ROS to give a fluorescent product. Figure 1a shows that monocytes from HDs become fluorescent when they are incubated with DCFH-DA and exposed to lipopolysaccharide, used as a positive control. This ROS production is prevented by pre-incubation with the NADPH oxidase inhibitor diphenyleneiodonium (DPI, Fig. 1a). By contrast, the spontaneous fluorescence of monocytes from HDs incubated with DCFH-DA was not reduced in the presence of DPI (Fig. 1a). Monocytes from certain COVID-19 patients became more fluorescent than monocytes from HDs after being exposed to DCFH-DA (Fig. 1b and 1c). Figure 1c shows the intensity of spontaneous monocytic ROS production in HDs, ICU and non-ICU patients. Non-ICU patients produced more ROS than HDs (22.2 ± 4.5 vs. 17.2 ± 4.6 mean ± SD arbitrary units (AU) of mean fluorescence intensity, $p = 0.003$) whereas ICU patients did not (16.4

± 3.9 vs. 17.2 ± 4.6 AU, p = 0.582). Yet, the ICU patients who survived presented lower monocytic ROS production than those who did not (15.6 ± 3.4 vs. 19.6 ± 4.1 AU, p = 0.021, Fig. 1d). To identify the monocyte subpopulations responsible for ROS production, we labeled the PBMCs exposed to DCFH-DA with anti-CD14 and anti-CD16 antibodies to identify classical (CD14hiCD16lo), intermediate (CD14+CD16+), and alternative (CD14loCD16hi) monocytes (Fig. 1e). Figure 1f shows that the intermediate and classical monocytes produced the highest amount of ROS. Compared with HDs, non-ICU participants had a higher percentage of intermediate monocytes (19.8 ± 9.4 vs. 12.7 ± 11.2%, p = 0.017, Fig. 1g) and ICU participants similar percentages (13.4 ± 10.6 vs. 12.7 ± 11.2%, p = 0.971, Fig. 1g). Logically, the proportions of intermediate monocytes and ROS-producing monocytes were correlated in COVID-19 patients (r = 0.373, p = 0.004, Fig. 1h).

Monocytes from COVID-19 patients induce DNA damage via ROS

ROS can oxidize proteins, lipids or DNA. We searched for the effect of monocytic ROS production on the DNA of bystander cells. For this purpose, we probed the presence of the phosphorylated form of the histone variant H2AX (γ–H2AX), a hallmark of chromosome breaks and DNA replication stress (14), in primary BJ fibroblasts co-cultured with PBMCs from COVID-19 patients. In this assay, PBMCs were co-cultured in transwells, i.e. with no cell-to-cell contact with BJ cells. Camptothecin, a topoisomerase I inhibitor which induces replication-dependent DNA lesions, was used as a positive control, whereas PBMCs from healthy donors were included as negative controls. We found that PBMCs in 8 out of the 25 patients we tested (32%), induced γ–H2AX nuclear foci in bystander BJ cells as exemplified in Figure 2a and 2b. Figure 2c shows that the formation of these foci was prevented by pre-incubating PBMCs with the ROS scavenger, N-acetylcysteine (NAC), or the NADPH oxidase inhibitor, DPI. This establishes that the γ–H2AX foci are indeed induced by ROS. To make really sure that the sources of DNA cells damaging ROS were

monocytes, we repeated the experiment after depleting patient PBMCs of monocytes using CD14-coated magnetic beads. Figure 2d shows that, whereas PBMCs and monocytes from the patient we analyzed induced DNA damage, monocyte-depleted PBMCs from the same patient did not.

PBMC DNA damage results in T-cell apoptosis during severe SARS-CoV-2 infection

ROS-induced DNA damage may provoke apoptosis (13). Therefore, we tested whether co-culturing with COVID-19 PBMCs might trigger apoptosis in HD PBMCs. Indeed, HD T-cells presented more phosphatidylserine at their surface, a marker of apoptosis, as measured by Annexin V labelling on day 6 when they were exposed to COVID-19 PBMCs able to induce DNA damage than when they were exposed to another healthy volunteer PBMCs (15.0 ± 1.5 vs. 10.8 ± 1.7 %, $p = 0.034$, Fig.2e). This programmed cell death provoked by COVID-19 PBMCs was entirely mediated by ROS, since the presence of NAC reduced apoptosis to the background level observed in the presence of HD PBMCs (11.8 ± 1.6 vs. 10.8 ± 1.7 %, $p = 0.638$, Fig.2e). By contrast, co-culturing with COVID-19 PBMCs unable to induce DNA damage or with HD PBMCs resulted in the same level of apoptosis (11.7 ± 2.1 vs. 10.8 ± 1.7 %, $p = 0.627$, Fig.2e). As a positive control, we used lipopolysaccharide-stimulated PBMCs, which triggered apoptosis in HD PBMCs (17.6 ± 1.6 vs 10.8 ± 1.7 %, $p = 0.007$, Fig.2e).

COVID-19 patient PBMCs present DNA damage

As the monocytes of certain COVID-19 patients release ROS which are able to cause DNA damage to neighboring cells, we analyzed whether the PBMCs of these patients presented DNA damage. To do this, we looked for the presence of γ–H2AX nuclear foci in their PBMCs. Figure 3a shows an example of a COVID-19 patient whose PBMCs harbor such DNA damage markers. Globally, the proportion of DNA-damaged PBMCs was higher in the 19 non-ICU patients (10.9 ± 3.7 % vs. 5.6 ± 1.7%, $p < 10^{-4}$), and the 28 ICU patients (13.3 ± 8.9% vs. 5.6 ± 1.7%, $p < 0.001$) than in age-

matched healthy donors we analyzed (Fig. 3b). COVID-19 patient PBMCs also harbored DNA double-strand breaks, as revealed by the labelling with an antibody specific for 53BP1, a protein known to aggregate at double-strand ends (15). In the example shown in Figure 3c, 16.8 ± 3.4 % of the patient PBMCs presented 53BP1 foci, a higher proportion than in the healthy donor (6.9 ± 1.6 %, p = 0.011). Next, we quantified CD4+ T-cell and CD8+ T-cell apoptosis in the participant peripheral blood. Figure 3d shows that Annexin V expression at the surface of both lymphocyte subpopulations, particularly on CD8+ T-cells, was more frequent in COVID-19 patients than in controls. As we had found that patient PBMCs producing ROS induced apoptosis *in vitro*, we searched for, and found in the participants a link between the level of their monocytic ROS production and their percentage of Annexin V-positive CD8+ T cells (r = 0.522, p = 0.005, Fig. 3e). Next, we tested whether the phenomenon we describe could result in lymphopenia in COVID-19 patients. To this aim, we looked for a correlation between the intensity of DNA damage in PBMCs and lymphopenia. As shown in Figure 3f, we observed an inverse correlation between the percentage of PBMCs with γ–H2AX foci and lymphocyte count in the patients and healthy volunteers we analyzed (r = -0.341, p = 0.025).

Angiotensin II induces monocytic ROS production

SARS-CoV-2 downregulates the cell surface expression of Angiotensin-converting enzyme 2 (ACE2), its main receptor, via ACE2 co-internalization and cleavage by the serine protease TMPRSS2 (16). Knowing that ACE2 converts Angiotensin II (AngII) into Angiotensin 1-7, this should result in an increase in AngII concentration (16). As AngII has been shown to induce ROS production in human mesangial cells (17), we tested whether this peptide was also able to provoke the release of ROS by human monocytes. Indeed, we observed that, like lipopolysaccharide, AngII increased the fluorescence of HD monocytes preincubated with DCFH-DA (Fig.4a). This effect was completely prevented by 1-hour preincubation with DPI (91,7 ± 15.3%, Fig.4b) or the

Angiotensin receptor 1 (AT1) antagonist losartan at 10µM (98,7 ± 4.5%, Fig.4c). Next, we checked to see whether the peripheral blood concentration of AngII was actually high in COVID-19 patients. Fig 4d shows that plasma levels of AngII in non-ICU volunteers (74.6 ± 40.5 vs. 41.9 vs. 37.9 pg/mL, p = 0.014), but not in ICU volunteers (35.4 ± 21.0 vs. 41.9 vs. 37.9 pg/mL, p = 0.828) were higher than those of normal volunteers. The lower level of AngII in ICU patients as compared with non-ICU patients might be the consequence of the increase in ACE2 expression reported in severe COVID-19 (18), driven by interferon (19), and/or reoxygenation (20). To test the hypothesis that AngII might be involved in the monocytic ROS overproduction that we had unveiled in certain patients, we looked for a link between AngII plasma levels and the intensity of ROS synthesis in HD, ICU and non-ICU participants. Figure 4e shows a clear correlation between these two parameters (r = 0.299, p = 0.027). This explains the fact that ROS expression was less intense in ICU patients than in non-ICU patients Thereafter, we checked whether AngII-stimulated monocytes could induce DNA damage in BJ cells. Indeed, this was the case, and the DNA damage was prevented by DPI (Fig. 4f) and the AT1 antagonist losartan (Fig. 4g). Furthermore, circulating levels of AngII strongly correlated with the ability of patient PBMCs to induce DNA damage in BJ cells (r = 0.704, p = 0.005, Fig. 4h).

Discussion

In this study, we discovered a new pathogenic mechanism, DNA damage due to AngII-driven ROS production by the monocytes of certain COVID-19 patients, and resulting in PBMC apoptosis (Extended Data Fig. 1).

ROS-induced PBMC programmed cell death may have various deleterious effects. First, it may result in an immune deficiency favoring coinfections with other viruses (21), bacteria (22) or mycoses (23), and in a poor immunological memory paving the way for SARS-CoV-2 reinfection. Second, regulatory T-cell apoptosis may account for the Treg deficiency observed in severe forms of COVID-19 (24), favoring immune activation. Third, CD8+ T-cell and NK cell loss due to programmed cell death might contribute to a cytokine storm. Indeed, these cytotoxic lymphocytes have been found to be involved in the downregulation of immune activation in the course of infections via their ability to kill T-cells, NK, and antigen presenting cells(25, 26). Accordingly, in primary hemophagocytic lymphohistiocytosis, mutations resulting in cytolytic deficiency may provoke cytokine storms (27). Thus, the programmed death of CD8+ T-cells and NK cells could impair a negative feedback on immune activation. Fourth, CD4+ T lymphocyte apoptosis, particularly follicular helper T- cell apoptosis which may account for the depletion of this subpopulation (28) might explain the poor isotype switch and B memory observed in severe forms (29).

The release of ROS could have direct effects in addition to these indirect effects. As ROS are known to activate the pro-inflammatory transcription factor NFkB(30) and the NLRP3 inflammasome (31), they could favor a cytokine storm in severe forms. Likewise, they might drive the differentiation of monocytes/macrophages into inflammatory M2 cells(32). Locally, the numerous monocytes/macrophages in the low respiratory tract could also participate in endothelial cell, alveolar and vascular damage via ROS (33).

As we found, *in vitro*, that ROS released by COVID-19 monocytes induce DNA damage and apoptosis, as the proportion of DNA-damaged PBMCs we measured in patients correlated with their lymphopenia (a major pronostic marker in COVID-19), and as we found a link between the level of monocytic ROS expression in ICU patients and their survival, our data and the well-documented proinflammatory effect of ROS argue for a role of this pathogenic pathway in the outcome of this disease. They could explain also why older people, males, patients with diabetes or prior cardiovascular diseases, who express low levels of ACE2 (34), present more often severe forms of COVID-19.

The mechanism we uncovered may also explain why SARS-CoV-2 variants with an enhanced affinity for their ACE2 receptor may be more pathogenic. Actually, these variants should provoke an increased ACE2 internalization, a higher level of AngII, a greater monocytic ROS production, and thereby more inflammation and more DNA damage resulting in lymphopenia and immune deficiency.

From a therapeutic viewpoint, our data may explain the beneficial effects of AT1 antagonists (35) and antioxidants (36) on COVID-19 observed in certain clinical trials. Given all the potential consequences of ROS release in severe COVID-19, therapeutic strategies aimed at reducing AngII signaling via AT1, ROS production, and apoptosis deserve more consideration (Supplementary Fig. 1).

Materials and Methods

Study Subjects. Adults with positive naso-pharyngeal swabs for SARS-CoV-2 RNA by RT-PCR were recruited at the Nîmes University Hospital following approval by the Île-de- France 1 Ethics Committee and after obtaining informed consent. Patients were either recruited on the day of their admission to an intensive care unit (ICU) for oxygen saturation <90% in ambient air or <95% with 5L/mn of oxygenotherapy and/or arterial oxygen tension (PaO2) of less than 60 mm Hg or upon admission to the Tropical and Infectious Diseases Department (non-ICU) for oxygen saturation <96% in ambient air. This study was approved by the French Ethics Committee, Île-de-France 1. All patients had provided written informed consent, and the trial was registered (Eudract/IDRCB 2020-A00875-34 and ClinicalTrials NCT04351711).

Cell-sorting and co-culture. Monocytes were sorted from PBMCs using CD14-coated microbeads (Miltenyi Biotech). Cells, pre-incubated or not with DPI or NAC for 3 hours at 37°C, were washed twice and cocultured in 1µm pore-size inserts with BJ placed on coverslips in 24-well companion plates. PBMCs or monocytes and BJ cells were co-cultured in 2:1 ratio in 1:1 DMEM and RPMI culture media supplemented with 10% heat-inactivated fetal bovine serum (FBS) for 3 days. Camptothecin (10µM) was used on BJ cells for 45 mn at 37°C. Lipopolysaccharide (1µg/ml) was added to the cells in 500µl final volume of RPMI without serum and incubated at 37°C for 30 minutes. Cells were washed and fixed for further staining.

Immunofluorescence. PBMC adherence on coverslips was obtained by using 20 µg/ml of poly-lysine in serum-free RPMI for 2 hours at room temperature. Coverslips with cocultured BJ cells were washed twice, fixed with 2% paraformaldehyde in PBS for 10 minutes, rinsed again with PBS, and permeabilized with 0.1% Triton-X-100 for 10 minutes at room temperature. Thereafter, coverslips were washed and blocked with PBS containing 10% FBS for 30 minutes. Cells were then

incubated with anti-γ-H2AX (Millipore, 1/500) for 1 hour or anti-53BP1 (Millipore, 1/300) monoclonal antibodies (mAb) in PBS with 10% FBS. Coverslips were rinsed three times with PBS and incubated with AF 546 anti-mouse IgG1 (Invitrogen, 1/2000) secondary antibody for 45 minutes in PBS with 10% FBS at room temperature. After washing with PBS, DNA was counter stained with DAPI (Sigma-Aldrich) for 5 minutes, and coverslips were mounted in fluorescence mounting medium (Prolong gold, Invitogen). Slides were kept overnight at 20°C in a dark room or drying. Images were obtained with a Zeiss ApoTome fluorescence microscope (63X magnification and 1.4 numerical aperture for BJ cells, 100X magnification and 1.46 numerical aperture for PBMC) with supporting software, and analyzed on Image J and FIJI software systems.

Flow Cytometry. The monoclonal antibodies used for cell surface staining were: CD3-APCA750, CD14-PE, CD16-APC, CD4-APC (Beckman Coulter), and CD3-BV421 (Biolegend). Annexin-V-PE (Biolegend) was used according to manufacturer's guidelines. For ROS quantification, 10^6 PBMCs were resuspended in 1µM DCFH-DA for 25min at room temperature. Data were acquired on a Navios flow cytometer (Beckman Coulter) from 20,000 gated events per sample and on a MACSQuant analyser 10 (Miltenyi Biotech), and analyzed using Kaluza software.

ELISA. AngII concentrations were determined using the Angiotensin II ELISA kit (Enzo Life Sciences).

Statistical analyses. Statistical analyses and graphical presentations were computed with GraphPad Prism version 6. Differences between two groups were analyzed using two-sided unpaired student's *t* test or Mann-Whitney test as appropriate. We used a two-sided Spearman rank test to evaluate correlations.

Acknowledgments: We are grateful to the persons who volunteered for this study, to Teresa Sawyers for the critical reading of the manuscript, to the biological resource center of the Nîmes University Hospital, and to BioMedTech core Facilities for their help with flow cytometry (INSERM US36, CNRS UMS2009, Paris, France). This study was supported by the University Hospital of Nîmes grant NIMAO/2020/COVID/PC-01 (PC), the Fondation Recherche Médicale and the Agence Nationale de Recherche grant 216261 (JE), and by AbbVie grant (PC).

References

1. F. Zhou, e. al., Clinical course and risk factors for mortality of adult inpatients with COVID-19 in Wuhan, China: a retrospective cohort study. *Lancet* **395**, 1054-1062 (2020).
2. X. Zhang *et al.*, Viral and host factors related to the clinical outcome of COVID-19. *Nature* **583**, 437-440 (2020).
3. B. J. Fan, e. al., Hematologic parameters in patients with COVID-19 infection. *Am J Hematol* **95**, E131-E134 (2020).
4. M. L. Reshi, RNA Viruses: ROS-Mediated Cell Death. *Int J Cell Biol* **2014**, 467452 (2014).
5. A. Casola, e. al., Oxidant tone regulates RANTES gene expression in airway epithelial cells infected with respiratory syncytial virus role in viral-induced interferon regulatory factor activation. *The Journal of biological chemistry* **276**, 19715-19722 (2001).
6. Y. M. Hosakote, e. al., Viral-mediated inhibition of antioxidant enzymes contributes to the pathogenesis of severe respiratory syncytial virus bronchiolitis. *Am J Resp Crit Care Med* **183**, 1550-1560 (2011).
7. Q. Li, e. al., The interaction of the SARS coronavirus non-structural protein 10 with the cellular oxido-reductase system causes an extensive cytopathic effect. *J Clin Virol* **34**, 133-139 (2005).
8. R. Vijay, e. al., Critical role of phospholipase A2 group IID in age-related susceptibility to severe acute respiratory syndrome-CoV infection. *The Journal of experimental medicine* **212**, 1851-1868 (2015).
9. A. C. Codo, e. al., Elevated Glucose Levels Favor SARS-CoV-2 Infection and Monocyte Response through a HIF-1α/Glycolysis-Dependent Axis. *Cell Metab* **32**, 437-446 (2020).
10. F. Violi, e. al., Nox2 activation in Covid-19. *Redox Biology* **36**, 101655 (2020).
11. A. Moghaddam, e. al., Selenium Deficiency Is Associated with Mortality Risk from COVID-19. *Nutrients* **12**, E2098 (2020).
12. T. Thomas, e. al., COVID-19 Infection Alters Kynurenine and Fatty Acid Metabolism, Correlating With IL-6 Levels and Renal Status *JCI Insight* **5**, e140327 (2020).
13. Z. Darzynkiewicz *et al.*, DNA damage signaling assessed in individual cells in relation to the cell cycle phase and induction of apoptosis. *Crit Rev Clin Lab Sci* **49**, 199-217 (2012).

14. V. Valdiglesias, S. Giunta, M. Fenech, M. Neri, S. Bonassi, gammaH2AX as a marker of DNA double strand breaks and genomic instability in human population studies. *Mutation research* **753**, 24-40 (2013).
15. S. Panier, S. J. Boulton, Double-strand break repair: 53BP1 comes into focus. *Nature reviews. Molecular cell biology* **15**, 7-18 (2014).
16. L. L. Xavier *et al.*, Does Angiotensin II Peak in Response to SARS-CoV-2? *Front Immunol* **11**, 577875 (2021).
17. Y. Chen *et al.*, NADPH oxidase-derived reactive oxygen species involved in angiotensin II-induced monocyte chemoattractant protein-1 expression in mesangial cells. *Zhonghua Bing Li Xue Za Zhi* **38**, 456-461 (2009).
18. F. Amati *et al.*, Expression profiles of the SARS-CoV-2 host invasion genes in nasopharyngeal and oropharyngeal swabs of COVID-19 patients. *Heliyon* **6**, e05143 (2020).
19. C. G. K. Ziegler *et al.*, SARS-CoV-2 receptor ACE2 is an interferon-stimulated gene in human airway epithelial cells and is detected in specific cell subsets across tissues *Cell* **181**, 1016-1035 (2020).
20. P. A. C. Wing *et al.*, Hypoxic and pharmacological activation of HIF inhibits SARS-CoV-2 infection of lung epithelial cells *Cell Rep* **35**, 109020 (2021).
21. M. A. Abouelkhair, Non-SARS-CoV-2 genome sequences identified in clinical samples from COVID-19 infected patients: Evidence for co-infections. *PeerJ* **8**, e10246 (2020).
22. G. Rodriguez-Nava *et al.*, A Retrospective Study of Coinfection of SARS-CoV-2 and Streptococcus pneumoniae in 11 Hospitalized Patients with Severe COVID-19 Pneumonia at a Single Center. *Med Sci Monit* **26**, e928754 (2020).
23. G. Segrelles-Calvo, G. R. de S Araújo, S. Frases, Systemic mycoses: a potential alert for complications in COVID-19 patients. *Future Microbiol* **15**, 1405-1413 (2020).
24. B. J. Meckiff *et al.*, Imbalance of Regulatory and Cytotoxic SARS-CoV-2-Reactive CD4 + T Cells in COVID-19. *Cell* **183**, 1-14 (2020).
25. J. Crouse *et al.*, Type I interferons protect T cells against NK cell attack mediated by the activating receptor NCR1. *Immunity* **40**, 961-973 (2014).
26. S. Madera *et al.*, Type I IFN promotes NK cell expansion during viral infection by protecting NK cells against fratricide. *The Journal of experimental medicine* **213**, 225-233 (2016).
27. M. Soy, P. Atagündüz, I. Atagündüz, G. T. Sucak, Hemophagocytic lymphohistiocytosis: a review inspired by the COVID-19 pandemic. *Rheumatol Int* **41**, 7-18 (2021).
28. Y.-Q. Duan *et al.*, Deficiency of Tfh Cells and Germinal Center in Deceased COVID-19 Patients. *Curr Med Sci* **40**, 618-624 (2020).
29. K. L. Newell *et al.*, Switched and unswitched memory B cells detected during SARS-CoV-2 convalescence correlate with limited symptom duration *medRxiv*, 2020.2009.2004.20187724 (2020).
30. M. J. Morgan, Z.-G. Liu, Crosstalk of reactive oxygen species and NF-κB signaling. *Cell Res* **21**, 103-115 (2011).
31. A. Harijith, D. L. Ebenezer, V. Natarajan, Reactive oxygen species at the crossroads of inflammasome and inflammation. *Front Physiol* **5**, 352 (2014).
32. B. Griess, S. Mir, K. Datta, M. Teoh-Fitzgerald, Scavenging reactive oxygen species selectively inhibits M2 macrophage polarization and their pro-tumorigenic function in part, via Stat3 suppression. *Free Radic Biol Med* **147**, 48-60 (2020).

33. A. F. Rendeiro *et al.*, The spatio-temporal landscape of lung pathology in SARS-CoV-2 infection. *medRxiv*, 2020.2010.2026.20219584 (2020).
34. P. Verdecchia, C. Cavallini, A. Spanevello, F. Angeli, The pivotal link between ACE2 deficiency and SARS-CoV-2 infection. *Eur J Intern Med* **76**, 14-20 (2020).
35. J. M. Saavedra, Angiotensin Receptor Blockers Are Not Just for Hypertension Anymore. *Physiology (Bethesda)* **36**, 160-173 (2021).
36. R. R. Mohanty , B. M. Padhy, S. Das, B. R. Meher, Therapeutic potential of N-acetyl cysteine (NAC) in preventing cytokine storm in COVID-19: review of current evidence. *Eur Rev Med Pharmacol Sci* **25**, 2802-2807 (2021).

Figures and Tables

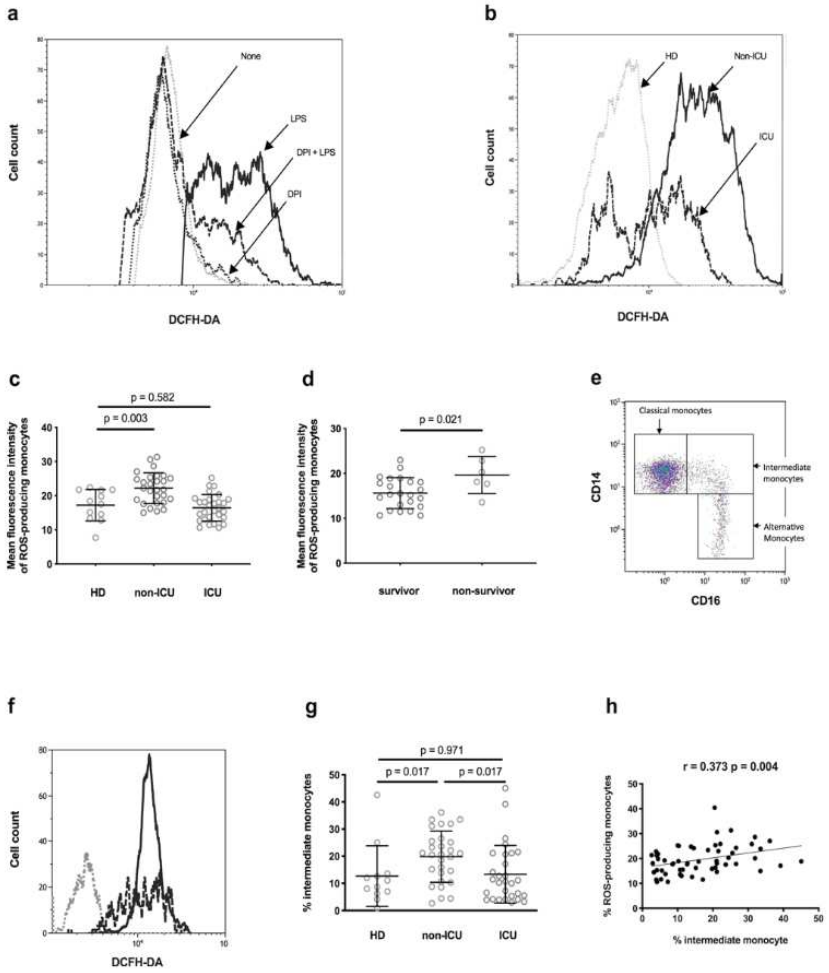

Figure 1. The monocytes from certain COVID-19 patients spontaneously produce ROS. (a) Fluorescence in monocytes from a healthy donor, pre-incubated (DPI + LPS, ---) or not (LPS, —) with DPI, exposed to DCFH-DA, and stimulated with lipopolysaccharide. As negative controls, fluorescence in the same monocytes pre-incubated (DPI, ···) or not (None, ···) with NADPH oxidase inhibitor DPI and exposed to DCFH-DA was analyzed. (b) Fluorescence in monocytes from a healthy donor (HD, ···), a non-ICU patient (non-ICU, —), and an ICU patient (ICU, ---) exposed to DCFH-DA. (c) Mean fluorescence intensity of ROS-producing monocytes from healthy donors (HD), non-ICU patients (non-ICU), and ICU patients (ICU) exposed to DCFH-DA. (d) Mean fluorescence intensity of ROS-producing monocytes from ICU patients who survived or not. (e) Identification of the classical, intermediate, and alternative monocyte subpopulations by flow cytometry. (f) Fluorescence in CD14hiCD16lo (---), CD14+CD16+ (—), and CD14loCD16hi (···) monocytes from an ICU patient exposed to DCFH-DA. (g) Percentages of CD14-CD16+ monocytes circulating in healthy (HDs), ICU and non-ICU donors. (h) Correlation between the proportions of intermediate and ROS-producing monocytes in ICU and non-ICU patients. Data are shown as means ± SD.

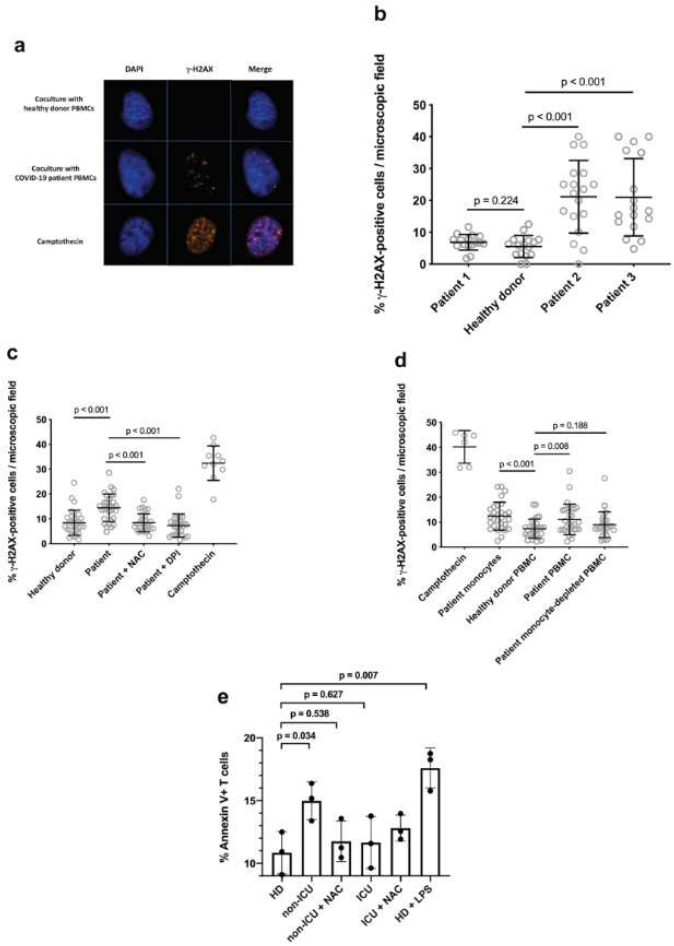

Figure 2. COVID-19 patient monocytes may induce DNA damage via ROS. (a) Detection of γ–H2AX foci by immunofluorescence in BJ cells co-cultured with PBMCs from a healthy donor or from a COVID-19 patient. Healthy donor's PBMCs treated with camptothecin were used as positive controls. (b) Quantification of the γ–H2AX foci induced in BJ fibroblasts by PBMCs from COVID-19 patients. The proportion of BJ cells presenting at least 5 foci per nucleus was quantified under microscopy. (c) γ–H2AX foci induced in BJ cells by COVID-19 patient's PBMCs are prevented by pre-incubating PBMCs with N-acetylcysteine (NAC) or diphenyleneiodonium (DPI). (d) Monocytes isolated from the PBMCs of a COVID-19 patient are able to induce DNA damage in BJ cells. The ability to induce γ–H2AX foci in the BJ fibroblasts of PBMCs from a COVID-19 patient, of the same PBMCs depleted of monocytes, and of monocytes isolated from these PBMCs was tested. (e) Intensity of phosphatidylserine expression at the surface of healthy donor PBMCs cocultured with non-ICU PBMCs able to induce DNA damage treated (non-ICU + NAC) or not (non-ICU) with N-acetylcysteine, or with ICU PBMCs unable to induce DNA damage treated (ICU + NAC) or not (ICU) with N-acetylcysteine, as detected by flow cytometry at day 6. Healthy donor PBMCs co-cultured with another healthy donor PBMCs (HD) or treated with lipopolysaccharide (HD + LPS) were used as negative and positive controls, respectively. Shown are biological replicates. Data are means ± SD and are representative of two experiments.

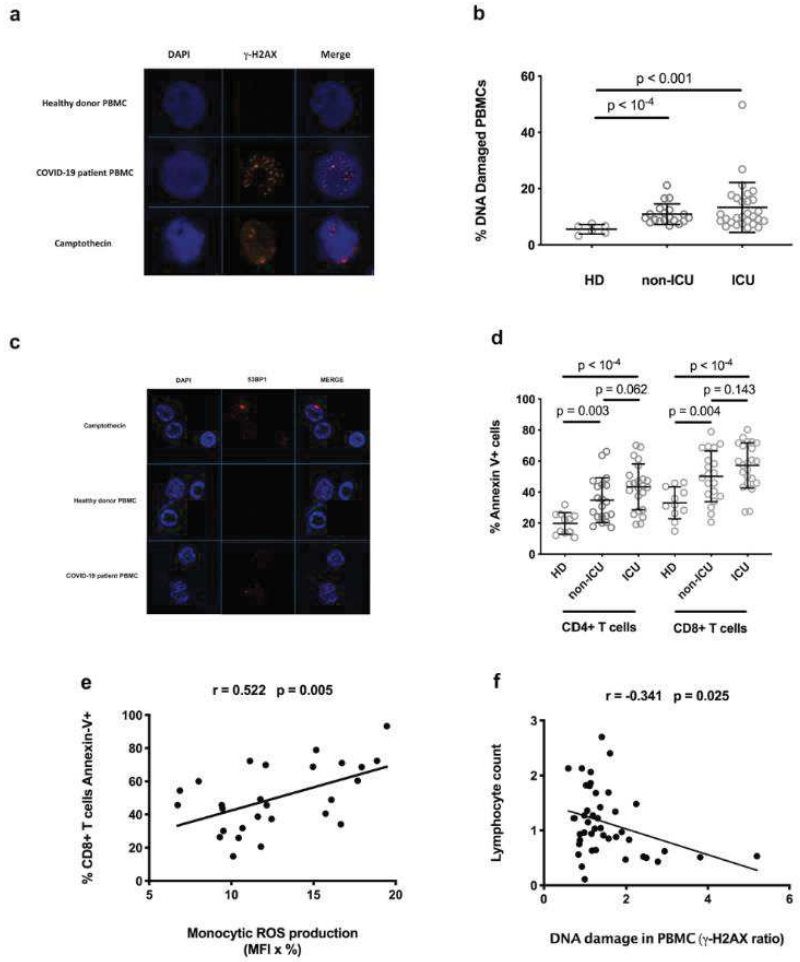

Figure 3. DNA damage in COVID-19 PBMCs. (a) PBMCs from a COVID-19 patient whose monocytes induce DNA damage in bystander BJ cells spontaneously present with γ–H2AX foci. PBMCs from a healthy donor treated or not with camptothecin were used as positive and negative controls, respectively. (b) Percentages of PBMCs harboring γ–H2AX foci in healthy donors (HD), non-ICU patients (non-ICU), and ICU patients (ICU). Data are shown as means ± SD. (c) PBMCs from a COVID-19 patient whose monocytes induce DNA damage in bystander BJ cells spontaneously present with □□□P□ foci. PBMCs from a healthy donor treated or not with camptothecin were used as positive and negative controls, respectively. One representative experiment out of two. (d) Annexin V expression on peripheral blood CD4+ T-cells and CD8+ T-cells of healthy donors (HD), non-ICU patients (non-ICU), and ICU patients (ICU). (e) Correlation between the amount of ROS produced by monocytes and the proportion of apoptotic CD8+ T cells in ICU and non-ICU patients. ROS production is expressed as the mean monocytic ROS production (mean fluorescence intensity of ROS-producing monocytes exposed to DCFH-DA) x percentage of monocytes producing ROS (percentage of fluorescent monocytes). (f) Correlation between the intensity of DNA damage in PBMC and lymphocyte counts in ICU patients. The intensity of DNA damage in PBMCs is expressed as the ratio (% patient PBMCs presenting γ–H2AX foci) : (% HD PBMCs presenting γ–H2AX foci).

20

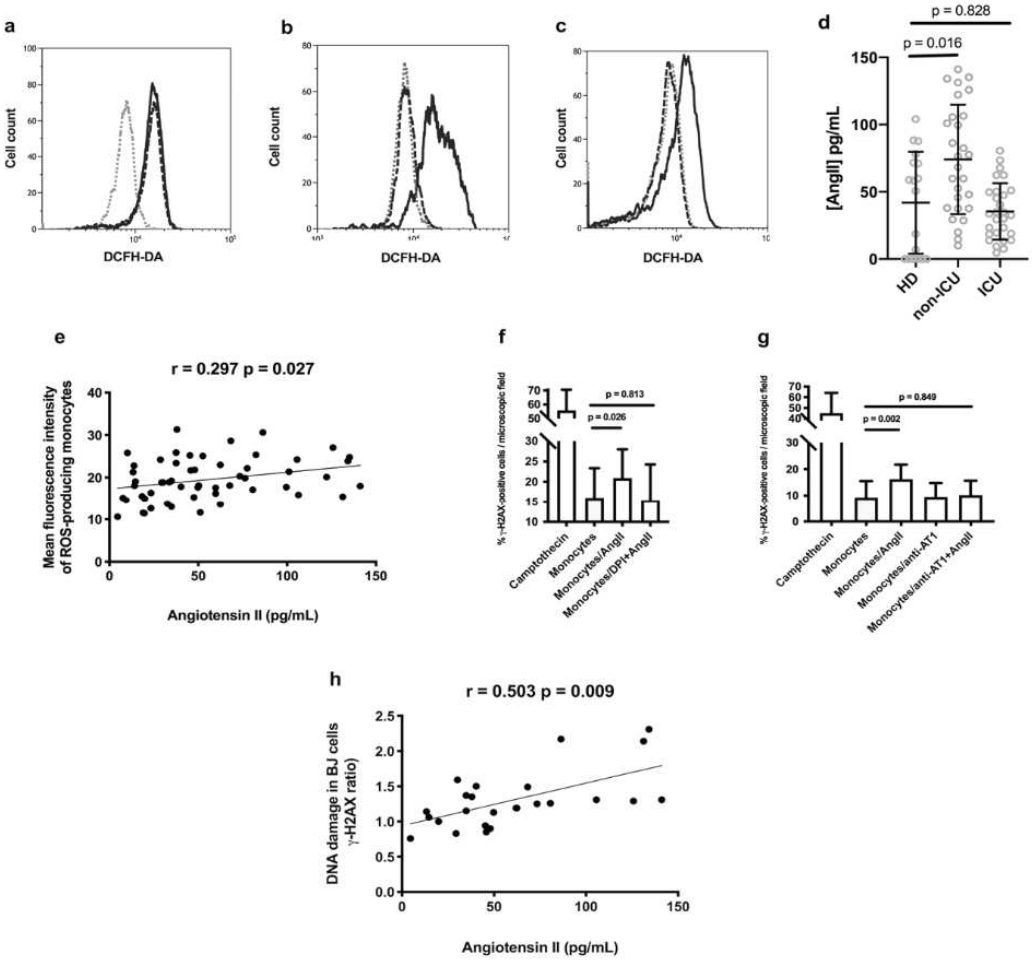

Figure 4. Angiotensin II induces ROS monocytic production and DNA damage. (a) Fluorescence in monocytes from a healthy donor, pre-incubated or not ( ) with lipopolysaccharide (---) or AngII (—), and exposed to DCFH-DA. One representative experiment out of three. (b) Fluorescence in monocytes from a healthy donor, pre-incubated or not ( ) with AngII (—) or with DPI and AngII (---), and exposed to DCFH-DA. One representative experiment out of three. (c) Fluorescence in monocytes from a healthy donor, pre-incubated or not ( ) with AngII (—), or with losartan and AngII (---), and exposed to DCFH-DA. One representative experiment out of three. (d) Plasma levels of AngII in patients and controls. (e) Correlation between plasma levels of AngII and mean fluorescence intensity of ROS-producing monocytes exposed to DCFH-DA in patients and controls. (f, g) Ability of healthy donor monocytes stimulated (Moncytes/AngII) or not (Monocytes) by AngII to cause γ-H2AX foci in bystander BJ cells (f, g). The effect or DPI (Monocytes/DPI+AngII, f) or AT1 antagonist (Monocytes/anti-AT1+AngII, g) preincubation on the ability of AngII-stimulated monocytes to induce DNA damage is shown. BJ exposed to camptothecin were used as a positive control (Camptothecin, f, g). (h) Correlation between plasma levels of AngII and the ability of patient PBMCs to induce γ–H2AX foci in bystander BJ cells. This ability is expressed as the ratio (% BJ cells presenting γ–H2AX foci in presence of patient s) : (% BJ cells presenting γ–H2AX foci in presence of HD PBMCs).

Table 1. Bioclinical characteristics of the patients enrolled

		Non-ICU patients (n=29)	ICU patients (n=29)	non-ICU vs ICU
Age (years)	Mean (SD)	66.1 (20.9)	69.3 (13.5)	
	Range	29.0-96.0	43.0-95.0	p = 0.702
Gender:				
Females	n (%)	16 (55)	13(45)	p = 0.600
Males	n (%)	13 (45)	16 (55)	
Any comorbidity	n (%)	12 (40)	12 (41)	p = 0.594
Diabetes	n (%)	7 (23)	7 (24)	p = 0.762
Cancer	n (%)	4 (13)	2 (7)	p = 0.783
Autoimmune disease	n (%)	1 (3)	0 (0)	p = 0.999
Chronic kidney failure	n (%)	0 (0)	2 (7)	p = 0.202
Duration of symptomatology (days)	Mean (SD)	6.8 (9.4)	11.8 (7.2)	p < 0.001
C-reactive protein (mg/L, normal range 0.9-1.8))	Mean (SD)	56.8 (68.1)	115.0 (81.3)	p = 0.003
Lactate dehydrogenase (IU/L, normal range 135-214)	Mean (SD)	214.8 (49.9)	416.4 (177.3)	p < 0.001
Absolute lymphocyte count ($x10^9$/L, normal range 0.9-1.8)	Mean (SD)	1.30 (0.53)	0.88 (0.59)	p = 0.004
Absolute monocyte count ($x10^9$/L, normal range 0.9-1.8)	Mean (SD)	0.70 (0.36)	0.46 (0.27)	p = 0.010

En conclusion nous proposons un modèle expliquant la lymphopénie observée dans le COVID-19 et les cibles thérapeutiques qui sont à envisager pour enrayer cette perte de lymphocytes (Figure7, présente en Figure 1 supplémentaire dans le manuscrit)

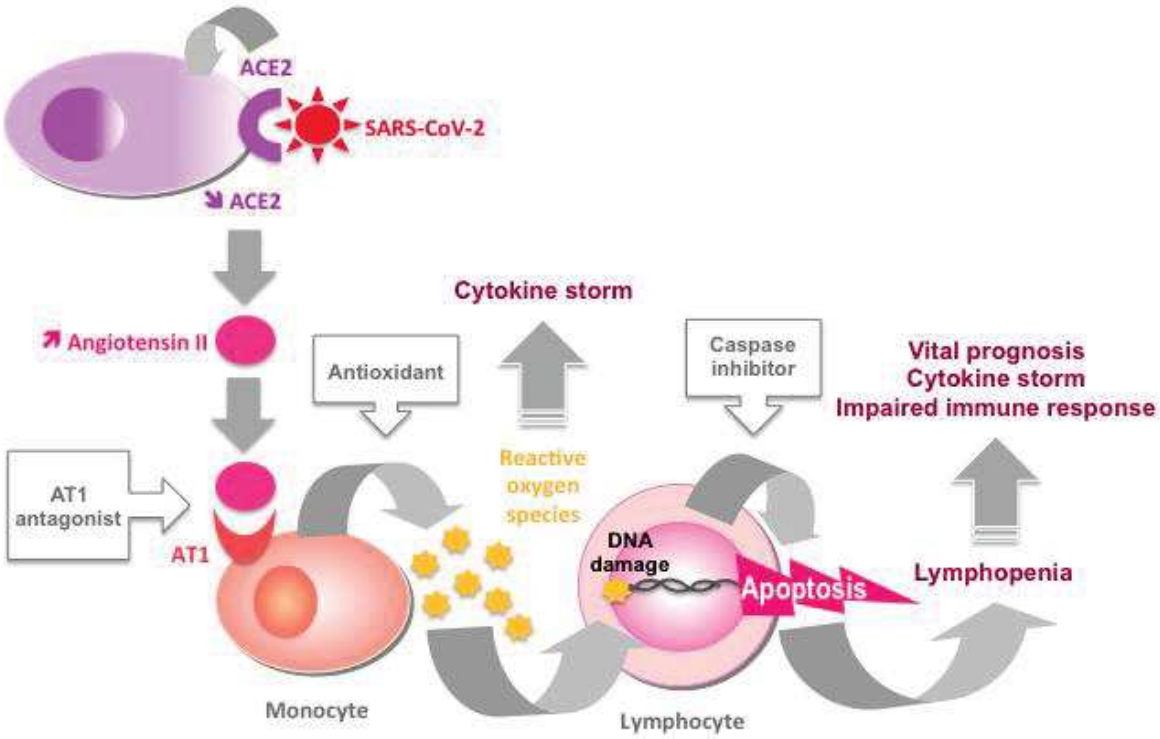

Figure 7 : Représentation schématique des données que nous avons collectées durant cette étude et les potentielles cibles thérapeutiques qui en découlent.

A partir de ces données et des connaissances actuelles sur le COVID-19 nous proposons l'hypothèse que l'internalisation d'ACE2 dans les cellules infectées par SARS-COV-2 réduit son action de clivage de l'angiotensine II en angiotensine 1-7. Il y aurait alors une accumulation d'angiotensine II circulant. Cette angiotensine II peut induire la production monocytaire de ROS, lesquels peuvent provoquer des dommages à l'ADN des cellules adjacentes, particulièrement aux LT et peut-être préférentiellement même aux LT8. Localement on peut aussi penser que les ROS relargués par les monocytes présents dans le tractus respiratoire inferieur participent à la lésion de ce dernier. Ces dommages à l'ADN vont enclencher l'apoptose de ces cellules et la lymphopénie observée. Comme dans la HLH primaire c'est un déficit de cytotoxicité LT8 et NK qui est à l'origine de l'orage cytokinique observé : on peut supposer un mécanisme similaire pour le COVID-19 (Jordan et al. 2011).

On peut penser que ces données sont contradictoires, puisque les patients dont les cellules produisent le plus de ROS ne sont pas en ICU, mais nous émettons l'hypothèse que chez ces patients, les monocytes produisent moins de ROS à cause de leur épuisement. Également, les cellules qui produisent le plus de ROS sont les monocytes intermédiaires, moins présents chez les ICU. On peut voir que le groupe de patients ICU a des concentrations d'Angiotensine II plus basse (Figure 4d). A ce stade de l'infection la concentration en virus circulant est plus faible (Boef et al. 2021) et il y devrait donc y avoir moins d'internalisation d'ACE2, ce qui peut expliquer qu'il y a moins d'Angiotensine II dans le plasma des patients ICU. A noter que le temps de demi-vie de l'angiotensine II et des ROS est très court (Al-Merani et al. 1978 ; D'Autréaux et Toledano 2007).

Il est intéressant de noter que l'antioxydant N-Acétylcystéine (NAC) a été mis en avant comme prometteur contre les symptômes du COVID-19 (Ibrahim et al. 2020). Il a déjà donné des résultats positifs dans d'autres infections chez l'Homme, dans des modèles *in vitro* et chez des rats infectés avec Influenza et le virus respiratoire syncitial, réduisant la mortalité (Wong, Lee, et Kua 2021; De Flora, Grassi, et Carati 1997). Les résultats cliniques pour le COVID-19 sont moins convaincants mais restent positifs pour le patient, avec une réduction du taux de CRP (Avdeev et al. 2021). Nous pensons qu'une prise plus anticipée d'antioxydant donnera des résultats plus visibles, puisque, suivant notre modèle, cela réduirait la lymphopénie chez ces patients.

Bloquer l'action de l'angiotensine II avec des sartans, médicaments antagonistes des récepteurs de l'angiotensine II a également été testé cliniquement pour des cas de COVID-19 : les résultats sont mitigés et très dépendants du stade auquel les patients ont été mis sous traitement (Rothlin et al. 2021; Puskarich et al. 2021).

Une étude est mise en place au CHU de Nîmes, consistant à tester l'hypothèse qu'une prise en charge précoce de patients SARS-COV-2 positif avec un traitement anti-AT_1R couplé à un antioxydant comme le NAC pourrait réduire la production de ROS dans les monocytes des patients. Nous espérons aussi que cette bithérapie puisse réduire le nombre de patients devant être admis en réanimation. Cette bithérapie a fait l'objet d'un dépôt de Brevet n° EP21306015, co-signé par les deux premiers et les deux derniers auteurs du manuscrit présenté.

F- PERSPECTIVES

I. PERSPECTIVES CONCERTANT LES PARTIES I A IV DES RESULTATS

Avec ces profils d'activation immunitaire, nous souhaitons plus largement participer à la création d'outils qui permettent de suivre au plus près la santé des personnes au long de leur vie. Que ce soit pour les PVVIH ou la population générale, nous souhaitons rendre le profilage plus accessible en trouvant les marqueurs clés qui caractérisent chaque profil. Ces outils auraient pour vocation d'anticiper voire d'éviter la survenue de pathologies liées à l'activation immunitaire. Les causes d'une pathologie sont bien sûr souvent multiples mais le profilage immunologique pourrait permettre certaines de ces causes pour chaque patient. Cela peut amener à une médecine plus personnalisée, jusqu'à étudier pour chaque patient les caractères phénotypiques des cellules immunitaires et estimer la balance bénéfice-risque d'une mise sous traitement anticipé de la personne (Fernandez et Giannarelli 2021).

II. PERSPECTIVES CONCERNANT LA PARTIE V DES RESULTATS

Pour aller plus loin, nous souhaitons comprendre les mécanismes qui entrainent la mort des T que nous avons observée. Quels types de ROS précisément sont produits par les monocytes ? Ces ROS pourraient activer la voie NFκB, ce qui impliquerait une production accrue de cytokines pro-inflammatoires que nous pourrions mesurer. L'Annexine-V est un marqueur précoce d'apoptose mais on peut se demander quelles voies sont impliquées. L'activation de p53 est-elle induite par les ROS dans les lymphocytes des patients ? Il est à noter que le gène *TP53* a été retrouvé plus exprimé dans les lymphocytes de certains patients positifs au SARS-COV-2 (Xiong et al. 2020). Je mets au point des lignées cellulaires transduites avec des petits ARN interférants ciblant l'ARN p53 afin de répondre à cette question. La pyroptose est-elle également impliquée (Huang et al. 2020) ?

Nous avons également commencé à étudier la dégranulation des perforines dans les cellules LT8 et les NK des patients de cette cohorte. Dans la HLH primaire, 40% des personnes atteintes de ce syndrome ont une mutation soit sur le gène qui code pour la perforine, soit au niveau de gènes impliqués dans la dégranulation des perforines (Karakike et Giamarellos-Bourboulis 2019). Il sera intéressant de voir si les patients COVID-19 ont un déficit en perforine et si tel est le cas de voir si ce déficit est primaire ou consécutif à une consommation.

Les conséquences de la lymphopénie dans le COVID-19 sont peu claires. Une lymphopénie importante est corrélée à la gravité des symptômes et à un pronostic défavorable (Q. Zhao et al. 2020; Tavakolpour et al. 2020).

La lymphopénie peut expliquer la perte des Tregs, observée dans les cas graves de COVID-19 (Meckiff et al. 2020), empêchant leur action de régulation négative sur les autres LT helper et favorisant l'orage cytokinique.

On peut penser à la qualité des anticorps produits dont l'affinité après une infection par SARS-COV-2 semble moins bonne que celle qui peut être observée pour les autre coronavirus humain (Liu et al. 2020). Des cas de personnes infectées deux fois au SARS-COV-2 dans un laps de temps assez court ont été rapportés (Pedro et al. 2021) parfois même avec des symptômes plus graves lors de la réinfection (Tillett et al. 2021) faisant penser à un défaut de mémoire des lymphocytes qui pourrait être consécutive à la lymphopénie.

La qualité de la mémoire immunitaire spécifique semble très variable après un COVID-19 et nécessite d'être étudiée plus en détail. Un rappel des patients COVID-19 inclus dans la cohorte de Nîmes est en cours pour étudier la qualité et la quantité des anticorps ainsi que des LB et LT mémoires chez ces patients pour tester l'hypothèse que cette qualité pourrait être inversement proportionnelle à l'activation immunitaire et à l'apoptose lymphocytaire en phase aigüe.

Dans une plus large perspective plusieurs infections virales induisent une lymphopénie. On peut bien sûr citer le VIH, mais également des filovirus du typer Marburg ou Ebola (Geisbert et al., 2000.), la rougeole (Quinet 1990), Influenza (Nichols, Niles, et Roberts 2001; Lalueza et al. 2019) et des orthopneumovirus comme le virus respiratoire syncitial (Roe et al. 2004). On peut observer une production de ROS accrue dans ces infections mais aussi une implication des monocytes. Nous pourrions rechercher ce qui déclenche cette production de ROS et si des points communs sont présents. Dans le contexte du VIH nous avons des éléments permettant de prouver qu'un autre GPCR est impliqué dans un mécanisme similaire à celui démontré ici pour le COVID-19, enclenchant des dommages à l'ADN et la mort de certaines cellules.

G- REFERENCES BIBLIOGRAPHIQUE

Agellon, Luis B., Matthew J. Toth, et Alan B. R. Thomson. 2002. « Intracellular Lipid Binding Proteins of the Small Intestine ». In *Cellular Lipid Binding Proteins*, édité par Jan F. C. Glatz, 79-82. Boston, MA: Springer US. https://doi.org/10.1007/978-1-4419-9270-3_10.

Aldaz, Pablo, Conchi Moreno-Iribas, Nerea Egüés, Fátima Irisarri, Yugo Floristan, Julio Sola-Boneta, Víctor Martínez-Artola, Mirian Sagredo, et Jesús Castilla. 2011. « Mortality by Causes in HIV-Infected Adults: Comparison with the General Population ». *BMC Public Health* 11 (1): 300. https://doi.org/10.1186/1471-2458-11-300.

Al-Merani, S A, D P Brooks, B J Chapman, et K A Munday. 1978. « The Half-Lives of Angiotensin II, Angiotensin II-Amide, Angiotensin III, Sar1-Ala8-Angiotensin II and Renin in the Circulatory System of the Rat. » *The Journal of Physiology* 278 (1): 471-90. https://doi.org/10.1113/jphysiol.1978.sp012318.

Avdeev, Sergey N., Viliya V. Gaynitdinova, Zamira M. Merzhoeva, et Zelimkhan G.-M. Berikkhanov. 2021. « N-Acetylcysteine for the Treatment of COVID-19 among Hospitalized Patients ». *Journal of Infection*, juillet, S0163445321003297. https://doi.org/10.1016/j.jinf.2021.07.003.

Babior, Bernard M. 2000. « Phagocytes and Oxidative Stress », 12.

Baroncelli, Silvia, Clementina Maria Galluzzo, Atim Molinari, Maria Franca Pirillo, Albertina Cavalli, Elisa Negri, Marco Floridia, et Anna Degli Antoni. 2020. « Markers of Microbial Translocation during Pregnancy: Differences among HIV+ Women of African and European Provenance ». *The Journal of Infection in Developing Countries* 14 (02): 184-90. https://doi.org/10.3855/jidc.11652.

Barre-Sinoussi, F, J. Chermann, F Rey, M. Nugeyre, S Chamaret, J Gruest, C Dauguet, et al. 1983. « Isolation of a T-Lymphotropic Retrovirus from a Patient at Risk for Acquired Immune Deficiency Syndrome (AIDS) ». *Science* 220 (4599): 868-71. https://doi.org/10.1126/science.6189183.

Batah, Sabrina Setembre, et Alexandre Todorovic Fabro. 2021. « Pulmonary Pathology of ARDS in COVID-19: A Pathological Review for Clinicians ». *Respiratory Medicine* 176 (janvier): 106239. https://doi.org/10.1016/j.rmed.2020.106239.

Bayati, Armin. 2020. « SARS-CoV-2 Infects Cells after Viral Entry via Clathrin-Mediated Endocytosis », 12.

Bergsbaken, Tessa, Susan L. Fink, et Brad T. Cookson. 2009. « Pyroptosis: Host Cell Death and Inflammation ». *Nature Reviews Microbiology* 7 (2): 99-109. https://doi.org/10.1038/nrmicro2070.

Boef, Anna G.C., Esther M. van Wezel, Lilli Gard, Kala Netkova, Mariëtte Lokate, Peter H.J. van der Voort, Hubert G.M. Niesters, et Coretta Van Leer Buter. 2021. « Viral Load Dynamics in Intubated Patients with COVID-19 Admitted to the Intensive Care Unit ». *Journal of Critical Care* 64 (août): 219-25. https://doi.org/10.1016/j.jcrc.2021.04.010.

Bösmüller, Hans, Selina Traxler, Michael Bitzer, Helene Häberle, Wolfgang Raiser, Dominik Nann, Leonie Frauenfeld, Antonio Vogelsberg, Karin Klingel, et Falko Fend. 2020. « The Evolution of Pulmonary Pathology in Fatal COVID-19 Disease: An Autopsy Study with Clinical Correlation ». *Virchows Archiv* 477 (3): 349-57. https://doi.org/10.1007/s00428-020-02881-x.

Boumaza, Asma, Laetitia Gay, Soraya Mezouar, Eloïne Bestion, Aïssatou Bailo Diallo, Moise Michel, Benoit Desnues, et al. 2021. « Monocytes and Macrophages, Targets of Severe Acute Respiratory Syndrome Coronavirus 2: The Clue for Coronavirus Disease 2019

Immunoparalysis ». *The Journal of Infectious Diseases* 224 (3): 395-406. https://doi.org/10.1093/infdis/jiab044.

Brenchley, Jason M, David A Price, Timothy W Schacker, Tedi E Asher, Guido Silvestri, Srinivas Rao, Zachary Kazzaz, et al. 2006. « Microbial Translocation Is a Cause of Systemic Immune Activation in Chronic HIV Infection ». *NATURE MEDICINE* 12 (12): 8.

Brook, Robert D., Robert L. Bard, Melvyn Rubenfire, Paul M. Ridker, et Sanjay Rajagopalan. 2001. « Usefulness of Visceral Obesity (Waist/Hip Ratio) in Predicting Vascular Endothelial Function in Healthy Overweight Adults ». *The American Journal of Cardiology* 88 (11): 1264-69. https://doi.org/10.1016/S0002-9149(01)02088-4.

Buchrieser, Julian, Jérémy Dufloo, Mathieu Hubert, Blandine Monel, Delphine Planas, Maaran Michael Rajah, Cyril Planchais, et al. 2020. « Syncytia Formation by SARS-CoV-2-infected Cells ». *The EMBO Journal* 39 (23). https://doi.org/10.15252/embj.2020106267.

Cappanera, Stefano, Michele Palumbo, Sherman H. Kwan, Giulia Priante, Lucia Assunta Martella, Lavinia Maria Saraca, Francesco Sicari, et al. 2021. « When Does the Cytokine Storm Begin in COVID-19 Patients? A Quick Score to Recognize It ». *Journal of Clinical Medicine* 10 (2): 297. https://doi.org/10.3390/jcm10020297.

Carbone, Michele, John Lednicky, Shu-Yuan Xiao, Mario Venditti, et Enrico Bucci. 2021. « Coronavirus 2019 Infectious Disease Epidemic: Where We Are, What Can Be Done and Hope For ». *Journal of Thoracic Oncology* 16 (4): 546-71. https://doi.org/10.1016/j.jtho.2020.12.014.

Casadevall, Arturo, Susan R. Weiss, et Michael J. Imperiale. 2021. « Can Science Help Resolve the Controversy on the Origins of the SARS-CoV-2 Pandemic? » *MBio* 12 (4). https://doi.org/10.1128/mBio.01948-21.

Cazein, Françoise. 2019. « Situation épidémiologique et dépistage du VIH et des autres IST / Epidemiological situation and screening for HIV and other STIs », 53.

Chen, I-Yin, Miyu Moriyama, Ming-Fu Chang, et Takeshi Ichinohe. 2019. « Severe Acute Respiratory Syndrome Coronavirus Viroporin 3a Activates the NLRP3 Inflammasome ». *Frontiers in Microbiology* 10 (janvier): 50. https://doi.org/10.3389/fmicb.2019.00050.

Chen, Ting, Dajing Guo, Jianguo Lu, Bo Xiang, Xiang Li, Jianghua Nie, Xiaojing He, et Kunhua Li. 2021. « The Role of Chest CT in Management of Asymptomatic SARS-CoV-2 Infections: A Longitudinal Multi-Center Study in Chongqing, China ». *International Journal of Medical Sciences* 18 (2): 520-27. https://doi.org/10.7150/ijms.50705.

Chen, Zeyu, et E. John Wherry. 2020. « T Cell Responses in Patients with COVID-19 ». *Nature Reviews Immunology* 20 (9): 529-36. https://doi.org/10.1038/s41577-020-0402-6.

Chocron, Richard, Baptiste Duceau, Nicolas Gendron, Nacim Ezzouhairi, Lina Khider, Antonin Trimaille, Guillaume Goudot, et al. 2021. « D-Dimer at Hospital Admission for COVID-19 Are Associated with in-Hospital Mortality, Independent of Venous Thromboembolism: Insights from a French Multicenter Cohort Study ». *Archives of Cardiovascular Diseases* 114 (5): 381-93. https://doi.org/10.1016/j.acvd.2021.02.003.

Coperchini, Francesca, Luca Chiovato, Laura Croce, Flavia Magri, et Mario Rotondi. 2020. « The Cytokine Storm in COVID-19: An Overview of the Involvement of the Chemokine/Chemokine-Receptor System ». *Cytokine & Growth Factor Reviews* 53 (juin): 25-32. https://doi.org/10.1016/j.cytogfr.2020.05.003.

Croxford, Sara, Aileen Kitching, Sarika Desai, Meaghan Kall, Michael Edelstein, Andrew Skingsley, Fiona Burns, et al. 2017. « Mortality and Causes of Death in People Diagnosed with HIV in the Era of Highly Active Antiretroviral Therapy Compared with the General

Population: An Analysis of a National Observational Cohort ». *The Lancet Public Health* 2 (1): e35-46. https://doi.org/10.1016/S2468-2667(16)30020-2.

Dale, David C., Laurence Boxer, et W. Conrad Liles. 2008. « The Phagocytes: Neutrophils and Monocytes ». *Blood* 112 (4): 935-45. https://doi.org/10.1182/blood-2007-12-077917.

Darcis, Gilles, Nathalie Maes, Alexander O. Pasternak, Anne-Sophie Sauvage, Frédéric Frippiat, Christelle Meuris, Françoise Uurlings, et al. 2020. « Detectability of HIV Residual Viremia despite Therapy Is Highly Associated with Treatment with a Protease Inhibitor-Based Combination Antiretroviral Therapy ». *Antimicrobial Agents and Chemotherapy* 64 (3). https://doi.org/10.1128/AAC.01902-19.

D'Autréaux, Benoît, et Michel B. Toledano. 2007. « ROS as Signalling Molecules: Mechanisms That Generate Specificity in ROS Homeostasis ». *Nature Reviews Molecular Cell Biology* 8 (10): 813-24. https://doi.org/10.1038/nrm2256.

De Flora, S., C. Grassi, et L. Carati. 1997. « Attenuation of Influenza-like Symptomatology and Improvement of Cell-Mediated Immunity with Long-Term N-Acetylcysteine Treatment ». *European Respiratory Journal* 10 (7): 1535-41. https://doi.org/10.1183/09031936.97.10071535.

Deeks, Steven G., Julie Overbaugh, Andrew Phillips, et Susan Buchbinder. 2015. « HIV Infection ». *Nature Reviews Disease Primers* 1 (1): 15035. https://doi.org/10.1038/nrdp.2015.35.

Désiré, Nathalie, Lorenzo Cerutti, Quentin Le Hingrat, Marine Perrier, Stefan Emler, Vincent Calvez, Diane Descamps, Anne-Geneviève Marcelin, Stéphane Hué, et Benoit Visseaux. 2018. « Characterization Update of HIV-1 M Subtypes Diversity and Proposal for Subtypes A and D Sub-Subtypes Reclassification ». *Retrovirology* 15 (1): 80. https://doi.org/10.1186/s12977-018-0461-y.

Doitsh, Gilad, Marielle Cavrois, Kara G. Lassen, Orlando Zepeda, Zhiyuan Yang, Mario L. Santiago, Andrew M. Hebbeler, et Warner C. Greene. 2010. « Abortive HIV Infection Mediates CD4 T Cell Depletion and Inflammation in Human Lymphoid Tissue ». *Cell* 143 (5): 789-801. https://doi.org/10.1016/j.cell.2010.11.001.

Dolganiuc, Angela, Catherine Garcia, Karen Kodys, et Gyongyi Szabo. 2006. « Distinct Toll-like Receptor Expression in Monocytes and T Cells in Chronic HCV Infection » 12 (8): 7.

Domingo, Francesca Reyes, Lisa A Waddell, Angela M. Cheung, Curtis L. Cooper, Veronica J. Belcourt, Alexandra M. E. Zuckermann, Tricia Corrin, et al. 2021. « Prevalence of Long-Term Effects in Individuals Diagnosed with COVID-19: A Living Systematic Review ». Preprint. Epidemiology. https://doi.org/10.1101/2021.06.03.21258317.

Dörffel, Yvonne, Christoph Lätsch, Bruno Stuhlmüller, Stefan Schreiber, Susann Scholze, Gerd R. Burmester, et Jürgen Scholze. 1999. « Preactivated Peripheral Blood Monocytes in Patients With Essential Hypertension ». *Hypertension* 34 (1): 113-17. https://doi.org/10.1161/01.HYP.34.1.113.

Edler, Carolin, Ann Sophie Schröder, Martin Aepfelbacher, Antonia Fitzek, Axel Heinemann, Fabian Heinrich, Anke Klein, et al. 2020. « Dying with SARS-CoV-2 Infection—an Autopsy Study of the First Consecutive 80 Cases in Hamburg, Germany ». *International Journal of Legal Medicine* 134 (4): 1275-84. https://doi.org/10.1007/s00414-020-02317-w.

Ejaz, Hasan, Abdullah Alsrhani, Aizza Zafar, Humera Javed, Kashaf Junaid, Abualgasim E Abdalla, Khalid O A Abosalif, Zeeshan Ahmed, et Sonia Younas. 2020. « COVID-19 and Comorbidities: Deleterious Impact on Infected Patients ». *Journal of Infection and Public Health*, 8.

Eloseily, Esraa M., et Randy Q. Cron. 2018. « Macrophage Activation Syndrome ». In *The Microbiome in Rheumatic Diseases and Infection*, édité par Gaafar Ragab, T. Prescott Atkinson, et Matthew L. Stoll, 151-82. Cham: Springer International Publishing. https://doi.org/10.1007/978-3-319-79026-8_14.

Engelberger, Rolf P., Andreas Limacher, Nils Kucher, Frédéric Baumann, Günther Silbernagel, Renée Benghozi, Dai-Do Do, Torsten Willenberg, et Iris Baumgartner. 2015. « Biological Variation of Established and Novel Biomarkers for Atherosclerosis: Results from a Prospective, Parallel-Group Cohort Study ». *Clinica Chimica Acta* 447 (juillet): 16-22. https://doi.org/10.1016/j.cca.2015.05.003.

Fajgenbaum, David C., et Carl H. June. 2020. « Cytokine Storm ». Édité par Dan L. Longo. *New England Journal of Medicine* 383 (23): 2255-73. https://doi.org/10.1056/NEJMra2026131.

Ferdenzi, Camille, Christophe Bousquet, Pierre-Emmanuel Aguera, Morgane Dantec, Christelle Daudé, Lesly Fornoni, Arnaud Fournel, et al. 2021. « Recovery From COVID-19-Related Olfactory Disorders and Quality of Life: Insights From an Observational Online Study ». *Chemical Senses* 46 (janvier): bjab028. https://doi.org/10.1093/chemse/bjab028.

Fernandez, Dawn M., et Chiara Giannarelli. 2021. « Immune Cell Profiling in Atherosclerosis: Role in Research and Precision Medicine ». *Nature Reviews Cardiology*, juillet. https://doi.org/10.1038/s41569-021-00589-2.

Ferreira, André C., Vinicius Cardoso Soares, Isaclaudia G. de Azevedo-Quintanilha, Suelen da Silva Gomes Dias, Natalia Fintelman-Rodrigues, Carolina Q. Sacramento, Mayara Mattos, et al. 2021. « SARS-CoV-2 Engages Inflammasome and Pyroptosis in Human Primary Monocytes ». *Cell Death Discovery* 7 (1): 43. https://doi.org/10.1038/s41420-021-00428-w.

Finkel, Yaara, Avi Gluck, Aharon Nachshon, Roni Winkler, Tal Fisher, Batsheva Rozman, Orel Mizrahi, et al. 2021. « SARS-CoV-2 Uses a Multipronged Strategy to Impede Host Protein Synthesis ». *Nature* 594 (7862): 240-45. https://doi.org/10.1038/s41586-021-03610-3.

Finkel, Yaara, Orel Mizrahi, Aharon Nachshon, Shira Weingarten-Gabbay, David Morgenstern, Yfat Yahalom-Ronen, Hadas Tamir, et al. 2021. « The Coding Capacity of SARS-CoV-2 ». *Nature* 589 (7840): 125-30. https://doi.org/10.1038/s41586-020-2739-1.

Follis, Kathryn E., Joanne York, et Jack H. Nunberg. 2006. « Furin Cleavage of the SARS Coronavirus Spike Glycoprotein Enhances Cell–Cell Fusion but Does Not Affect Virion Entry ». *Virology* 350 (2): 358-69. https://doi.org/10.1016/j.virol.2006.02.003.

Forrester, Steven J., George W. Booz, Curt D. Sigmund, Thomas M. Coffman, Tatsuo Kawai, Victor Rizzo, Rosario Scalia, et Satoru Eguchi. 2018. « Angiotensin II Signal Transduction: An Update on Mechanisms of Physiology and Pathophysiology ». *Physiological Reviews* 98 (3): 1627-1738. https://doi.org/10.1152/physrev.00038.2017.

Freund, Adam, Arturo V. Orjalo, Pierre-Yves Desprez, et Judith Campisi. 2010. « Inflammatory Networks during Cellular Senescence: Causes and Consequences ». *Trends in Molecular Medicine* 16 (5): 238-46. https://doi.org/10.1016/j.molmed.2010.03.003.

Funderburg, Nicholas, Morgan Boucher, Abdus Sattar, Manjusha Kulkarni, Danielle Labbato, Bruce I. Kinley, et Grace A. McComsey. 2016. « Rosuvastatin Decreases Intestinal Fatty Acid Binding Protein (I-FABP), but Does Not Alter Zonulin or Lipopolysaccharide Binding Protein (LBP) Levels, in HIV-Infected Subjects on Antiretroviral Therapy ». *Pathogens and Immunity* 1 (1): 118. https://doi.org/10.20411/pai.v1i1.124.

Furuhashi, Masato, Norihito Moniwa, Hideki Takizawa, Nobuyuki Ura, et Kazuaki Shimamoto. 2020. « Potential Differential Effects of Renin-Angiotensin System Inhibitors on SARS-

CoV-2 Infection and Lung Injury in COVID-19 ». *Hypertension Research* 43 (8): 837-40. https://doi.org/10.1038/s41440-020-0478-1.

Ganneru, Brunda, Harsh Jogdand, Vijaya Kumar Daram, Dipankar Das, Narasimha Reddy Molugu, Sai D. Prasad, Srinivas V. Kannappa, et al. 2021. « Th1 Skewed Immune Response of Whole Virion Inactivated SARS CoV 2 Vaccine and Its Safety Evaluation ». *IScience* 24 (4): 102298. https://doi.org/10.1016/j.isci.2021.102298.

Gao, F, L Yue, D L Robertson, S C Hill, H Hui, R J Biggar, A E Neequaye, T M Whelan, D D Ho, et G M Shaw. 1994. « Genetic Diversity of Human Immunodeficiency Virus Type 2: Evidence for Distinct Sequence Subtypes with Differences in Virus Biology ». *Journal of Virology* 68 (11): 7433-47. https://doi.org/10.1128/jvi.68.11.7433-7447.1994.

Geisbert, Thomas W, Lisa E Hensley, Tammy R Gibb, Keith E Steele, Nancy K Jaax, et Peter B Jahrling. s. d. « Apoptosis Induced In Vitro and In Vivo During Infection by Ebola and Marburg Viruses », 16.

Gomes, Caio P., Danilo E. Fernandes, Fernanda Casimiro, Gustavo F. da Mata, Michelle T. Passos, Patricia Varela, Gianna Mastroianni-Kirsztajn, et João Bosco Pesquero. 2020. « Cathepsin L in COVID-19: From Pharmacological Evidences to Genetics ». *Frontiers in Cellular and Infection Microbiology* 10 (décembre): 589505. https://doi.org/10.3389/fcimb.2020.589505.

Gonçalves, Priscila H., Thomas S. Uldrick, et Robert Yarchoan. 2017. « HIV-Associated Kaposi Sarcoma and Related Diseases ». *AIDS* 31 (14): 1903-16. https://doi.org/10.1097/QAD.0000000000001567.

Greter, Melanie, Julie Helft, Andrew Chow, Daigo Hashimoto, Arthur Mortha, Judith Agudo-Cantero, Milena Bogunovic, et al. 2012. « GM-CSF Controls Nonlymphoid Tissue Dendritic Cell Homeostasis but Is Dispensable for the Differentiation of Inflammatory Dendritic Cells ». *Immunity* 36 (6): 1031-46. https://doi.org/10.1016/j.immuni.2012.03.027.

Griendling, Kathy K, Candace A Minieri, Jeremy D Ollerenshaw, et R Wayne Alexander. s. d. « Angiotensin II Stimulates NADH and NADPH Oxidase Activity in Cultured Vascular Smooth Muscle Cells. », 8.

Guaraldi, G., G. Orlando, S. Zona, M. Menozzi, F. Carli, E. Garlassi, A. Berti, E. Rossi, A. Roverato, et F. Palella. 2011. « Premature Age-Related Comorbidities Among HIV-Infected Persons Compared With the General Population ». *Clinical Infectious Diseases* 53 (11): 1120-26. https://doi.org/10.1093/cid/cir627.

Hahn, Alfred W.A., Uwe Jonas, Fritz R. Bühler, et Thérèse J. Resink. 1994. « Activation of Human Peripheral Monocytes by Angiotensin II ». *FEBS Letters* 347 (2-3): 178-80. https://doi.org/10.1016/0014-5793(94)00531-1.

Hammer, Scott M., David A. Katzenstein, Michael D. Hughes, Holly Gundacker, Robert T. Schooley, Richard H. Haubrich, W. Keith Henry, et al. 1996. « A Trial Comparing Nucleoside Monotherapy with Combination Therapy in HIV-Infected Adults with CD4 Cell Counts from 200 to 500 per Cubic Millimeter ». *New England Journal of Medicine* 335 (15): 1081-90. https://doi.org/10.1056/NEJM199610103351501.

Haque, SK Manirul, Omar Ashwaq, Abdulla Sarief, et Abdul Kalam Azad John Mohamed. 2020. « A Comprehensive Review about SARS-CoV-2 ». *Future Virology* 15 (9): 625-48. https://doi.org/10.2217/fvl-2020-0124.

Harijith, Anantha, David L. Ebenezer, et Viswanathan Natarajan. 2014. « Reactive Oxygen Species at the Crossroads of Inflammasome and Inflammation ». *Frontiers in Physiology* 5 (septembre). https://doi.org/10.3389/fphys.2014.00352.

Hoffmann, Markus, Hannah Kleine-Weber, Nadine Krüger, Marcel Müller, Christian Drosten, et Stefan Pöhlmann. 2020. « The Novel Coronavirus 2019 (2019-NCoV) Uses the SARS-Coronavirus Receptor ACE2 and the Cellular Protease TMPRSS2 for Entry into Target Cells ». Preprint. Molecular Biology. https://doi.org/10.1101/2020.01.31.929042.

Hoffmann, Markus, Hannah Kleine-Weber, et Stefan Pöhlmann. 2020. « A Multibasic Cleavage Site in the Spike Protein of SARS-CoV-2 Is Essential for Infection of Human Lung Cells ». *Molecular Cell* 78 (4): 779-784.e5. https://doi.org/10.1016/j.molcel.2020.04.022.

Horáková, Dagmar, Ladislav Štěpánek, Vladimír Janout, Jana Janoutová, Dalibor Pastucha, Helena Kollárová, Alena Petráková, Lubomír Štěpánek, Roman Husár, et Karel Martiník. 2019. « Optimal Homeostasis Model Assessment of Insulin Resistance (HOMA-IR) Cut-Offs: A Cross-Sectional Study in the Czech Population ». *Medicina* 55 (5): 158. https://doi.org/10.3390/medicina55050158.

Huang, Chaolin, Yeming Wang, Xingwang Li, Lili Ren, Jianping Zhao, Yi Hu, Li Zhang, et al. 2020. « Clinical Features of Patients Infected with 2019 Novel Coronavirus in Wuhan, China ». *The Lancet* 395 (10223): 497-506. https://doi.org/10.1016/S0140-6736(20)30183-5.

Hulo, Chantal, Edouard de Castro, Patrick Masson, Lydie Bougueleret, Amos Bairoch, Ioannis Xenarios, et Philippe Le Mercier. 2011. « ViralZone: A Knowledge Resource to Understand Virus Diversity ». *Nucleic Acids Research* 39 (suppl_1): D576-82. https://doi.org/10.1093/nar/gkq901.

Ibrahim, Homam, Andras Perl, Deane Smith, Tyler Lewis, Zachary Kon, Ronald Goldenberg, Kinan Yarta, Cezar Staniloae, et Mathew Williams. 2020. « Therapeutic Blockade of Inflammation in Severe COVID-19 Infection with Intravenous N-Acetylcysteine ». *Clinical Immunology* 219 (octobre): 108544. https://doi.org/10.1016/j.clim.2020.108544.

Ireland, H, C Konstantoulas, J Cooper, E Hawe, S Humphries, H Mather, A Goodall, J Hogwood, I Juhanvague, et J Yudkin. 2005. « EPCR Ser219Gly: Elevated SEPCR, Prothrombin F1+2, Risk for Coronary Heart Disease, and Increased SEPCR Shedding in Vitro ». *Atherosclerosis* 183 (2): 283-92. https://doi.org/10.1016/j.atherosclerosis.2005.02.028.

Jakubzick, Claudia V., Gwendalyn J. Randolph, et Peter M. Henson. 2017. « Monocyte Differentiation and Antigen-Presenting Functions ». *Nature Reviews Immunology* 17 (6): 349-62. https://doi.org/10.1038/nri.2017.28.

Jensen, Benjamin AH, et Andre Marette. 2020. « Microbial Translocation in Type 2 Diabetes: When Bacterial Invaders Overcome Host Defence in Human Obesity ». *Gut* 69 (10): 1724-26. https://doi.org/10.1136/gutjnl-2020-321288.

Jordan, Michael B., Carl E. Allen, Sheila Weitzman, Alexandra H. Filipovich, et Kenneth L. McClain. 2011. « How I Treat Hemophagocytic Lymphohistiocytosis ». *Blood* 118 (15): 4041-52. https://doi.org/10.1182/blood-2011-03-278127.

Jose, Ricardo J, et Ari Manuel. 2020. « COVID-19 Cytokine Storm: The Interplay between Inflammation and Coagulation ». *The Lancet Respiratory Medicine* 8 (6): e46-47. https://doi.org/10.1016/S2213-2600(20)30216-2.

Junqueira, Caroline. 2021. « SARS-CoV-2 Infects Blood Monocytes to Activate NLRP3 and AIM2 Inflammasomes, Pyroptosis and Cytokine Release », 36.

Justin Rucker, A., et Steven D. Crowley. 2017. « The Role of Macrophages in Hypertension and Its Complications ». *Pflügers Archiv - European Journal of Physiology* 469 (3-4): 419-30. https://doi.org/10.1007/s00424-017-1950-x.

Kang, M A, E-Y So, A L Simons, D R Spitz, et T Ouchi. 2012. « DNA Damage Induces Reactive Oxygen Species Generation through the H2AX-Nox1/Rac1 Pathway ». *Cell Death & Disease* 3 (1): e249-e249. https://doi.org/10.1038/cddis.2011.134.

Kanwar, Bittoo, David Favre, et Joseph M McCune. 2010. « Th17 and Regulatory T Cells: Implications for AIDS Pathogenesis »: *Current Opinion in HIV and AIDS* 5 (2): 151-57. https://doi.org/10.1097/COH.0b013e328335c0c1.

Karakike, Eleni, et Evangelos J. Giamarellos-Bourboulis. 2019. « Macrophage Activation-Like Syndrome: A Distinct Entity Leading to Early Death in Sepsis ». *Frontiers in Immunology* 10 (janvier): 55. https://doi.org/10.3389/fimmu.2019.00055.

Ke, Zunlong. 2020. « Structures and Distributions of SARS-CoV-2 Spike Proteins on Intact Virions », 21.

Keyhanian, Kiandokht, Raffaella Pizzolato Umeton, Babak Mohit, Vahid Davoudi, Fatemeh Hajighasemi, et Mehdi Ghasemi. 2021. « SARS-CoV-2 and Nervous System: From Pathogenesis to Clinical Manifestation ». *Journal of Neuroimmunology* 350 (janvier): 577436. https://doi.org/10.1016/j.jneuroim.2020.577436.

Kim, Dongwan, Joo-Yeon Lee, Jeong-Sun Yang, Jun Won Kim, V. Narry Kim, et Hyeshik Chang. 2020. « The Architecture of SARS-CoV-2 Transcriptome ». *Cell* 181 (4): 914-921.e10. https://doi.org/10.1016/j.cell.2020.04.011.

Klein, Steffen, Mirko Cortese, Sophie L. Winter, Moritz Wachsmuth-Melm, Christopher J. Neufeldt, Berati Cerikan, Megan L. Stanifer, Steeve Boulant, Ralf Bartenschlager, et Petr Chlanda. 2020. « SARS-CoV-2 Structure and Replication Characterized by in Situ Cryo-Electron Tomography ». *Nature Communications* 11 (1): 5885. https://doi.org/10.1038/s41467-020-19619-7.

Laforge, Mireille, Carole Elbim, Corinne Frère, Miryana Hémadi, Charbel Massaad, Philippe Nuss, Jean-Jacques Benoliel, et Chrystel Becker. 2020. « Tissue Damage from Neutrophil-Induced Oxidative Stress in COVID-19 ». *Nature Reviews Immunology* 20 (9): 515-16. https://doi.org/10.1038/s41577-020-0407-1.

Lalueza, Antonio, Dolores Folgueira, Carmen Díaz-Pedroche, Pilar Hernández-Jiménez, Blanca Ayuso, Cristina Castillo, Jaime Laureiro, Hernando Trujillo, Marta Torres, et Carlos Lumbreras. 2019. « Severe Lymphopenia in Hospitalized Patients with Influenza Virus Infection as a Marker of a Poor Outcome ». *Infectious Diseases* 51 (7): 543-46. https://doi.org/10.1080/23744235.2019.1598572.

Latinne, Alice. 2020. « Origin and Cross-Species Transmission of Bat Coronaviruses in China », 15.

Lau, Eva. 2016. « The Role of I-FABP as a Biomarker of Intestinal Barrier Dysfunction Driven by Gut Microbiota Changes in Obesity », 7.

Li, Shufen, Yulan Zhang, Zhenqiong Guan, Huiling Li, Meidi Ye, Xi Chen, Jun Shen, et al. 2020. « SARS-CoV-2 Triggers Inflammatory Responses and Cell Death through Caspase-8 Activation ». *Signal Transduction and Targeted Therapy* 5 (1): 235. https://doi.org/10.1038/s41392-020-00334-0.

Lin, Xian-Dan, Wen Wang, Zong-Yu Hao, Zhao-Xiao Wang, Wen-Ping Guo, Xiao-Qing Guan, Miao-Ruo Wang, et al. 2017. « Extensive Diversity of Coronaviruses in Bats from China ». *Virology* 507 (juillet): 1-10. https://doi.org/10.1016/j.virol.2017.03.019.

Liou, Geou-Yarh, et Peter Storz. 2010. « Reactive Oxygen Species in Cancer ». *Free Radical Research* 44 (5): 479-96. https://doi.org/10.3109/10715761003667554.

Liu, Tiancheng, Jessica Hsiung, Su Zhao, Jessica Kost, Deepika Sreedhar, Carl V. Hanson, Kjerstie Olson, et al. 2020. « Quantification of Antibody Avidities and Accurate Detection of

SARS-CoV-2 Antibodies in Serum and Saliva on Plasmonic Substrates ». *Nature Biomedical Engineering* 4 (12): 1188-96. https://doi.org/10.1038/s41551-020-00642-4.

Lubbe, Lizelle, Gyles E. Cozier, Delia Oosthuizen, K. Ravi Acharya, et Edward D. Sturrock. 2020. « ACE2 and ACE: Structure-Based Insights into Mechanism, Regulation and Receptor Recognition by SARS-CoV ». *Clinical Science* 134 (21): 2851-71. https://doi.org/10.1042/CS20200899.

Maca, J., O. Jor, M. Holub, P. Sklienka, F. Bur a, M. Burda, V. Janout, et P. ev ik. 2017. « Past and Present ARDS Mortality Rates: A Systematic Review ». *Respiratory Care* 62 (1): 113-22. https://doi.org/10.4187/respcare.04716.

Maciel, Rafael Aguiar, Helena Moreira Klück, Madeleine Durand, et Eduardo Sprinz. 2018. « Comorbidity Is More Common and Occurs Earlier in Persons Living with HIV than in HIV-Uninfected Matched Controls, Aged 50 Years and Older: A Cross-Sectional Study ». *International Journal of Infectious Diseases* 70 (mai): 30-35. https://doi.org/10.1016/j.ijid.2018.02.009.

Mangalmurti, Nilam, et Christopher A. Hunter. 2020. « Cytokine Storms: Understanding COVID-19 ». *Immunity* 53 (1): 19-25. https://doi.org/10.1016/j.immuni.2020.06.017.

Marcus, Julia L., Wendy A. Leyden, Stacey E. Alexeeff, Alexandra N. Anderson, Rulin C. Hechter, Haihong Hu, Jennifer O. Lam, et al. 2020. « Comparison of Overall and Comorbidity-Free Life Expectancy Between Insured Adults With and Without HIV Infection, 2000-2016 ». *JAMA Network Open* 3 (6): e207954. https://doi.org/10.1001/jamanetworkopen.2020.7954.

Maucourant, Christopher, Iva Filipovic, Andrea Ponzetta, Soo Aleman, Martin Cornillet, Laura Hertwig, Benedikt Strunz, et al. 2020. « Natural Killer Cell Immunotypes Related to COVID-19 Disease Severity ». *Science Immunology* 5 (50): eabd6832. https://doi.org/10.1126/sciimmunol.abd6832.

Meckiff, Benjamin J., Ciro Ramírez-Suástegui, Vicente Fajardo, Serena J. Chee, Anthony Kusnadi, Hayley Simon, Simon Eschweiler, et al. 2020. « Imbalance of Regulatory and Cytotoxic SARS-CoV-2-Reactive CD4+ T Cells in COVID-19 ». *Cell* 183 (5): 1340-1353.e16. https://doi.org/10.1016/j.cell.2020.10.001.

Mehta, Puja, Daniel F McAuley, Michael Brown, Emilie Sanchez, Rachel S Tattersall, et Jessica J Manson. 2020. « COVID-19: Consider Cytokine Storm Syndromes and Immunosuppression ». *The Lancet* 395 (10229): 1033-34. https://doi.org/10.1016/S0140-6736(20)30628-0.

Meinhardt, Jenny. 2021. « Olfactory Transmucosal SARS-CoV-2 Invasion as a Port of Central Nervous System Entry in Individuals with COVID-19 ». *Nature Neuroscience* 24: 13.

Melo, Guilherme Dias de, Françoise Lazarini, Sylvain Levallois, Charlotte Hautefort, Vincent Michel, Florence Larrous, Benjamin Verillaud, et al. 2021. « COVID-19–Related Anosmia Is Associated with Viral Persistence and Inflammation in Human Olfactory Epithelium and Brain Infection in Hamsters ». *Science Translational Medicine* 13 (596): eabf8396. https://doi.org/10.1126/scitranslmed.abf8396.

Miller, William C, Nora E Rosenberg, Sarah E Rutstein, et Kimberly A Powers. 2010. « Role of Acute and Early HIV Infection in the Sexual Transmission of HIV »: *Current Opinion in HIV and AIDS* 5 (4): 277-82. https://doi.org/10.1097/COH.0b013e32833a0d3a.

Moreno, S, Cf Perno, Pw Mallon, G Behrens, P Corbeau, J-P Routy, et G Darcis. 2019. « Two-Drug *vs* . Three-Drug Combinations for HIV-1: Do We Have Enough Data to Make the Switch? » *HIV Medicine* 20 (avril): 2-12. https://doi.org/10.1111/hiv.12716.

Nguyen, Hoang Linh, Pham Dang Lan, Nguyen Quoc Thai, Daniel A. Nissley, Edward P. O'Brien, et Mai Suan Li. 2020. « Does SARS-CoV-2 Bind to Human ACE2 More Strongly Than Does SARS-CoV? » *The Journal of Physical Chemistry B* 124 (34): 7336-47. https://doi.org/10.1021/acs.jpcb.0c04511.

Nichols, Joan E., Jean A. Niles, et Norbert J. Roberts. 2001. « Human Lymphocyte Apoptosis after Exposure to Influenza A Virus ». *Journal of Virology* 75 (13): 5921-29. https://doi.org/10.1128/JVI.73.13.5921-5929.2001.

Nolan, David. 2003. « Metabolic Complications Associated with HIV Protease Inhibitor Therapy »: *Drugs* 63 (23): 2555-74. https://doi.org/10.2165/00003495-200363230-00001.

O'Driscoll, Megan, Gabriel Ribeiro Dos Santos, Lin Wang, Derek A. T. Cummings, Andrew S. Azman, Juliette Paireau, Arnaud Fontanet, Simon Cauchemez, et Henrik Salje. 2021. « Age-Specific Mortality and Immunity Patterns of SARS-CoV-2 ». *Nature* 590 (7844): 140-45. https://doi.org/10.1038/s41586-020-2918-0.

Orekhov, Alexander N., Varvara A. Orekhova, Nikita G. Nikiforov, Veronika A. Myasoedova, Andrey V. Grechko, Elena B. Romanenko, Dongwei Zhang, et Dimitry A. Chistiakov. 2019. « Monocyte Differentiation and Macrophage Polarization ». *Vessel Plus* 2019 (mars). https://doi.org/10.20517/2574-1209.2019.04.

Otsuka, Ryo, et Ken-ichiro Seino. 2020. « Macrophage Activation Syndrome and COVID-19 ». *Inflammation and Regeneration* 40 (1): 19. https://doi.org/10.1186/s41232-020-00131-w.

Pan, Pan, Miaomiao Shen, Zhenyang Yu, Weiwei Ge, Keli Chen, Mingfu Tian, Feng Xiao, et al. 2021. « SARS-CoV-2 N Protein Promotes NLRP3 Inflammasome Activation to Induce Hyperinflammation ». *Nature Communications* 12 (1): 4664. https://doi.org/10.1038/s41467-021-25015-6.

Parham, Peter, 1950-. 2005. *The immune system*. Second edition. New York, NY : Garland Science, [2005] ©2005. https://search.library.wisc.edu/catalog/999960176602121.

Paul, Oindrila, Jian Qin Tao, Leslie Litzky, Michael Feldman, Kathleen Montone, Chamith Rajapakse, Christian Bermudez, et Shampa Chatterjee. 2021. « Vascular Inflammation in Lungs of Patients with Fatal Coronavirus Disease 2019 (COVID-19) Infection: Possible Role for the NLRP3 Inflammasome ». Preprint. Cardiovascular Medicine. https://doi.org/10.1101/2021.03.19.21253815.

Peacock, Thomas P., Daniel H. Goldhill, Jie Zhou, Laury Baillon, Rebecca Frise, Olivia C. Swann, Ruthiran Kugathasan, et al. 2021. « The Furin Cleavage Site in the SARS-CoV-2 Spike Protein Is Required for Transmission in Ferrets ». *Nature Microbiology* 6 (7): 899-909. https://doi.org/10.1038/s41564-021-00908-w.

Peacock, Thomas P., Carol M. Sheppard, Jonathan C. Brown, Niluka Goonawardane, Jie Zhou, Max Whiteley, PHE Virology Consortium, Thushan I. de Silva, et Wendy S. Barclay. 2021. « The SARS-CoV-2 Variants Associated with Infections in India, B.1.617, Show Enhanced Spike Cleavage by Furin ». Preprint. Microbiology. https://doi.org/10.1101/2021.05.28.446163.

Pedro, Nicole, Cláudio N. Silva, Ana C. Magalhães, Bruno Cavadas, Ana M. Rocha, Ana C. Moreira, Maria Salomé Gomes, et al. 2021. « Dynamics of a Dual SARS-CoV-2 Lineage Co-Infection on a Prolonged Viral Shedding COVID-19 Case: Insights into Clinical Severity and Disease Duration ». *Microorganisms* 9 (2): 300. https://doi.org/10.3390/microorganisms9020300.

Polak, Samuel B., Inge C. Van Gool, Danielle Cohen, Jan H. von der Thüsen, et Judith van Paassen. 2020. « A Systematic Review of Pathological Findings in COVID-19: A Pathophysiological Timeline and Possible Mechanisms of Disease Progression ». *Modern Pathology* 33 (11): 2128-38. https://doi.org/10.1038/s41379-020-0603-3.

Psomas, Christina, Mehwish Younas, Christelle Reynes, Renaud Cezar, Pierre Portalès, Edouard Tuaillon, Adeline Guigues, et al. 2016. « One of the Immune Activation Profiles Observed in HIV-1-Infected Adults with Suppressed Viremia Is Linked to Metabolic Syndrome: The ACTIVIH Study ». *EBioMedicine* 8 (juin): 265-76. https://doi.org/10.1016/j.ebiom.2016.05.008.

Puskarich, Michael A., Nathan W. Cummins, Nicholas E. Ingraham, David A. Wacker, Ronald A. Reilkoff, Brian E Driver, Michelle H. Biros, et al. 2021. « A Multi-Center Phase II Randomized Clinical Trial of Losartan on Symptomatic Outpatients with COVID-19 ». *EClinicalMedicine* 37 (juillet): 100957. https://doi.org/10.1016/j.eclinm.2021.100957.

Quinet, B. 1990. « Rougeole et immunosuppression ». *Médecine et Maladies Infectieuses* 20 (8-9): 480-83. https://doi.org/10.1016/S0399-077X(05)80825-X.

Raj, Resal. 2021. « Analysis of Non-Structural Proteins, NSPs of SARS-CoV-2 as Targets for Computational Drug Designing ». *Biochemistry and Biophysics Reports* 25 (mars): 100847. https://doi.org/10.1016/j.bbrep.2020.100847.

Rajagopalan, S, S Kurz, T Münzel, M Tarpey, B A Freeman, K K Griendling, et D G Harrison. 1996. « Angiotensin II-Mediated Hypertension in the Rat Increases Vascular Superoxide Production via Membrane NADH/NADPH Oxidase Activation. Contribution to Alterations of Vasomotor Tone. » *Journal of Clinical Investigation* 97 (8): 1916-23. https://doi.org/10.1172/JCI118623.

Ray, Paul D., Bo-Wen Huang, et Yoshiaki Tsuji. 2012. « Reactive Oxygen Species (ROS) Homeostasis and Redox Regulation in Cellular Signaling ». *Cellular Signalling* 24 (5): 981-90. https://doi.org/10.1016/j.cellsig.2012.01.008.

Ren, Yujie, Ting Shu, Di Wu, Jingfang Mu, Chong Wang, Muhan Huang, Yang Han, et al. 2020. « The ORF3a Protein of SARS-CoV-2 Induces Apoptosis in Cells ». *Cellular & Molecular Immunology* 17 (8): 881-83. https://doi.org/10.1038/s41423-020-0485-9.

Reusch, Nico, Elena De Domenico, Lorenzo Bonaguro, Jonas Schulte-Schrepping, Kevin Baßler, Joachim L. Schultze, et Anna C. Aschenbrenner. 2021. « Neutrophils in COVID-19 ». *Frontiers in Immunology* 12 (mars): 652470. https://doi.org/10.3389/fimmu.2021.652470.

Rha, Min-Seok, Hye Won Jeong, Jae-Hoon Ko, Seong Jin Choi, In-Ho Seo, Jeong Seok Lee, Moa Sa, et al. 2021. « PD-1-Expressing SARS-CoV-2-Specific CD8+ T Cells Are Not Exhausted, but Functional in Patients with COVID-19 ». *Immunity* 54 (1): 44-52.e3. https://doi.org/10.1016/j.immuni.2020.12.002.

Rodrigues, Tamara S., Keyla S.G. de Sá, Adriene Y. Ishimoto, Amanda Becerra, Samuel Oliveira, Leticia Almeida, Augusto V. Gonçalves, et al. 2021. « Inflammasomes Are Activated in Response to SARS-CoV-2 Infection and Are Associated with COVID-19 Severity in Patients ». *Journal of Experimental Medicine* 218 (3): e20201707. https://doi.org/10.1084/jem.20201707.

Roe, M. F. E., D. M. Bloxham, D. K. White, R. I. Ross-Russell, R. T. C. Tasker, et D. R. O'Donnell. 2004. « Lymphocyte Apoptosis in Acute Respiratory Syncytial Virus Bronchiolitis: Respiratory Syncytial Virus and Lymphocyte Apoptosis ». *Clinical & Experimental Immunology* 137 (1): 139-45. https://doi.org/10.1111/j.1365-2249.2004.02512.x.

Roncati, Luca, Vincenzo Nasillo, Beatrice Lusenti, et Giovanni Riva. 2020. « Signals of Th2 Immune Response from COVID-19 Patients Requiring Intensive Care ». *Annals of Hematology* 99 (6): 1419-20. https://doi.org/10.1007/s00277-020-04066-7.

Rothlin, Rodolfo Pedro, Mariano Duarte, Facundo Germán Pelorosso, Liliana Nicolosi, M. Victoria Salgado, Héctor Miguel Vetulli, et Eduardo Spitzer. 2021. « Angiotensin Receptor Blockers for COVID-19: Pathophysiological and Pharmacological Considerations About Ongoing and Future Prospective Clinical Trials ». *Frontiers in Pharmacology* 12 (mars): 603736. https://doi.org/10.3389/fphar.2021.603736.

Roy, Jérôme, Jean-Marie Galano, Thierry Durand, Jean-Yves Le Guennec, et Jetty Chung-Yung Lee. 2017. « Physiological Role of Reactive Oxygen Species as Promoters of Natural Defenses ». *The FASEB Journal* 31 (9): 3729-45. https://doi.org/10.1096/fj.201700170R.

Rubio, Camila Peres, et José Joaquin Cerón. 2021. « Spectrophotometric Assays for Evaluation of Reactive Oxygen Species (ROS) in Serum: General Concepts and Applications in Dogs and Humans ». *BMC Veterinary Research* 17 (1): 226. https://doi.org/10.1186/s12917-021-02924-8.

Sandler, Netanya G., et Daniel C. Douek. 2012. « Microbial Translocation in HIV Infection: Causes, Consequences and Treatment Opportunities ». *Nature Reviews Microbiology* 10 (9): 655-66. https://doi.org/10.1038/nrmicro2848.

Santos, Wagner Gouvea dos. 2020. « Natural History of COVID-19 and Current Knowledge on Treatment Therapeutic Options ». *Biomedicine & Pharmacotherapy* 129 (septembre): 110493. https://doi.org/10.1016/j.biopha.2020.110493.

Schubert, Katharina, Evangelos D. Karousis, Ahmad Jomaa, Alain Scaiola, Blanca Echeverria, Lukas-Adrian Gurzeler, Marc Leibundgut, Volker Thiel, Oliver Mühlemann, et Nenad Ban. 2020. « SARS-CoV-2 Nsp1 Binds the Ribosomal MRNA Channel to Inhibit Translation ». *Nature Structural & Molecular Biology* 27 (10): 959-66. https://doi.org/10.1038/s41594-020-0511-8.

Schultze, Joachim L., et Anna C. Aschenbrenner. 2021. « COVID-19 and the Human Innate Immune System ». *Cell* 184 (7): 1671-92. https://doi.org/10.1016/j.cell.2021.02.029.

Sereti, Irini, Richard M. Dunham, John Spritzler, Evgenia Aga, Michael A. Proschan, Kathy Medvik, Catherine A. Battaglia, et al. 2009. « IL-7 Administration Drives T Cell–Cycle Entry and Expansion in HIV-1 Infection ». *Blood* 113 (25): 6304-14. https://doi.org/10.1182/blood-2008-10-186601.

Shang, Jian, Yushun Wan, Chuming Luo, Gang Ye, Qibin Geng, Ashley Auerbach, et Fang Li. 2020. « Cell Entry Mechanisms of SARS-CoV-2 ». *Proceedings of the National Academy of Sciences* 117 (21): 11727-34. https://doi.org/10.1073/pnas.2003138117.

Sharp, P. M., et B. H. Hahn. 2011. « Origins of HIV and the AIDS Pandemic ». *Cold Spring Harbor Perspectives in Medicine* 1 (1): a006841-a006841. https://doi.org/10.1101/cshperspect.a006841.

Skowyra, Artur, Tomasz Mikuła, Magdalena Suchacz, Agnieszka Skowyra, et Alicja Wiercińska-Drapało. 2015. « The Role of Serum I-FABP Concentration in Assessment of Small Intestine Mucosa among HIV-Infected Patients ». *European Journal of Inflammation* 13 (2): 75-81. https://doi.org/10.1177/1721727X15586660.

Smiley, Casey L, Peter F Rebeiro, Carina Cesar, Pablo F Belaunzaran-Zamudio, Brenda Crabtree-Ramirez, Denis Padgett, Eduardo Gotuzzo, et al. 2021. « Estimated Life Expectancy Gains with Antiretroviral Therapy among Adults with HIV in Latin America and the Caribbean: A Multisite Retrospective Cohort Study ». *The Lancet HIV* 8 (5): e266-73. https://doi.org/10.1016/S2352-3018(20)30358-1.

Sokoya, T., H. C. Steel, M. Nieuwoudt, et T. M. Rossouw. 2017. « HIV as a Cause of Immune Activation and Immunosenescence ». *Mediators of Inflammation* 2017: 1-16. https://doi.org/10.1155/2017/6825493.

Song, Cheng-Bo, Le-Le Zhang, Xian Wu, Ya-Jing Fu, Yong-Jun Jiang, Hong Shang, et Zi-Ning Zhang. 2020. « CD4+CD38+ Central Memory T Cells Contribute to HIV Persistence in HIV-Infected Individuals on Long-Term ART ». *Journal of Translational Medicine* 18 (1): 95. https://doi.org/10.1186/s12967-020-02245-8.

Srinivas, Upadhyayula Sai, Bryce W.Q. Tan, Balamurugan A. Vellayappan, et Anand D. Jeyasekharan. 2019. « ROS and the DNA Damage Response in Cancer ». *Redox Biology* 25 (juillet): 101084. https://doi.org/10.1016/j.redox.2018.101084.

Steins, Martin B., Teresa Padró, Chang-Xun Li, Rolf M. Mesters, Helmut Ostermann, Dieter Hammel, Hans H. Scheld, Wolfgang E. Berdel, et Joachim Kienast. 1999. « Overexpression of Tissue-Type Plasminogen Activator in Atherosclerotic Human Coronary Arteries ». *Atherosclerosis* 145 (1): 173-80. https://doi.org/10.1016/S0021-9150(99)00030-1.

Tavakolpour, Soheil, Taha Rakhshandehroo, Erin X. Wei, et Mohammad Rashidian. 2020. « Lymphopenia during the COVID-19 Infection: What It Shows and What Can Be Learned ». *Immunology Letters* 225 (septembre): 31-32. https://doi.org/10.1016/j.imlet.2020.06.013.

Tay, Matthew Zirui, Chek Meng Poh, Laurent Rénia, Paul A. MacAry, et Lisa F. P. Ng. 2020. « The Trinity of COVID-19: Immunity, Inflammation and Intervention ». *Nature Reviews Immunology* 20 (6): 363-74. https://doi.org/10.1038/s41577-020-0311-8.

Taylor, Barbara S., Magdalena E. Sobieszczyk, Francine E. McCutchan, et Scott M. Hammer. 2008. « The Challenge of HIV-1 Subtype Diversity ». *New England Journal of Medicine* 358 (15): 1590-1602. https://doi.org/10.1056/NEJMra0706737.

Taylor, Stephen, Marta Boffito, Saye Khoo, Erasmus Smit, et David Back. 2007. « Stopping Antiretroviral Therapy ». *AIDS* 21 (13): 1673-82. https://doi.org/10.1097/QAD.0b013e3281c61394.

Tillett, Richard L, Joel R Sevinsky, Paul D Hartley, Heather Kerwin, Natalie Crawford, Andrew Gorzalski, Chris Laverdure, et al. 2021. « Genomic Evidence for Reinfection with SARS-CoV-2: A Case Study ». *The Lancet Infectious Diseases* 21 (1): 52-58. https://doi.org/10.1016/S1473-3099(20)30764-7.

Totura, Allison L., et Sina Bavari. 2019. « Broad-Spectrum Coronavirus Antiviral Drug Discovery ». *Expert Opinion on Drug Discovery* 14 (4): 397-412. https://doi.org/10.1080/17460441.2019.1581171.

Vandestienne, Marie, Yujiao Zhang, Icia Santos-Zas, Rida Al-Rifai, Jeremie Joffre, Andreas Giraud, Ludivine Laurans, et al. 2021. « TREM-1 Orchestrates Angiotensin II–Induced Monocyte Trafficking and Promotes Experimental Abdominal Aortic Aneurysm ». *Journal of Clinical Investigation* 131 (2): e142468. https://doi.org/10.1172/JCI142468.

Varanat, M., E.M. Haase, J.G. Kay, et F.A. Scannapieco. 2017. « Activation of the TREM-1 Pathway in Human Monocytes by Periodontal Pathogens and Oral Commensal Bacteria ». *Molecular Oral Microbiology* 32 (4): 275-87. https://doi.org/10.1111/omi.12169.

Vitte, Joana, Aïssatou Bailo Diallo, Asma Boumaza, Alexandre Lopez, Moïse Michel, Jérôme Allardet-Servent, Soraya Mezouar, et al. 2020. « A Granulocytic Signature Identifies COVID-19 and Its Severity ». *The Journal of Infectious Diseases* 222 (12): 1985-96. https://doi.org/10.1093/infdis/jiaa591.

V'kovski, Philip, Annika Kratzel, Silvio Steiner, Hanspeter Stalder, et Volker Thiel. 2021. « Coronavirus Biology and Replication: Implications for SARS-CoV-2 ». *Nature Reviews Microbiology* 19 (3): 155-70. https://doi.org/10.1038/s41579-020-00468-6.

Vora, Setu M., Judy Lieberman, et Hao Wu. 2021. « Inflammasome Activation at the Crux of Severe COVID-19 ». *Nature Reviews Immunology*, août. https://doi.org/10.1038/s41577-021-00588-x.

Walls, Alexandra C., Young-Jun Park, M. Alejandra Tortorici, Abigail Wall, Andrew T. McGuire, et David Veesler. 2020. « Structure, Function, and Antigenicity of the SARS-CoV-2 Spike Glycoprotein ». *Cell* 181 (2): 281-292.e6. https://doi.org/10.1016/j.cell.2020.02.058.

Wang, Hui Di, Shanqin Xu, Douglas G. Johns, Yue Du, Mark T. Quinn, Antonio J. Cayatte, et Richard A. Cohen. 2001. « Role of NADPH Oxidase in the Vascular Hypertrophic and Oxidative Stress Response to Angiotensin II in Mice ». *Circulation Research* 88 (9): 947-53. https://doi.org/10.1161/hh0901.089987.

Westmeier, Jaana, Krystallenia Paniskaki, Zehra Karaköse, Tanja Werner, Kathrin Sutter, Sebastian Dolff, Marvin Overbeck, et al. 2020. « Impaired Cytotoxic CD8 $^{+}$ T Cell Response in Elderly COVID-19 Patients ». Édité par Peter Palese. *MBio* 11 (5). https://doi.org/10.1128/mBio.02243-20.

Wiernik, E., S. Kab, M. Goldberg, et M. Zins. 2019. « Interaction entre l'obésité abdominale et l'indice de masse corporelle dans le risque cardiométabolique : résultats de la cohorte Constances ». *Revue d'Épidémiologie et de Santé Publique* 67 (mai): S140. https://doi.org/10.1016/j.respe.2019.03.113.

Wong, Kon Ken, Shaun Wen Huey Lee, et Kok Pim Kua. 2021. « N-Acetylcysteine as Adjuvant Therapy for COVID-19 – A Perspective on the Current State of the Evidence ». *Journal of Inflammation Research* Volume 14 (juillet): 2993-3013. https://doi.org/10.2147/JIR.S306849.

Wu, Zunyou, et Jennifer M. McGoogan. 2020. « Characteristics of and Important Lessons From the Coronavirus Disease 2019 (COVID-19) Outbreak in China: Summary of a Report of 72 314 Cases From the Chinese Center for Disease Control and Prevention ». *JAMA* 323 (13): 1239. https://doi.org/10.1001/jama.2020.2648.

Xiong, Yong, Yuan Liu, Liu Cao, Dehe Wang, Ming Guo, Ao Jiang, Dong Guo, et al. 2020. « Transcriptomic Characteristics of Bronchoalveolar Lavage Fluid and Peripheral Blood Mononuclear Cells in COVID-19 Patients ». *Emerging Microbes & Infections* 9 (1): 761-70. https://doi.org/10.1080/22221751.2020.1747363.

Xu, Jing, Jiahui Wang, Xiaoli Wang, Ruoming Tan, Xiaoling Qi, Zhaojun Liu, Hongping Qu, et al. 2020. « Soluble PD-L1 Improved Direct ARDS by Reducing Monocyte-Derived Macrophages ». *Cell Death & Disease* 11 (10): 934. https://doi.org/10.1038/s41419-020-03139-9.

Younas, M, C Psomas, J Reynes, et P Corbeau. 2016. « Immune Activation in the Course of HIV-1 Infection: Causes, Phenotypes and Persistence under Therapy ». *HIV Medicine* 17 (2): 89-105. https://doi.org/10.1111/hiv.12310.

Younas, Mehwish, Christina Psomas, Christelle Reynes, Renaud Cezar, Lucy Kundura, Pierre Portales, Corinne Merle, et al. 2019. « Microbial Translocation Is Linked to a Specific Immune Activation Profile in HIV-1-Infected Adults With Suppressed Viremia ». *Frontiers in Immunology* 10 (septembre): 2185. https://doi.org/10.3389/fimmu.2019.02185.

Yu, Pian, Xu Zhang, Nian Liu, Ling Tang, Cong Peng, et Xiang Chen. 2021. « Pyroptosis: Mechanisms and Diseases ». *Signal Transduction and Targeted Therapy* 6 (1): 128. https://doi.org/10.1038/s41392-021-00507-5.

Zaravinos, Apostolos, John Bizakis, et Demetrios A. Spandidos. 2009. « Prevalence of Human Papilloma Virus and Human Herpes Virus Types 1-7 in Human Nasal Polyposis ». *Journal of Medical Virology* 81 (9): 1613-19. https://doi.org/10.1002/jmv.21534.

Zhang, Jinghe, Haibo Wu, XiaoHong Yao, Dingyu Zhang, Yonggang Zhou, Binqing Fu, Wei Wang, et al. 2021. « Pyroptotic Macrophages Stimulate the SARS-CoV-2-Associated Cytokine Storm ». *Cellular & Molecular Immunology* 18 (5): 1305-7. https://doi.org/10.1038/s41423-021-00665-0.

Zhang, Jixiang, Xiaoli Wang, Vikash Vikash, Qing Ye, Dandan Wu, Yulan Liu, et Weiguo Dong. 2016. « ROS and ROS-Mediated Cellular Signaling ». *Oxidative Medicine and Cellular Longevity* 2016: 1-18. https://doi.org/10.1155/2016/4350965.

Zhang, Ke, Lisa Miorin, Tadashi Makio, Ishmael Dehghan, Shengyan Gao, Yihu Xie, Hualin Zhong, et al. 2021. « Nsp1 Protein of SARS-CoV-2 Disrupts the MRNA Export Machinery to Inhibit Host Gene Expression ». *Science Advances* 7 (6): eabe7386. https://doi.org/10.1126/sciadv.abe7386.

Zhao, Miao-Miao. 2021. « Cathepsin L Plays a Key Role in SARS-CoV-2 Infection in Humans and Humanized Mice and Is a Promising Target for New Drug Development ». *Signal Transduction and Targeted Therapy*, 12.

Zhao, Qianwen, Meng Meng, Rahul Kumar, Yinlian Wu, Jiaofeng Huang, Yunlei Deng, Zhiyuan Weng, et Li Yang. 2020. « Lymphopenia Is Associated with Severe Coronavirus Disease 2019 (COVID-19) Infections: A Systemic Review and Meta-Analysis ». *International Journal of Infectious Diseases* 96 (juillet): 131-35. https://doi.org/10.1016/j.ijid.2020.04.086.

Zhao, Zhuangzhuang, Pan Qin, et Yao-Wei Huang. 2021. « Lysosomal Ion Channels Involved in Cellular Entry and Uncoating of Enveloped Viruses: Implications for Therapeutic Strategies against SARS-CoV-2 ». *Cell Calcium* 94 (mars): 102360. https://doi.org/10.1016/j.ceca.2021.102360.

Zheng, Jian, Yuhang Wang, Kun Li, David K Meyerholz, Chantal Allamargot, et Stanley Perlman. 2021. « Severe Acute Respiratory Syndrome Coronavirus 2–Induced Immune Activation and Death of Monocyte-Derived Human Macrophages and Dendritic Cells ». *The Journal of Infectious Diseases* 223 (5): 785-95. https://doi.org/10.1093/infdis/jiaa753.

Zhou, Hong, Jingkai Ji, Xing Chen, Yuhai Bi, Juan Li, Qihui Wang, Tao Hu, et al. 2021. « Identification of Novel Bat Coronaviruses Sheds Light on the Evolutionary Origins of SARS-CoV-2 and Related Viruses ». *Cell* 184 (17): 4380-4391.e14. https://doi.org/10.1016/j.cell.2021.06.008.

Zhou, Peng, Xing-Lou Yang, Xian-Guang Wang, Ben Hu, Lei Zhang, Wei Zhang, Hao-Rui Si, et al. 2020. « A Pneumonia Outbreak Associated with a New Coronavirus of Probable Bat Origin ». *Nature* 579 (7798): 270-73. https://doi.org/10.1038/s41586-020-2012-7.

Ziegler, Carly G.K., Samuel J. Allon, Sarah K. Nyquist, Ian M. Mbano, Vincent N. Miao, Constantine N. Tzouanas, Yuming Cao, et al. 2020. « SARS-CoV-2 Receptor ACE2 Is an Interferon-Stimulated Gene in Human Airway Epithelial Cells and Is Detected in Specific Cell Subsets across Tissues ». *Cell* 181 (5): 1016-1035.e19. https://doi.org/10.1016/j.cell.2020.04.035.

Zweigner, Janine, Hans-Joachim Gramm, Oliver C. Singer, Karl Wegscheider, et Ralf R. Schumann. 2001. « High Concentrations of Lipopolysaccharide-Binding Protein in

Serum of Patients with Severe Sepsis or Septic Shock Inhibit the Lipopolysaccharide Response in Human Monocytes ». *Blood* 98 (13): 3800-3808. https://doi.org/10.1182/blood.V98.13.3800.